

ABSTRACT

Title of Document: ENERGY-POSITIVE METHODS OF
WASTEWATER TREATMENT—
AN EXAMINATION OF ANAEROBIC
DIGESTION & BIO-ELECTROCHEMICAL
TECHNOLOGY

Kyla Gregoire, Doctor of Philosophy, 2013,
Civil & Environmental Engineering

Directed By: Dr. Leonard Tender, Branch Head
US Naval Research Lab, Washington, D.C.

The results presented here demonstrate plausibility of a hybrid Anaerobic Digester-Microbial Fuel Cell (AD-MFC) system for anaerobic primary (AD) and secondary (MFC) treatment and resource recovery from high-strength wastewater. We empirically determine the treatment efficiencies and energy densities achieved by the AD and MFC processes, both separately and when integrated as primary and secondary unit operations. On the basis of current production, undigested wastewater yielded an stable anodic current of 131 A/m^3 when continuously fed to triplicate MFCs (chronoamperometry, E_{an} , -0.200V vs. Ag/AgCl). Substrate limitations in digested sludge reduced anodic current— 36 A/m^3 , 17 A/m^3 , and 9 A/m^3 were achieved from 6d, 13d, and 21d digestate, respectively. Cathodic limitations severely

limited power/energy production by the MFC, with maximum power output of 11 W/m³ (69 mW/m²). Presumably, this was due to mass transport of oxygen reduction intermediates.

When AD and MFC processes are de-coupled (i.e. each fed with undigested wastewater), the energy realized from AD (as biogas) was, on average, 29.6 kJ per m³ wastewater treated (8.2 Wh/m³), whereas the MFC produced, on average, 2.1 kJ per m³ wastewater treated (0.58 Wh/m³). On the basis of COD removal, AD separately generated 9,110 kJ per kg COD removed (2,530 Wh/kg COD) whereas MFC separately generated 0.18 kJ per kg COD removed (0.05 Wh/kg COD). When combined as primary and secondary unit processes with a 6-d digestion period (reaction period which yielded the highest net energy production), the energy output from AD (as biogas) was 23.9 kJ per m³ wastewater; the energy output from MFC (as electrical power) was 2.1 kJ per m³ wastewater.

MFC treatment rates exceeded 90% COD removal, 80% VS removal and 80% TS removal, likely owing to the upflow, baffled reactor design that maximized interaction between wastewater and the anodic biofilm. Results indicate an inverse logarithmic relationship between digester retention time and subsequent MFC current production, i.e. maximal MFC current production is achieved with undigested waste, and an inverse linear relationship between digester retention time and subsequent COD/VS removal in MFCs. Breakthroughs must be made to address cathodic limitations of MFCs, before scaling is practically or economically viable.

ENERGY-POSITIVE METHODS OF WASTEWATER TREATMENT — AN
EXAMINATION OF ANAEROBIC DIGESTION &
BIOELECTROCHEMICAL TECHNOLOGY

By

Kyla Gregoire

Dissertation submitted to the Faculty of the Graduate School of the
University of Maryland, College Park, in partial fulfillment
of the requirements for the degree of
Doctor of Philosophy
2013

Advisory Committee:
Dr. Leonard Tender (chair)
Dr. Alba Torrents (co-advisor)
Dr. Stephanie Lansing (co-advisor)
Dr. Allen Davis
Dr. Baoxia Mi
Dr. Eric Wachsman

© Copyright by
Kyla Gregoire
2013

In Memory of my Mother,

Edith Anne Gregoire

Acknowledgements

To Greg Carter, my boyfriend, my support system, and my most patient advisor over the last six years—this would not have happened without you, and I am so grateful to have you in my life. To my friends and family—thank you for your love, support, encouragement, and most of all, for your endless supply of poop jokes.

Infinite thanks go my NRL advisor, Lenny Tender, for believing in me and giving me the opportunity to work on a project I am passionate about. Not many graduate students have the full, uncompromising support of an advisor, and I have been incredibly lucky to have worked with you. Also, I am sorry to have made your lab smell like butyric acid for the last two years.

Many thanks to my co-advisors and committee members: Dr. Alba Torrents for the flexibility and trust you have imparted on me during grad school; Dr. Stephanie Lansing for your co-advising on the Gates project and for the opportunity to be involved in the Haiti project, which has made a tremendous impact on my graduate career; Dr. Allen Davis for an education in reactor design that has benefitted my research immensely; Dr. Baoxia Mi for your kind words and advice with teaching ENCE215; and Dr. Eric Wachsman for your much appreciated service as the Dean's representative on my committee.

Thank you also to the US Naval Research Laboratory and especially the Center for Bio-Molecular Science & Technology for hosting me in your labs and facilities. I have been very lucky to work at a first-class research institution during my PhD, and my research has benefitted immensely from the opportunities provided by NRL.

To all of my lab mates during graduate school—Maia Tatinclaux, Sarah Glaven, Rachel Snider, Jeff Erickson and all others of NRL; Andrew Moss, Kate Klavon, Holly Bowen, Veronika Zhiteneva, Sean Lai, Preston Postl, and all others of UMD. Thank you for your camaraderie, laughter, and, most of all, for your education in all things anaerobic and electrochemical.

Many thanks to the various wastewater treatment plant operators, scientists and managers that I pinged for advice during the initial phase of this project—your field is fascinating to me, and I'm grateful for the informal education. In particular, thank you to Greg Phillips of DC Water for your assistance with nutrient analysis, and patience during my infinite sample dilutions.

Funding for this project was provided by the Bill & Melinda Gates Foundation, the US Naval Research Laboratory, the University of Maryland's Institute for International Affairs, as well as a fellowship from the A. James Clark School of Engineering. This project would not have been possible without their financial support, and I am grateful to each of them.

Table of Contents

Acknowledgements.....	iii
Table of Contents	v
List of Tables	viii
List of Figures	ix
Chapter 1 : Introduction.....	1
1.1 Dissertation Summary.....	1
1.2 Sustainable Development & Water-Energy Nexus.....	4
1.3 Need for ‘Waste-to-Energy’ in the Developing World.....	8
1.4 Technological Need for AD-MFC	10
1.5 Hypothesis & Objectives	11
Chapter 2 : LITERATURE REVIEW	Error! Bookmark not defined.
2.1 Human Waste and Treatment Fundamentals	13
2.1.1 Environmental Composition of High Strength Wastewater	13
2.1.2 Aerobic BOD Removal.....	14
2.1.3 Sanitation Options for the Developing World	19
2.2 Anaerobic Digestion	21
2.2.1 Benefits and Dissemination of Biogas Technology.....	21
2.2.2 Biochemical Principles Governing AD	23
2.2.3 Process Design Considerations for AD.....	25
2.2.4 Low-Cost Digestion Review.....	26
2.3 Bioelectrochemical Systems & the Microbial Fuel Cell.....	29
2.3.1 Microbial Fuel Cell Principles	29
2.3.2 Fuel Cell Performance Metrics—Energy, Voltage, Current, and Power	34
2.3.3 Waste-fed MFCs	38
2.4 Bioenergetics of BOD Removal through Aerobic Respiration, Methanogenesis, and Anode Respiration.....	43
Chapter 3 : Hybrid Anaerobic Digester-Microbial Fuel Cell for Energy & Nutrient Capture from Latrine Sludge	52
3.1 Section 1 Introduction.....	52
3.2 Materials & Methods	58
3.2.1 Digester Substrate & Inoculum Sampling	58
3.2.2 AD-MFC Reactor Designs & Fabrication	59
Digesters	59
MFCs.....	60
3.2.3 Digester Loading & Operation.....	63
3.2.4 MFC Electrochemical Analysis	65
3.2.5 MFC Loading & Operation.....	66
3.2.6 Environmental & Microbiological Analyses	68
Aqueous Samples.....	68
Gas Samples.....	70
3.3 Results & Discussion	70
3.3.1 Digestion—Treatment Efficiencies	70

Organic Matter & Solids	70
3.3.2 Organic Acid Transformations	76
3.3.3 Nutrient Transformations.....	78
3.3.4 Coliform Removal	81
3.3.5 Digestion—Energy Production.....	82
3.3.6 Microbial Fuel Cell—Treatment Efficiencies	87
Organics	87
3.3.7 Coliform Removal	92
Anodic Current Production.....	92
Voltammetry	97
Cathodic Losses and Power Output	101
3.4 Conclusions.....	106
3.5 Acknowledgements.....	107
Chapter 4 : Microbial Fuel Cell Field Deployment for Secondary Treatment and Resource Recovery from Anaerobic Digestion Effluent	108
4.1 Introduction.....	108
4.2 Materials & Methods	112
4.2.1 Digester Study Site	112
4.2.2 Sampling and Environmental Analysis.....	114
4.2.3 MFC Reactor Designs & Fabrication	115
4.2.4 MFC Loading & Operation.....	117
4.2.5 MFC Electrochemical Analysis	118
4.3 Results & Discussion	121
4.3.1 Digester Treatment Efficiencies from Field Study.....	121
4.3.2 Microbial Fuel Cell—Treatment Efficiencies	126
Organics Removal.....	126
4.3.3 Microbial Fuel Cell—Energy Production.....	129
2-Electrode Current/Power—Field Experiments.....	129
4.3.4 Cathodic Overpotential & pH Effects.....	135
4.3.5 Laboratory Experiments.....	137
4.3.6 Voltammetry	143
4.3.7 Mass Balance of Wastewater Treatment & Energy Production	144
4.4 Conclusions.....	145
Acknowledgements.....	146
Chapter 5 : Iron(II)-Dependent Denitrification by a High-Current Density Bio-Cathode	148
5.1 Introduction.....	148
5.2 Materials & Methods	157
5.2.1 Sampling	157
5.2.2 Aqueous Enrichment for Iron(II)-Dependent Denitrifying Organisms	157
5.2.3 Electrochemical Enrichment Experiments.....	159
Experimental Set-Up.....	159
Electrochemical Analysis.....	160
5.2.4 Environmental Analyses	161
5.2.5 Confocal Microscopy.....	161
5.2.6 Phylogenetic DNA Analysis and Clone Library Generation	162

5.3	Results & Discussion	163
5.3.1	Aqueous Phase Enrichment	163
5.3.2	Cathodic Enrichment	164
	<i>Current Profiles</i>	164
	<i>Voltammetry</i>	170
	<i>Non-turnover CV</i>	177
5.3.3	Confocal Imaging	180
5.3.4	NO ₂ -NO ₃ Transformations—Treatment Efficiencies	181
5.4	Conclusions	184
5.5	Acknowledgements	185
	Chapter 6 : Sand-Modified Anode for Increased Power Generation from Benthic Microbial Fuel Cell	186
6.1	Introduction	186
6.2	Materials & Methods	191
6.2.1	Lab-Scale BMFC Evaluation	191
6.2.2	Field Deployment of Sand-Modified BMFC	196
6.3	Results & Discussion	198
6.3.1	Sediment Characterization	198
6.3.2	Laboratory Evaluation	199
6.3.3	Field Deployment	205
6.4	Conclusions	208
6.5	Acknowledgements	208
	Bibliography	225

List of Tables

TABLE 2-1 ENVIRONMENTAL CHARACTERIZATION OF HIGH-STRENGTH WASTEWATER & EXCRETA SAMPLES	14
TABLE 2-2 PROCESS DESIGN COMPARISON OF ANAEROBIC AND AEROBIC METHODS OF BOD REMOVAL	18
TABLE 2-3 CRITERIA FOR EVALUATION OF SANITATION TECHNOLOGIES FOR THE DEVELOPING WORLD	19
TABLE 2-4 REVIEW OF DIRECT AND INDIRECT BENEFITS OF ANAEROBIC DIGESTION FOR WASTE TREATMENT	22
TABLE 2-5 ENERGETIC AND PHYSIO-CHEMICAL CHARACTERISTICS OF BIOGAS (BUYSMAN, 2009)	23
TABLE 2-6 SUMMARY OF KEY PROCESS DESIGN CRITERIA FOR AD (LETTINGA 1995; AMANI, NOSRATI ET AL. 2010).....	25
TABLE 2-7 REVIEW OF COD REMOVAL AND MAXIMUM POWER DENSITIES ACHIEVED IN MFCs FED WITH ACTUAL WASTEWATER	42
TABLE 2-8 CALCULATED BACTERIAL CELLULAR YIELDS FOR PURPORTED WASTE-TO-ENERGY PROCESSES	50
TABLE 3-1 ENVIRONMENTAL COMPOSITION OF SUBSTRATE AND INOCULUM SOURCES AS PROXIES FOR LATRINE SOLIDS.....	58
TABLE 3-2 ENVIRONMENTAL COMPOSITION, TREATMENT EFFICIENCIES, AND TREATMENT RATES DURING DIGESTION OF LATRINE SOLIDS IN BMP 4. DATA IS PRESENTED AS MEAN \pm SD (N = 3).	75
TABLE 3-3. ORGANIC ACID PROFILES DURING BMP RUN 2	78
TABLE 3-4 CUMULATIVE METHANE PRODUCTION DURING DIGESTION OF HIGH-STRENGTH WASTEWATER DURING THREE BMPs. CH ₄ PRODUCTION IS NORMALIZED BY VOLUME (mL CH ₄ /mL SUBSTRATE), AND BY COD (mL CH ₄ /g COD REMOVED). VALUES ARE REPORTED AS MEAN \pm SD	83
TABLE 3-5 SUMMARY OF ENVIRONMENTAL CHARACTERISTICS, TREATMENT EFFICIENCIES, AND TREATMENT RATES DURING MFC TREATMENT. DATA IS PRESENTED AS MEAN \pm SD.	91
TABLE 4-1. PHYSICAL AND HYDRODYNAMIC DESIGN CHARACTERISTICS OF DIGESTERS	114
TABLE 4-2. SUMMARY OF ENVIRONMENTAL INDICATORS AND TREATMENT PERFORMANCE FROM DIGESTERS TREATING DORMITORY, COW, AND SWINE WASTE. DATA IS PRESENTED AS THE MEAN \pm STANDARD DEVIATION (N).	125
TABLE 4-3 EMPIRICAL MASS BALANCE FOR COD, VS, AND ENERGY PRODUCED BY AD-MFC TREATMENT; LABORATORY MFC DATA WAS USED FOR ALL CALCULATIONS.....	145
TABLE 5-1. REDOX HALF REACTIONS AND ASSOCIATED FORMAL POTENTIALS RELEVANT TO BIO- CATHODES	153
TABLE 5-2 NITRATE-NITROGEN REMOVAL RATES FROM DENITRIFYING CATHODE	182
TABLE 5-3 NITRITE- AND AMMONIA-NITROGEN REMOVAL RATES FROM DENITRIFYING CATHODE	182
TABLE 6-1 REVIEW OF BENTHIC MICROBIAL FUEL CELLS TO DATE	189
TABLE 6-2 PHYSICAL & CHEMICAL CHARACTERISTICS OF SEDIMENT COLLECTED FROM THE TUCKERTON, NJ SALT MARSH AND THE SAN DIEGO, CA MARINE STATION	199
TABLE 6-3 PERFORMANCE SUMMARY FROM LAB-SCALE CONTROL & SAND-MODIFIED ANODES	205
TABLE 6-4 SUMMARY OF ANALYTICAL METHODS USED FOR ENVIRONMENTAL ANALYSIS OF SAMPLES	209
TABLE 6-5 SUMMARY OF CALCULATIONS AND RESULTS FROM SMA ASSAY ON METHANOGENIC INOCULUM	215
TABLE 6-6. SUMMARY OF ELECTROCHEMICAL PERFORMANCE OF MFCs FED WITH AGRICULTURAL DIGESTATE IN LABORATORY EXPERIMENTS. VALUES ARE PRESENTED AS MEAN \pm STANDARD DEVIATION (N).	219
TABLE 6-7. SUMMARY OF ELECTROCHEMICAL PERFORMANCE OF MFCs FED WITH AGRICULTURAL DIGESTATE	222
TABLE 6-8 EMPIRICAL MASS BALANCE FOR COD, VS, AND ENERGY PRODUCED BY AD-MFC TREATMENT PROCESS; COMBINED LAB & FIELD DATA	223
TABLE 6-9 EMPIRICAL MASS BALANCE FOR COD, VS, AND ENERGY PRODUCED BY AD-MFC TREATMENT PROCESS; FIELD MFC DATA WAS USED FOR ALL CALCULATIONS.....	223

List of Figures

FIGURE 1-1 SPATIAL REPRESENTATION OF GLOBAL WATER RELATED DISEASE, SHOWING WATER RELATED DEATHS AS WELL AS FERTILIZER USAGE (UNEP AND CORCORAN 2010).....	5
FIGURE 1-2 PUBLIC HEALTH RETURNS ON INTERNATIONAL INVESTMENTS IN SAFE WATER AND SANITATION AT TWO DIFFERENT INVESTMENT AND IMPLEMENTATION SCENARIOS (UNEP AND CORCORAN 2010).....	6
FIGURE 1-3 GHG EMISSIONS BY INDUSTRIAL SECTOR IN 2004.....	7
FIGURE 2-1 DIVISION OF ENERGY REQUIREMENTS FROM THE BLUE PLAINS WASTEWATER TREATMENT PLANT IN WASHINGTON, D.C.	15
FIGURE 2-2 SCHEMATIC REPRESENTATION OF THE MICROBIOLOGICAL PATHWAYS RELEVANT TO ORGANIC MATTER DECOMPOSITION VIA ANAEROBIC DIGESTION AND ANODE RESPIRATION.....	24
FIGURE 2-3 PHOTOGRAPHIC AND SCHEMATIC (NOT-TO-SCALE) REPRESENTATION OF LOW-COST DIGESTER DESIGNS, WHERE (A) AND (B) ILLUSTRATE TUBULAR, PLUG-FLOW DIGESTERS; AND (C) AND (D) ILLUSTRATE A MODIFIED FLOATING DRUM DESIGN, THAT USES A 55 GALLON DRUM (COURTESY: NCAT, 2011).....	26
FIGURE 2-4 SCHEMATIC DEPICTION OF THE CROSS-SECTION OF TYPICAL TWO-CHAMBER MFC (TENDER, 2013).....	32
FIGURE 2-5 SCHEMATIC DEPICTION OF TYPICAL SINGLE-CHAMBER MFC (TENDER, 2013).....	33
FIGURE 2-6 SIMULATED VOLTAGE VS. CURRENT AND POWER VS. CURRENT POLARIZATION PLOTS FOR A TWO-CHAMBER MFC IN WHICH MEMBRANE RESISTANCE TO ION FLOW IS PROGRESSIVELY INCREASED	38
FIGURE 2-7 SCHEMATIC SHOWING THE DIVISION OF ELECTRON EQUIVALENTS FROM ELECTRON DONOR TO CELL SYNTHESIS AND ENERGY PRODUCTION (COURTESY: RITTMAN & MCCARTY, 2000).....	45
FIGURE 2-8 FROM MARA ET AL. (2003); SCHEMATIC REPRESENTATION OF HETEROTROPHIC METABOLISM OF ORGANIC MATTER. PATHWAYS ILLUSTRATE (1) CARBON FLOW FROM ORGANIC MATTER TO CARBON DIOXIDE; (2) ELECTRON FLOW FROM DONOR TO ACCEPTOR; AND (3) ENERGY CAPTURE AS ATP IN SUBSTRATE.....	48
FIGURE 3-1 CARTOON DIAGRAM OF BATCH ANAEROBIC DIGESTER ($V: 1.5L; OD: 3 IN.$) LIKED TO GAS TIPPING BUCKET TO MONITOR BIOGAS PRODUCTION, AND DUAL-CHAMBER, CONTINUOUS FLOW MICROBIAL FUEL CELL ($V_{AN}=V_{CATH}=100 ML$).	60
FIGURE 3-2 PHOTOS OF LAB-SCALE AD-MFC REACTORS USED TO EVALUATE TREATMENT AND ENERGY PRODUCTION FROM LATRINE SLUDGE.....	61
FIGURE 3-3 AVERAGE COD (IN BLACK), VS (IN GREY), AND TS (HASHED) DURING DIGESTION OF LATRINE SOLIDS DURING BMP2 (FIGURE A) AND BMP4 (FIGURE B). DATA POINTS REPRESENT THE AVERAGE \pm STANDARD DEVIATION (MG/L COD, MG/L VS, OR MG/L TS; $n = 3-9$).....	72
FIGURE 3-4 AVERAGE TOTAL COD (SOLID SYMBOLS) AND SCOD (OPEN SYMBOLS) DURING DIGESTION OF LATRINE SOLIDS DURING BMP3. DATA POINTS REPRESENT THE MEAN \pm SD (MG/L COD, $n = 4-6$).....	75
FIGURE 3-5 PROFILES OF NH_3-N AND $ORG-N$ CONCENTRATIONS IN WASTEWATER SAMPLES BEFORE AND AFTER DIGESTION DURING BMPs 2, 3, AND 4. DATA IS PRESENTED AS MEAN \pm SD (MG/L NH_3-N OR MG/L $ORG-N$).....	79
FIGURE 3-6 NH_3-N AND NO_2+NO_3-N CONCENTRATIONS DURING DIGESTION. DATA IS PRESENTED AS MEAN \pm SD (MG/L NH_3-N OR MG/L NO_2+NO_3-N).....	80
FIGURE 3-7 CUMULATIVE METHANE PRODUCTION (FIGURE A) AND BIOGAS COMPOSITION (FIGURE B) DURING BMP RUN 4. DATA POINTS REPRESENT THE MEAN \pm SD (ML CH_4 OR % CH_4) OF TRIPLICATE REACTORS THAT WERE TERMINATED AT 6 D (OPEN DIAMOND SYMBOLS), 13 D (OPEN CIRCLE SYMBOLS), AND 21 D (CLOSED DIAMOND SYMBOLS) OF DIGESTION.	84
FIGURE 3-8 PERCENTAGE OF THE TOTAL BIOGAS/METHANE CAPTURED AS A FUNCTION OF DIGESTION PERIOD, DURING BMP2 (CLOSED SYMBOLS); BMP3 (OPEN DIAMONDS); AND BMP4 (OPEN CIRCLES).....	ERROR! BOOKMARK NOT DEFINED.
FIGURE 3-9. CUMULATIVE METHANE PRODUCTION AS A FUNCTION OF INFLUENT COD LOADING (MG/L). DATA POINTS REPRESENT THE AVERAGE OF TRIPLICATE COD MEASUREMENTS AT DAY 0 OF DIGESTION. OPEN CIRCLES REPRESENT THE 2 ND DIGESTION TRIAL; SOLID CIRCLES REPRESENT THE 3 RD DIGESTION TRIAL.....	86

FIGURE 3-10. MFC INFLUENT AND EFFLUENT CONCENTRATIONS OF COD (FIGURE A; MG//L); AND VS (FIGURE B; MG/L) WHEN FED WITH UNDIGESTED WASTEWATER (IN BLUE), 6D DIGESTATE (IN GREEN), 13D DIGESTATE (IN TEAL), AND 21 D DIGESTATE (IN PURPLE) ...**ERROR! BOOKMARK NOT DEFINED.**

FIGURE 3-11. AVERAGE REMOVAL RATES OF COD FROM THE FOUR DIFFERENT WASTE FEEDS (0D, 5D, 10D, AND 35D DIGESTED LATRINE SOLIDS). REMOVAL RATES WERE CALCULATED ON THE BASIS OF HYDRAULIC RETENTION TIME (5 MIN).....**ERROR! BOOKMARK NOT DEFINED.**

FIGURE 3-12. RELATIONSHIP BETWEEN THE HYDRAULIC RETENTION TIME FOR DIGESTION (0-35 D) AND THE RESULTING CURRENT (MA/M2) AND COD REMOVAL FROM THE DIGESTATE WHEN POWERING THE MFCs. CURRENT VALUES (OPEN CIRCLES) REPRESENT THE AVERAGE, STEADY-STATE CURRENT DENSITY FROM TRIPPLICATE MFCs OPERATED IN CHRONOAMPEROMETRIC MODE WITH A FIXED ANODE POTENTIAL OF -200 mV vs. Ag/AgCL.....**ERROR! BOOKMARK NOT DEFINED.**

FIGURE 3-13 CHRONOAMPEROMETRIC PLOT OF THE FORMATION OF BIOELECTRICAL ACTIVITY AND SUSTAINED CURRENT PRODUCTION OF AN ENVIRONMENTAL SLUDGE BIOFILM AT CARBON CLOTH ELECTRODES IN TRIPPLICATE MFCs; CONTINUOUS FLOW EXPERIMENT WITH 3.6 H HRT; EAN: -0.2V vs. Ag/AgCL. OSCILLATIONS IN CURRENT PRODUCTION WERE DUE TO PUMP ON/OFF CYCLING EVERY 58 MIN.93

FIGURE 3-14. CHRONOAMPEROMETRIC CURVES SHOWING RELATIONSHIP BETWEEN DIGESTION PERIOD (5, 10, OR 35 D) AND SUSTAINED CURRENT PRODUCTION AT CARBON CLOTH ELECTRODES; CONTINUOUS FLOW EXPERIMENT WITH 3.6 H HRT; EAN: -0.2V vs. Ag/AgCL.....95

FIGURE 3-15 CHRONOAMPEROMETRIC SHOWING THE EFFECT OF SODIUM ACETATE ADDITIONS ON CURRENT PRODUCTION, UNDER THE FLOW OF 10D DIGESTATE; 5 MIN HRT; EAN: -0.2V vs. Ag/AgCL.96

FIGURE 3-16. REPRESENTATIVE VOLTAMMOGRAMS OF UNDIGESTED WASTE BIOFILMS RECORDED AT (A) THE TIME OF INOCULATION; (B) THE ONSET OF CATALYTIC ACTIVITY; AND (C) MAXIMUM CATALYTIC ACTIVITY. SCAN WAS RECORDED AT 0.001 V/S FROM -0.8 V TO +0.3 V AND BACK TO -0.8 V vs. Ag/AgCL, 3M KCL**ERROR! BOOKMARK NOT DEFINED.**

FIGURE 3-17 REPRESENTATIVE VOLTAMMOGRAMS OF UNDIGESTED WASTE BIOFILMS (SOLID LINES) AND GEOBACTER SULFURREDUCTENS, STRAIN DL1 (DASHED LINE) RECORDED AT 0.001 V/S FROM -0.8 V TO +0.3 V AND BACK TO -0.8 V vs. Ag/AgCL, 3M KCL.99

FIGURE 3-18. REPRESENTATIVE VOLTAMMETRY FROM MFC ANODE FED WITH UNDIGESTED SLUDGE. SCAN PARAMETERS: $v = 0.001$ V/s, EAN: -0.8 V TO +0.3 V, AND RETURN.....100

FIGURE 3-19. REPRESENTATIVE VOLTAMMOGRAMS OF AN WASTEWATER BIOFILM FED WITH (A) 0 D; (B) 5 D; (C) 10 D; AND (D) 35 D DIGESTATE. VOLTAMMOGRAMS WERE RECORDED AT MAXIMUM BIOFILM ACTIVITY. SCAN PARAMETERS: $v = 0.001$ V/s, EAN: -0.8 V TO +0.3 V, AND RETURN....101

FIGURE 3-20. POWER, CELL VOLTAGE, AND ELECTRODE POTENTIALS DURING FUEL CELL POLARIZATION WHEN MFC ANODE IS FED WITH UNDIGESTED LATRINE SOLIDS. POLARIZATION WAS RECORDED FROM OCV TO 0.005 V AT 0.1667 mV/s; ELECTRODE POTENTIALS WERE RECORDED AGAINST Ag/AgCL, 3M KCL.104

FIGURE 3-21. POWER, CELL VOLTAGE, AND ELECTRODE POTENTIALS DURING FUEL CELL POLARIZATION WHEN MFC ANODE IS FED WITH 5 D DIGESTATE. POLARIZATION WAS RECORDED FROM OCV TO 0.005 V AT 0.1667 mV/s; ELECTRODE POTENTIALS WERE RECORDED AGAINST Ag/AgCL, 3M KCL.105

FIGURE 4-1. UN-MECHANIZED, ANAEROBIC DIGESTERS TREATING AGRICULTURAL WASTE ON THE CAMPUS OF EARTH UNIVERSITY (LIMON, COSTA RICA). PHOTO ON LEFT SHOWS BIOGAS COLLECTION IN POLYETHYLENE BAGS WITH PVC CONNECTIONS. PHOTO ON RIGHT SHOWS A TWO-STAGE DIGESTER TREATING SWINE WASTE, ALONG WITH SUSPENDED BIOGAS COLLECTION BAGS.113

FIGURE 4-2. PHOTO (A) AND SCHEMATIC (B) SHOWING THE FRONT VIEW OF DUAL CHAMBER, PLUG-FLOW MFC REACTOR. SCHEMATIC (NOT TO SCALE) PROVIDES DIMENSIONING OF REACTOR AND BAFFLED FLOW CHAMBER. (V_{AN} , 101 mL; V_{CATH} , 202 mL; ANODE DEPTH, 0.5 IN; CATHODE DEPTH, 1 IN.116

FIGURE 4-3. TS AND VS CONCENTRATIONS (MG/L) AT DIGESTER INFLUENT (SOLID BARS) AND DIGESTER EFFLUENT (HASHED BARS). TS LEVELS ARE REPRESENTED IN BLACK; VS LEVELS ARE REPRESENTED IN GREY.....122

FIGURE 4-4. COD CONCENTRATIONS (MG/L) FROM FIELD EXPERIMENTS FOR: (1) DIGESTER INFLUENT (BLUE); (2) DIGESTER EFFLUENT (RED); (3) MFC INFLUENT (GREEN); AND (4) MFC EFFLUENT (PURPLE). VALUES ARE PRESENTED AS THE MEAN (SAMPLE SIZE), AND ERROR BARS REPRESENT THE STANDARD DEVIATION.....126

FIGURE 4-5. LABORATORY COD (RED) AND VS (BLACK) LEVELS AT THE INFLUENT (SOLID BARS) AND EFFLUENT (HASHED BARS) OF THE MFCs WHEN OPERATED AT A FIXED ANODE POTENTIAL OF -0.200V vs. Ag/AgCl. TRIPLICATE MFCs WERE EACH SAMPLED A MINIMUM OF TWO TIMES. DATA VALUES REPRESENT THE MEAN (N), AND ERROR BARS REPRESENT THE STANDARD DEVIATION. ..127

FIGURE 4-6. COD (RED) AND VS (BLACK) REMOVAL RATES FROM MFCs FED WITH SWINE, COW, AND DORMITORY DIGESTATE. REMOVAL EFFICIENCIES WERE CALCULATED AS A PERCENTAGE DECREASE FROM INFLUENT TO EFFLUENT (% , HASHED BARS) AND AS A DAILY RATE (KG/M³/D, SOLID BARS).128

FIGURE 4-7. CONVERGENCE OF ANODE (DIAMOND SYMBOLS) AND CATHODE (TRIANGLE SYMBOLS) POTENTIALS DURING BIOFILM DEVELOPMENT OF MFCs OPERATED IN THE FIELD. ANODES WERE FED WITH DIGESTATE FROM A DAIRY MANURE DIGESTER (DASHED LINE, CLOSED SYMBOL), SWINE MANURE DIGESTER (SOLID LINE, OPEN SYMBOL), AND DORMITORY WASTEWATER DIGESTER (SOLID LINE, CLOSED SYMBOL). AFTER HOUR 60, THE CATHOLYTE WAS REPLACED DAILY WITH PH 3 SEAWATER.131

FIGURE 4-8. CURRENT PRODUCTION (MA/M²) DURING BIOFILM DEVELOPMENT OF MFCs FED WITH DIGESTATE FROM A DAIRY MANURE DIGESTER (FILLED SYMBOLS, SOLID LINE), SWINE MANURE DIGESTER (OPEN SYMBOLS, DASHED LINE), AND DORMITORY WASTEWATER DIGESTER (CLOSED SYMBOLS, DASHED LINE); CONTINUOUS FLOW EXPERIMENT WITH 2.8 H HRT; V_{CELL}: 0.350 V.132

FIGURE 4-9. POLARIZATION ANALYSIS PERFORMED IN-COUNTRY ON MFCs FED WITH DIGESTATE FROM A DAIRY MANURE DIGESTER (BLACK LINES), SWINE MANURE DIGESTER (BLUE LINES), AND DORMITORY WASTEWATER DIGESTER (PURPLE LINES). POLARIZATION WAS PERFORMED THROUGH REDUCTIONS IN EXTERNAL RESISTANCE FROM 200,000 Ω TO 2 Ω, AND RECORDING STABLE CURRENT PRODUCTION AFTER 25 MIN. FIGURE (A) SHOWS POWER (MW/M²; SOLID LINES), AND CELL VOLTAGE (V; DASHED LINES), AS A FUNCTION OF AND CURRENT (MA/M²). FIGURE (B) SHOWS ANODE POTENTIALS (CLOSED SYMBOLS) AND CATHODE POTENTIALS (OPEN SYMBOLS) AS A FUNCTION OF CURRENT (MA/M²).134

FIGURE 4-10. CURRENT PRODUCTION FROM LAB TRIALS OF MFCs FED WITH SWINE (BLUE), COW (BLACK), AND DORMITORY (PURPLE) DIGESTATE; CONTINUOUS FLOW EXPERIMENT WITH 5 MIN HRT. FIGURE A DISPLAYS CURRENT PRODUCTION WITH A FIXED ANODE POTENTIAL OF -0.200V vs. Ag/AgCl; FIGURE B DISPLAYS CURRENT PRODUCTION WITH A FIXED CELL VOLTAGE OF 0.200V.138

FIGURE 4-11 CHRONOAMPEROMETRIC PLOT OF CURRENT AS A FUNCTION OF TIME DURING LAB TRIALS OF TRIPLICATE MFCs FED WITH DORMITORY DIGESTATE, ILLUSTRATING EFFECT OF SUBSTRATE CONCENTRATION ON CURRENT WHEN DIGESTATE IS SPIKED WITH SODIUM ACETATE (10 mM NAAC). CURRENT PRODUCTION IS DISPLAYED AT A FIXED ANODE POTENTIAL OF -0.200V vs. Ag/AgCl.139

FIGURE 4-12. CURRENT PRODUCTION FROM TRIPLICATE MFCs FED WITH DORMITORY DIGESTATE; CONTINUOUS FLOW EXPERIMENT WITH 5 MIN HRT; V_{CELL}: .200V. VALUES REPRESENT THE AVERAGE, STABLE CURRENT FOR THE EXPERIMENTAL CONDITION.140

FIGURE 4-13. POLARIZATION ANALYSIS FROM LAB TRIALS OF MFCs FED WITH SWINE (BLUE), COW (BLACK), AND DORMITORY (PURPLE) DIGESTATE. POWER CURVES (SOLID LINES); CELL VOLTAGE (DASHED LINES); CATHODE POTENTIAL (OPEN SYMBOLS); ANODE POTENTIAL (CLOSED SYMBOLS).142

FIGURE 4-14. REPRESENTATIVE VOLTAMMOGRAMS FROM MFCs FED WITH COW (BLACK), SWINE (BLUE), AND DORMITORY (PURPLE) DIGESTATE. VOLTAMMOGRAM FROM UNDIGESTED LATRINE SOLIDS (RED LINE) IS PROVIDED FOR COMPARISON OF MAGNITUDE OF CURRENT PRODUCTION AND CURRENT-POTENTIAL DEPENDENCY. SCANS WERE RECORDED AT 0.001 V/S FROM -0.8 V TO +0.3 V AND BACK TO -0.8 V vs. Ag/AgCl, 3M KCl.....144

FIGURE 5-1 PHOTOGRAPHS OF UN-INOCULATED SERUM BOTTLES, WHERE MILKY COLOR RESULTS FROM FeCO₃ PRECIPITATES (A); SERUM BOTTLES IMMEDIATELY AFTER INOCULATION WITH SEDIMENT ENRICHMENTS (B); AND SERUM BOTTLES CONTAINING ENVIRONMENTAL ENRICHMENTS SEVEN DAYS AFTER INOCULATION, SHOWING DEVELOPMENT OF ORANGE-BROWN PRECIPITATE,

CONSISTENT WITH Fe(III) PRECIPITATION THROUGH MICROBIAL OXIDATION OF FERROUS CARBONATES (C).	164
FIGURE 5-2 CURRENT PROFILE DURING BIOFILM GROWTH OF DENITRIFYING CELLS. DN1 AND DN2 WERE MAINTAINED AT FIXED POTENTIALS OF 0V AND -0.25V vs. Ag/AgCl, 3M KCl. FIGURE INSET SHOWS ENLARGED CURRENT PROFILE FROM DN1 CELL. RAW CURRENT WAS NORMALIZED TO CATHODE SURFACE AREA (8.30 CM ²).	165
FIGURE 5-3 CHRONOAMPEROMETRY SHOWING CURRENT PRODUCTION FROM DENITRIFYING BIO-CATHODE ON GRAPHITE ROD (SOLID LINE) AND CARBON CLOTH (DASHED LINE). ELECTRODES WERE MAINTAINED AT -0.25V vs. Ag/AgCl AND CURRENT WAS NORMALIZED BY GEOMETRIC SURFACE AREA (GRAPHITE ROD, 8.30 CM ² ; CARBON CLOTH, 12.9 CM ²).	168
FIGURE 5-4 CHRONOAMPEROMETRIC PLOT (EWE, -0.25V vs. Ag/AgCl) ILLUSTRATING THE DECLINE IN CURRENT TO BACKGROUND LEVELS WITHIN 24 H OF FLOWING MEDIA WITHOUT NITRATE AS AN ELECTRON ACCEPTOR TO THE DN2-T1 BIO-CATHODE.	170
FIGURE 5-5 VOLTAMMOGRAMS CAPTURED IMMEDIATELY BEFORE AND AFTER INOCULATION WITH THE ENVIRONMENTAL ENRICHMENTS. SCAN BEFORE INOCULATION IS FEATURELESS, CONSISTENT WITH ABIOLOGICAL, ANOXIC CONDITIONS. SCANS AFTER INOCULATION SHOW ABIOLOGICAL OXIDATION AND REDUCTION OF FERROUS AND FERRIC IRON, RESPECTIVELY (v = 1 mV/s FROM +0.55V TO -0.6V vs. Ag/AgCl).	171
FIGURE 5-6 REPRESENTATIVE SLOW SCAN VOLTAMMOGRAMS OF CATHODES AT THE ONSET OF CATALYTIC ACTIVITY, v = 0.0002 V/s. DN1 (DASHED LINE) AND DN2 (SOLID LINE) WERE GROWN AT FIXED POTENTIALS OF 0V AND -0.25V vs. Ag/AgCl, RESPECTIVELY.	173
FIGURE 5-7 SLOW-SCAN VOLTAMMETRY OF ORIGINAL NO ₃ -REDUCING BIO-CATHODE (DN2) AT VARIOUS POINTS ALONG THE GROWTH CURVE. SCAN PARAMETERS: 0.2 mV/s; EWE: +350 mV TO -500 mV AND BACK TO +350 mV vs. Ag/AgCl.	173
FIGURE 5-8 REPRESENTATIVE VOLTAMMOGRAMS OF THE ORIGINAL BIO-CATHODE (DN2) CATHODE AT MAXIMAL CURRENT PRODUCTION. SCANS WERE PERFORMED AT 0.2, 2, 10, 20, 100, AND 200 mV/s, E: +0.3V TO -0.5V AND BACK TO +0.3V vs. Ag/AgCl.	175
FIGURE 5-9 FIRST DERIVATIVE ANALYSIS OF VOLTAMMOGRAMS OF THE DN2-T1 BIO-CATHODE. VOLTAMMOGRAMS WERE RECORDED IMMEDIATELY AFTER CATHODES REACHED MAXIMUM STABLE CURRENT OPERATION (IN GREY) AND 18 DAYS LATER (IN BLACK); SCAN PARAMETERS: 0.2 mV/s FROM +0.3 V TO -0.5V AND BACK TO +0.3V vs. Ag/AgCl.	176
FIGURE 5-10 REPRESENTATIVE NON-TURNOVER VOLTAMMOGRAMS FROM BIO-CATHODE DN2, CAPTURED AT I < 4 uA IN THE ABSENCE OF NO ₃ - AS ELECTRON ACCEPTOR. SCANS WERE RECORDED AT 2 mV/s (GREEN LINE), 5 mV/s (PURPLE LINE), AND 10 mV/s (TEAL LINE).	178
FIGURE 5-11 RELATIONSHIP BETWEEN HEIGHT OF VISIBLE REDOX PEAKS (A, B, C, D IN FIGURE 5-9) AND THE SQUARE ROOT OF SCAN RATE DURING NON-TURNOVER VOLTAMMETRY. LINEAR REGRESSION LINES ARE OVERLAID WITH CORRELATION COEFFICIENT. BASELINE CORRECTION WAS ACCOUNTED FOR IN CALCULATING PEAK HEIGHT.	180
FIGURE 5-12 CONFOCAL LASER SCANNING MICROSCOPY IMAGES PERFORMED ON CARBON CLOTH, MODIFIED WITH DENITRIFYING BIO-CATHODE. IMAGES SHOW THE PRESENCE OF DNA AT THE ELECTRODE SURFACE.	181
FIGURE 6-1 LAB-SCALE BMFC REACTOR (NOT TO SCALE). 2-L BEAKER IS FILLED WITH 800 mL MARINE SEDIMENT AND 1200 mL ARTIFICIAL SEAWATER. GRAPHITE PLATE ANODE IS EMBEDDED IN THE SEDIMENT, CARBON CLOTH CATHODE IS SUSPENDED IN OVERLYING SEAWATER, AND Ag/AgCl REFERENCE.	193
FIGURE 6-2 SCHEMATIC OF SAND-MODIFIED ANODE USED FOR LAB EVALUATIONS (NOT TO SCALE)	193
FIGURE 6-3 SCHEMATIC OF SAND-MODIFIED ANODE	196
FIGURE 6-4 PHOTOS OF (A) ASSEMBLED, DEPLOYABLE ANODE; (B) CONTROL ANODE; AND (C) SAND-MODIFIED ANODE	197
FIGURE 6-5 REPRESENTATIVE GROWTH CURVES OF LAB-SCALE BMFCs USING TUCKERTON, NJ SALT MARSH SEDIMENT. EXPERIMENTS CONDUCTED IN THREE-ELECTRODE MODE, WHERE E _{AN} : 0.3V vs. Ag/AgCl. ALL CURRENT MEASUREMENTS WERE NORMALIZED BY ANODE SURFACE AREA (50.67 CM ²).	200
FIGURE 6-6 REPRESENTATIVE GROWTH CURVES OF LAB-SCALE BMFCs USING SAN DIEGO BAY (SPAWAR) MARINE SEDIMENT. EXPERIMENTS CONDUCTED IN THREE-ELECTRODE MODE, WHERE	

EAN: 0.3V vs. Ag/AgCl. ALL CURRENT MEASUREMENTS WERE NORMALIZED BY ANODE SURFACE AREA (50.67 CM ²).	200
FIGURE 6-7 REPRESENTATIVE POLARIZATION AND IV PLOTS FROM LAB-SCALE BMFCs WITH SAND-MODIFIED ANODES, USING TUCKERTON, NJ SALT MARSH SEDIMENT. BMFC WAS HELD AT OPEN CIRCUIT FOR 24-48 HRS. PRIOR, THEN SCANNED FROM OPEN CIRCUIT TO 0.1V; SCAN RATE OF 0.1 mV/s. ALL CURRENT/POWER MEASUREMENTS WERE NORMALIZED BY ANODE SURFACE AREA (50.67 CM ²).....	201
FIGURE 6-8 REPRESENTATIVE VOLTAMMETRY OF CONTROL ANODES USING TUCKERTON, NJ SALT MARSH SEDIMENT (RUMFS 100410 BATCH). SCANS PERFORMED AT 0.1 mV/s FROM 0.3V --> -0.5V vs. Ag/AgCl. ALL CURRENT MEASUREMENTS WERE NORMALIZED BY ANODE SURFACE AREA (50.67 CM ²).....	204
FIGURE 6-9 REPRESENTATIVE VOLTAMMETRY OF SAND-MODIFIED ANODES USING TUCKERTON, NJ SALT MARSH SEDIMENT (RUMFS 100410 BATCH). SCANS PERFORMED AT 0.1 mV/s FROM 0.3V --> -0.5V vs. Ag/AgCl. ALL CURRENT MEASUREMENTS WERE NORMALIZED BY ANODE SURFACE AREA (50.67 CM ²).....	204
FIGURE 6-10 CURRENT DENSITY FROM CONTROL AND SAND-MODIFIED BMFCs DEPLOYED AT TUCKERTON, NJ SALT MARSH. CURRENT PRODUCTION WAS NORMALIZED BY ANODE SURFACE AREA OF 0.259 M ²	206
FIGURE 6-11 POWER DENSITY FROM CONTROL AND SAND-MODIFIED BMFCs DEPLOYED AT TUCKERTON, NJ SALT MARSH. POWER PRODUCTION WAS NORMALIZED BY ANODE SURFACE AREA OF 0.259 M ²	207
FIGURE 6-12 CUMULATIVE CH ₄ PRODUCTION DURING SMA ASSAY ON METHANOGENIC INOCULUM ..	215
FIGURE 6-13 AVERAGE TS IN MG/L DURING DIGESTION OF LATRINE SOLIDS DURING BMP2 (SOLID SYMBOLS); BMP3 (OPEN DIAMONDS); AND BMP4 (OPEN CIRCLES). DATA POINTS REPRESENT THE MEAN ± SD (MG/L COD, N = 4-6).....	216
FIGURE 6-14. AVERAGE COD (IN BLACK) AND VS (IN GREY) DURING DIGESTION OF WASTEWATER IN BMP4. DATA POINTS REPRESENT THE MEAN ± SD (MG/L COD, N = 4-6).....	216
FIGURE 6-15. AVERAGE COD (SOLID SYMBOLS) AND VS (OPEN SYMBOLS) DURING DIGESTION OF LATRINE SOLIDS DURING BMP2 (FIGURE A) AND BMP4 (FIGURE B). DATA POINTS REPRESENT THE AVERAGE ± STANDARD DEVIATION (MG/L COD OR MG/L VS) OF TRIPPLICATE REACTORS....	217
FIGURE 6-16. REPRESENTATIVE VOLTAMMOGRAMS FROM MFCs FED WITH COW (BLACK), SWINE (BLUE), AND DORMITORY (PURPLE) DIGESTATE. SCANS WERE RECORDED AT 0.001 V/s FROM -0.8 V TO +0.3 V AND BACK TO -0.8 V vs. Ag/AgCl, 3M KCL	220
FIGURE 6-17. DEVELOPMENT OF ANODE POTENTIAL (TRIANGULAR SYMBOLS) AND CURRENT PRODUCTION (CIRCULAR SYMBOLS) FROM MFCs FED WITH HUMAN (CLOSED SYMBOLS, SOLID LINE); COW (CLOSED SYMBOLS, DASHED LINE); AND SWINE (OPEN SYMBOLS, SOLID LINE) DIGESTATE; CONTINUOUS FLOW EXPERIMENT, V _{CELL} : 0.35V.....	221
FIGURE 6-18. CURRENT PRODUCTION (mA) DURING BIOFILM DEVELOPMENT OF MFCs FED WITH COW (BLUE), SWINE (GREEN), AND DORMITORY (RED) DIGESTATE; CONTINUOUS FLOW EXPERIMENT WITH 2.8 h HRT; V _{CELL} : 0.350 V.	221
FIGURE 6-19. TOTAL SOLIDS (TS) AND VOLATILE SOLIDS (VS) AT THE INFLUENT AND EFFLUENT OF DORMITORY, COW, AND SWINE DIGESTERS. VALUES ARE PRESENTED AS THE MEAN (SAMPLE SIZE), AND ERROR BARS REPRESENT THE STANDARD DEVIATION.	222

Chapter 1 : Introduction

1.1 Dissertation Summary

The critical need for effective human waste treatment across the developing world is matched by demand for low-cost sources of energy. Innovative wastewater technologies that exploit the nutrient and energy content of human excreta (e.g., 4.5 g total N per L urine; 1 kWh per kg carbohydrate) are needed to incentivize economically viable, environmentally sustainable treatment (Jonsson, Stinzing et al. 2004, Pham, Rabaey et al. 2006). If implemented, such technologies would reduce the burden of diarrheal disease and childhood mortality in the developing world while providing useful energy to the community. The focus of this dissertation is the integration of two such technologies—low-cost anaerobic digestion (AD) and the microbial fuel cell (MFC)—as primary and secondary unit processes for high-strength wastewaters (e.g. pit latrine sludge, septage). While AD and MFC can be configured for implementation in developing communities, neither performs to its full potential as a stand-alone system. We therefore proposed and investigated integration of an AD with a MFC as primary and secondary unit processes, respectively, for high-strength wastewaters (e.g. pit latrine sludge, septage) to increase overall treatment effectiveness and provide energy capture in the form of biogas and electricity.

The first study, described in Chapter 3 of this dissertation, investigated the energy capture and treatment potential of bench-scale AD-MFC systems treating high-strength wastewater obtained from the Blue Plains Advanced WWTP in

Washington DC. Ten replicate ADs and triplicate MFCs were designed in-house and operated at UMD and NRL laboratories over the course of one year, and were evaluated on the basis of biogas (AD) and electricity (MFC) production, organics, solids, and coliform removals, and nutrient transformations. Using a continuous flow of undigested sludge, we achieved volumetric current densities that are near the upper limit of what has been observed to date (i.e., $> 100 \text{ A/m}^3$), and that greatly exceed the upper limit of real waste-fed MFCs. Very high rates of organic removal (as measured by chemical oxygen demand, COD), as well as fecal coliform loads, were also achieved— greater than $100 \text{ kg COD/m}^3/\text{d}$ and 4-5 log fecal coliform removal, respectively. Later experiments with digested sludge revealed highly consistent correlations between digestion period, energy/electricity capture, and treatment efficiencies. These correlations can be used as a means to best optimize AD-MFC operations for energy and/or treatment efficiencies.

The second study, described in Chapter 4 of this dissertation, investigated performance of bench-scale MFC systems that were fed the effluent of low cost, tubular digesters treating agricultural and human waste in Costa Rica. This study similarly assessed energy and treatment efficacy of the MFC, and further focused on the challenges associated with field deployment and scaling of the technology, especially with respect to fundamental electrochemical challenges that remain at the cathode reaction of MFCs.

The third study, described in Chapter 5 of this dissertation, investigated the potential for biological catalysis of nitrate reduction (i.e. denitrification) as the cathode reaction for MFCs. A fundamental challenge to implementation of MFCs is

abiological oxygen reduction at the cathode, where circum-neutral temperature and pH conditions required by MFCs severely limit the rates of reaction. This study represents one component of a larger effort by the lab to elucidate and address cathodic limitations in the MFC. Microbial enrichment strategies for cathode-dependent biofilms were established, and results demonstrate the first electrochemical characterization of a denitrifying bio-cathode with high current production (i.e., > 3 A/m² of cathodic current). This approach is particularly appealing for wastewater-fed MFCs because denitrification is valuable waste treatment process. Moreover, it makes possible single-chamber anaerobic MFCs that would not require costly and ineffective oxygen-exclusion membranes.

The fourth study, described in chapter 6 of this dissertation, investigated a novel strategy to partially address mass transport limitations at the anode of benthic microbial fuel cells (BMFCs). BMFCs are comprised of an anode embedded in marine sediment and cathode floating in the overlying seawater for the purpose of powering oceanographic sensors. BMFCs in which the anodes were encapsulated in a highly porous layer of sand prior to embedment in sediment were initially evaluated in the laboratory, where they generated significantly more energy than control anodes ($p < 0.05$), with a 148% increase in maximum current production ($n = 9$) in lab evaluation. Control and sand-modified anode BMFCs were subsequently deployed off the coast of New Jersey, where the sand-modified anode maintained a greater than 50% advantage in power production for more than 1000 hours.

The first two studies described in this dissertation on the investigation of integrated AD-MFC treatment of wastewater were performed from 2011 – 2013.

They comprised the basis of an awarded Phase I proposal to the Bill & Melinda Gates Foundation which supported the research. The third study on the investigation of cathodic denitrification was conducted from September 2012 – April 2013 and was funded by the US Naval Research Laboratory. The fourth study on the investigation of sand modification of the BMFC anodes was conducted from April 2010 – September 2011 and was also funded by the US Naval Research Laboratory. The outcomes of the work include: four invited conference talks; one keynote address; one undergraduate student award (ENCE411); four scientific journal articles (to be submitted by November, 2013); project funding for anaerobic digestion deployments in Haiti (USAID-DIV grant); and project funding for MFC deployment at the DC WATER Blue Plains WWTP in D.C.

1.2 Sustainable Development & Water-Energy Nexus

A tenuous balance exists between global poverty alleviation, economic development, and environmental sustainability. In the face of climate change, population growth, and water scarcity, the premise of traditional civil works programs as catalysts for economic growth becomes less justifiable (Daly 1997, Sneddon, Howarth et al. 2006). The long-term public health and economic benefits from infrastructure improvements like centralized water, electricity, or highway/interstate programs cannot be overstated; however, the environmental impacts of such improvements are not insignificant, e.g., concrete production contributes 2.4% of global CO₂ emissions from industrial and energy sources; traditional hydroelectric

dams that accelerate erosion and affect aquatic migratory patterns; groundwater extraction near coastlines that leads to saltwater intrusion, and so on and so forth (Marland, Boden et al. 1989, Mihelcic, Crittenden et al. 2003, Davidson, Matthews et al. 2007). In the context of emerging economies, these environmental impacts need to be taken into account to avoid the long-term remedial measures that many western countries currently face at significant (e.g. ground and surface water remediation).

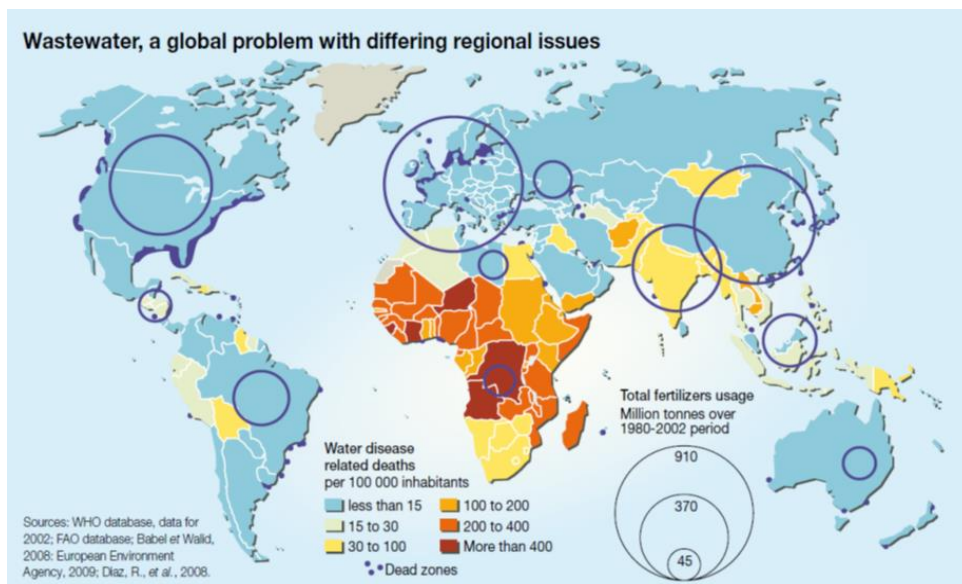


Figure 1-1 Spatial representation of global water related disease, showing water related deaths as well as fertilizer usage (UNEP and Corcoran 2010)

Examples of the global poverty alleviation, economic development, and environmental sustainability conundrum are easily viewed through the lens of civil engineering in the US, especially in the emerging concept of the ‘*Water-Energy Nexus*’ (Voinov and Cardwell 2009, Rothausen and Conway 2011). The centralized distribution of potable water, as well as the collection and treatment of sewage, have

resulted in some of the largest gains in public health and workforce productivity in US history.

More recently, this has been validated by economic analyses of foreign aid to developing communities, where the return on a US\$1 investment in sanitation is estimated to be between US\$5 – US\$28, based on averted diarrheal disease and the associated time and productivity savings (Hutton and Haller 2004, Haller, Hutton et al. 2007, UNEP and Corcoran 2010). Global representations of water related disease and the public health returns on international investments in safe water and sanitation are illustrated in Figures 1-1 and 1-2.

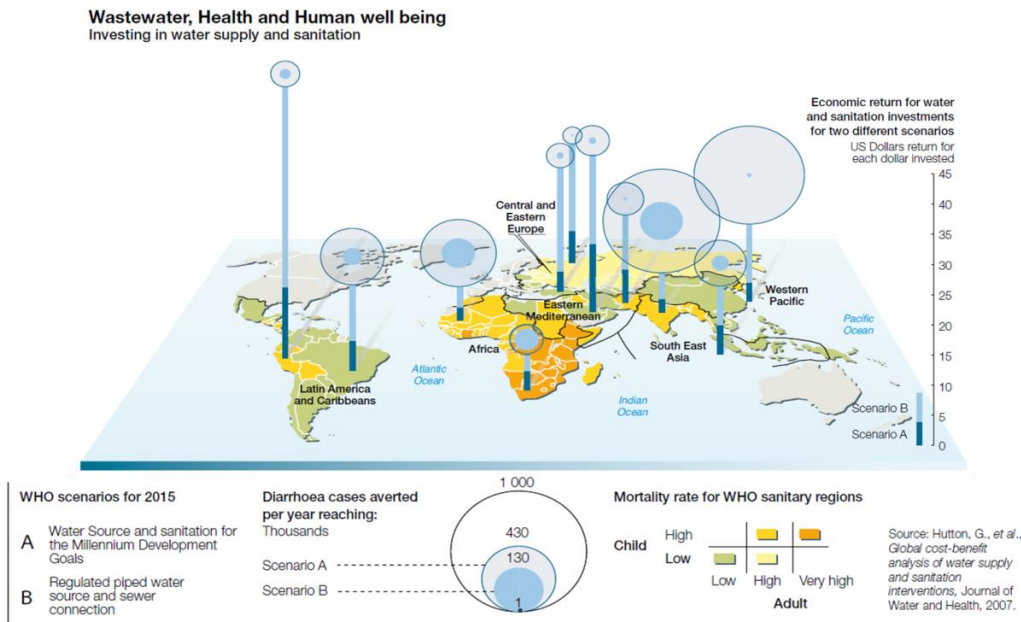


Figure 1-2 Public health returns on international investments in safe water and sanitation at two different investment and implementation scenarios (UNEP and Corcoran 2010)

The energy and economic demands of centralized distribution, collection, and treatment of water and wastewater are however enormous. The cumulative energy

demand of the water and wastewater sectors accounts for roughly 4% of the US annual energy budget, equating to 1,170 billion kWh or US\$4 billion annually (Goldstein, Newmark et al. 2008, Rothausen and Conway 2011) or 3,730 kWh per capita. Not considering economic sustainability, the implementation of similar, centralized waterworks programs in developing countries would greatly impact global energy consumption. The associated greenhouse gas emissions would be on the order of 0.67 kg CO₂/m³ of water and wastewater treated per capita (Friedrich, Pillay et al. 2009, Rothausen and Conway 2011). Presently water and wastewater treatment account for 2.8% of global greenhouse gas emissions (LeBlanc, Matthews et al. 2009), as illustrated in Figure 1-3.

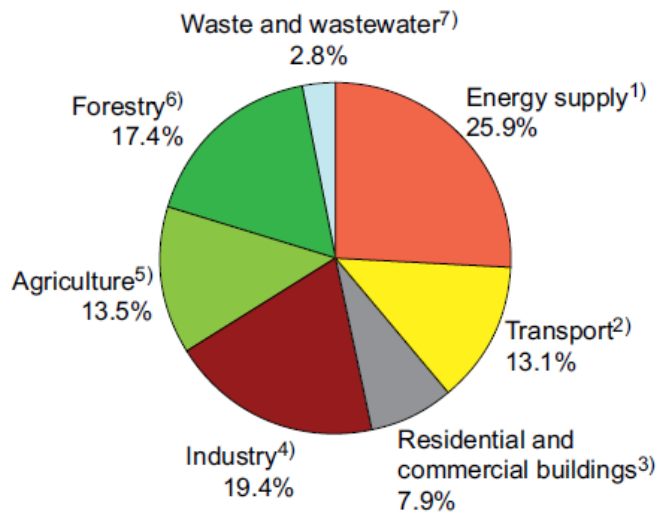


Figure 1-3 GHG emissions by industrial sector in 2004 (Oliver et al, 2005; 2006)

In the US, the scale of these energy demands and associated environmental and economic impacts is drawing attention from climate change specialists,

economists, and policy analysts. Much of the science and engineering driving water and wastewater treatment evolved prior to environmental legislation, and was primarily driven by public health necessity and a qualitative understanding of environmental health—e.g. minimization of fecal-oral route through closed conveyance; end-of-pipe treatment. Progress in relevant basic science research (e.g. microbial kinetics; pathogen inactivation; redox chemistry) has been rapid, but transition into more effective and environmentally sound water and wastewater technology has been slow to evolve. The energy expenditures for modern wastewater treatment is a striking example, requiring between 0.29 – 1.21 kWh for every cubic meter of sewage treated (Mitchel and Gu 2010, Rothausen and Conway 2011). As a point of reference, the Blue Plains Advanced WWT in Washington DC, which serves 2.5 million people, consumes on average 864 MWh treating 4 million cubic meters of sewage per day. Much of this energy is used to oxidize organic matter and nutrients to lesson oxygen demand on receiving water bodies, despite a scientific understanding of organic matter as biochemical energy reserves. This understanding has been applied elsewhere (e.g. biomass energy); however, its application to wastewater treatment has been extremely limited (e.g. 10% of wastewater treatment plants in the U.S. employ anaerobic digestion) (USEPA and CHP 2001).

1.3 Need for ‘Waste-to-Energy’ in the Developing World

Much progress has been made to meet the UN’s Millennium Development Goal (MGD) of improving worldwide access to clean water by 2015; however, progress on sanitation has been minimal, e.g. Sub-Saharan Africa has seen a 22%

increase in access to improved water sources but only 3% increase in improved sanitation (1990 to 2010); and it is projected that there will be a net increase in the number of people without access to improved sanitation by 2015 (UN 2010).

One attributing factor to these numbers is the capital and energy intensive nature of wastewater collection and treatment described above. Costs for traditional, aqueous conveyance and treatment exceed that of drinking water by at least 50% (McCullough, Moreau et al. 1993). As such, feasibility studies in many developing nations, such as Haiti, have concluded that the construction and operation and maintenance costs for wastewater treatment would exceed the local population's capacity to pay (Grau, Cathala et al. 2009). These costs however would be offset by reduction of the economic burden of water-associated diseases - over half the world's hospital beds are filled, at any given time, with people suffering from water-related diseases (Corcoran, Nellesmann et al. 2010). Nonetheless, the capital intensive, energy intensive and environmentally unsustainable nature of traditional centralized wastewater collection and treatment processes makes them unrealistic goals for developing countries.

Moreover, the need for low-cost energy sources in the developing world is similarly well documented: 1.4 billion people currently lack access to electricity, which is somewhat deflated by the large fraction who only have access to traditional biomass and coal as their fuel sources (Legros, Havet et al. 2009). All of these factors point to the need for significant investment in both the developed and developing world to advance technologies that exploit rather than demand energy for the treatment of human waste.

1.4 Technological Need for AD-MFC

The integration of anaerobic digestion with microbial fuel cells (AD-MFC) described in this dissertation aims to provide a technological solution to meet the critical needs of (1) effective human waste treatment and (2) decentralized, renewable energy for application in resource-limited settings. Established methods of decentralized waste treatment (e.g. lagoons, composting latrines) fail to exploit the large nutrient and energy content of human excreta (e.g., 4.5 g total N per L urine; 1 kWh per kg carbohydrate) and are often unsuitable for urban settings. Moreover, the aeration-dependent processes used in most centralized treatment are energy-intensive, making their operations and maintenance costs infeasible for developing countries. Innovative wastewater technologies are therefore required that exploit the nutrient and energy content of human excreta are needed to incentivize sanitation as economically viable and environmentally sustainable (Jonsson, Stinzing et al. 2004, Pham, Rabaey et al. 2006). If widely implemented, such technologies could reduce the burden of diarrheal disease and childhood mortality in the developing world while providing useful energy to the community.

Described here is integration of two such technologies—low-cost anaerobic digestion (AD) and the microbial fuel cell (MFC)—as primary and secondary unit processes for high-strength wastewaters (e.g. pit latrine sludge, septage). Both AD and MFC can be implemented with developing community appropriate materials. Neither performs however to its full potential as a stand-alone system. Specifically, ADs generate maximum energy with high-strength wastes, whereas MFCs are most efficient with low- to medium-strength wastes. By utilizing the MFC as a secondary

treatment process for AD, it may be possible to increase overall energy production and achieve more complete wastewater treatment. An MFC in-series after digestion may also improve overall process stability by improving buffering capacity, decreasing retention times and optimizing food/microorganism ratios). Notably, while AD has been demonstrated as a viable treatment method in a developing country, MFC technology has not.

Results from this investigation provide a technical baseline to evaluate scale-up of AD-MFC systems in a developing country setting. If successful, this technology represents a method to exploit the large energy and nutrient content of human excreta, and one that will work within the framework of decentralized sanitation. The dissemination of such a technology would provide an economic benefit to the local population, thus incentivizing sanitation and reducing the burden of waterborne disease in the developing world.

1.5 Hypothesis & Objectives

It was hypothesized that an AD-MFC system will yield (1) a nutrient-rich effluent with low organic and pathogen loads (< 100 mg COD/L with < 1% coliforms); (2) viable quantities of biogas (60-80% CH₄) for use in cooking and heating; and (3) continuous power generation for small devices. Compared to either as a stand-alone system, we propose that integration of the technologies will increase energy production and achieve more complete wastewater treatment. Specific objectives of the research were as follows:

1. To design and fabricate (10) batch, anaerobic reactors for digestion, and (3) dual-chamber, flow-through MFC reactors.
2. To quantify baseline power generation and electrochemical performance of these prototypes.
3. To evaluate the quantity and quality of nutrients in the effluent from AD & MFC, as well as solids, COD, and coliform reductions during treatment.
4. To evaluate the optimal retention times for AD & MFC, with the goal of balancing energy recovery with treatment efficiency.
5. To install bench-scale MFCs to the effluent of existing, full-scale digesters, repeating objectives 3 & 4 above to obtain field data.
6. To optimize the cathodic MFC reaction through the development and characterization of a denitrifying bio-cathode.

Chapter 2 : Literature Review

2.1 Human Waste and Treatment Fundamentals

2.1.1 Environmental Composition of High Strength Wastewater

The composition of domestic sewage varies widely but is largely comprised of water (>95%), as well as biodegradable organic material, organics & inorganic nutrients, and other micro & macro pollutants. Dietary, cultural, and socio-economic factors influence nutrient concentrations in human waste, but, on average, each liter of human urine contains 3-7 g of total nitrogen (TN), and 0.4 – 0.8 g of total phosphorus (TP); each kilogram of feces (dry matter) contains, on average, 5-13 g TN and 3-5 g TP (Jonsson, Stinzing et al. 2004, Langergraber and Muellegger 2005). Assuming per capita waste production of 1.4 L urine/day and 102 g feces (dry weight)/day, the annual nutrient loading rates from fecal sludge (combined urine and feces) are 2.1-4.0 kg TN/cap/year and 0.3-0.6 kg TP/cap/year. The organic content of human waste is largely contained in the fecal matter, where each gram contains 46-78 g chemical oxygen demand (COD) (Chaggu, Sanders et al. 2007).

With respect to combined waste streams, wastewater ‘strength’ is largely dictated by the degree of dilution from grey water (kitchens, showers, etc.) and/or conveyance water (e.g. flush toilets), and is characterized by the concentration of organic matter, either as biological or chemical oxygen demand (BOD, COD) or alternatively, by the concentration of solids, either as total solids (TS), suspended solids (SS) or volatile solids (VS). Owing to smaller volumes of gray and stormwater,

wastewater in the developing world is typically classified as high-strength, with COD concentrations exceeding 10 g COD/L (Strauss, Larmie et al. 1997). For comparison, the COD content of wastewater resulting from centralized collection in the US is typically 300 – 1,000 mg/L (Metcalf, Eddy et al. 2010). Fecal coliforms, as an indicator of microbial pollution, are found at concentrations of 10^4 – 10^9 MPN per 100 mL in high strength wastewater (Jimenez, Mara et al. 2010). Table 2-1 reviews the concentrations of key environmental parameters in wastewater, septage, sludge, and excreta samples.

Table 2-1 Environmental Characterization of High-Strength Wastewater & Excreta Samples

Wastewater Source	COD (g/L)	Total Solids (g/L, %)	Total Volatile Solids (g/L, %)	NH ₃ -N (mg/L)	Total Nitrogen (mg/L)	COD/TN	Total Phosphorus (mg/L)
Septage (UNEP 1998)	25 - 40	10 - 25			200-700		100-300
Latrine Sludge (Montangero and Strauss 2002)	20-50	> 3.5%		2,000-5,000	NA	NA	NA
Septage (Montangero and Strauss 2002)	< 10	< 3%		< 1,000	NA	NA	NA
Septage (Kootatep, Surinkul et al. 2004)	15.7	15.4	11.1	415	> 1,100	< 14	
Feces (Kujawa-Roeleveld and Zeeman 2006)	45.7-54.5 g/cap/d				1,500 – 2,000 g/cap/d		300 – 700 g/cap/d
Urine (Kujawa-Roeleveld and Zeeman 2006)	10 -12 g/cap/d				7,000 – 11,000 g/cap/d		600 – 1,000 g/cap/d

2.1.2 Aerobic BOD Removal

Modern wastewater treatment plants (WWTPs) range from comparatively simplistic, single-stage processes (e.g. stabilization ponds, lagoons) to highly-

engineered, multi-staged facilities. In the US, where federal and/or state standards regulate treatment levels, effluent discharged must not exceed 30 mg BOD/L, 30 mg TSS/L (Metcalf, Eddy et al. 2010). European regulations are somewhat more stringent, with maximum discharge limits of 25 mg BOD/L, 125 mg COD/L, 35 mg SS/L, 10 mg TN/L, 1 mg TP/L (Mara 2003). The unit operations driving advanced wastewater treatment in the US have been extensively reviewed by Metcalf & Eddy (2010) and Tchobanoglous (2003).

Secondary treatment processes, typically involving physical aeration of waste to promote aerobic oxidation, are responsible for the majority of organics, solids, and pathogen removal (i.e., 85% BOD and TSS Removal). They are also energy intensive, accounting the largest fraction of a WWTP energy budget (Pham, Rabaey et al. 2006, Logan and Rabaey 2012, Wang, Ma et al. 2013).

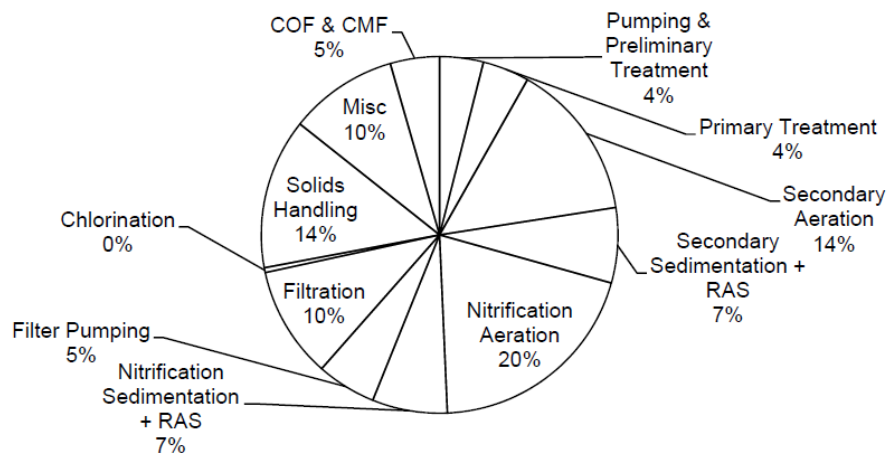
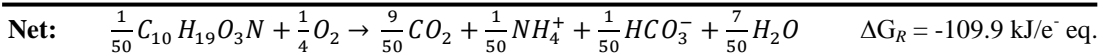
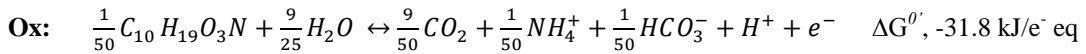


Figure 2-1 Division of energy requirements from the Blue Plains Wastewater treatment plant in Washington, D.C.

In activated sludge (AS) processes, the most common form of secondary treatment, heterotrophic organisms are maintained in suspended growth reactors,

where they catalyze the oxidation of organic matter, coupled to the reduction of dissolved oxygen, as described by the following redox reactions, where wastewater is approximated as $C_{10}H_{19}O_3N$ (Metcalf, Eddy et al. 2010):



Much of the engineering of secondary treatment is driven by the biological thermodynamics and kinetics pertaining to aerobic respiration, with the goal of maximizing the rates of these reactions, i.e. the rate of BOD removal. Reactor design is typically governed by a 1-5 d solids retention time (SRT) and 6-8 h hydraulic retention time (HRT). Organic loading rates for AS are typically 0.16 – 1.6 kg BOD/m³/day, and recommended food-to-microbe (F/M) ratio are 0.091 – 0.23 kg BOD/L MLVSS/day, (Lee and Lin 2000, Tchobanoglous, Burton et al. 2003). Aerobic BOD removal is catalyzed by a host of organisms, including bacteria (predominated by *Pseudomonas*), protozoa (ciliates, amoeba), and multicellular organisms (rotifers, water bears, nematodes) (Madigan, Martinko et al. 1997, Bitton 2005). Dense flocs (i.e. aggregates) of these cells form in suspension, which can then be settled out as ‘activated sludge’.

Physical aeration of the waste is necessary to maintain dissolved oxygen levels for aerobic metabolism (i.e. > 3 mg DO/L). Specific oxygen supply rates are

dependent on wastewater strength, and the efficiency of mechanical aerators/diffusers varies widely, but on average 8 m³ of air is required per m³ of medium-strength domestic wastewater, corresponding to an energy demand of 0.50 – 0.75 kWh per kg COD removed (Lee and Lin 2000). As one example, in the case of the Blue Plains Advanced WWTP in Washington, D.C., which treats, on average, 2 billion L/d, this equates to 16 MW for aeration, enough to power 1600 average US households.

As described by the governing redox reactions, the high energetic yield for organisms (-109.9 kJ/mol electron equivalent; -5,495 kJ/mol wastewater) facilitates rapid kinetics for the process and a relatively short HRT (e.g. 6-8 hr HRT). It also results in high cell yield (*Y*), whereby biomass resulting from cellular growth accumulate in AS tanks at a rate of $\approx 0.4 - 0.9$ kg VSS_{cells} per kg BOD removed (see theoretical calculation in Section 2.3). Consequently, biomass must be regularly wasted from tanks and disposed of hygienically, resulting in additional energy/cost demands due removal, treatment, and disposal of sludge (Metcalf, Eddy et al. 2010).

Biochemical differences between aerobic and anaerobic waste treatment govern much of the engineering and design of systems (summarized in Table 2-2), and can be used to compare AS to anaerobic digestion (AD), and to proposed bioelectrochemical system (BES) technology (i.e., microbial fuel cells (MFCs)). On the basis of cell (sludge) yields, anaerobic processes (e.g. methanogenesis), generate ≤ 0.1 kg VSS_{cells} per kg BOD removed (calculations outlined in Section 2.3). Because they do not require biomass wasting, this can greatly simplify operation and maintenance, reduce the hazards associated with additional sludge disposal, and reduce cost and energy savings (Mara 2003, Tchobanoglous, Burton et al. 2003).

Anaerobic processes are typically capable of treating significantly higher organic loading rates, on the order of 1-5 kg COD/m³/day for low-cost digestion systems; 10-40 kg COD/m³/day for high-rate reactors (e.g. the up flow anaerobic sludge blanket, UASB) (Bogte, Breure et al. 1993, Mara 2003, Appels, Baeyens et al. 2008). Higher loading rates correspond to reduced reactor volume, and thus reduced capital costs.

Anaerobic treatment is often reported as being less stable than aerobic methods, where control of environmental parameters, such as pH, temperature, and inhibitory compounds, is of greater importance for maintaining a healthy microbial community. Additionally, the relatively slow growth rate of anaerobic organisms (typically modeled as methanogens) contributes to long start-up times (1-2 months, or 2-3 HRTs for mesophilic conditions), and significantly longer required retention times (i.e. 30-60 HRT days low-cost, tubular digesters).

Table 2-2 Process design comparison of Anaerobic and Aerobic methods of BOD removal

Anaerobic	Aerobic
Recommended Organic Loading Rate	
High rate systems: 10 – 40 kg COD/m ³ /d (e.g. UASB) Conventional & Low-Cost Systems: 1-4 kg COD/m ³ /d (e.g. tubular or conventional AD)	0.5 – 1.5 kg COD/m ³ /d (e.g. activated sludge processes)
Biomass Yield	
0.05 – 0.15 kg VSS/kg COD (primarily dependent on substrate)	0.35 – 0.45 kg VSS/kg COD (fairly constant irrespective of substrate)
Start-up Time	
1-3 months; or 1-3 HRTs	1-2 weeks

2.1.3 Sanitation Options for the Developing World

When evaluating the practicality, economics, and sustainability of wastewater treatment options in the developing world, the following general criteria have been developed by Mara (2003):

Table 2-3 Criteria for Evaluation of Sanitation Technologies for the Developing World

Criteria	Details
Low Cost	Includes capital and operation and maintenance (O&M)
Simplicity	Construction; O&M complexities
Energy Usage	Preferably zero to avoid significant operating costs
Chemical Usage	Low, preferably zero, especially environmentally hazardous disinfectants, e.g. chlorine
Small Land Footprint	Where applicable, e.g. urban, peri-urban slums
Treatment Efficiencies	To meet effluent requirements
Low sludge production	Avoid additional cost, energy for treatment

Wastewater treatment methods that involve centralized collection, and/or capital and energy-intensive methods (e.g. activated sludge) can often be ruled out on the basis of one or more of these criteria. Energy-neutral, land-based treatment methods of wastewater treatment (e.g. lagoons, stabilization ponds) have proven effective in rural areas (Strauss, Larmie et al. 1997, Jimenez, Mara et al. 2010); however, they require centralized collection and a large (10-15 m² per person) footprint not suitable for urban settings. From an environmental perspective, land-based treatment also poses a number of challenges; namely, the production of

methane from such open-air processes serves as a point source for greenhouse gases (El-Fadel and Massoud 2001).

It has been demonstrated in a multitude of geographic and economic levels that decentralized wastewater treatment represents not only cost savings, but also significant environmental and public health benefits (Schönning and Stenström 2004, Langergraber and Muellegger 2005, Katukiza, Ronteltap et al. 2012). Septic tanks, which often serve the majority of the middle- and upper class in urban centers, can be an effective decentralized technique if installed in appropriate soils and maintained consistently, but otherwise, can rapidly contaminate groundwater and surface waters. Pit latrines, which currently meet the sanitation needs of most of the world's rural poor, represent another method of decentralized sanitation, but effective treatment is greatly dependent on characteristics of the underlying soils and hydrology. Unlined latrines built in areas with high water tables (< 2 m to water table) or porous soils can quickly result in contamination of surface and shallow groundwater. Furthermore, when the underlying pit fills, it is often capped and the latrine is reconstructed over a newly dug pit, representing an additional point source for organic and fecal pollution. Composting latrines, both dry and source-separated, represent an ecological method of waste management that does not rely on the addition of water or energy to treat the waste. In dry systems, urine is diverted to a holding tank before dilution and direct crop application as liquid fertilizer. Feces falls into a separate chamber under the latrine, where dry absorbent materials (wood ash, straw) must be added to maintain conditions conducive to aerobic microbial and fungal degradation (e.g. 40-70% moisture). Depending on temperature, pH, and moisture content, the period required

for pathogen reduction to ≤ 200 MPN/g ranges from three months to a year (Stenström 2001, Redlinger, Graham et al. 2002). The dry compost can subsequently be applied as fertilizer to non-consumable crops. Importantly though, none of these techniques is capable of exploiting the biochemical energy present in domestic wastewater, and especially from the most common high-strength sources, like septage or pit sludge.

2.2 Anaerobic Digestion

2.2.1 Benefits and Dissemination of Biogas Technology

The use of anaerobic digestion (AD) for waste treatment and energy production has been practiced at a household level since the early 20th century, with China and India serving as the proving ground for many of the low-cost designs (Buysman 2009). To date, there are an estimated 30 million household digesters installed globally, with a high concentration in China, India, Nepal, and Bangladesh (Jiang, Sommer et al. 2011, Austin and Morris 2012, Rajendran, Aslanzadeh et al. 2012, Thien Thu, Cuong et al. 2012). In the US, where digestion is often only economically viable at an industrial scale, the number is comparatively small (Klavon, Lansing et al. 2013). Approximately 1,500 systems have been installed at wastewater plants (representing ~10% of the total number of WWTPs in operation in the U.S.), and an addition 175 are currently installed on large-scale agricultural operations (USEPA and CHP 2001, Klavon, Lansing et al. 2013).

As stated previously, anaerobic methods of wastewater treatment are often considered to be economically and technologically more practical for the developing world, owing to the climatic conditions (15-30°C) and to the high organic loading rates that result from decentralized sanitation. AD represents one such method that benefits from these criteria, and, importantly, delivers a host of direct and indirect benefits for users, as summarized in Table 2-4, adapted from Buysman (2009) and Rajendran et al., (2012).

Table 2-4 Review of direct and indirect benefits of anaerobic digestion for waste treatment

Benefit of AD	Details; Reporting authors
Improved sanitation	Elimination of fecal-oral route of pathogen transmission; increased productivity (Gadre, Ranade et al. 1986; Barreto, Genser et al. 2007; Buysman 2009)
Renewable and low-cost energy	Biogas ($\approx 65\%$ methane); 395 mL CH ₄ per g COD (Marchaim 1992, Rajendran, Aslanzadeh et al. 2012)
Organic fertilizer	production and associated increases in crop yields (Garfi, Ferrer-Martí et al. 2011; Garfi, Gelman et al. 2011)
Indoor air quality	Biogas offsets use of traditional biomass for fuel (Smith and Mehta 2003; Rehfuess, Mehta et al. 2006)
Elimination of odor	Anaerobic (i.e. sealed) reactor architecture
Environmental benefits	GHG mitigation, BOD, pathogen removal from waste streams, avoided deforestation, chemical fertilizer substitution (El-Fadel and Massoud 2001)

The energy produced by digestion is termed ‘biogas’ and is a mixture of methane (50-70%), carbon dioxide (30-40%), and other trace compounds (2% H₂O, < 1% H₂S, NH_{3,g}). Energetic and physio-chemical properties of biogas are summarized in Table 2-5 (adapted from Buysman, 2009):

Table 2-5 Energetic and physio-chemical characteristics of biogas (Buysman, 2009)

Biogas Property	Value
Energy Content (HHV)	20-25 MJ/m ³
Ignition Temperature	650 – 750 °C
Density	1.2 kg/m ³
Critical pressure	75-89 bar
Critical temperature	-82.5°C

2.2.2 Biochemical Principles Governing AD

The biochemical processes governing anaerobic digestion of organic matter are markedly similar to that of BES technology. Both processes rely on a consortium of bacterial (and archaeal, in the case of AD) populations to perform the following sequential, and often symbiotic reactions (Lettinga and Lexmond 2001):

- **Hydrolysis** of lipids, complex polymers (e.g. cellulose, polysaccharides), and particulate organics to their monomeric fractions (e.g. sugars, amino acids)
- **Fermentation (i.e. acidogenesis)** of the solubilized monomers into organic acids, CO₂, and H₂
- **Acetogenesis** of high molecular weight acids (e.g. butyrate, formate) to acetate, H₂, and CO₂

Where AD and BES technologies differ is in the ultimate mineralization of organic matter, typically represented as the oxidation of acetate coupled to either the **reduction of CO₂ (i.e. CH₄ production in AD)** or **reduction of an electrode (i.e. current production in BES)**. The chain reactions and syntrophic relationships

associated with anaerobic digestion and anode respiration are described in the following figure:

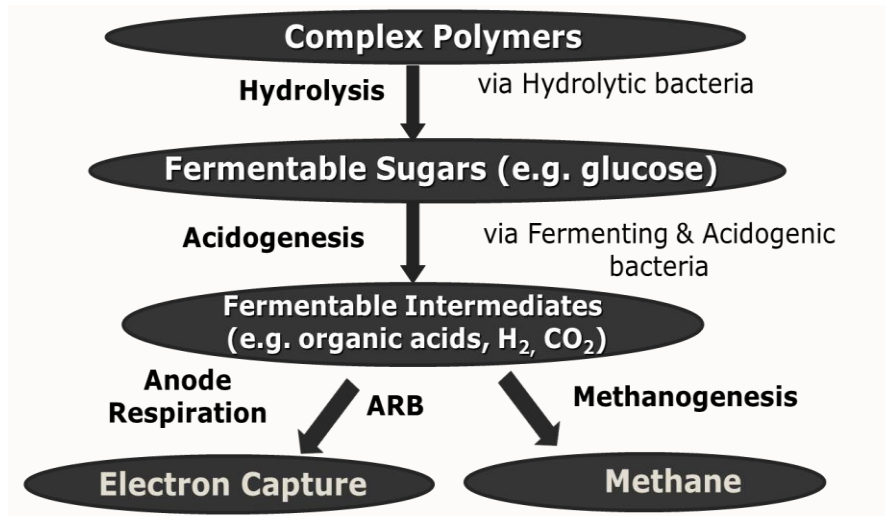
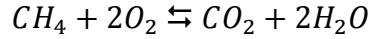


Figure 2-2 Schematic representation of the microbiological pathways relevant to organic matter decomposition via anaerobic digestion and anode respiration.

Although acetate is regarded as the most important precursor to methane production (substrate for acetoclastic methanogens), a number of hydrogenotrophic (i.e. H₂ oxidizing) species have also been identified (Gerardi 2003, Mara and Horan 2003). All known methanogenic species are neutrophilic and strictly anaerobic, requiring a relatively narrow pH window (6.5 – 8) and highly reduced conditions for growth (Lettinga 1995). The final step of methanogenesis is frequently reported as the rate-limiting step in kinetic models of AD, presumably due to the small energetic yields from the reaction (see section 2.3) and their low growth rates (i.e. 1 – 9 d doubling period) (McCarty 1975, Lettinga 1995, Mara and Horan 2003).

Assuming 100% conversion efficiencies (e.g. no biomass yield), and STP (i.e. 25.3 L/mol), theoretical methane production can be estimated as **395 mL CH₄/g**

COD removed, where the combustion of methane can be reported as a theoretical COD value (ThCOD, 64 g O₂/mol CH₄), as illustrated in the following reaction:



2.2.3 Process Design Considerations for AD

Similar to activated sludge, much of the engineering of AD reactors is driven by the biological thermodynamics and kinetics pertaining to methanogens, with the goal of maximizing rates methane production and organic matter turnover. In addition to the prolonged long start-up time (2-3 X HRT), a host of additional process considerations govern AD design and have been reviewed by Amani et al., (2010), Lettinga et al., (1995), and others:

Table 2-6 Summary of key process design criteria for AD (Lettinga 1995, Amani, Nosrati et al. 2010)

Process Parameter	Specification
Carbon-Nitrogen (C/N) Ratios	COD:N ~ 30:1 – 150:1, where 40:1 is most commonly recommended
Organic loading rates (OLR)	High rate AD, 3-35 kg COD/m ³ /d; Conventional AD, 1-5 kg COD/m ³ /d
Temperature	Mesophilic range, 30-37°C; Thermophilic range, 55-60°C
HRT	12-100 d
Buffering capacity	Sufficient alkalinity to buffer VFA production (e.g. 2,000 – 3,000 mg/L as CaCO ₃)
Inhibitory compounds	Metals, > 100 mg/L VFAs, > 150 mg/L NH ₃

2.2.4 Low-Cost Digestion Review

Low-cost digester designs are typically sized to meet either household or community energy needs, where the volume is dependent on flow rate, loading rate, HRT, as described in the previous section. The designs most commonly reported on in the developing world include: (1) fixed-dome or ‘hydraulic’ digester; (2) floating drum or ‘KVIC’ digester; and (3) plug flow or ‘tubular’ digester (Figure 2-3). A pertinent review of the respective design criteria and performance from each type has been conducted by Rajendran et al., (2012) and Buysman (2009).

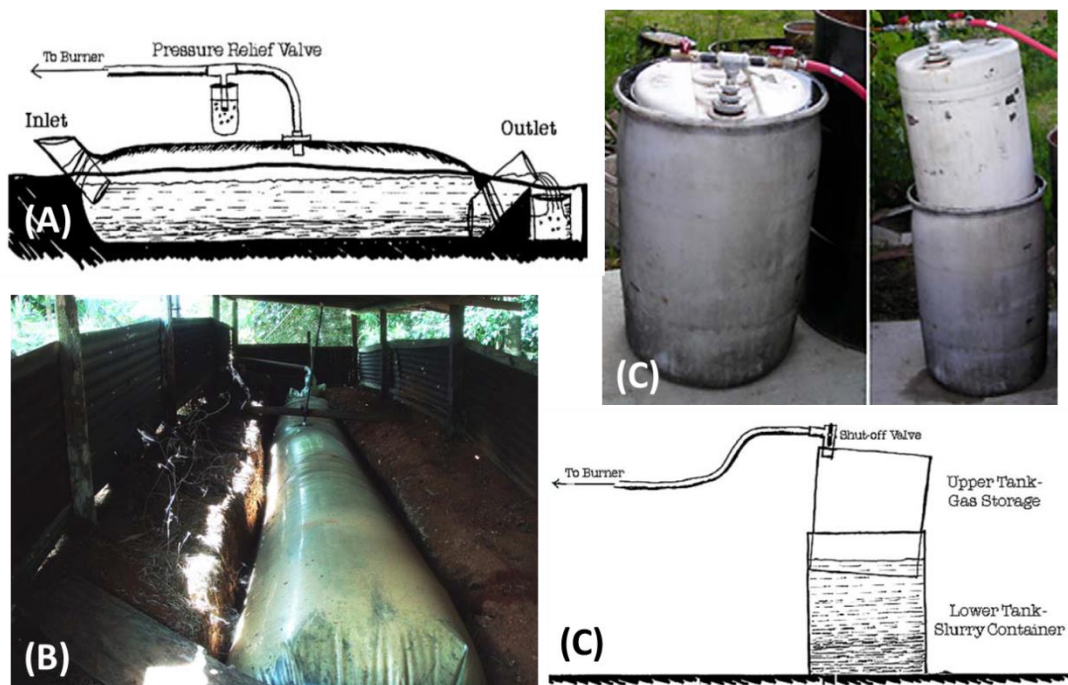


Figure 2-3 Photographic and schematic (not-to-scale) representation of low-cost digester designs, where (A) and (B) illustrate tubular, plug-flow digesters; and (C) and (D) illustrate a modified floating drum design, that uses a 55 gallon drum (Courtesy: NCAT, 201

The popularity of membrane-based, tubular digester has increased of late, likely owing to the modular, deployable design, low cost, and simplicity of

construction (Ferrer, Garfí et al. 2011, Garfí, Gelman et al. 2011, Rajendran, Aslanzadeh et al. 2012). Notably, this design is not subject to gas leakage that can result from imperfections in masonry construction, as is often the case with fixed-dome designs, (Marchaim 1992, Rajendran, Aslanzadeh et al. 2012). Instead, both manure and gas are collected in membrane-based bags (e.g. polyethylene, PVC, geomembrane), where gas can be subsequently transported by flexible or rigid tubing, or by physical transport of gas bags.

Similar to conventional AD designs, the recommended organic loading of tubular systems in mesophilic conditions is typically between 1-3 kg VS/m³/d; recommended solids content is 5-10% (w/w) (Mara 2003, Rajendran, Aslanzadeh et al. 2012).

A large range of specific biogas production rates has been reported (Buysman 2009, Rajendran, Aslanzadeh et al. 2012); however, values typically fall in the range of **0.26 – 0.55 m³ biogas/kg VS/day**. Importantly, many studies do not report data on COD or solids removal, or do not specify VS_{added} versus VS_{removed}; making it difficult to compare digester efficiencies. Instead, many studies report in units of m³ biogas produced per m³ reactor volume per day, or m³ biogas per kg VS_{added} or per kg COD_{added}.

One of the earliest reports comparing plug flow and continuously mixed designs demonstrated enhanced biogas production from the PFR—from 2.13 m³ biogas/m³ reactor/d (CSTR) to 2.32 m³ biogas/m³ reactor/d (PFR), both at 15 d HRT (Hayes 1979, Marchaim 1992). Specific biogas yield was also enhanced, from 0.281 m³ biogas/kg VS_{added} (CSTR) to 0.337 m³ biogas/kg VS_{added} (PFR). Both were dairy

digesters operated in relatively ideal conditions (12.9% solids loading) and were maintained as research systems on a university campus, which likely contributed to their high production rates, in comparison to other low-cost PFR studies.

In an early report of low-cost tubular systems, digesters sited in rural communities in Vietnam generated $\sim 0.24 \text{ m}^3 \text{ biogas/m}^3 \text{ digester volume/day}$, which provided > 4 hours of cooking fuel per day (An, Preston et al. 1997). More recent analysis on low-cost tubular designs has centered in Latin America. Lansing et al., (2008a; 2008b) evaluated two low-cost agricultural systems, operated in tropical conditions (Limon, Costa Rica). Daily biogas production from each system was $0.32 \text{ m}^3 \text{ biogas/m}^3 \text{ digester volume/day}$ (dairy manure; $\text{OLR} \sim 0.15 \text{ kg COD/m}^3/\text{d}$) and $0.10 \text{ m}^3 \text{ biogas/m}^3 \text{ digester volume/day}$ (swine manure; $\text{OLR} \sim 0.20 \text{ kg COD/m}^3/\text{d}$). On the basis of VS, this equates to $4.0 \text{ m}^3 \text{ biogas/kg VS}_{\text{added}}/\text{d}$ (dairy) and $1.0 \text{ m}^3 \text{ biogas/kg VS}_{\text{added}}/\text{d}$ (swine). High efficiencies for COD and solids removal were reported from both systems—86.1% COD and 80.3% VS (dairy); 91.9% COD and 83.0% VS (swine).

Reports by Garfi and colleagues (Ferrer, Garfi et al. 2011, Garfi, Ferrer-Martí et al. 2011) evaluated similar tubular systems fed with cow manure, but sited in a mountainous region of Peru (Cusco, Peru), where they were subject to psychrophilic conditions (i.e. $10 - 20^\circ\text{C}$), along with significant diurnal temperature fluctuations. By employing a greenhouse design, they were, notably, able to achieve comparable specific production rates of $0.32 - 0.36 \text{ m}^3 \text{ biogas/kg VS}_{\text{added}}$, and a maximum volumetric production of $0.47 \text{ m}^3 \text{ biogas/m}^3/\text{day}$ ($\text{OLR}, 1.29 \text{ kg VS/m}^3/\text{d}$) from household-scale (i.e. $< 8 \text{ m}^3$) systems. Daily biogas production provided sufficient

fuel for 2-3 hours of cooking, equivalent to 40-60% of the energy requirements for a family of 3-5 members (Ferrer, Garfí et al. 2011, Garfí, Ferrer-Martí et al. 2011).

2.3 Bioelectrochemical Systems & the Microbial Fuel Cell

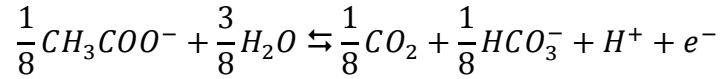
2.3.1 Microbial Fuel Cell Principles

Fuel cells are commonly described as devices that directly and continuously convert chemical energy into electrical power, via the oxidation of a substrate coupled to the reduction of an oxidant (Barbir 2005). They operate without combustion steps and do not require recharging, unlike voltaic batteries. They do however, require a continuous supply of fuel and oxidant to maintain current.

In the case of abiotic fuel cells, a reduced fuel (e.g. hydrogen or methanol) is oxidized at the anode, yielding electrons, which conducted through an external circuit to the cathode, where they are consumed by the reduction of an oxidant, such as oxygen. Abiotic fuel cells typically require non-renewable catalysts, such as platinum, to catalyze the oxidation of electrochemically active fuels (Barbir 2005, Lovley 2006).

The microbial fuel cell (MFC), which represents one application of bioelectrochemical system (BES) technology, operates on similar principles: it continuously converts the biochemical energy present in organic or inorganic material into electricity using bacteria, rather than platinum, as the catalyst to oxidize fuels (Bennetto, Stirling et al. 1983, Logan, Hamelers et al. 2006). In the case of organic

wastes, the biological oxidation of a substrate (e.g. acetate) is accompanied by the release of CO₂, protons, and electrons, according to:



A select but ubiquitous class of environmental microorganisms, termed anode respiring bacteria (ARB), will form a robust biofilm on the surface of non-corrosive anode (e.g., graphite) that catalyze the anodic reaction by coupling oxidation of organic matter to reduction of the anode. A fraction of the original energy release from organic matter is utilized by ARB for anabolic purposes (i.e. Y_h, 0.406 g VSS/g ThCOD, described in Section 2.3). In natural environments, the remaining electrons are captured by a thermodynamically favorable terminal electron acceptor (TEA), such as oxygen, nitrate, and carbon dioxide. In the case of the MFC, the anode serves as the TEA, and the rate at which ARB can transfer electrons to the anode is termed their *catalytic activity*, measured in C/s (A), and which is governed in part by the thermodynamic potential (i.e. V vs. SHE) of the anode. By capturing a certain fraction of the energy release for cell growth, the biofilm is able to derive sufficient benefit from the catalytic process to sustain itself, such that catalytic activity does not wane over time.

Electrical current is subsequently produced when electrons are conducted from anode to cathode via an external circuit (i.e. conductive wire plus resistor), where they are consumed by the reduction of an oxidant. Oxygen reducing cathodes are most commonly utilized, whereby protons and electrons react with dissolved oxygen to form water molecules, mainly by either four-electron or two-electron pathways:



Four-electron oxygen reduction is typically observed with highly active catalysts (e.g. Pt, Pd), while the two-electron mechanism is associated with less active catalysts (e.g. graphite).

As in abiotic fuel cells, the electrical power that is generated by an MFC results from the difference in electrochemical potentials of the anode and cathode that are governed by their respective half-reactions (oxidation of organic matter at the anode catalyzed by ARB, and oxidation of oxygen and the cathode). This difference in electrochemical potentials results in a voltage between the electrodes (cell voltage, V) that drives current from the anode through the external circuit to the cathode, where the resulting power delivered to the external circuit is described by Ohm's Law (i.e. $V = IR$; $P = IV$, where I is current and R is resistance of the external circuit). To maintain pH and electroneutrality, protons must be continuously removed from, or balanced with hydroxyls, in the anode chamber. In the case of **two-chamber MFCs** with oxygen reducing cathodes (as depicted in Figure 2-4; Tender 2013), this is typically accomplished with an ion selective membrane (e.g. Nafion), which physically separates anode and cathode half-cells. The purpose of the membrane is two-fold: to avoid oxygen intrusion into the anodic half-cell, which can reduce Coulombic efficiency (ratio of organic matter degradation resulting in electrical current production to total amount of organic matter degradation occurring in the anodic chamber) and poison the ARB biofilm, and to enable the selective flow of charged ions (e.g. H^+ diffusion through Nafion) that maintains charge and pH

neutrality. Importantly, such membranes were designed for the high-temperature, low pH, high pressure conditions typically associated with abiological fuel cells. Numerous investigations have concluded that membrane-associated internal resistance in MFCs contribute significant Ohmic resistance, and are the limiting factor in ultimate current/power outputs (Rozendal, Sleutels et al. 2008, Sleutels, Hamelers et al. 2009, Choi, Chae et al. 2011). This is especially the case in wastewater fed MFCs, where the relatively large number of cationic species in wastewater (e.g. Ca^{2+} , Mg^{2+} , K^{+}) contributes to cationic membrane inefficiencies (i.e. transport of other cations is preferential over H^{+}). As such, anion exchange membranes (AEM) have demonstrated somewhat higher efficiencies in waste-fed MFCs, though significant membrane losses still occur (Rozendal, Sleutels et al. 2008, Sleutels, Hamelers et al. 2009, Popat, Ki et al. 2012).

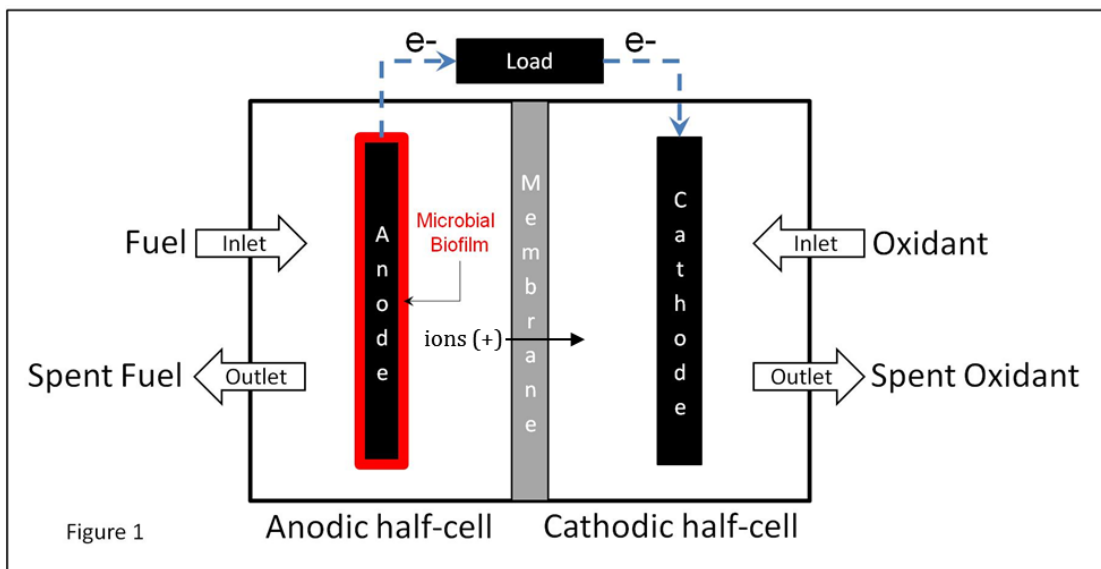


Figure 2-4 Schematic depiction of the cross-section of typical two-chamber MFC (Tender, 2013)

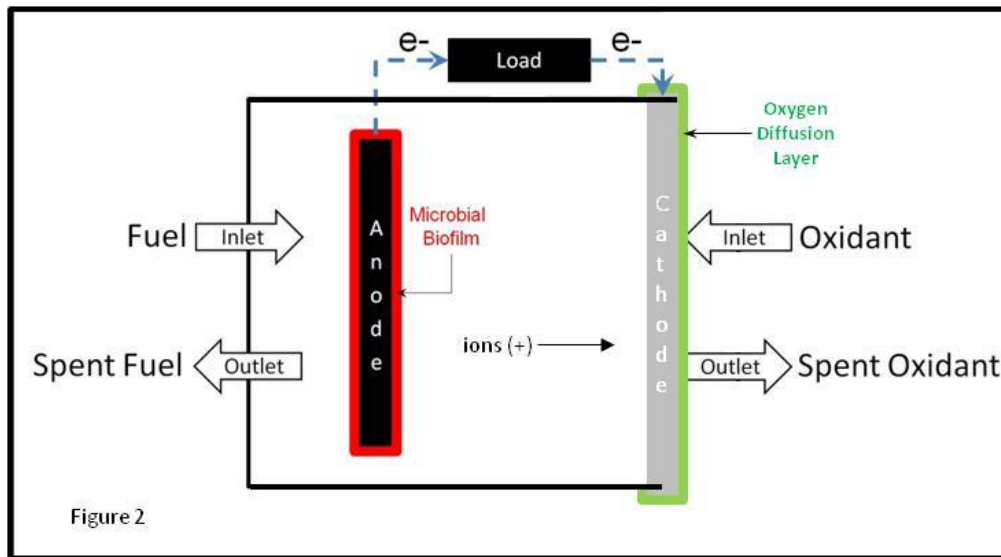


Figure 2-5 Schematic depiction of typical single-chamber MFC (Tender, 2013)

In the case of a **single-chamber (membraneless) MFC** (depicted in Figure 2-5) (Tender, 2013), which is the most common alternative MFC design, a permeable cathode (typically carbon cloth) is used to seal the open end of the anodic chamber. The cathode is made impermeable to water through the use of ‘water-proofing’—typically accomplished with multiple applications of polytetrafluoroethylene (PTFE, i.e. Teflon) solutions painted onto the cathode surface (Liu and Logan 2004, Cheng, Liu et al. 2006). In this way, the oxygen from ambient air is allowed to diffuse through the semi-breathable cloth and react with catalytically active sites on the cathode (i.e. the side in contact with the anodic solution). While this configuration eliminates the membrane-associated internal resistance, such MFCs exhibit other limitations. Most notably is the intrusion of oxygen into the anodic chamber owing to incomplete reduction of oxygen at the cathode surface, which typically results in

reductions in Coulombic efficiency (Liu and Logan 2004, Hu 2008, Du, Xie et al. 2011).

A common MFC uses acetate as the fuel, either added to water or as found in wastewater, and oxygen as the oxidant. The net MFC reaction is thus described by the following chemical equation:

Net Reaction: $\text{CH}_3\text{COOH} + 2\text{O}_2 \rightarrow 2\text{CO}_2 + 2\text{H}_2\text{O}$, $\Delta G^0 = - 875 \text{ kJ/mole of acetate}$

This reaction is the result of two coupled half-reactions, the oxidation of acetate occurring at the anode, and the reduction of oxygen occurring at the cathode:

Anodic half-reaction: $\text{CH}_3\text{COOH} + 2\text{H}_2\text{O} \rightarrow 2\text{CO}_2 + 8\text{H}^+ + 8\text{e}^-$

Cathodic half-reaction: $2\text{O}_2 + 8\text{H}^+ + 8\text{e}^- \rightarrow 4\text{H}_2\text{O}$

2.3.2 Fuel Cell Performance Metrics—Energy, Voltage, Current, and Power

Like other fuel cells and batteries, the performance of an MFC is characterized by its voltage (V): the amount of energy imparted to the load per electron flowing through the load; current (I): the rate at which electrons flow through the load; and power (P): the rate at which energy is imparted to the load (P) where power is the product of current and voltage ($P = I V$) (USDOE and EG&G 2004, Barbir 2005). As in the case of fuel cells and batteries, voltage and current are interdependent. The maximum voltage that can be generated by a MFC, referred to as the open circuit voltage (OCV), occurs when the resistance of the load is very high such that essentially no current flows from anode to cathode. The theoretical open

circuit voltage is related to the free energy of the net reaction (ΔG^0) of the MFC by the following reaction:

$$\text{OCV} = -\Delta G^0/nF$$

Where n is the number of electrons released per molecule of fuel oxidized (eight in the case of acetate) and F is the Faraday constant (96,487 coulombs/mole of electrons) yielding 1.13 V for an acetate and oxygen consuming MFC. The importance of OCV in characterizing a MFC is that it represents that upper limit of voltage (energy per electron) that a given MFC can deliver based on the specific net reaction occurring (i.e., the fuel and oxidant used). Conversely, when the MFC is operated at short circuit, such that resistance between anode and cathode is very small, current is then able to flow as quickly as can be generated by the MFC (referred to as limiting current, I_L).

Neither open circuit nor short circuit conditions result in power being generated by the MFC. To assess the potential for power production from an MFC, a technique referred to as polarization analysis is performed. Starting at open circuit, current is increased from zero by systematically decreasing the external resistance, and subsequently decreasing cell voltage and increasing current, where for each amount of external resistance $P = IV$. Maximum power is produced at some intermediate resistance/cell voltage combination between open and closed circuit. The resulting voltage vs. current and power vs. current polarization plots, which are analogous to those used to study battery and fuel cell performance, provide a significant amount of information about the specific MFC being analyzed.

Irreversible losses (i.e. Ohmic, activation, mass transport) at electrodes and/or the membrane have been observed in all MFC configurations to date, and have the cumulative effect of increasing the anode potential and decreasing the cathode potential, thereby reducing overall cell voltage (Barbir 2005, Chang, Moon et al. 2006, Rismani-Yazdi, Carver et al. 2008). In the case of MFCs, observed values of OCV are typically much lower than the predicted value, i.e. $\sim 0.6 - 0.8$ V, and are the results of limitations at anode, cathode, membrane, or some combination thereof.

To illustrate the effect of membrane losses, for example, on current/power, figure 2-6 (Tender 2013) depicts simulated voltage vs. current plots (black curves) and corresponding power vs. current polarization plots (red curves) for three related MFCs with sequentially increasing membrane resistance. These plots were simulated by numerically partitioning the cell voltage (V) into two components, one that is utilized to drive ions through the membrane (wasted), the other utilized to drive electrons through the external electrical circuit (resulting in power generation), where the flux of ions (expressed as current) is equal to the current through the external circuit, where the standard Butler-Volmer relationship is used to describe the rate vs. electrode potential dependency of the two electrode reactions (Tender, Carter et al. 1994), and where the cathode is assumed to be extremely large so as not to be the limiting factor. Here, j is current density (current normalized by volume of the MFC), j_L is the limiting current density (maximum current density the MFC can achieve at short circuit for which voltage is 0), V is voltage, V_{OC} is the open circuit voltage (maximum voltage the MFC can achieve at open circuit for which current density is 0), W is power density normalized by volume of the MFC), and W_L is the

limiting power density (product of open circuit potential and limiting current density). Curves labeled A correspond to those expected for a MFC that is limited in performance by the anode, achieved in practice by using an anode with very small surface area to the membrane and to the cathode (Logan 2008). The shape of power curve A (red; resembling that of a shark fin) is indicative of such an anodic limitation; in this case, maximum power density occurs when current density is very close to the closed circuit current. In the case of a wastewater-fed MFC, this would represent an idealized system where maximum substrate turnover (i.e. BOD removal) coincided with maximum power production. Curves labeled B correspond to those expected for the same MFC when there is non-negligible resistance to ion flow due to poor membrane performance, resulting in downward curvature of the power vs. current polarization plot, reduced power density, and maximum power density occurring at lower current density than in the case of A. Curves labeled C correspond to those expected for the same MFC when there is significant resistance to ion flow due to very poor membrane performance, resulting in a semicircular power density vs. current density polarization (as typically observed for real MFCs), where maximum power density is considerably lower than in the two other cases.

Such losses can be quantified (and minimized) experimentally by controlling the potential of the electrode, as in three electrode configurations, with a potentiostat, or by adjusting current flow from anode to cathode (via a variable resistor). This allows the potential difference between the redox potential of the substrate and the anode potential to be increased, making the insoluble electrode preferential for

bacterial reduction relative to alternative processes like fermentation, while still maximizing MFC voltage (Logan, Hamelers et al. 2006).

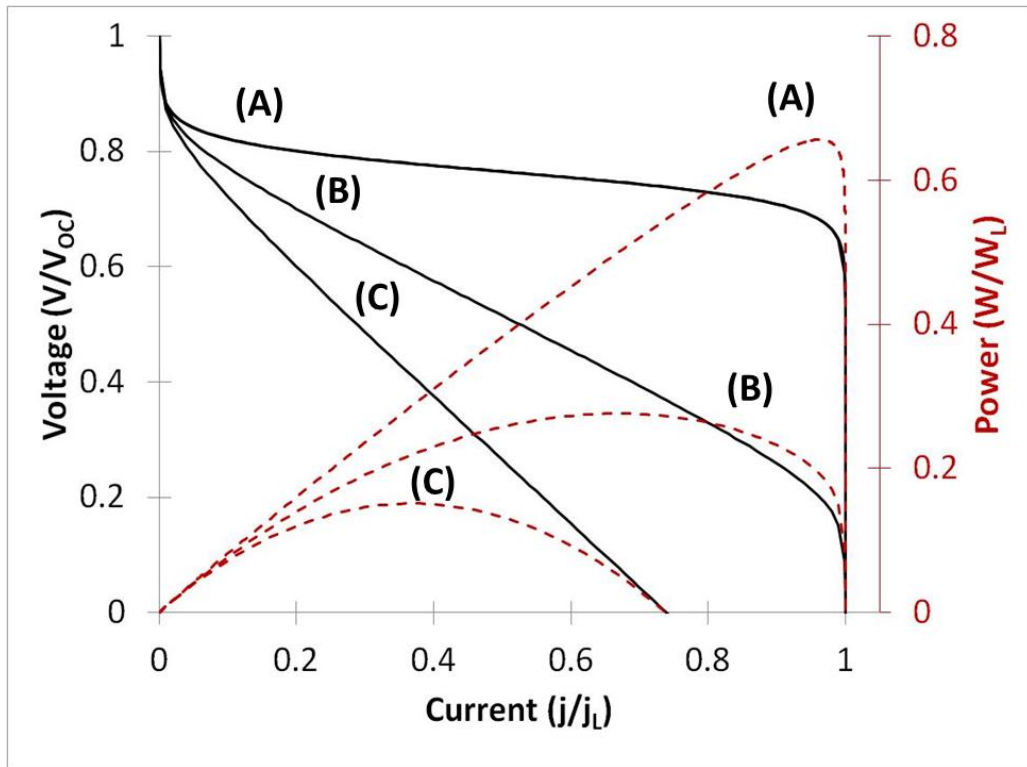


Figure 2-6 Simulated voltage vs. current and power vs. current polarization plots for a two-chamber MFC in which membrane resistance to ion flow is progressively increased

2.3.3 Waste-fed MFCs

A commonly proposed application of MFC and other bioelectric technology is for the simultaneous treatment and energy recovery from domestic and industrial waste streams (Aelterman 2006, Rozendal, Hamelers et al. 2008, McCarty, Bae et al. 2011, Logan and Rabaey 2012). The vast majority of MFC literature to-date has utilized synthetic waste streams, which are typically derivatives of acetate- or glucose-based, mineral media recipes (Rozendal, Hamelers et al. 2008, Fornero, Rosenbaum et al. 2010, Pant, Van Bogaert et al. 2010). The use of an acetate-based

media ensures optimal microbiological and electrochemical conditions (e.g. optimized substrate dilution rates; minimize solution resistance), and thus provides valuable baseline data to evaluate MFC performance, and especially the catalytic activity by ARB. Importantly though, the environmental characteristics of dilute, and especially high-strength, wastewater are vastly different than microbiological media. Waste composition, in addition to being highly variable, is ill-optimized in many ways for maximizing fuel cell performance—concentrations of acetate, the most common ARB substrate, are often too low (e.g., < 5 mM CH₃COO⁻) to optimize the catalytic activity (i.e. anodic current); the presence of cellulose and other hydrolysable compounds increases required retention times and encourages growth of hydrolytic and fermentative species which do not contribute to current; and the low buffering capacity contributes to pH gradients within the anodic biofilm; the negligible conductivity of wastewater (~ 1 mS/cm) adds solution resistance to the transport of protons; and the presence of fermentation intermediates (e.g., H₂S) and heavy metals (e.g., FeCl₃ coagulant) would be a significant challenge to known cathode catalysts (e.g., Platinum) and membranes (Rozendal, Hamelers et al. 2008, Pant, Van Bogaert et al. 2010, Logan and Rabaey 2012). The effect(s) that each of these parameters has on anode, cathode, and membrane losses has been studied at a very limited extent (Vega, Chartier et al. 2010, Choi, Chae et al. 2011).

The maximum reported electrical output from an MFC has increased exponentially over the last ten years, with a maximum 1.55 kW/m³ (2.77 W/m²) reported under optimal conditions (Fan, Hu et al. 2007). Much of this progress though has been reported with highly refined media, as described above. Also, and perhaps

more significantly, scaling of MFC power with reactors > 1.0 L has not been demonstrated under any operational conditions, and many of the studies reporting high power densities (i.e., > 1 W/m² or > 100 W/m³) utilized < 0.1 L reactors, or reported on stacked fuel cell configurations to reduce cathode limitations (Fornero, Rosenbaum et al. 2010, Pant, Van Bogaert et al. 2010, Logan 2012).

Progress on real waste-fed MFCs has been significantly more limited, and a review of reported COD removal rates (% and kg/m³/d) and power production (mW, mW/m², and W/m³) from systems fed with domestic or high-strength wastewater is summarized in Table 2-7. Reports utilizing a ferricyanide catholyte or acetate-amended waste streams were omitted from the review. Percent COD removal numbers are qualified with the reactor's HRT (for flow systems) or batch cycle period (for batch loaded systems).

Many of the systems were performed as batch, or fed-batch, experiments at small (< 0.1 L) volumes. This is problematic because of (1) the highly heterogeneous nature of domestic wastewater; (2) the low substrate (e.g., acetate) concentrations described above; and (3) the prolonged retention times (e.g., > 10 d HRT), which provide little meaning to COD removal rates in comparison to other BOD removal processes. Studies with *G. sulfurreducens* (the most studied, highest current generating ARB) have shown that, when fed with media containing 10 mM sodium acetate, dilutions rates > 0.09 h⁻¹ are required to maintain maximum catalytic activity (Strycharz, Malanoski et al. 2011). Thus, the low power output from batch wastewater studies may be due to rapid depletion of substrate by ARB, rather than inhibition by the waste stream. One side-by-side comparison of identical, flow

reactors showed an 82% reduction in maximum power under the flow of primary effluent wastewater, rather than a buffered, acetate (1g/L; ~ 10 mM) media, though a comparison of retention times for the acetate stream was not provided (Hays et al., 2011).

Notably, Min & Logan (2004) achieved relatively high power and COD removal at retention times that are competitive with activated sludge processes (i.e. 19 W/m³ and 79% COD removal at 4 h HRT). The design of this reactor, a flat plate assembly with a serpentine flow path, yielded a high surface area per volume ratio, likely enhancing catalytic activity, and thus COD removal, by maximizing the interaction between the waste stream and the anodic biofilm. A number of these reports, including the reactor by Min & Logan, utilized a platinum-based cathode catalyst (e.g., 0.5 mg Pt/cm²) to accelerate rates of oxygen reduction at neutral pH. It is unclear how quickly, and to what degree, platinum is fouled at the cathode of wastewater-fed MFCs; however, reports on H₂S fouling in abiological fuel cells would suggest this to be a significant problem (Zhang 2008).

Scaling of MFC reactors, and optimization of actual waste-fed systems, remains a primary challenge to practical implementation of BES for wastewater treatment, with significant space in the literature for meaningful contribution in these areas.

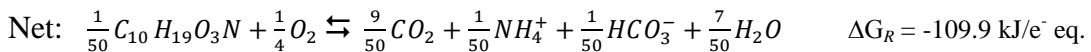
Table 2-7 Review of COD removal and maximum power densities achieved in MFCs fed with actual wastewater

Waste Source	V_{an}^a or V_{cath}^c (L)	A_{an}^a or A_{cath}^c (cm^2)	COD_{in} (mg/L^c or $kg/m^3/d^m$)	COD Removal (% ^p or $kg/m^3/d^m$)	P_{max} (mW/m^2)	P_{max} (W/m^3)	P_{max} (mW)	Citation
1° Effluent	1.0 ^a 0.1 ^c	20 ^a 20 ^c	300 ^c	< 15%	25	0.05	0.05	Rodrigo, 2007
1° Effluent	0.022 ^a	100 ^a	300 ^c	42% (1 h HRT) 79% (4 h HRT)	72 (1 h HRT) 42 (4 h HRT)	32 (1 h HRT) 19 (4 h HRT)	0.72 (1 h HRT) 0.42 (4 h HRT)	Min & Logan, 2004
1° Effluent	0.014 ^a	7 ^a	390 ^c	83% (21 d HRT)	230	12	0.16	Hays, Zhang, 2011
Acetate (1 g/L)	0.014 ^a	7 ^a	780 ^c	NR	1300	65	0.91	Hays, Zhang, 2011
1° Effluent & 1° Sludge (Batch Mode)	0.028 ^a	7 ^c	440 – 490 ^c 0.8 – 0.9 ^m	≥ 88% (HRT NR)	334	10	0.23	Ahn & Logan, 2010
1° Effluent & 1° Sludge (Flow Mode)	0.028 ^a	7 ^c	54 ^m	~ 20% (0.2 h HRT)	422	13	0.36	Ahn & Logan, 2010
1° Sludge	1.8 ^a	NR	14,000 ^c	70% (> 9 d HRT)	NR	6.4	10.8	Ge, Zhang, 2013
Digested Sludge	1.8 ^a	NR	16,700 ^c	36% (> 9 d HRT)	NR	3.2	5.4	Ge, Zhang, 2013
2° Sludge	0.426 ^a 0.336 ^c	NR	15,830 ^c	88% (> 30 d HRT)	NR	13	5.5	Zhang.. Ren, 2012
Digested Sludge	1 ^a	330 ^a 380 ^c	NR	NR	130	4.3	4.3	Weld, 2010

2.4 Bioenergetics of BOD Removal through Aerobic Respiration, Methanogenesis, and Anode Respiration

As stated previously, secondary treatment is responsible for the majority of organic, solids, and pathogen removal in a WWTP, and is frequently hypothesized to be replaced by BES technology. The biological thermodynamics of AS thus provide a useful, albeit simplified, comparison for understanding AS, AD, and MFC energetics and the theoretical energy value of domestic wastewater. For the purpose of this review, focus will be placed on the bioenergetics of BOD removal through (1) Aerobic respiration (i.e. activated sludge); (2) Methanogenesis (i.e. anaerobic digestion); and (3) Iron reduction (i.e. anode respiration, as in a MFC).

The redox reactions, and associated thermodynamics, of aerobic wastewater treatment can be described as follows, where we approximate wastewater (electron donor) as $C_{10}H_{19}O_3N$, oxygen serves as the terminal electron acceptor (TEA) for respiration, and values of Gibb's free energy ($\Delta G^{0'}$) represent biological standard conditions (25°C, 1 atm, 1 M activity except $[H^+] = 10^{-7}$):



In the context of biological energetics, the net energy release of the reaction is significant (ΔG_R , -109.9 kJ/mol e^- ; -5,495 kJ/mol wastewater), but a fraction of this energy is used for cell synthesis, and thus ΔG_R is not necessarily indicative of the energy that may go to energy yielding processes (e.g. CO_2 reduction; anode respiration). To estimate theoretical energetic yields, biomass yield (Y) and the associated parameters of f_e and f_s (fraction of electrons going to energy and cell synthesis, respectively) must first be evaluated.

From an energetic perspective, removal of the energy (i.e. organic matter, COD, BOD) from wastewater is attained via two pathways: (1) through biological energy losses (as heat) to the surroundings (i.e. biological inefficiencies); and (2) through anabolic transformations of wastewater organics into biomass (Mara and Horan 2003). The cumulative energy yield from these two pathways is referred to as the **biomass yield coefficient (Y)** for organisms and is represented as a fraction of the original organic matter present in the wastewater (i.e. the mass of cells formed per mass of organic material utilized). In other words, specific yield describes the division of electrons from the original organic material to new cellular mass, where the remainder are captured by the terminal electron acceptor (TEA) for energetic gains, either by the organism or by the energy conversion process.

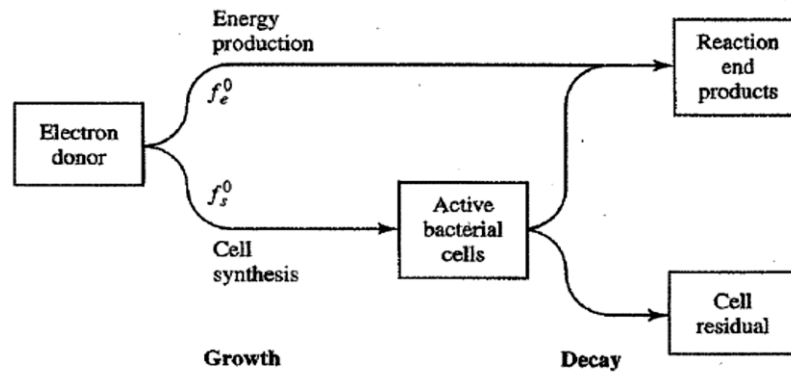


Figure 2-7 Schematic showing the division of electron equivalents from electron donor to cell synthesis and energy production (Courtesy: Rittman & McCarty, 2000)

An understanding of the flow of electrons from substrate to TEA thus provides a useful starting point for comparing theoretical energy gains from anaerobic digestion vs. bioelectric technology, where the f_e value can be thought of as an energetic efficiency factor, comparable to the empirically based measures of Coulombic efficiency in MFCs.

Following the methods proposed by McCarty (1971) and Rittman & McCarty (2001), estimations for Y , f_e , and f_s can be developed using the following stoichiometric equations for heterotrophic metabolism:

$$\Delta G_s = \frac{\Delta G_p}{K^m} + \Delta G_c + \frac{\Delta G_N}{K} \quad \text{Equation 2-1}$$

$$f_e + f_s = 1.0 \quad \text{Equation 2-2}$$

$$K \Delta G_R \left(\frac{f_e}{f_s} \right) = -\Delta G_s \quad \text{Equation 2-3}$$

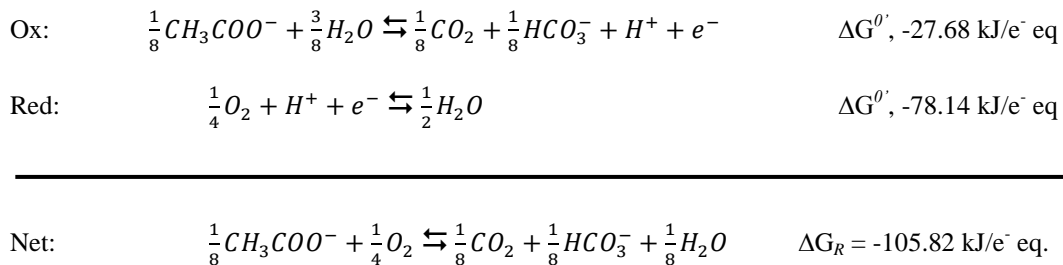
$$Y = \frac{f_s}{\text{Th.COD of cell tissue}} \quad \text{Equation 2-4}$$

- ΔG_s = free energy to convert 1 e⁻ eq of carbon to cells
- ΔG_p = free energy to convert 1 e⁻ eq of carbon to pyruvate
= +81.2 kJ/e⁻ eq (acetate/pyruvate)
- ΔG_R = free energy release from oxidation-reduction
- K = fraction of energy captured by bacteria ($K \approx 0.4-0.8$)
- $m = +1$ if $\Delta G_p > 0$
= -1 if $\Delta G_p < 0$
- ΔG_c = free energy to convert 1 e⁻ eq of pyruvate to cells
= +31.41 kJ/e⁻ eq. cells
- ΔG_N = free energy required to reduce N to NH₃
= +17.46 kJ/e⁻ eq cells (NO₃⁻)
= + 13.61 kJ/e⁻ eq cells (NO₂⁻)
= +15.85 kJ/e⁻ eq cells (N₂)
= 0.00 kJ/e⁻ eq cells (NH₄⁺)
- f_e = e⁻ mole substrate oxidized per e⁻ mole substrate used
(fraction of electron donor used for energy/TEA)
- f_s = e⁻ mole substrate used for cell synthesis per e⁻ mole substrate used
(fraction of electrons used for cell synthesis)
- Th.COD of cell tissue = 1.42 g cell COD per g cell VSS

In the following example calculations, we calculate theoretical f_e values for the two waste-to-energy technologies under investigation—AD and MFC—as a means for comparing the theoretical energy conversion by the microbiological processes (i.e. methanogenesis vs. anode respiration). As a baseline, we also calculate f_e values for activated sludge—the energy-demanding wastewater treatment process used by the majority of advanced wastewater treatment plants in the US. Acetate (CH₃COO⁻) is

assumed as the organic carbon source and electron donor for all three processes, as it is the substrate commonly utilized by heterotrophic metabolism, either by methanogens, ARB, or aerobic organisms. The bacterial efficiency factor (K) is assumed to be 60% based on Metcalf & Eddy (2010) and ammonium is assumed as the nitrogen source ($\Delta G_n = 0 \text{ kJ/e}^- \text{ eq}$).

For the case of activated sludge, the redox reactions associated with aerobic acetate oxidation are as follows:



The significant energy release (ΔG_R , -105.8 kJ/mol e⁻; -846 kJ/mol acetate) is comparable to that of wastewater, where both substrates create a large energetic potential for aerobically respiring organisms. To calculate the fraction of free energy diverted to cell synthesis, we assume pyruvate as the intermediate compound, as it is produced immediately before the division of electrons between substrate level phosphorylation (i.e. no electron release) and oxidative phosphorylation (i.e. electron release to terminal electron acceptor). Figure 2-8 illustrates the position of pyruvate in the division of energy, as well as overall carbon and energy flows during heterotrophic catabolism.

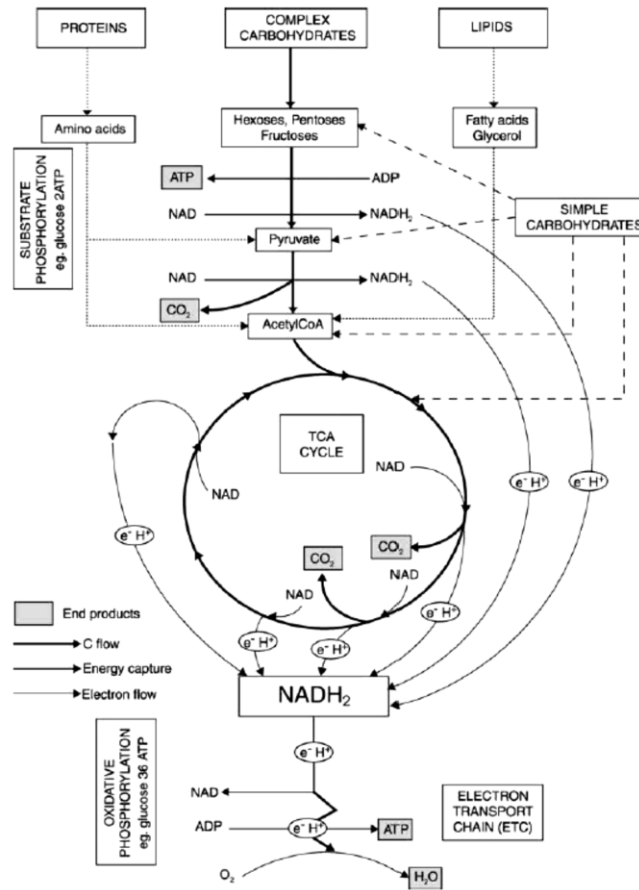


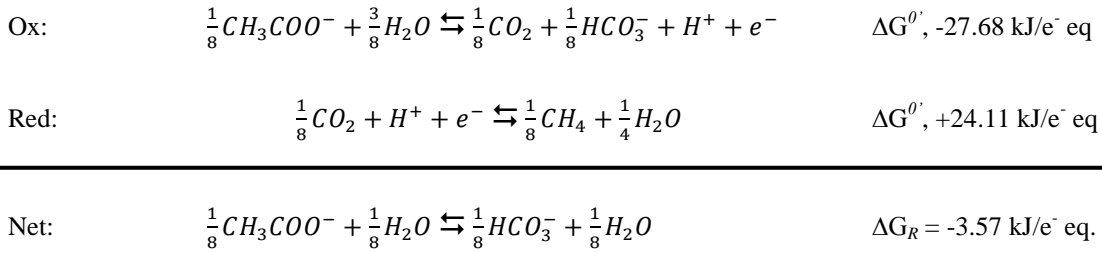
Figure 2-8 From Mara et al. (2003); Schematic representation of heterotrophic metabolism of organic matter. Pathways illustrate (1) carbon flow from organic matter to carbon dioxide; (2) electron flow from donor to acceptor; and (3) energy capture as ATP in substrate.

Using similar steps, the free energy release from coupling acetate oxidation to the formation of pyruvate ($\text{CH}_3\text{COCOO}^-$) is thus $81.2 \text{ kJ/e}^- \text{ eq}$ (ΔG_p). Substituting into equation 2-1, the value of ΔG_s is calculated to be $+44.94 \text{ kJ/e}^- \text{ eq}$ (constant value when acetate serves as electron donor). Further substitution into equation 2-3X yields a f_e/f_s ratio of 0.707. Using the relationship in equation 2-2, values of f_e and f_s for aerobic respiration on acetate are thus calculated to be 0.41 and 0.59, respectively. That is, 59% of the electrons liberated through substrate oxidation will go to the synthesis of new cells, and the remaining **41% of electron equivalents will go to energy yielding**

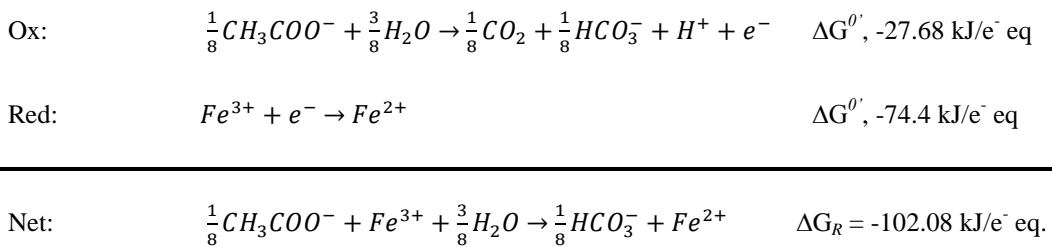
processes (i.e. oxygen reduction). Assuming a COD value for cell tissue of 1.42 g COD per g VSS (VSS as proxy for biomass), **the cell yield for the process (Y) can also be calculated as 0.42 g VSS/g COD (Metcalf, Eddy et al. 2010).**

Experimentally measured values of cell yield for activated sludge are typically within close range of this theoretical value (i.e. Y_{emp} , 0.42 – 0.45 g VSS/g COD) (Mara and Horan 2003, Tchobanoglous, Burton et al. 2003, Metcalf, Eddy et al. 2010).

In the case of anaerobic respiration, we can use similar stoichiometric relationships to assess the electron yields and associated theoretical energy gains from anaerobic digestion and bioelectric technology. The redox reactions associated with **acetoclastic methanogenesis** are as follows:



Similarly, for acetate oxidation coupled to **iron reduction** (i.e. anode respiration by metal-reducing organisms):



Again using acetate as the electron donor and ammonium as the nitrogen source, we calculate a ΔG_s of 44.94 kJ/e⁻ eq for both processes. Following from the steps outlined above and equations 2-1 through 2-4, we can determine cell yield coefficients, f_e , and f_s for each of the potential waste-to-energy processes, which are summarized in Table 2-8.

Table 2-8 Calculated bacterial cellular yields for Purported Waste-to-Energy Processes

Associated Wastewater Process	Growth Condition	Electron Donor/ Acceptor	ΔG_R (kJ/mol)	Biomass Yield (g VSS/ g COD)	f_e	f_s	$f_e(\Delta G_R)$ (kJ/mol)
Activated Sludge	Aerobic	Acetate/ Oxygen	-846.6	0.420	0.410	0.590	-347.1
Anaerobic Digestion	Anaerobic	Acetate/ CO ₂	-28.56	0.032	0.954	0.046	-27.2
Anode Respiration	Anaerobic	Acetate/ Fe ³⁺	-816.6	0.406	0.423	0.577	-345.4

As can be seen in Table 2-8 there are significant differences between the theoretical energy released from substrate oxidation (ΔG_R) and the fraction of oxidizable substrate (f_e) that is available for energy production. In the case of methanogenesis, significantly less free energy is available through acetate oxidation/CO₂ reduction; however 95.4% of substrate-available electrons will be oxidized for an energetic benefit (i.e. CH₄ production).

Importantly however, calculation of Y and f_e are likely influenced by differences in the energetics of fixed-film or attached growth (e.g., the MFC), versus suspended growth (e.g., AS or AD) process. There have been many reports of Coulombic efficiencies exceeding 42%, especially in MFCs fed with refined substrates

(e.g., acetate). One hypothesis is that the energetic requirements of the anodic biofilm decline as the biofilm matures, until a steady-state condition is reached, where cells can turn over acetate to produce current without any energetic yield. Though this is speculative, a comparison of bio-energetic calculations with empirical data may serve to better understand and predict the theoretical energy that can be extracted from digestion and/or bioelectrochemical technology.

Chapter 3 : Hybrid Anaerobic Digester-Microbial Fuel Cell for Energy & Nutrient Capture from Latrine Sludge

3.1 Introduction

Critical needs exist for effective human waste treatment and low-cost sources of energy across the developing world (Legros, Havet et al. 2009, UNEP and Corcoran 2010). Consequently, a large space exists for innovative technologies that exploit the large reserves of biochemical energy and nutrients present in human excreta for energy generation (e.g., 4.5 g total N per L urine; 1 kWh per kg carbohydrate) (Jonsson, Stinzinger et al. 2004, Pham, Rabaey et al. 2006). The production of value-added products from waste treatment (e.g. decentralized energy, high-value fertilizers) could serve as a means for incentivizing cultural acceptance of new technology, as well as maintenance and upkeep of sanitation facilities. The study reported here, explores integration of two waste-to-energy technologies—low-cost anaerobic digestion (AD) and the microbial fuel cell (MFC)—as primary and secondary unit processes for high-strength wastewaters, such as pit latrine sludge or septage.

Owing to the negligible volumes of gray and storm water, waste streams resulting from decentralized sanitation are typically classified as high-strength, and contain large stores of biochemical energy (as measured by chemical oxygen demand, COD, or biological oxygen demand, BOD), as well as high nutrient and pathogen loads (e.g. >10g COD/L, >10g TS/L, >1 g NH₃-N/L, and 10⁴ – 10⁹ fecal coliforms per 100 mL) (Montangero and Strauss 2002, Jimenez, Mara et al. 2010). Table 3-1

summarizes the composition of different high-strength waste streams common to decentralized sanitation. In addition to the high organic loads, the climatic conditions of many developing countries (i.e. 15-30°C) are beneficial to anaerobic methods of waste treatment, like anaerobic digestion (AD). In tropical or sub-tropical climates, mesophilic conditions can be maintained without heating or insulation of digesters, yielding more favorable economic and energy returns for the systems (Lansing, Viquez et al. 2008, Klavon, Lansing et al. 2013). Un-mechanized, low-cost digester designs (e.g. 50 gal drums, tubular polyethylene bags), in particular, have demonstrated success in a number of countries (e.g. Costa Rica, Mexico, China) (Bhat, Chanakya et al. 2001, Chaggu, Sanders et al. 2007, Lansing, Botero et al. 2008, Buysman 2009, Arthur, Baidoo et al. 2011, Rajendran, Aslanzadeh et al. 2012). They are capable of treating high organic loads (e.g. 3.2 – 7.2 kg VS/m³/day) at moderate hydraulic retention times (i.e. 20-40 d HRT), and produce methane gas at rates of $\approx 0.2 - 0.35 \text{ m}^3 \text{ CH}_4/\text{kg COD}$, making them competitive with more capital-intensive digester designs (e.g. heated and continuously stirred tank reactors, CSTRs) (Marchaim 1992, Lansing, Viquez et al. 2008, Klavon, Lansing et al. 2013). A second, value-added product of digestion is the liquid digester effluent (i.e. the digestate), which contains high levels of soluble nitrogen, primarily as NH₃, and phosphorus, and can be land applied as fertilizer (Schievano, D'Imporzano et al. 2011). Importantly though, practical limitations on reactor volume, temperature, and operating conditions mean that a fraction of the material will not be fully oxidized, leading to incomplete oxidation of organic matter and an effluent stream with relatively poor quality (e.g. > 200 mg BOD/L) (Marchaim 1992, Lansing, Viquez et al. 2008). This often

necessitates secondary processes (e.g. treatment wetlands) that increase costs without adding value or resource-recovery (Mowat, Singh et al. 1986).

The second waste-to-energy process evaluated in this study is the MFC—an emerging technology that couples microbial degradation of organic matter (e.g. acetate) with direct production of electricity in a biologically-based fuel cell (Rabaey and Verstraete 2005, Logan, Hamelers et al. 2006). When fed with complex waste streams like wastewater, the metabolic pathways most commonly used to describe the conversion of organic matter to current are as follows—a consortia of hydrolytic and fermentative organisms metabolize glucose and other carbohydrates, producing intermediates (e.g. organic acids, primarily as acetate, lactate) which can subsequently be utilized as the electron donor for anode respiring bacteria (ARB), which colonize the anode surface and are contained within the anodic half-cell (Parameswaran, Torres et al. 2009). Dissimilatory metal reducing bacteria (DMRB) such as *Geobacter sulfurreducens*, *Shewanella putrefaciens*, are commonly identified in ARB biofilms, where they serve as microbial catalysts to couple organic acid oxidation to the reduction of a non-consumed electrode. This process is analogous to Fe(III) reduction by DMRB in sediments (Lovely 1993). The anodic process is coupled with the reduction of an oxidant (e.g. oxygen) at the cathode, contained within the cathodic half-cell, where electrical current/power is proportional to the rate at which electrons can be transported from anode to cathode using an external circuit.

The anodic reaction of MFCs fed with simple substrates (e.g. acetate) is relatively well-understood, with reaction rates (expressed as current density) reaching an apparent limit of 10 Am^{-2} electrode surface area catalyzed by pure culture

organisms (e.g. *G. sulfurreducens*) or mixed, environmental biofilms (Torres, Krajmalnik-Brown et al. 2009, Strycharz, Malanoski et al. 2011). This upper limit for current equates to a theoretical COD removal rate (R_{COD}) of 71.6 g ThCOD/m²/d, where:

$$R_{COD} = \frac{I M ThCOD}{F n A} \left(\frac{86,400 \text{ s}}{d} \right)$$

Where I is current (C/s); M is the molecular weight of the oxidizable substrate (g/mol); ThCOD is the theoretical COD of the substrate which in the case of acetate is 1.067 g O₂/g acetate (i.e. 2 mol O₂ consumed per mol acetate oxidize and incorporating a molar weight ratio); F is the Faraday constant (96,487 C mol⁻¹ electrons); n is the number of electrons released per molecule of substrate oxidized (n = 8 in the case of acetate); and A is the geometric surface area of the anode (m²).

Importantly, this calculation assumes that the electrode surface is relatively smooth and that the entire surface area is electrochemically active (i.e., portions of the anode are not obstructed to mass transport of reactants or products). For MFCs utilizing 3-dimensional high surface area anodes with ill-defined surfaces such as graphite granules or carbon fiber brushes, the use of volumetric current density (A/m³) based on volume of the anodic half-cell is likely to yield a more accurate, and higher, predictor of volumetric COD removal (g COD/m³/d).

Wastewater-fed MFCs have proven efficient at generating electrical power from low- to medium-strength influents (\approx 50-150 W/m³ of reactor volume), particularly when fed with acetate buffered media as a synthetic waste stream (Logan

2008). When fed with high-strength wastes however, MFCs exhibit dramatic decreases in Coulombic efficiency (the fraction of released electrons that results in electricity production) and relationships between organic load and resulting current and power that do not agree with known dilution rates (Min, Kim et al. 2005, Feng, Wang et al. 2008). Additionally, many existing MFC reactors are ill-optimized for mass transport of substrate to the anode, which exacerbates the predominance of fermentative and methanogenic organisms in biological wastes and results in conversion inefficiencies and lost resource recovery (Min, Kim et al. 2005, Pham, Rabaey et al. 2006, Foley, Rozendal et al. 2010, Weld and Singh 2011).

The work reported here evaluates the possibility for enhanced treatment and energy recovery by using AD and MFC as primary and secondary waste treatment processes, respectively, for high-strength wastewater. Based on the above reports, it was hypothesized that the use of the partially degraded digester effluent (the ‘digestate’) may serve as an optimized substrate for the MFC, in that digestate is depleted of fermentable resources and potentially higher in organic acid concentrations. Additionally, a hybrid AD-MFC system would enable additional resource recovery and treatment capacity of high strength wastewaters. Specific objectives of research were as follows:

1. To design and fabricate (10) batch, anaerobic reactors for digestion, and (3) dual-chamber, flow-through MFC reactors
2. To quantify baseline power generation and electrochemical performance from the prototypes

3. To evaluate the quantity and quality of nutrients in the effluent from AD & MFC, as well as solids, COD, and coliform reductions during treatment
4. To evaluate the effect of digester retention time (reaction times: 0-, 7-, 13-, and 21-d) on AD-MFC performance, with the goal of balancing energy recovery and treatment efficiency.

Results indicate an inverse logarithmic relationship between digester retention time and subsequent MFC current production, i.e. maximal MFC current production is achieved with undigested waste, and an inverse linear relationship between digester retention time and subsequent COD/VS removal in MFCs. Digestion produced biogas as the energy source, at a rate equivalent to 29.6 kJ per m³ wastewater treated (8.2 Wh/m³). The MFC produced direct electrical power as the energy source, at a rate equivalent to 2.1 kJ per m³ wastewater treated (0.58 Wh/m³). On the basis of COD, AD generated 9,110 kJ per kg COD removed (2,530 Wh/kg COD); MFC generated 0.18 kJ per kg COD removed (0.05 Wh/kg COD). Cathodic limitations ultimately constrained power/energy production by the MFC, presumably due to mass transport of oxygen reduction intermediates. With an improved MFC cathode, a five-fold increase in power (from ~10 W/m³ to ~50 W/m³) could be realized (based on 130 A/m³ anodic current densities observed under potentiostated configurations; and where V_{cell} , 0.4V coincides with P_{max}). This would translate into an estimated energy yield of 15 kJ per m³ wastewater treated in a MFC.

3.2 Materials & Methods

3.2.1 Digester Substrate & Inoculum Sampling

Grab sampling was performed at a number of points along the solids treatment line of a nearby wastewater treatment plant to identify a proxy substrate for high-strength wastewater (Blue Plains Facility, Washington, D.C.). Samples were analyzed on the basis of key environmental characteristics, as outlined in Table 3-1, to provide comparability with latrine sludge. All samples were preserved at 4°C and analyzed within 24 h for COD, total solids (TS), volatile solids (VS), pH, and alkalinity, as described in Section 3.2.6. Approximately 100 mL of each sample was preserved separately for nutrient analysis, according to the methods outlined in Section 3.2.6.

Table 3-1 Environmental Composition of Proxy Substrate and Inoculum Sources

Sample Name	COD (mg/L)	Total Solids (mg/L, %)	Volatile Solids (mg/L, %)	NH4-N (mg/L)	TN (mg/L)	COD/ TN	TP (mg/L)
Septage ^{ab}	25,000 – 40,000	10,000 – 25,000		< 1,000	200-700		100- 300
Latrine Sludge ^b	20,000- 50,000	> 3.5%		2,000- 5,000	NA		
WASA Gravity Thickened Solids	50,700	36,600 (3.6%)	30,000 (82.0%)		1,163.4	43.55	21.97
Alexandria WW Digestate		43,400 (4.44%)	34,300 (78.96%)				

^a UNEP (1998); ^b EAWAG (2002)

For digestion experiments, approximately 7 L and 3 L of primary and gravity settled solids, respectively, were collected from the Blue Plains facility and used as the digestion substrate. The same sampling points provided the inoculum and substrate for

MFC experiments performed on '0-d' digestate. The methanogenic inoculum for digestion was collected from the effluent of a mesophilic, gas-mixed anaerobic digester, being maintained on domestic wastewater solids at a second, nearby treatment plant (V_l , 1.5 MG) (Alexandria Sanitation Authority, Alexandria, VA). Both digestion substrate and inoculum were collected and stored without headspace for ≤ 5 h before being added to bench digesters.

Concurrent with anaerobic digestion, a sub-sample of the inoculum was tested for specific methanogenic activity (SMA), following the methods of (Sørensen and Ahring 1993). Activity on acetate (1g/L $\text{NaCH}_3\text{COO}^-$) and glucose (1 g/L $\text{C}_6\text{H}_{12}\text{O}_6$) were, respectively, 0.019 g $\text{COD-CH}_4/\text{g VSS/d}$ and 0.023 $\text{COD-CH}_4/\text{g VSS/d}$ after 72 h (see methods and results in Appendix A).

3.2.2 AD-MFC Reactor Designs & Fabrication

Digesters

Batch anaerobic reactors were designed to mimic low-cost digester designs that utilize 55 gal drums and can be placed within a latrine superstructure. This design does not require a flushing mechanism, and thus simplifies waste conveyance. Ten batch digesters were constructed from 3 in. clear PVC tubing, pressure test caps, and mating flanges, and were fitted with liquid and gas sampling ports using threaded or barbed adaptors, flexible tubing, and butyl rubber septa. The linked AD-MFC system is illustrated in Figure 3-1, and photographs of the assembled reactors are in Figure 3-2.

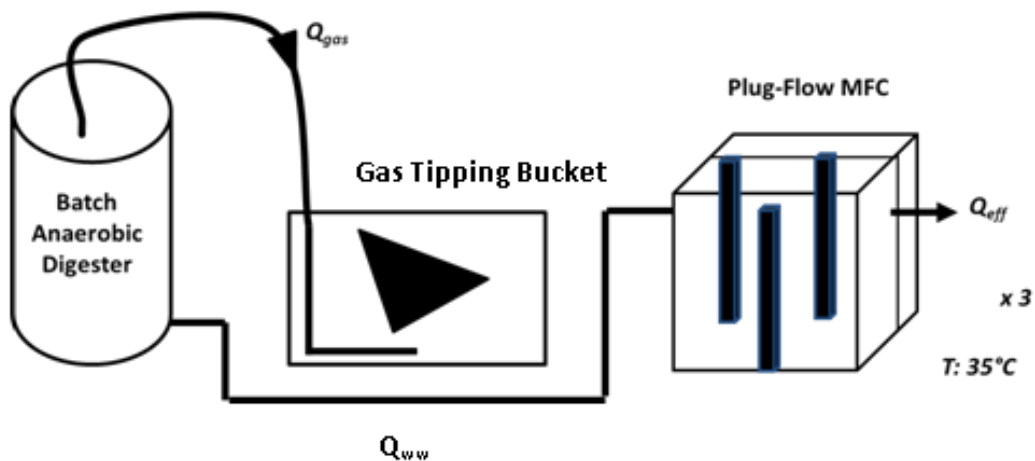


Figure 3-1 Cartoon diagram of batch anaerobic digester ($V: 1.5L$; $OD: 3\text{ in.}$) linked to gas tipping bucket to monitor biogas production, and dual-chamber, continuous flow Microbial Fuel Cell ($V_{an}=V_{cath}=100\text{ mL}$).

The empty volume of each digester was 1.5 L. The headspace of each digester was linked via flexible tubing to a gas flow meter, which recorded real-time gas production rates using a tipping bucket mechanism and data logger. A reed switch affixed to the outside of each flow meter was triggered by a magnet positioned at the apex of the gas collection volume. Each time the meter ‘tipped’, the reed switch was sent into ‘high’ position, which was captured by a microcontroller in the data logger, and a continuous recording of biogas production was captured from each reactor.

MFCs

Six dual-chamber MFC reactors were designed and machined in-house using a CNC milling machine (Haas Mini Mill), using stock from Plexiglas and graphite block (G10 grade; Mersen Graphite). Criteria of the designed was to (1) minimize membrane losses, i.e. spacing between the anode and cathode; (2) maximize the ratio of cell volume to exposed electrode surface area, (3) minimize lateral resistance across the

electrode, and (4) maintain the reference electrode in the anodic chamber to minimize solution/membrane resistance. See Appendix A for design diagrams and milling specifications. The reactors, displayed in Figure 3-2, achieve plug-flow conditions (10:1 L:W, 1:1.5 W:D), mimicking the large-scale, baffled anaerobic reactors that achieve high levels of treatment efficiency with minimum volume in wastewater unit operations (Barber and Stuckey 1999). These reactors also mimic the serpentine design of abiological, PEM or hydrogen, fuel cells to minimize electrochemical and mass transport losses (Pozio, Giorgi et al. 2002, Kim, Hyun et al. 2009).

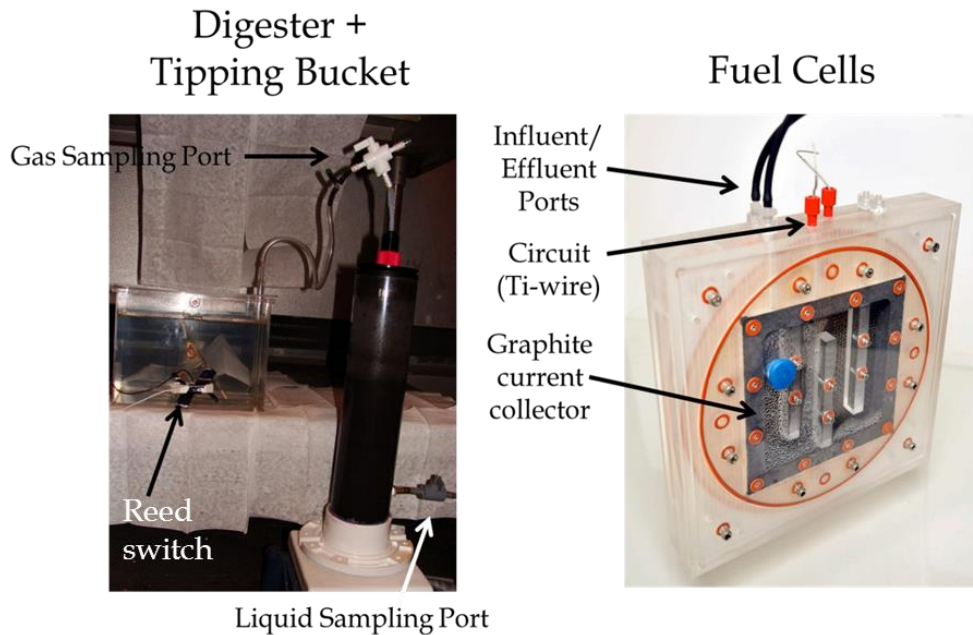


Figure 3-2 Photos of lab-scale AD-MFC reactors used to evaluate treatment and energy production from latrine sludge

Importantly, a baffled MFC reactor has a number of practical and theoretical benefits for high-strength wastewater treatment, including: (1) scalability; (2) constructible with locally-sourced materials (e.g. concrete or stone masonry); (3) minimization of stagnant areas; (4) increasing treatment efficiency by maximizing

exposure to the anode and anodic bacteria; and (5) the option of a secondary treatment process (e.g. denitrification) at the cathode reaction.

Anodic and cathodic volumes were 101 mL and 202 mL, respectively, and exposed anode geometric surface area was 12.80 cm x 12.80 cm ($A_{an} = 163.88 \text{ cm}^2$) for each. Untreated carbon cloth (CC6, Fuel Cell Earth Mfg.) was used as anode and cathode material. Approximately 100 mL of graphite granules (Grade 4012; Asbury Graphite; 0.935 cm diam.) were also added to the cathode chamber to increase surface area and reduce cathode overpotential. The hydraulic retention time (HRT) of the MFC was defined as:

$$HRT = \frac{V}{Q}$$

Where V is volume of the anodic chamber (0.1 L), and Q is the flow rate of wastewater to the anode chamber (L/min).

Graphite frame (Mersen Graphite; G10 grade) and titanium wires were used as current collectors for the external circuit at both electrodes, using press-fit connection between nylon screws, Ti-wire and graphite. Electrical resistance of the graphite-titanium connection was checked with a high input impedance handheld multimeter (Fluke 179), and found to be less than 5 Ω for all electrodes. To minimize electrode spacing and the associated ohmic losses, electrodes were physically compressed on either side of an anion exchange membrane (AMI-2000; Ultrex Corp.) that separated anodic and cathodic chambers and ensured a redox/oxygen gradient. Removal of residual organic matter and metals from graphite was achieved via 24-hr soaks in 1M NaOH and 1 M HCl, respectively, followed by neutralization in DIW. A Ag/AgCl, 3M

KCl reference electrode (BioAnalytical Systems, Inc.) that was mounted in the anodic half to enable application of a defined potential to the anode in a 3-electrode configuration with the cathode serving as the counter electrode.

3.2.3 Digester Loading & Operation

Biochemical methane potential (BMP) assays were conducted using the undigested primary and gravity settled solids as substrate, and were performed on three different occasions, referred to as **BMP2** (January 2012), **BMP3** (April 2012), and **BMP4** (December 2012). Experiments were performed following the methods of (Owen, Stuckey et al. 1979) with the following modifications: nine of the digesters (labeled as AD1-9 in figures) were batch loaded with inoculum and substrate to achieve an inoculum-to-substrate ratio of 1 g VS inoculum : 1 g VS substrate, allowing for 20% (v/v) headspace, resulting in an aqueous volume of 1.1 L. Primary and gravity settled solids were mixed to achieve a substrate organic load of approximately 20,000 mg COD/L and 20,000 mg VS/L. Owing to the heterogeneous nature of the samples, actual COD and VS loadings were highly variable, from 5,000-30,000 mg COD/L and 5,000-22,000 mg VS/L. One reactor (labeled as AD10 in figures) was loaded with inoculum only, and was used to quantify methane production from residual organics in the inoculum (deducted from AD1-9 biogas production). Sodium bicarbonate was added at a rate of 6g L NaHCO₃ per L to buffer organic acid production. Previous studies conducted by our lab group evaluated biogas production from actual latrine sludge during BMP assays with and without the addition of mineral media, and found only insignificant increases in biogas yield (3.9% increase; p =

0.58), suggesting that high solids wastewater contains sufficient micro- and macronutrients for diverse microbial growth (Lansing et al., 2013; manuscript in preparation). Thus, no microbial media was added to the batch assays performed here. All reactors were leak- and gas-tested prior to use. After addition of substrate and bicarbonate, reactors were de-gassed for 20 min under an 80/20 N₂/CO₂ mixture (AirGas; ultra-high purity) to remove residual oxygen prior to addition of methanogenic inoculum, and headspace was de-gassed for 10 min prior to sealing. Reactors were inverted several times before connection to gas flow meters and data loggers, and manually agitated 1-2 times per day thereafter.

For all BMP trials, all ten reactors and tipping buckets were started concurrently, and operated in an environmental chamber maintained at 30°C to represent mesophilic digestion. Biogas was sampled and composition was analyzed via GC on a daily basis for the first 5 days, and 2-3 times per week thereafter. For the first digestion experiment (BMP2), three reactors were terminated on day 7, and the remaining seven (including control) were terminated on day 47. For BMP3, four reactors were terminated on day 19, and the remaining six (including control) were terminated on day 26. For BMP4, triplicate digesters were terminated on day 6, day 13, and day 21; the control was also terminated on day 21. Data from BMPs 2, 3, and 4 were used to evaluate and confirm treatment efficacy by digesters. The effluent from BMP4 (referred to as BMP4 digestate) also served as the substrate for MFCs, to evaluate MFC energy and nutrient capture at three different digestion periods (6 d, 13 d, and 21 d HRTs).

3.2.4 MFC Electrochemical Analysis

All electrochemical analysis was performed using a Solartron 1470E multichannel potentiostat (Solartron analytical) and Multistat software program (Scribner Associates). The anodic biofilms were grown via chronoamperometry (i.e. 3-electrode configuration), whereby the anode (working electrode, WE) was maintained at a fixed potential of -0.200 V vs. Ag/AgCl, 3M KCl reference electrode (RE; ≈ 0 V vs. SHE) located in the anodic half-cell and the cathode serving as the counter electrode/auxiliary electrode (CE). By maintaining the anode at -0.200 V vs. Ag/AgCl, we aim to enrich for species capable of highly efficient anode reduction at relatively low thermodynamic potentials (e.g. *Geobacter spp.*) (Torres, Krajmalnik-Brown et al. 2009, Marsili, Sun et al. 2010). Controlling the anode potential during biofilm growth also ensures that any overpotential that develops at the cathode will not create thermodynamic constraints on anode respiration (i.e. reducing E_{an} such that it is not an energetically favorable electron acceptor). In turn, this maximizes current production and organic matter oxidation.

Slow-scan cyclic voltammetry (CV) of the anodes was performed at (1) the start of the experiment; (2) the onset of catalytic activity; and (3) maximum current production (i_{max}). CVs were performed in-situ under the same three-electrode configuration, and scan parameters were as follows: the initial cathodic scan ($v < 0$) swept the anode potential from $E_i = -0.800$ V vs. Ag/AgCl to $E_f = +0.300$ V vs Ag/AgCl, and was followed immediately by a anodic scan from +0.300 V vs. Ag/AgCl to -0.800 V vs. Ag/AgCl; all scans were performed at rates (v) of 1, 2, and 5 mV/sec. In preliminary experiments, it was determined that voltammetric scan rates $>$

1 mV/s distorted limiting current and peak potentials. Thus, only 0.001 V/s scans are displayed in this report.

Once a stable, maximum current was achieved under potentiostated conditions (attributed to a fully grown anodic biofilm), the MFCs were switched to two-electrode configuration by connecting the potentiostat's reference and counter/auxiliary electrode leads to the cathode (i.e. the reference is not used), and were given 24-48 hr to reach a stable open circuit voltage (OCV). Polarization was then performed, whereby the cell voltage (V_{cell}) was swept from OCV to 0.005V at a rate of 0.1 mV/s. Point measurements of anode and cathode potentials vs. the reference electrode during polarization were also recorded with a high input impedance multimeter (Fluke 179) to separate electrode losses. Following polarization, power output was characterized under two-electrode configuration, where the cathode was poised 0.100 - 0.350 V positive of the anode, such that cell voltage was fixed to achieve maximum power production. Power was calculated via Ohm's law (i.e. $P = iV$), and all current and power measurements were normalized by anode geometric surface area (163.88 cm²) and/or anodic volume (101 mL). All experiments were conducted, at a minimum, in triplicate, and statistical analysis on resulting current/power densities were conducted using the Student's t-test at $\alpha > 0.05\%$ and $t_{crit}: 2.552$.

3.2.5 MFC Loading & Operation

Available protocols for inoculation and enrichment of wastewater-fed MFCs are relatively non-standardized, particularly for the optimization of MFCs with actual (vs. synthetic acetate- or glucose-fed) waste streams. Thus, we propose the following methodology, modified from established inoculation and electrochemical

characterization procedures for pure culture MFCs (Richter, Nevin et al. 2009, Strycharz, Malanoski et al. 2011). This protocol minimizes inhibitory effects from: (1) mass transport limitations of a high-solids substrate; (2) substrate limitations of batch-fed MFC; and (3) cathodic overpotentials at neutral pH that limit treatment efficiencies and current/power production. This method additionally enables a clear evaluation of the anodic (i.e. treatment) capacity of a wastewater-fed MFC and provides an upper limit on what treatment and current can be achieved in an optimized fuel cell configuration.

Undigested wastewater solids (mixtures primary and secondary settled solids to achieve ≈ 10 g VS/L), that had been sampled and maintained in headspace-free conditions for ≤ 5 h, were initially batch fed to the anode chamber of triplicate MFCs to serve as both inoculum and substrate. Under a three-electrode configuration (E_{an} - 0.200V vs. Ag/AgCl), flow was turned off until the onset of catalytic activity (i.e. current production) was observed. At which point, the MFCs were switched to a low flow rate using a peristaltic pump (Fisher FH100X) on a timer interval (2 min 'on', 58 min 'off'), resulting in an effective flow rate (Q_{eff}) of **0.46 - 0.66 mL/min (HRT of 2.8 - 3.6 h)**, where variations in sludge viscosity created slight differences in flow rate.

Continuous flow of the wastewater continuously replenished organic matter to ARB biofilm, and minimized stagnation and solids settling. During biofilm growth, the same mixture of solids served as the substrate, except that pH was maintained at 6.5, and solids were coarse filtered with two layers of cheesecloth to eliminate tubing clogs. No attempts were made thereafter to control for oxygen levels in the sludge. Flow of the undigested solids was maintained until maximum, steady-state current was

achieved. At which point, treatment efficiencies were characterized by sampling from the influent and effluent lines of each of the reactors a minimum of four times. MFCs were subsequently switched to a recycled flow at a flow rate of 10-20 mL/min (HRT: 5-10 min) for ≥ 3 d to quantify trade-offs in current production vs. treatment efficiencies with a decreased retention time.

After characterization with undigested waste, MFCs were then fed with 5, 10, or 20 d digestate to quantify maximal current, power, and treatment with reduced digestion periods. Similar loading and operation was followed, except that treatment and steady-state current were evaluated under recycled flow (Q: 20 mL/min; HRT: 5 min) to minimize substrate limitations in the MFC. Each digestate was recycled for ≥ 10 d, until current dropped below 1 mA. In some cases, sodium acetate (10 mM) was later added to the wastewater reservoir to evaluate substrate limitations in the digestate. Before switching to a new digestate source, stable current was re-established with undigested solids, such that biofilm re-growth did not affect evaluation of current/power production from the different digestate materials.

3.2.6 Environmental & Microbiological Analyses

Aqueous Samples

Aqueous samples were collected and preserved for analysis at the following times: (1) during sampling of digestion substrate and inoculum; (2) pre- and post-digestion for each retention time; (3) pre- and post-MFC at HRTs between 5 min and 1.5 h and 5 d. For pH, Alkalinity, COD, TS, VS, TKN and fecal coliforms, aqueous samples were preserved at 4°C and analyzed within 7-d. For organic acids, NH₃-N,

and $\text{NO}_2+\text{NO}_3\text{-N}$, samples were acidified (5N H_2SO_4 , $\text{pH}<2$), centrifuged ($6,000 \times g$) for 20min, and supernatant was filtered to $<0.22 \mu\text{m}$ and stored at 4°C until analysis.

Samples were analyzed for solids (TS, VS), COD, and Alkalinity according to Standard Methods (APHA, AWWA et al. 2005). Nutrient concentrations were determined by continuous flow colorimetry using an autoanalyzer with autosampler (Bran & Luebbe TRAACS 2000). Analysis for $\text{NH}_3\text{-N}$, $\text{NO}_2+\text{NO}_3\text{-N}$, TKN, and TP was performed following EPA methods 350.1, 353.1, 351.2, and 365.4, respectively (O'Dell 1993, O'Dell 1993, O'Dell 1993). Aqueous samples collected for organic acids were injected onto a Varian 450 HPLC equipped with a Refractive Index Detector. The mobile phase was a 0.005 M sulfuric acid solution, and the column was a PL Hi-Plex H+ ion exchange column, at 65°C , with a flow rate of $0.6 \text{ mL}/\text{min}$. The injection volume was $40 \mu\text{L}$.

Total coliforms were quantified using the MPN-dilution method for detection of lactose fermenting organisms, modified for analysis of high solids wastewater samples as follows: 10^{-1} - 10^{-12} dilutions (v/v) of aqueous samples were incubated in tryptic soy broth (TSB) at 37°C for 24 h. One test tube was filled with TSB but was not inoculated and served as the control. An MPN calculator (USEPA MPN Calculator, v 2.0) was used to estimate total coliform densities as the no CFU/100 mL based on the number of tubes showing positive growth after inoculation. A sub-set of samples were also analyzed for fecal coliform density, where the same steps were followed, except that dilutions were incubated at 44°C , and $0.5 \mu\text{L}$ of each dilution was subsequently plated onto MacConkey agar, and again incubated at 44°C for 24 h. A UV light was used to check agar plates for colony growth.

Gas Samples

During digestion, biogas was sampled from ports in each reactor's gas line using a gas-tight syringe (Vici Corp.; 1 mL) and injected onto an HP7890 gas chromatograph (GC) for determination of methane content. The GC was equipped with a thermal conductivity detector (TCD) and an Agilent capillary column (19095P-Q04; 30 m x 530 μ m x 40 μ m). Inlet, oven, and detector temperatures were 250°C, 60°C, and 250°C, respectively, and helium served as the carrier gas.

3.3 Results & Discussion

3.3.1 Digestion—Treatment Efficiencies

Organic Matter & Solids

In all BMP trials, discernible and statistically significant ($p < 0.05$) removal of organic matter and solids was achieved through digestion, as measured by COD, VS, and TS reductions in wastewater samples before and after digestion. Reported treatment rates are conservative estimates for digestion, and do not account for the quantity of recalcitrant matter added with the methanogenic inoculum.

Average COD, TS, VS, and coliform concentrations are displayed as a function of batch digestion period during BMP Run 2 and Run 4 in Figure 3-3. A

summary of these values, as well as fecal coliforms, is provided for BMP 4 in Table 3-2, where the effluent from BMP 4 served as feed for all MFC experiments and was used to calculate cumulative removal rates from the combined AD-MFC system. From the initial COD loading of $16,700 \pm 1,780$ mg/L, digesters removed approximately 25% of COD after 6 d, 33% after 13 d, and 38% after 21 d. On a volumetric basis, this corresponds to removal rates of 0.720, 0.440, and 0.190 kg COD/m³/day at day 6, day 13, and day 21, respectively. VS removal followed a similar pattern, where the starting concentration ($10,010 \pm 787$ mg VS/L) was reduced by 11% by day 6, 24% by day 13, and 25% by day 21. On a volumetric basis, this corresponds to 0.186, 0.188, and 0.072 kg VS/m³/day removal rates at day 6, day 13, and day 21, respectively. Presumably, this reflects the initial, rapid breakdown of readily-degradable organics (e.g. glucose, organic acids), followed by slower hydrolytic and fermentative processes (Yadvika, Santosh et al. 2004).

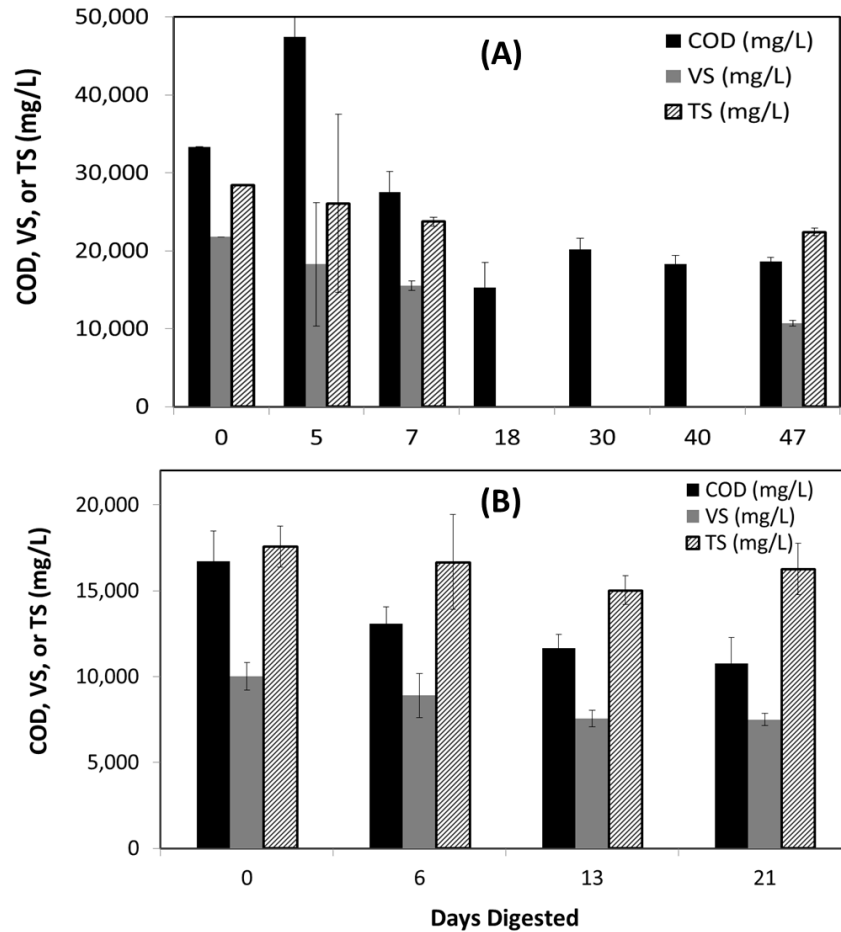


Figure 3-3 Average COD (in black), VS (in grey), and TS (hashed) during digestion of latrine solids during BMP2 (Figure A) and BMP4 (Figure B). Data points represent the average \pm standard deviation (mg/L COD, mg/L VS, or mg/L TS; n = 3-9).

TS removal rates were lower than COD or VS in all cases, where average TS removal during BMPs 2 and 4 was 21% and 7% at the end of digestion (47 d and 21 d, respectively). This corresponds to volumetric removal rates of 0.127 kg TS/m³/d (BMP2) and 0.040 kg TS/m³/d (BMP 4). Reduced TS removal is consistent with the understanding of TS as a measure of both organic solids (VS) as well as indigestible solids (e.g. silicates, clays, etc.); physical, rather than biological, treatment processes (e.g. sedimentation) are often more effective for TS removal from waste streams. In the case of BMP 4, starting TS concentrations (17,600 mg/L) were comprised of 57%

VS, but after 21 days of digestion, this fraction had reduced to 46%, which is consistent with the hypothesis that much of the inoculum and substrate was relatively resistant to batch digestion. Also consistent with this hypothesis, the reduction in COD within the inoculum-only (control) digester was statistically insignificant ($p > 0.05$) from Day 0 to Day 21 (BMP4), highlighting the low availability of biologically relevant substrate in the inoculum. If the quantity of recalcitrant matter associated with the inoculum is accounted for (e.g. g COD remaining after inoculum digestion), all digesters achieved 100% removal of COD and VS by Day 21.

The COD and VS removal rates obtained in this study are comparable to what has been observed in other lab-scale, batch digesters, but are lower than those reported by continuous-flow, full-scale digesters (e.g. 80-90% removal at $> 1 \text{ kg COD/m}^3/\text{day}$ loading)(Metcalf, Eddy et al. 2010). Reduced removal of organic pollutants (e.g. $< 50\%$ COD removal) is frequently reported in batch digestion or BMP literature (Rajan, Lin et al. 1989; Lin, Ma et al. 1999). This is commonly attributed to the addition of recalcitrant organic matter associated with the methanogenic inoculum. While an inoculum is necessary to ensure sufficient methanogenic activity (i.e. to provide kinetic enhancements) in batch loaded systems, it often contains a large fraction of indigestible organic matter that elevates COD concentrations but is not biologically relevant (Owen, Stuckey et al. 1979, Sørensen and Ahring 1993). In the current study, previously digested wastewater solids served as the inoculum, where waste-to-substrate ratios were approximately 1 g VS substrate/g VS inoculum. Converted on a mass basis, the inoculum thus represented 41 - 49% (w/w) of the

original COD added (e.g. $\approx 9,800$ mg COD_{inoc} of $\approx 19,100$ mg COD_{added}), and 42 – 55% (w/w) of the original VS (e.g. $\approx 6,300$ mg VS_{inoc} of $\approx 11,500$ mg VS_{added}).

Digestibility of the substrate was also assessed during the second BMP (BMP 3), as measured by the ratio of soluble to total COD (SCOD and TCOD, respectively). Average SCOD concentrations of inoculum and undigested wastewater were 470 mg SCOD/L and 1,730 mg/L, respectively, corresponding to SCOD/TCOD ratios of 1.85% and 2.95%, respectively. SCOD accounted for < 4% of all COD at all sampling points during BMP3. Thus, only a small fraction of COD existed as soluble, biologically relevant organic matter. From a starting concentration of 1,140 mg SCOD/L, digesters removed 83% of SCOD after 26 d, resulting in an effluent concentration of 500 mg/L (Figure 3-4). Digesters were thus able to remove much of the solubilized organic matter, supporting the hypothesis that overall treatment was hampered by the presence of recalcitrant matter.

Similar ratios of SCOD/TCOD in wastewater solids have been previously reported, and a large body of work has been amassed on the effect of various physio-chemical pre-treatment methods used to increase SCOD and to quantify its relationship to digestibility (Rajan, Lin et al. 1989, Lin, Ma et al. 1999, Amani, Nosrati et al. 2010). Similar to the results reported here, others have achieved < 50% COD removal during batch digestion of wastewater solids without pre-treatment of hydrolysis (Rajan, Lin et al. 1989, Lin, Ma et al. 1999, Elbeshbishy, Nakhla et al. 2012).

Similar BMP or batch AD studies have calculated removal rates that account for the quantity of recalcitrant matter associated with the inoculum (i.e. by subtracting

the mass of COD remaining after digestion of the control, inoculum-only, reactor), and have thus reported > 90% COD removal rates in batch-fed systems (Atayol and Sofuoğlu 2003). As demonstrated though, all complex waste streams, and certainly high-strength wastewater, will contain some fraction of recalcitrant organic matter (i.e. lignin, sediments, or silts), making 100% COD removal infeasible by a full-scale system at any practical retention time.

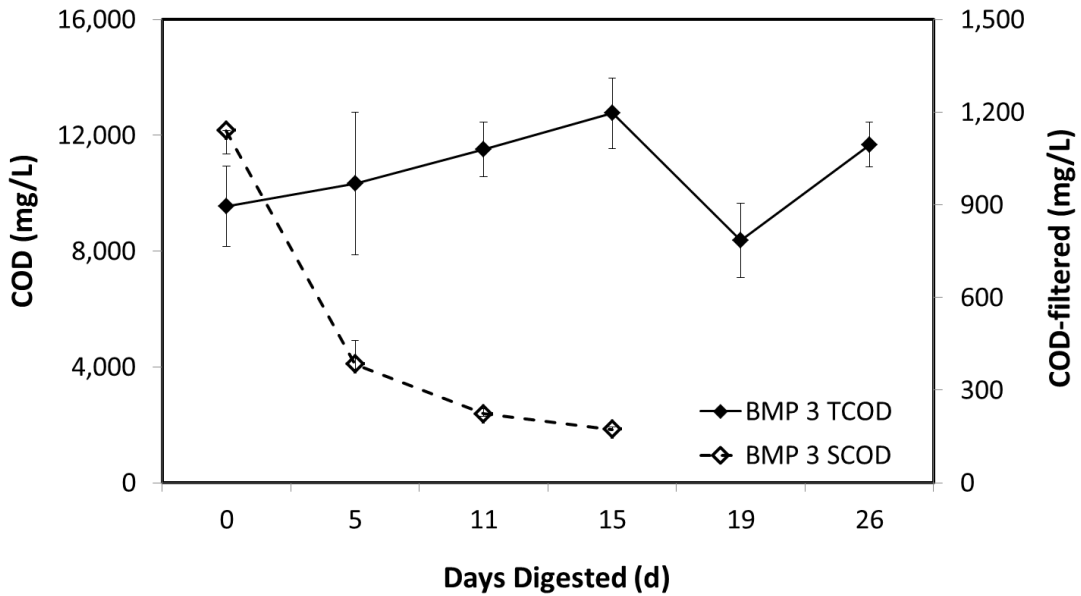


Figure 3-4 Average total COD (solid symbols) and SCOD (open symbols) during digestion of latrine solids during BMP3. Data points represent the Mean \pm SD (mg/L COD, n = 4-6)

Table 3-2 Environmental composition, treatment efficiencies, and treatment rates during digestion of latrine solids in BMP 4. Data is presented as mean \pm SD (n = 3).

	Days Digested			
	0 d	6 d	13 d	21 d
Avg COD (mg/L)	16,700 \pm 1,780	13,100 \pm 990	11,700 \pm 780	10,700 \pm 1,550

Avg COD Removal (%)	0.00%	24.6%	32.7%	38.0%
Avg COD Removal (kg/m³/day)	0.000	0.710	0.440	0.190
Avg TS (mg/L)	17,570 ± 1,200	16,700 ± 2,760	15,000 ± 840	16,300 ± 1,500
Avg TS Removal (%)	0.00%	5.14%	14.43%	7.42%
Avg TS Removal (kg/m³/day)	0.000	0.150	0.200	0.040
Avg VS (mg/L)	10,010 ± 790	8,900 ± 1,270	7,570 ± 470	7,500 ± 350
Avg VS Removal (%)	0.00%	11.1%	24.4%	25.1%
Avg VS Removal (kg/m³/day)	0.000	0.186	0.188	0.072
Total Coliform (MPN/100 mL)	9.52x10 ⁹ ± 5.52x10 ⁷	5.85x10 ⁶ ± 2.35x10 ⁶	1.07x10 ⁶ ± 7.17x10 ⁵	8.44 X 10 ³ ± 8.97 X 10 ³
Fecal Coliform (MPN/100 mL)	9.59x10 ⁴	4.8	0.36	17.8
Total Coliform Removal (%)	0	99.80 ± 0.200%	99.99 ± 0.002%	99.99 ± 0.020%
Fecal Coliform Removal (% , log)	0	99.995% (4-log)	>99.999% (5-log)	99.98% (3-log)

3.3.2 Organic Acid Transformations

One hypothesis of this study was that partial degradation of the waste by digestion would provide the MFCs with an influent that was relatively low in bulk organic load (i.e. kg COD/m³/d), but enriched with the simple organics (e.g. acetate) that are the primary carbon sources for ARB. In this way, the digester effluent would serve as a naturally optimized substrate for electricity generation by the MFC. To evaluate this, organic acid profiles were performed during BMP Run 2—at day 0, day 7, and day 47—and are summarized in Table 3-3. An initial enrichment for the lowest molecular weight organic acids was observed at day 7 of digestion, where the average acetate level in digestate samples was 9.4 ± 1.0 mM, representing a 10-fold increase, relative to their starting concentrations. Importantly, the acetate levels observed at day

7 are comparable to concentrations in optimized, synthetic media for anode respiring bacteria (ARB) like *G. sulfurreducens*, which yields high levels of current in MFCs (e.g. 5-7 A/m²) under the flow of media containing 10 mM acetate as the carbon source and electron donor. This result is also consistent with the higher current production that resulted from MFCs fed with 6 d, compared to 13 d or 21 d digestate from BMP4 (See Section 3.5.1 for description of current production from MFCs). Interestingly, while prolonged digestion did reduce the maximum electrical current achieved by the MFCs, it did not reduce treatment efficiencies (as described in Section 3.4.1), which suggests that power production from field MFCs could be manipulated without sacrificing treatment by augmenting with supplementary organics (e.g. vinegar, molasses).

Propionate concentrations increased from 2.7 to 36 mM (2,600 mg/L) after seven days of digestion. Levels exceeding 900 mg/L (12.5 mM) have previously been reported to cause significant inhibition of methanogenesis, contributing to VFA accumulation and pH declines (Wang, Zhang et al. 2009) however, no evidence of pH decline or prolonged propionate accumulation was found after 47 days in the batch digesters. Prolonged digestion (47 d) yielded more than 10-fold increases in butyrate levels, where concentrations increased from 0 mM at the start of digestion, to 1.7 mM by day 7, and 22 mM by day 47. There is no evidence to suggest that butyrate directly contributes to inhibition, but is often an indicator of stress on methanogens, where depletion of primary substrates (i.e. acetate, H₂) leads to population declines and the accumulation of less thermodynamically favorable substrates (Wang, Zhang et al. 2009). This is also consistent with accepted digestion models that describe a

syntrophic relationship between fermenters, acidogenic bacteria, and methanogens, where their respective growth rates, as well as kinetics of the associated reactions, dictate (Mosey 1983, Bernard, Hadj-Sadok et al. 2001).

Table 3-3. Organic acid profiles during BMP Run 2

	Influent Substrate	7d Digestate	47d Digestate	Toxicity Threshold
Final pH		7.67-7.97	7.67-7.97	<6.8; >7.2 ^a
Acetate (mM)	0.92	9.42 ± 1.01	0.54 ± 0.42	
Propionate (mM)	2.77	36.1 ± 0.59	1.79 ± 0.38	
Butyrate (mM)	0	1.71 ± 1.71	21.8 ± 1.69	
Valerate (mM)	0	0	0	
Total (mM)		47.2 (3,389 mg/L)	24.1 (2,083 mg/L)	>5,000 mg/L ^b

^a Chen, Cheng, & Creamer (2008); ^b Parkin & Owen (1986); Data is represented as Mean ± SE.

3.3.3 Nutrient Transformations

Unless indicated, nutrient transformations were calculated as the difference in concentrations pre- and post-digestion, where concentrations on the final day of digestion were used (day 47 for BMP2, day 26 for BMP3, and day 21 for BMP4). Solubilization of nitrogen was observed during each BMP run, as evidenced by 70 – 100% increases in ammonia-nitrogen (NH₃-N) pre- and post-digestion. The effluent of BMP2, BMP3, and BMP4 contained, respectively, 1,220 ± 39 mg/L NH₃-N, 820 ± 35 mg/L NH₃-N, and 600 ± 34 mg/L NH₃-N (n = 3-6). The increase in NH₃-N was accompanied by a decline (6.0 - 21%) in organic nitrogen (calculated as the difference in TKN and NH₃-N), as illustrated in Figure 3-5. The net increase in NH₃-N was

greater than the net decrease in Org-N—in BMP2, NH₃-N levels increased by 508 mg/L, while Org-N declined by 215 mg/L; in BMP3, NH₃-N levels increased by 402 mg/L, while Org-N declined by 188 mg/L. These transformations support the use of digester effluent (digestate) as a high-value, nutritive fertilizer, with high levels of soluble NH₃-N and a reduced fraction of Org-N.

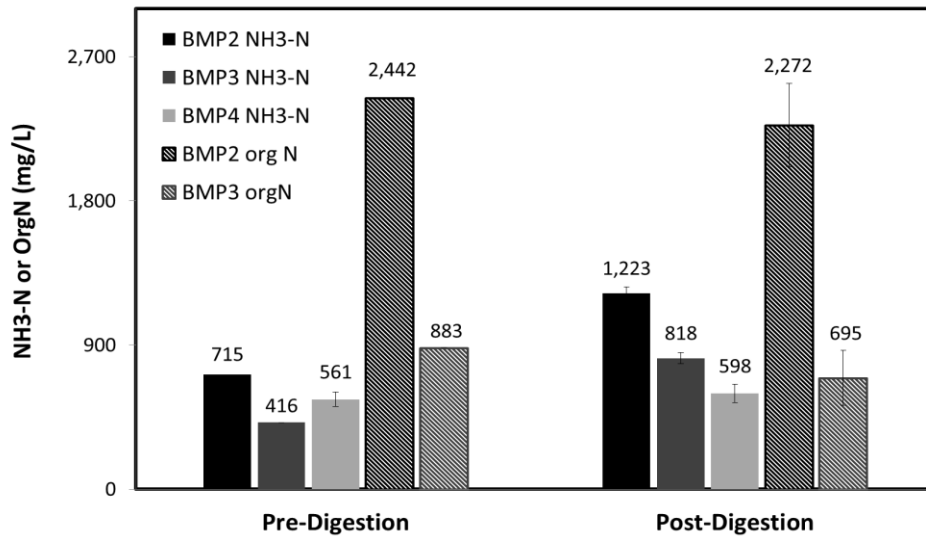


Figure 3-5 Profiles of NH₃-N and Org-N concentrations in wastewater samples before and after digestion during BMPs 2, 3, and 4. Data is presented as mean± SD (mg/L NH₃-N or mg/L Org-N)

Eight of nine digesters during the initial BMP trial (BMP2) yielded effluent ammonia concentrations that neared inhibitory levels for methanogenic organisms (>1,200 mg/L NH₃-N). The slightly alkaline conditions of the digestate (7.67-7.97 pH) would exacerbate any ammonia toxicity by yielding a higher ratio of free vs. combined ammonia (Hansen, Angelidaki et al. 1998). While only one of the three digestion trials (BMP Run 2) exceeded 1,000 mg/L in the effluent, the possibility of ammonia inhibition should be considered for any scale-up efforts, where urine loads

from undiluted human waste will affect C:N ratios and may require a secondary carbon source (e.g. food scraps, sawdust) and/or urine diversion efforts.

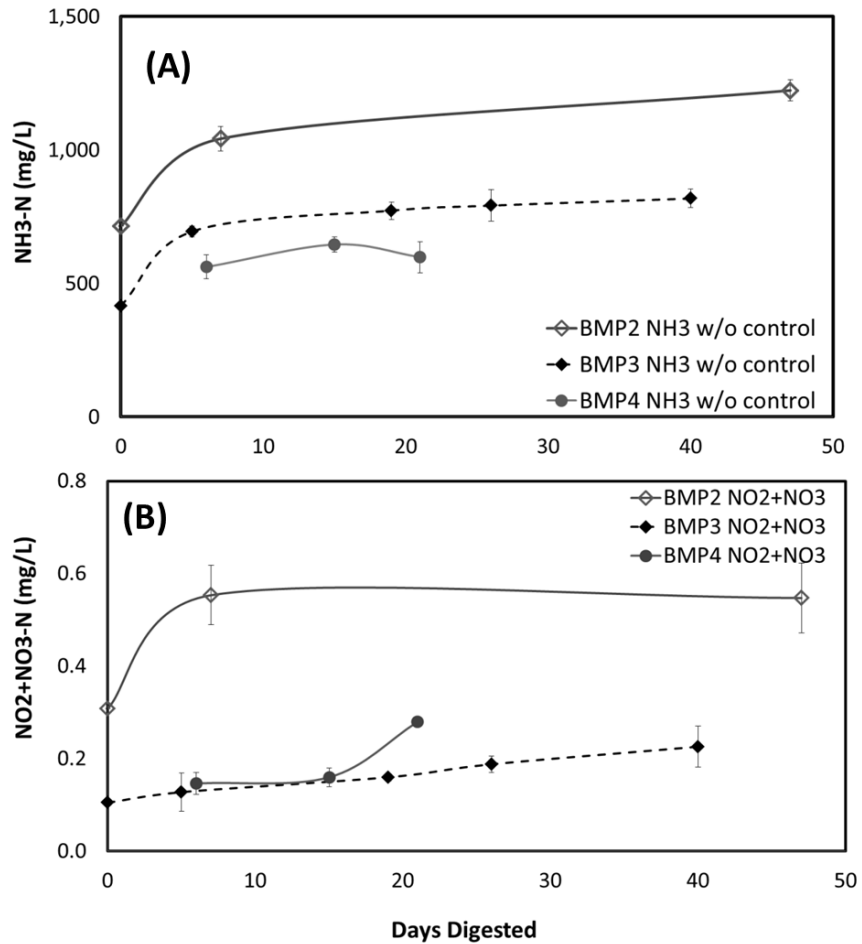


Figure 3-6 NH3-N and NO2+NO3-N concentrations during digestion. Data is presented as mean ± SD (mg/L NH3-N or mg/L NO2+NO3-N)

Nitrate-nitrite (NO₂+NO₃-N) levels in wastewater samples remained near detection limits (< 1 mg/L) and contributed minimally to the overall nutrient profile at all digestion periods (Figure 3-6). Phosphorus (TP) concentrations were also minimally affected by digestion, and averaged 463 mg/L after digestion. The digested

sludge contained, on average, 0.40 mg/L $\text{NO}_2^- + \text{NO}_3^- - \text{N}$; 1,040 mg/L $\text{NH}_3 - \text{N}$; 1,890 mg/L TKN; and 463 mg/L TP. If land applied as a fertilizer, this represents an N:P ratio of approximately 4:1.

3.3.4 Coliform Removal

Coliform analysis was carried out on wastewater samples digested for 0, 6, 13, and 21 d during BMP Run 4. For all digestion periods, a minimum 2-log removal (>99%) of total coliforms, and greater than 3-log removal (> 99.9%) of fecal coliforms was achieved. Total coliform loads were reduced from $9.5 \times 10^9 \pm 5.5 \times 10^7$ MPN/mL (influent) to $8.4 \times 10^3 \pm 8.9 \times 10^3$ MPN/mL (effluent) after 21 days digestion (BMP4). Fecal coliforms were similarly reduced—from 9.6×10^4 MPN/mL (influent) to 17.8 MPN/mL (effluent). Although initial total coliform density in the control (inoculum-only) digester was lower than the other reactors (2.5×10^5 MPN/mL), removal rates from the control were also lower (92%, 1-log removal), and digester effluent contained $> 1 \times 10^4$ MPN/mL after digestion. Normalized on the basis of effluent TS levels, the digested wastewater solids contained 1,090 MPN per g TS after 21 days of digestion. US federal regulations require $< 1,000$ MPN per g TS for status as ‘Class A’ Biosolids, and $< 2,000,000$ MPN per g TS for ‘Class B’ Biosolids (40 CFR Part 503 Regs), where class A biosolids are considered inert and can be used in bulk by the general public without restrictions on crop type, land access or harvesting methods; Class B biosolids are also suitable for land application but are restricted on the basis of crop type and harvesting methods, and site access. These results indicate that the product of mesophilic, batch digestion of septage or latrine solids would likely

produce a product comparable to Class A biosolids, with minimal public health or environmental risk if applied as a fertilizer for crops.

3.3.5 Digestion—Energy Production

Biogas and methane production from high-strength wastewater were evaluated in 30 identical batch reactors over the course of three trials, and are reported as per volume latrines solids digested (mL CH₄/mL substrate) and per mass COD removed (mL CH₄/g COD), as summarized in Table 3-4. On a volumetric basis, BMP2 produced the largest volume of methane, where reactors terminated at a 7d HRT produced 1.18 ± 0.58 mL CH₄/mL wastewater, and reactors terminated after 47 d produced 4.24 ± 0.74 mL CH₄/mL. BMPs 3 and 4 produced, on average, 77% less methane than BMP4, and methane was primarily captured in the first 10 days of digestion. Digesters terminated on day 19 and day 26 (BMP3) produced nearly the same volume CH₄ per mL substrate. Triplicate reactors terminated on day 6 of BMP4 produced 0.67 ± 0.19 mL CH₄/mL.

Table 3-4 Cumulative methane production during digestion of high-strength wastewater during three BMPs. CH₄ production is normalized by volume (mL CH₄/mL substrate), and by COD (mL CH₄/g COD removed). Values are reported as Mean ± SD

	Cumulative CH ₄ (mL CH ₄ /mL Substrate)			Cumulative CH ₄ (mL CH ₄ /g COD Removed) (η, %)		
	BMP2	BMP3	BMP4	BMP2	BMP3	BMP4
Day 6	-	-	0.67 ± 0.19		-	153 ± 90 (38%)
Day 7	1.18 ± 0.57	-	-	214 ± 70 (54%)	-	-
Day 13	-	-	0.51 ± 0.30	-	-	135 ± 58 (34%)
Day 19	-	0.97 ± 0.48	-	-	-	-
Day 21	-	-	0.90 ± 0.48	-	-	144 ± 60 (36%)
Day 26	-	0.96 ± 0.59	-	-	-	-
Day 47	4.24 ± 0.74	-	-	288 ± 48 (73%)	-	-
Biogas %CH ₄	59% ± 9.6%	55 ± 18%	59% ± 2.1%			

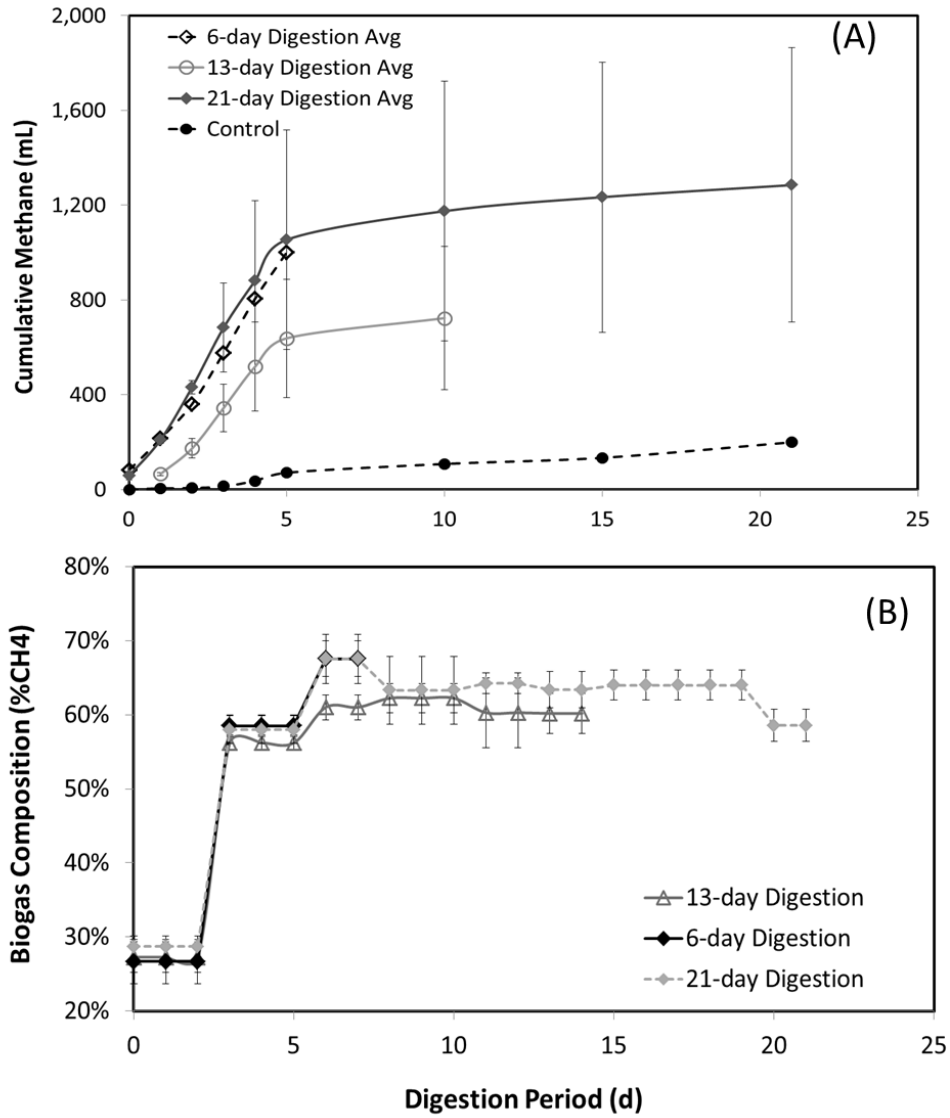


Figure 3-7 Cumulative Methane Production (Figure A) and Biogas composition (Figure B) during BMP Run 4. Data points represent the Mean \pm SD (mL CH₄ or %CH₄) of triplicate reactors that were terminated at 6 d (open diamond symbols), 13 d (open circle symbols), and 21 d (closed diamond symbols) of digestion.

The average methane content of biogas during BMP2, 3, and 4 was 59% \pm 9.6%, 55 \pm 18%, and 59% \pm 2.1%, respectively, though concentrations reached 76% during BMP2, 71% during BMP3, and 64% during BMP4. This is consistent with commonly accepted values for biogas composition from wastewater solids (Parkin and Owen 1986). Declines in methane production below 60% appeared to coincide with

the depletion of substrate, as evidenced by negligible gas production. At the end of digestion, the methane content of BMP 2, 3, and 4 biogas 54%, 55%, and 59%, respectively.

In all BMP trials, over 80% of methane was captured in the first 10 days and 95% by day 20 (illustrated in Figure 3-8)—a timeline comparable to what has been reported elsewhere (Raposo, De la Rubia et al. 2012). This initial, high rate of methane production may be a function of the batch-loading and/or the methanogenic inoculum, which is provided, in part, to ensure rapid kinetics for the BMP assay.

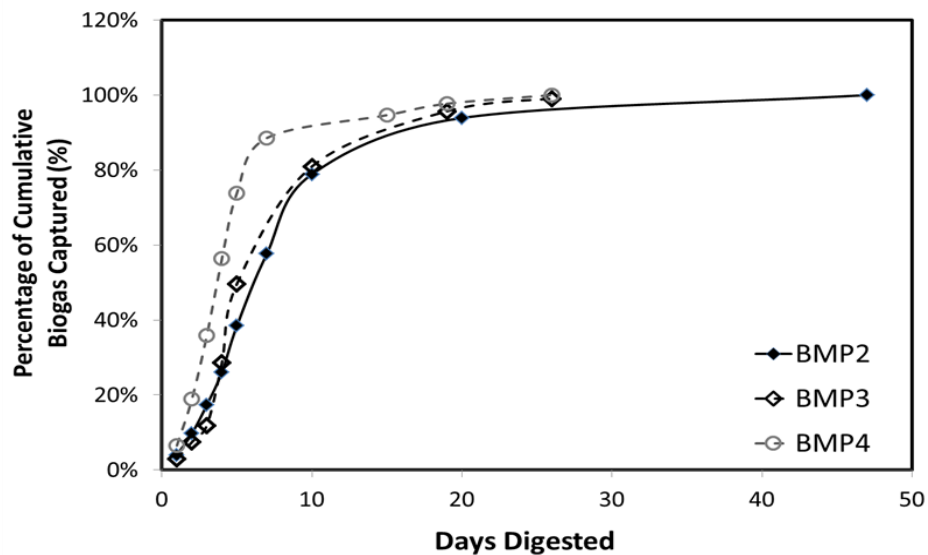


Figure 3-8. Percentage of the total biogas/methane captured as a function of digestion period, during BMP2 (closed symbols); BMP3 (open diamonds); and BMP4 (open circles).

Volumetric rates of methane production were primarily a function of the COD loading ($p < 0.001$), as illustrated in Figure 3-9. The stoichiometric relationship of 395 mL CH_4 per g COD destroyed (based on combustion equivalent of CH_4 ; See Chapter 2) was thus used as a more accurate predictor of BMP process efficiency, as has been

noted elsewhere (Metcalf, Eddy et al. 2010, Moody, Burns et al. 2011). A summary of conversion efficiencies is also provided in Table 3-4 for BMPs 2 and 4. Negligible removal of COD was detected during BMP3, resulting in erroneously high conversion rates. During BMP2, latrine solids produced 214 -288 mL CH₄ per g COD removed, where longer digestion periods increased conversion efficiencies. This is equivalent to a 54 – 73% conversion efficiency. Efficiencies were somewhat lower in BMP4—from 135 – 153 mL CH₄ per g COD removed (equivalent to 34 – 38% efficiency). The average conversion rate (254 L CH₄ per kg COD removed), equates to an energy density of 9.09 MJ/kg COD removed (HHV: 35.8 MJ/m³ CH₄) (McCarty 1975, Buysman 2009).

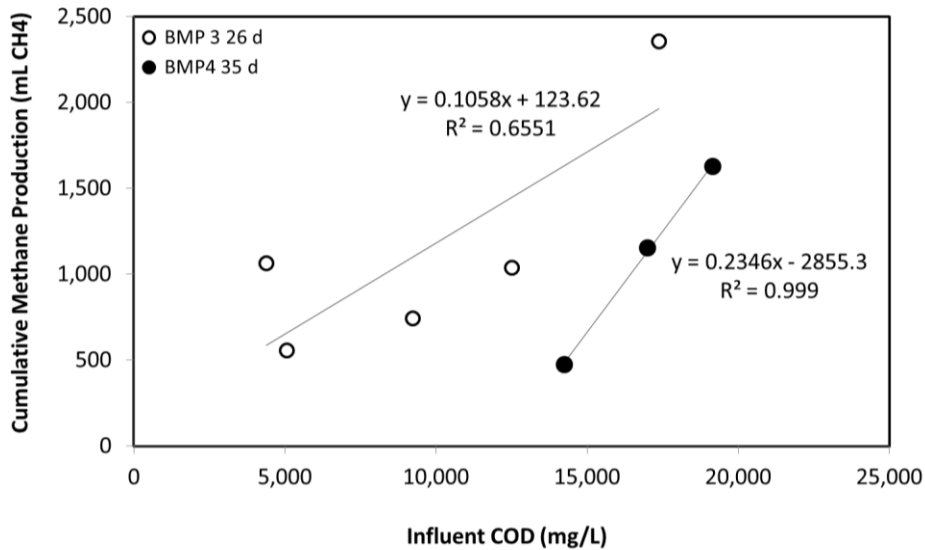


Figure 3-9. Cumulative methane production as a function of influent COD loading (mg/L). Data points represent the average of triplicate COD measurements at day 0 of digestion. Open circles represent the 2nd digestion trial; Solid circles represent the 3rd digestion trial.

There was significant variability in the calculated efficiencies (i.e. SD represented >40% of the mean efficiency in all trials). This variability can likely be attributed to

the heterogeneous and semi-solid nature of the substrate, which contributes to inaccuracies in COD measurements. This heterogeneity, as well as the large fraction of recalcitrant materials, is likely also the cause of the inefficiencies observed (i.e., conversion rates less than 395 mL per g COD removed). Batch digestion (i.e. the BMP assay) is often a conservative estimate of the degradability and methane potential of a substrate, and thus, biogas production from human waste in full-scale digesters would likely meet or exceed the values reported herein (Jensen, Ge et al. 2011). This is supported by reports on low-cost tubular digesters that have reported conversion rates > 395 mL per g COD removed (Lansing, Viquez et al. 2008), and additionally, by other BMP assays performed by the lab on the methane potential of latrine sludge, sampled from a pit latrine in Cange, Haiti. On a volumetric basis, the latrine sludge generated 7.5 – 16.6 L CH₄ per L sludge digested, approximately 10-times the volumetric rates reported here. This was likely attributable to the substrate's COD content (456 g/L), though removal rates, and thus conversion efficiencies, could not be discerned (Lansing et al., in preparation).

3.3.6 Microbial Fuel Cell—Treatment Efficiencies

Organics

Despite 20-40 d retention times, the effluent from digesters often still contains organic matter at levels that are unsafe for aquatic discharge (e.g. > 200 mg COD/L), and require post-treatment (e.g., treatment wetlands). Because this was also the case in this study, further reductions in COD, solids, and coliforms by the MFC were

necessary to achieve a final effluent safe for discharge. Treatment efficiencies for undigested waste were evaluated at HRTs between 5 min ($Q = 20$ mL/min; continuous recycle) and 3.6 h (no recycle; $Q = 0.46$ mL/min). When solids were recycled, treatment was evaluated at current-dependent intervals until substrate was depleted ($I < 1$ mA raw current). (Q_{eff}) of **0.46 - 0.66 mL/min (HRT of 2.8 -3.6 h)**.

Table 3-5 and Figures 3-10, 3-11, and 3-12 summarize MFC treatment performance when fed with digester effluent after 6d, 13d, and 21d digestion (BMP Run 4). Rates of organic matter removal were exceedingly high (i.e., > 1000 kg COD/m³/d), in comparison with other real waste-fed MFCs (Moon, Chang et al. 2005, Jiang, Curtis et al. 2011). At an HRT of 217 min, MFCs removed, on average, 95%, 72%, and 65% of COD, TS, and VS from undigested latrine sludge, corresponding to removal rates of 352, 338, and 272 kg/m³/day.

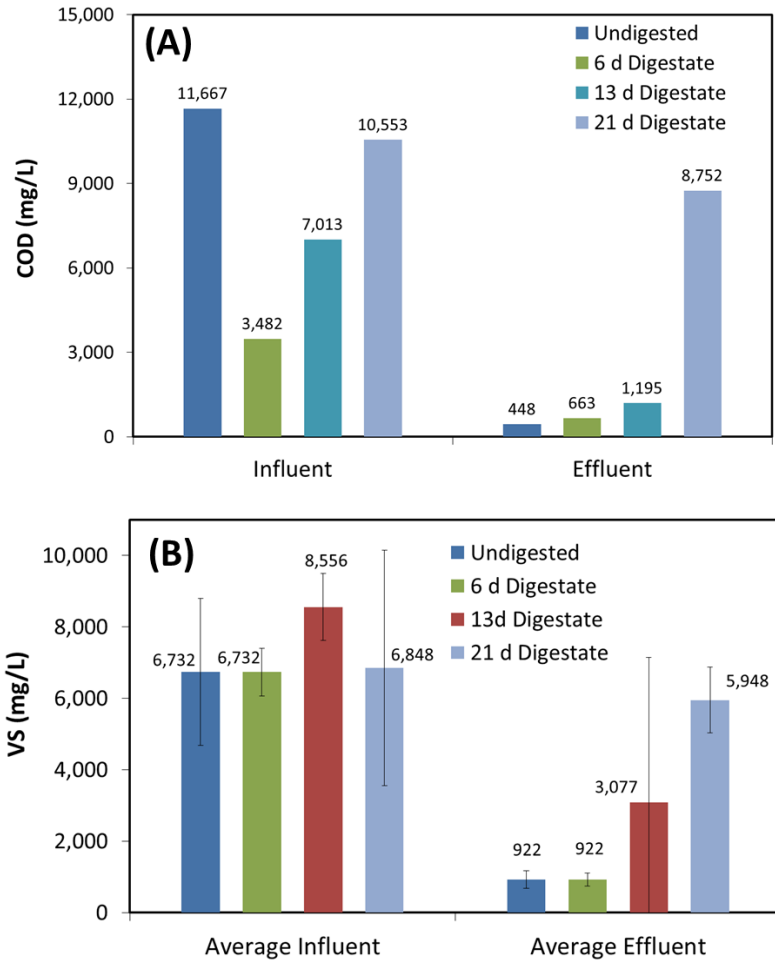


Figure 3-10. MFC influent and effluent concentrations of COD (Figure A; mg/L); and VS (Figure B; mg/L) when fed with undigested wastewater (in blue), 6d digestate (in green), 13d digestate (in red), and 21 d digestate (in light blue).

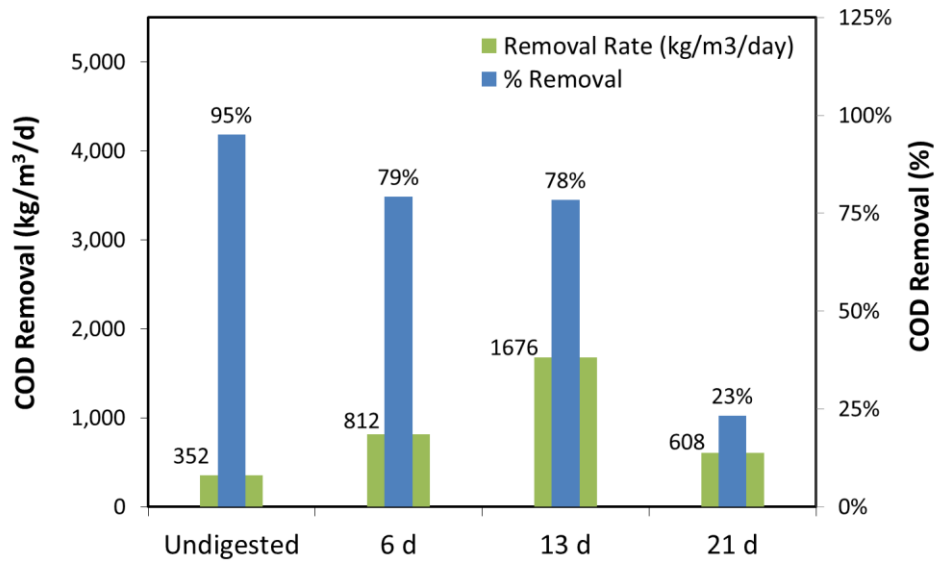


Figure 3-11. Average removal rates of COD from the four different waste feeds (0d, 6d, 13d, and 21d digested latrine solids). Removal rates were calculated on the basis of hydraulic retention time (5 min).

Digester retention time was found to be inversely correlated with MFC percentage removal rates, as illustrated in Figure 3-12), i.e. increased digestion time led to reduced rates of contaminant removal, as measured by percentage reductions in COD, TS, or VS. This is likely explained by the fraction of indigestible, recalcitrant material present in waste streams—as digestion proceeds, the fraction of recalcitrant-to-biologically relevant organic matter likely increases. Importantly however, overall removal rates of contaminant removal (kg/m³/d) do not appear to be affected by digestion period, indicating that the MFC is functioning as a highly stable unit operation for wastewater treatment.

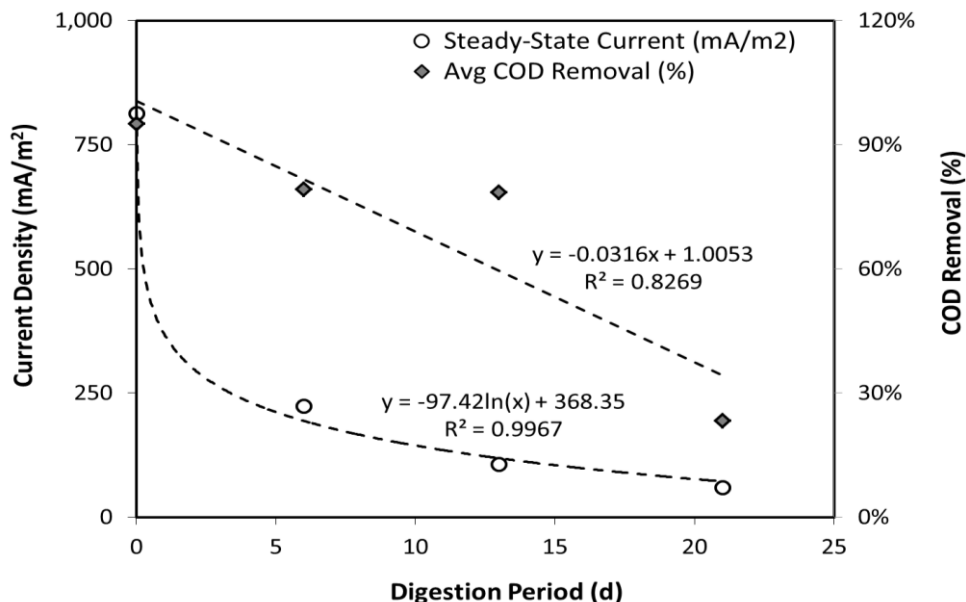


Figure 3-12. Relationship between the hydraulic retention time for digestion (0-21 d) and the resulting current (mA/m^2) and COD removal from the digestate when powering the MFCs. Current values (open circles) represent the average, steady-state current density from triplicate MFCs operated in chronoamperometric mode with a fixed anode potential of $-0.200 \text{ V vs. Ag/AgCl}$

Table 3-5 Summary of environmental characteristics, treatment efficiencies, and treatment rates during MFC treatment. Data is presented as mean \pm SD.

	Undigested	6-d Digestate	13-d Digestate	21-d Digestate
COD_{in} (mg/L)	11,667	3,482	7,013	10,553
COD_{eff} (mg/L)	448	663	1,195	8,752
COD Removal (%)	95.0%	79.2%	78%	23.3%
COD Loading ($\text{kg}/\text{m}^3/\text{d}$)	322	1,000	2,020	3,040
COD Removal ($\text{kg}/\text{m}^3/\text{d}$)	352	812	1,675	608
VS_{in} (mg/L)	6,732	3,631	4,792	6,848
VS_{eff} (mg/L)	922	1,709	3,077	5,948
VS Removal (%)	65.4%	56.6%	35.8%	20.4%
VS Loading ($\text{kg}/\text{m}^3/\text{d}$)	292	1,046	1,380	1,970
VS Removal ($\text{kg}/\text{m}^3/\text{d}$)	272	554	494	349
TS_{in} (mg/L)	9,548	8,437	10,360	13,897
TS_{eff} (mg/L)	1,583	5,493	7,660	12,361
TS Removal (%)	72.3%	32.3%	26.1%	16.1%

TS Loading (kg/m ³ /d)	402	2,430	2,980	4,000
TS Removal (kg/m ³ /d)	339	848	778	563

3.3.7 Coliform Removal

Coliform removal from MFCs was lower than what was observed during digestion of wastewater. Undigested solids achieved >99.0% (1-log) removal of fecal coliforms, reducing loads from $1.5 \times 10^6 \pm 1.5 \times 10^6$ MPN/mL to $7.7 \times 10^4 \pm 7.2 \times 10^4$ MPN. Digested solids (5 d digestate only was evaluated) achieved negligible, additional reductions, where fecal densities actually increased slightly in the MFC effluent—from 4.5 ± 2.8 MPN/mL to 24 ± 31 MPN/mL. Coliform densities were highly variable, and in both cases, the standard error accounted for 58% of the standard deviation.

3.3.8 Microbial Fuel Cell—*Electrochemical Evaluation*

Anodic Current Production

Anodic biofilms of the triplicate MFCs (labeled as MFC 1, 2, and 3 in figures) were grown under the continuous flow of undigested solids and achieved stable current production of $131 \text{ A/m}^3 \pm 21.5 \text{ A/m}^3$ ($813 \text{ mA/m}^2 \pm 133 \text{ mA/m}^2$) after approximately 120 h of growth (Figure 3-13). This level of current production was maintained for > 500 hours with no evidence of biofouling or other deterioration of biological catalysis

at the anode. Oscillations in current production of $\sim \pm 30 \text{ A/m}^3$ were observed and coincided with substrate introductions at the anode (pump on/off cycling every 58 min). Under conditions of continuous recycled flow, these oscillations were not observed. Reductions in current were observed as substrate was depleted from the waste, typically between 86 and 120 h of recycled flow, and coincided with reductions in COD and solids, as described in Section 3.3.6, where the final effluent contained $< 448 \pm 91 \text{ mg COD/L}$ and $< 922 \pm 244 \text{ mg VS/L}$ ($n \geq 3$), as well as visible clearing of the sludge and reductions in settled solids.

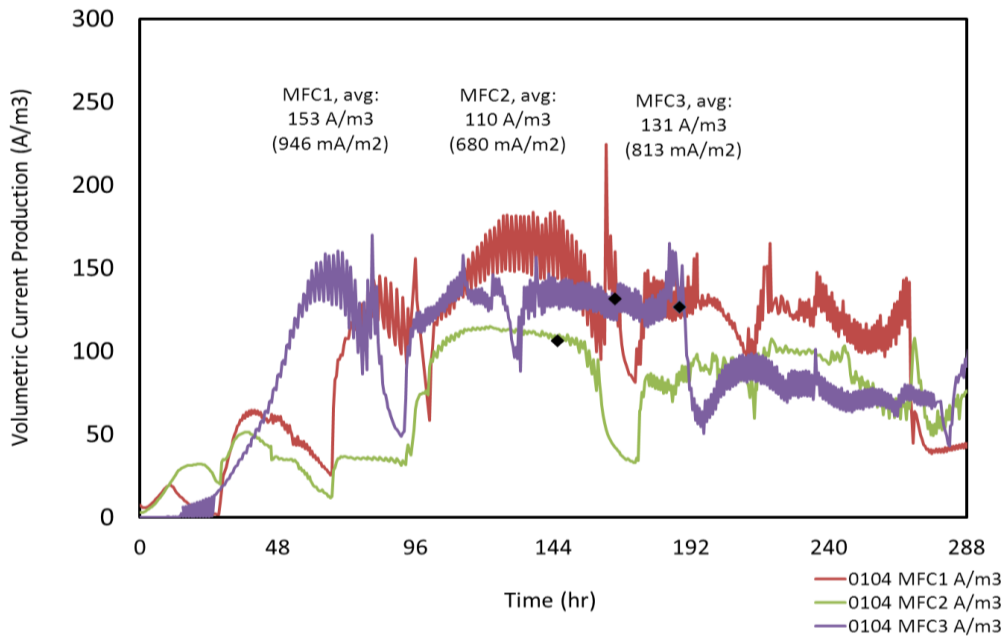


Figure 3-13 Chronoamperometric plot of the formation of bioelectrical activity and sustained current production of an environmental sludge biofilm at carbon cloth electrodes in triplicate MFCs; continuous flow experiment with 3.6 h HRT; Ean: -0.2V vs. Ag/AgCl. Oscillations in current production were due to pump on/off cycling every 58 min.

Between testing of the three digested wastes, undigested sludge was fed to MFCs to recover a stable level of current production. Each time a comparable, average current production was achieved (100-252 A/m³) with peak currents reaching 300

A/m^3 (1860 mA/m^2). This nears the upper limit of volumetric current reported to date from MFCs, and, to the authors' knowledge, represents the highest volumetric current that has been achieved by a waste-fed fuel cell to date. We attribute the high level of volumetric current and treatment achieved in this study to features of the reactor design (i.e., high SRT, maximized interaction between waste and ARB), as outlined in Section 2.2.2. Baffled, anaerobic reactors are known for efficient treatment of high strength wastes, and an increased resilience to non-uniform organic loading rates (Bachmann, Beard et al. 1985, Barber and Stuckey 1999).

Amending the undigested sludge with acetate ($0.82 \text{ g/L NaCH}_3\text{COO}^-$) resulted in an additional current increase of only 7.3% (from 156 A/m^3 to 167 A/m^3), suggesting that high-strength wastewater contains sufficient ARB substrate to sustain a high level of current production. Further, acetate amendments resulted in approximately 48 h of sustained current production under recycled flow conditions. In comparison, more than 100 h of current production was sustained with a complete replacement of the sludge volume, suggesting that hydrolytic/fermentative processes within the MFC were yielding sufficient ARB substrate for a longer period of time. This type of syntrophic relationship between fermentative and anode respiring species has been previously reported (Parameswaran, Torres et al. 2009, Parameswaran, Zhang et al. 2010).

Latrine sludge digested during BMP Run 4 (labeled as '5 d', '10 d', and '35 d' Digestate in Figures) was subsequently fed to triplicate MFCs, and flow was recycled (3 L total volume) until substrate was depleted, as evidenced by a decline in current production to $< 100 \text{ mA/m}^2$ ($< 1 \text{ mA}$ raw current). To avoid carry-over bias between

samples, undigested solids were used to recover maximum, stable current production ($> 100 \text{ A/m}^3$) between each of the digested sludges (confirmed with voltammetry at maximum current).

The wastewater digested for the shortest period, 6 d, produced the greatest current in the MFC. As indicated by organic acid analysis, short digestion period may serve as pseudo-fermentation for the waste. The 5 d digestate yielded an average, peak current of $36 \text{ A/m}^3 \pm 6.1 \text{ A/m}^3$ ($223 \text{ mA/m}^2 \pm 36 \text{ mA/m}^2$) after approximately 150 hr of continuous flow, and was able to maintain $> 1 \text{ mA}$ raw current for $> 350 \text{ h}$. Sludges digested for 10 or 35 d were able to sustain current $> 1 \text{ mA}$ for no longer than 48 hr, and in both cases the average, peak current was significantly reduced—10 d digestate yielded $17 \pm 0.8 \text{ A/m}^3$ ($106 \text{ mA/m}^2 \pm 4.9 \text{ mA/m}^2$) after approximately 48 hr of flow; 35 d digestate yielded $9 \pm 0.4 \text{ A/m}^3$ ($59 \pm 2.8 \text{ mA/m}^2$).

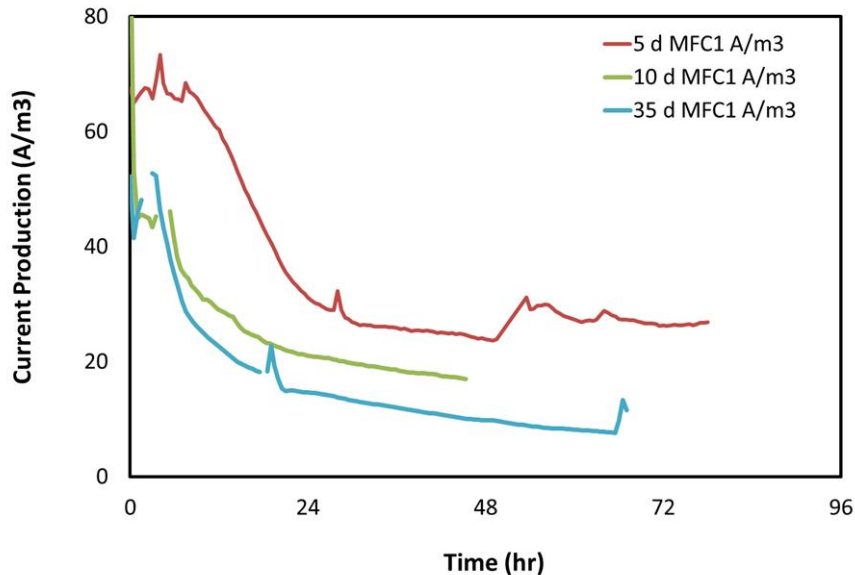


Figure 3-14. Chronoamperometric curves showing relationship between digestion period (5, 10, or 35 d) and sustained current production at carbon cloth electrodes; continuous flow experiment with 5 min HRT; Ean: -0.2V vs. Ag/AgCl.

After current declined to < 1 mA (~ 140 h), the 10 d digestate was amended with sodium acetate (10 mM $\text{NaCH}_3\text{COO}^-$) to confirm that reduced current densities were due to substrate limitations rather than inhibition by digestion-related products (e.g. NH_3). All anodes responded positively to the acetate, yielding an average, peak current of 140 ± 40 A/m^3 ($1,072 \pm 140$ mA/m^2)—more than an eight-fold increase over the un-amended digestate, and comparable to the stable level of current that was observed with the undigested material. Acetate amendments were repeated three times to confirm the current response, each time after current dropped below 1 mA.

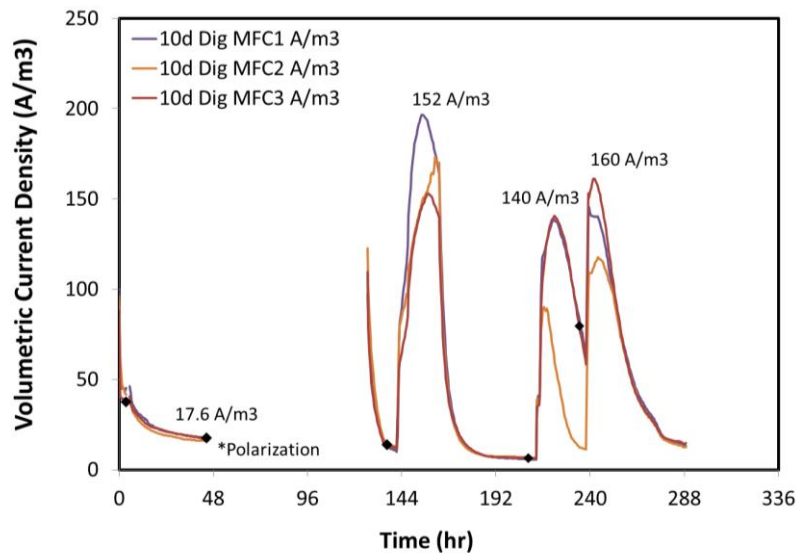


Figure 3-15 Chronoamperometric showing the effect of sodium acetate additions on current production, under the flow of 10d digestate; 5 min HRT; Ean: -0.2V vs. Ag/AgCl .

This is consistent with previous studies that have elucidated acetate as the primary reductant for metal reducing bacteria (Lovley and Phillips 1988, Liu, Cheng et al. 2005). Because of the limited volume of digestate available, it was not possible

to discern whether reducing the dilution rate of substrate to the anode (i.e. reduced MFC retention time, larger digestate volume) could alleviate substrate deficiencies. The few pilot studies of MFC/MEC technology to date have found that the concentration of simple, easily degradable organic acids in actual waste streams may be insufficient to grow or sustain current production by MFCs (Cusick, Bryan et al. 2011, Jiang, Curtis et al. 2011). Importantly, this work demonstrates that high-strength, raw wastes can in fact yield significant current production, on par with that of known ARB (e.g. 5 A/m² from *G. sulfurreducens*, strain DL1), as well as high-rate removal of organic matter and solids from high-strength wastes. Critical to such performance is the maintenance of a thermodynamically favorable anode potential (i.e. > -300 mV vs. Ag/AgCl), which is directly related to the ability of ARB to efficiently couple organic matter oxidation with anode reduction (see Section 3.5.2 for further description).

Voltammetry

Slow scan voltammetry enabled evaluation of anodic losses, as well as comparison of our wastewater biofilm with that of known ARB strains. Voltammetry was performed in-situ during the course of anodic biofilm growth (illustrated in Figure 3-16) and at maximum catalytic activity with undigested sludge (illustrated in Figures 3-17 and 3-18). CVs captured during feeding with the four different digestates all exhibited a

current-potential dependency, consistent with the Nernst-Monod model that has previously been used to model ARB kinetics (Fricke, Harnisch et al. 2008, Marsili, Sun et al. 2010, Strycharz, Malanoski et al. 2011).

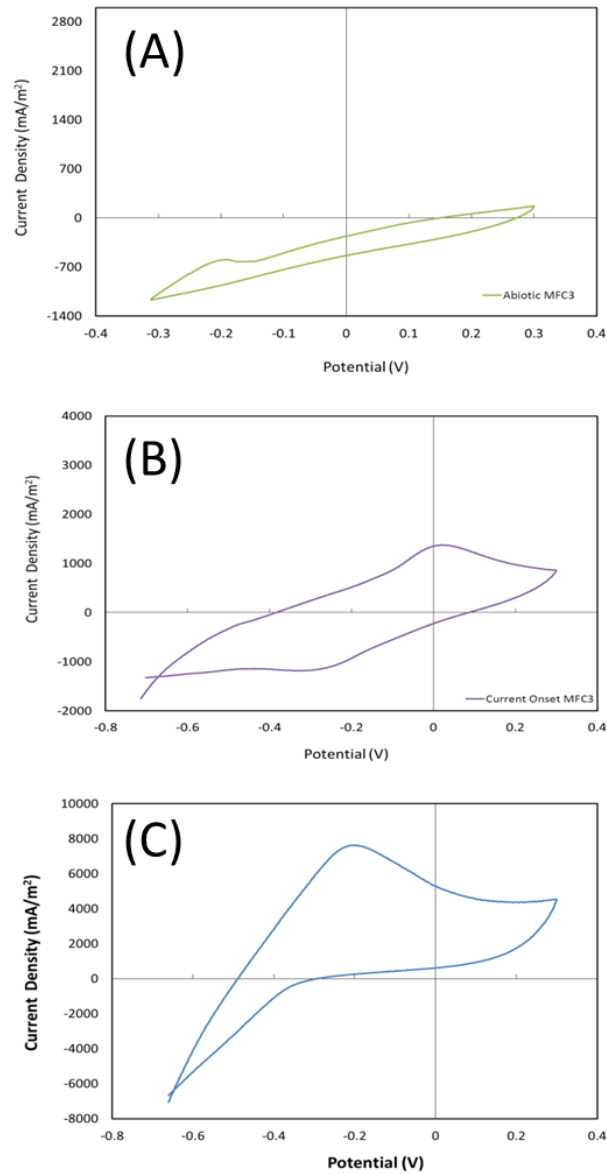


Figure 3-16. Representative voltammograms of undigested waste biofilms recorded at (a) the time of inoculation; (b) the onset of catalytic activity; and (c) maximum catalytic activity. Scan was recorded at 0.001 V/s from -0.8 V to +0.3 V and back to -0.8 V vs. Ag/AgCl, 3M KCl

Voltammograms of *Geobacter sulfurreducens*, strain DL1 and undigested, waste-fed anodes in the same MFC (Figure 3-17) exhibit similar mid-point (formal) potentials (~ -0.35 to -0.40 V vs. Ag/AgCl), representing the potential at which one-half of the limiting current can be achieved. Oxidative peaks were also observed for waste-fed anodes (E_{an} ~ -200 mV; range of -140 to -300 mV vs. Ag/AgCl), consistent with lower rates of mass transport of the electron donor (e.g., acetate) to the anode, consistent with the lower current response from digested waste.

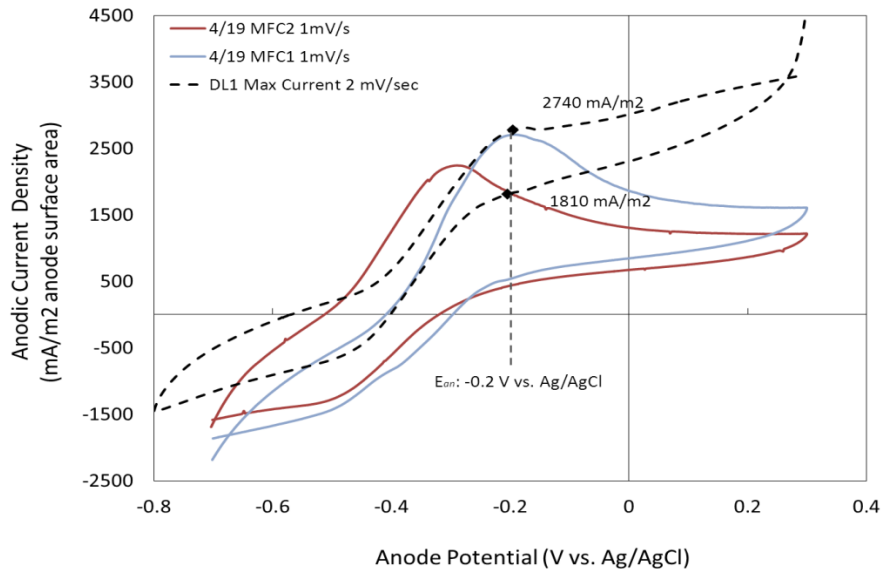


Figure 3-17 Representative voltammograms of undigested waste biofilms (solid lines) and *Geobacter sulfurreducens*, strain DL1 (dashed line) recorded at 0.001 V/s from -0.8 V to $+0.3$ V and back to -0.8 V vs. Ag/AgCl, 3M KCl.

Even though the waste feed was relatively heterogeneous and was not controlled for organic content, or other environmental parameters, CV shape, mid-point potential, and limiting current were highly consistent across the span of more

than one month (Figure 3-18). Anodes exhibited negative (cathodic) catalytic behavior at potentials less than -500 mV vs. Ag/AgCl.

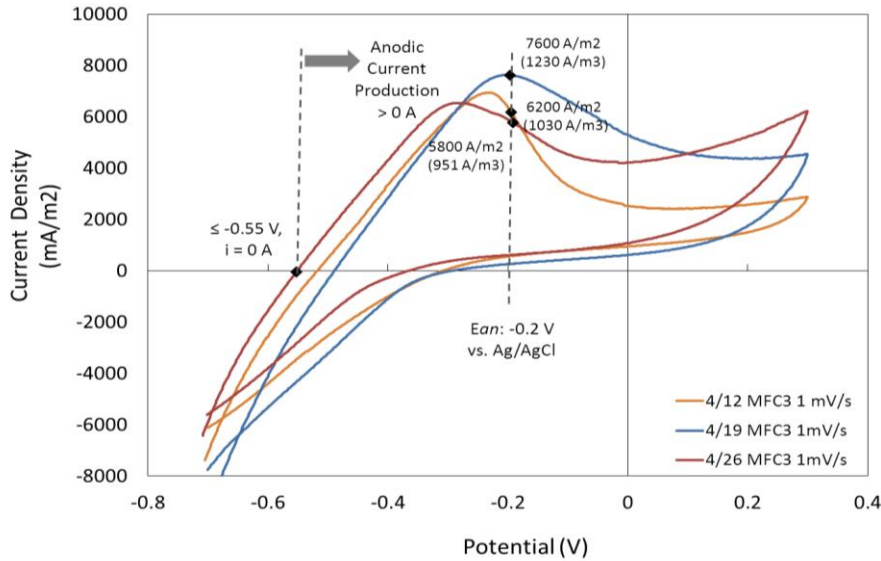


Figure 3-18. Representative voltammetry from MFC anode fed with undigested sludge. Scan parameters: $v = 0.001$ V/s, $E_{an} = -0.8$ V to $+0.3$ V, and return.

In all cases, the onset of anodic current production began at anode potentials ≥ -420 mV, with curves approaching saturation at potentials > -200 mV. This is consistent with the relatively small current response that was recorded when the cell voltage was fixed, i.e. when the cathode is limiting, the anode potential is driven to potentials too low to be an energetically favorable electron acceptor and thus limit current/power production as well as treatment efficiencies. The cathodic (return) scan showed a significant, negative deviation from the initial, anodic sweep. This phenomenon has been previously reported, albeit to a lesser degree, by (Strycharz, Malanoski et al. 2011), is not well understood, and is attributed to non-metabolic uptake of electrons by the anodic biofilm. Significant reductions in CV peak height,

and limiting current density were observed in digestate fed anodes (Figure 3-19), which is consistent with the reductions in current density observed during chronoamperometric experiments.

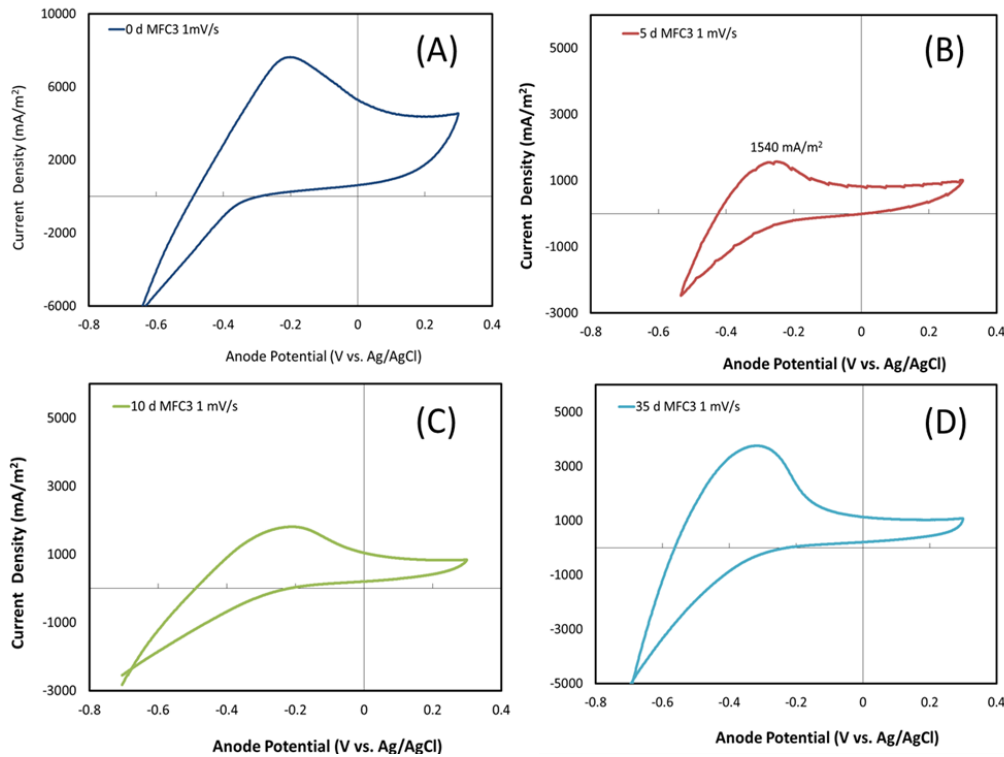


Figure 3-19. Representative voltammograms of an wastewater biofilm fed with (a) 0 d; (b) 5 d; (c) 10 d; and (d) 35 d digestate. Voltammograms were recorded at maximum biofilm activity. Scan parameters: $v = 0.001$ V/s, $E_{an} = -0.8$ V to $+0.3$ V, and return.

Cathodic Losses and Power Output

Most recent and pertinent MFC literature has concluded that the oxygen reduction reaction (ORR) that supplies the cathodic process in most abiotic fuel cells is ill-optimized in the MFC, owing to the circum-neutral pH and temperature conditions required for biological growth (i.e. pH7, 30°C). Findings from this study corroborate

this, with cathodic overpotentials ($E_c^{0'}$) approaching 900 mV (i.e. a reduction in $E_{cath}^{0'}$ from +0.4V to -0.4 V vs. Ag/AgCl at maximum current production), which caused a cessation of appreciable power production. Cathodes initially neared the theoretical limits for oxygen reduction at neutral pH ($E_{cath,OCV}$: +550 mV) but declined by >300 mV after 72 h OCV, prior to the onset of catalytic activity. During chronoamperometric conditions at maximum current (E_{an} : -200 mV), cathodes were driven as low as -900 mV to compensate for the high rate of charge transfer at the anode. This result could be indicative of a number of membrane/cathode limitations, e.g. that a rapid accumulation of charge occurred at the cathode, even with minimal anode activity (i.e. open circuit); or that anionic substances present in the waste (e.g. S^{2-}) were transported across the AEM to create a competing reduction reaction at a less favorable potential. Importantly, these findings all point to the need for characterizing MFC performance in both two- and three-electrode configurations, so as to evaluate limitations of individual electrodes.

Two-electrode methods of characterizing the MFC (i.e. polarization; maintaining a fixed cell voltage) were inadequate for evaluating differences in anode performance and power output under the various waste feeds. In all cases, cathodic losses dominated and constrained current/power production in this MFC configuration. Relationships between anode performance and the waste material should thus only be evaluated when cathode performance is non-limiting (i.e. three electrode potentiostatic; cyclic voltammetry). Reported power numbers, either from polarization or from operation at a fixed cell voltage, are only indicative of the overall

MFC configuration and should not be taken as indicative of the anodic process or the maximum power extractable from high-strength wastes, such as latrine sludge.

This was demonstrated by the cathodic activation losses, which increased significantly during biofilm growth. Cathodes achieved an OCP of +400 mV vs. Ag/AgCl at the start of the experiment, prior to biofilm growth and current discharge. After the anode reached maximal current production ($> 100 \text{ A/m}^3$) however, cathode OCPs dropped to $< 115 \text{ mV}$ vs. Ag/AgCl (while the MFC was equilibrated at OCV). At maximum current production ($\sim 7 \text{ mA}$ raw current from undigested waste), cathode potentials dropped to $< -300 \text{ mV}$ vs. Ag/AgCl at open circuit ($E_{cath,OCP} : -104 - 112 \text{ mV}$ vs. Ag/AgCl, 3M KCl) and significant cathode polarization upon current discharge (See Figure 3-20).

Maximum power, obtained by polarization analysis, varied from $7-11 \text{ W/m}^3$ ($44 - 69 \text{ mW/m}^2$), with no significant difference observed among the four digestion periods. As evidenced by significant differences in anode performance (e.g. current production at a fixed anode potential, voltammetric signatures), this cannot be attributed to insignificant differences in the biochemical energy reserves of the different waste sources. As measured by a deviation in potential from OCP to $0.005 V_{cell}$, the average anode and cathode polarization was 147 mV and 383 mV , respectively. Cathode losses have been reported frequently in MFC literature (Oh, Min et al. 2004, He, Huang et al. 2008, Popat, Ki et al. 2012); however, they are somewhat exacerbated in the current configuration, which may be due to complexities created by the use of real, high-strength waste.

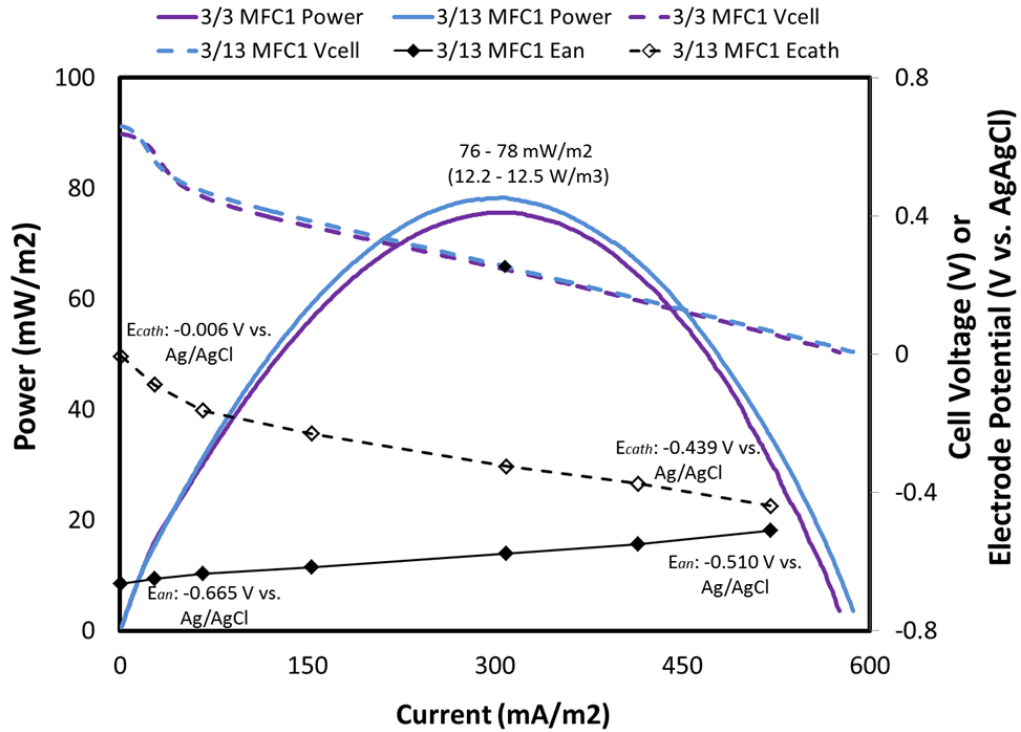


Figure 3-20. Power, cell voltage, and electrode potentials during fuel cell polarization when MFC anode is fed with undigested latrine solids. Polarization was recorded from OCV to 0.005 V at 0.1667 mV/s; electrode potentials were recorded against Ag/AgCl, 3M KCl.

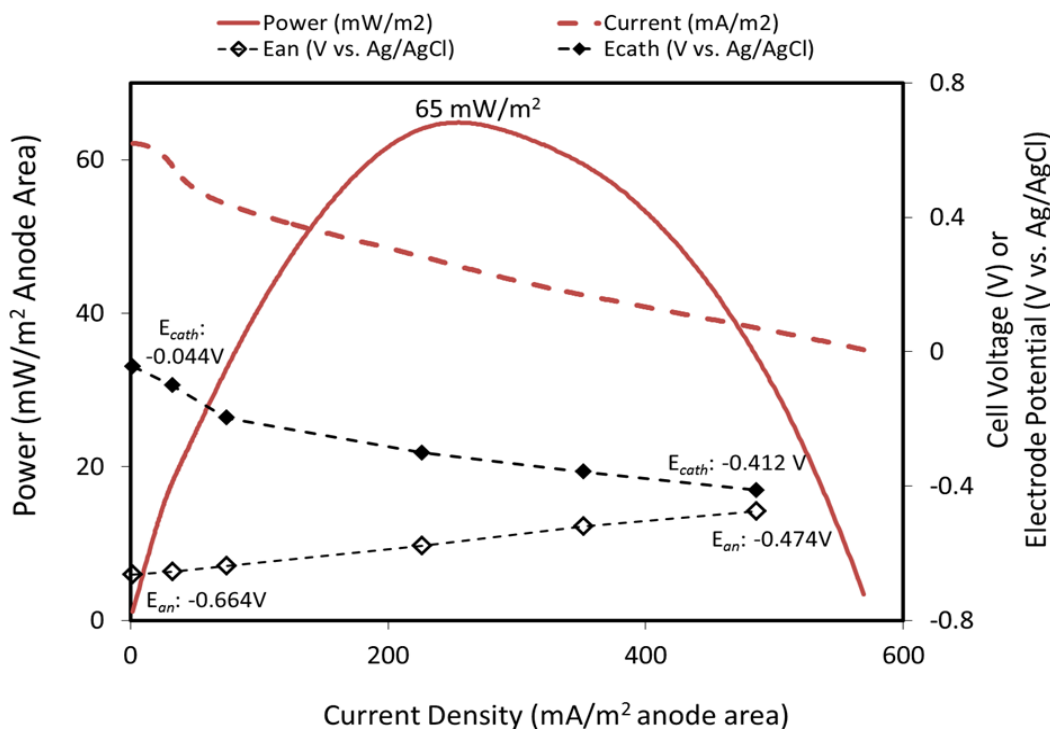


Figure 3-21. Power, cell voltage, and electrode potentials during fuel cell polarization when MFC anode is fed with 5 d digestate. Polarization was recorded from OCV to 0.005 V at 0.1667 mV/s; electrode potentials were recorded against Ag/AgCl, 3M KCl.

A number of cathode iterations were evaluated, e.g. greater than 100-fold increase cathode surface area; employing Pt- and MnO-loaded cathodes; phosphate buffered, or salt-based catholytes to improve buffering/conductivity; the use of ambient air (21% O₂) versus O₂-saturated water (< 1% O₂); 50 mM potassium ferricyanide catholyte; and the addition of dilute acids and bases at the cathode to ameliorate pH effects. The replacement of bare graphite granules with granules that had been loaded with a manganese oxide catalyst (8-10% MnO on Vulcan carbon; uncharacterized; synthesized by J. Biffinger, NRL) resulted in a 200 mV increase in cathode OCP (from ~0 mV to +200 mV vs. Ag/AgCl, 3M KCl); however, no difference in cathode potential, or fuel cell power output were observed at maximum

current production. Potassium ferricyanide as the catholyte (50 mM) yielded measureable, albeit unsustainable, improvements in cathode potential and power production—up to 242 mW/m² (690 mA/m²) in an undigested sludge-fed MFC.

3.4 Conclusions

The results presented here demonstrates plausibility of a hybrid AD-MFC system for anaerobic treatment and resource recovery from fecal sludge. We empirically demonstrate the energy densities that can be gleaned from waste using the AD-MFC process. AD produced, on average, 29.6 kJ per m³ wastewater treated (8.2 Wh/m³); MFC produced, on average, 2.1 kJ per m³ undigested wastewater treated (0.58 Wh/m³). On the basis of COD, AD generated 9,110 kJ per kg COD removed (2,530 Wh/kg COD); MFC generated 0.18 kJ per kg COD removed (0.05 Wh/kg COD). Substrate limitations in digested sludge reduced current densities—36 A/m³, 17 A/m³, and 9 A/m³ were achieved from 6d, 13d, and 21d digestate, respectively.

Cathodic limitations severely limited power/energy production by the MFC, with maximum power output of 11 W/m³ (69 mW/m²). Presumably, this was due to mass transport of oxygen reduction intermediates. With an improved MFC cathode, a five-fold increase in power (from ~10 W/m³ to ~50 W/m³) could be realized (based on 130 A/m³ anodic current densities observed under potentiostated configurations; and where V_{cell} , 0.4V coincides with P_{max}). This would translate into an estimated energy yield of 15 kJ per m³ wastewater treated.

The MFC treatment was exceeding efficient—averaging 96% COD, 86% VS, and 83% TS removal from undigested waste. Results indicate an inverse logarithmic

relationship between digester retention time and subsequent MFC current production, i.e. maximal MFC current production is achieved with undigested waste, and an inverse linear relationship between digester retention time and subsequent COD/VS removal in MFCs. Breakthroughs must be made to address cathodic limitations of MFCs, before scaling is practically or economically viable.

3.5 Acknowledgements

This work was supported by the Bill & Melinda Gates Foundation (Grant No. 01566000547) as well as the US Naval Research Laboratory. K.G. was also supported by a fellowship from the A. James Clark School of Engineering at UMD. We thank Joel Gregory at the Alexandria Sanitation Authority for digester sampling assistance, and Mark Ramirez and Greg Phillips at DC WATER for assistance with sampling and nutrient analysis. Justin Biffinger (NRL-DC) assisted with organic acid analysis. John Palmisano and Marius Pruessner (NRL-DC) fabricated the circuit board for biogas data logging. Walter Mulbry (USDA-BARC) and Heekwon Ahn provided the anaerobic reactors and gas flowmeters.

Chapter 4 : Microbial Fuel Cell Field Deployment for Secondary Treatment and Resource Recovery from Anaerobic Digestion Effluent

4.1 Introduction

Low-cost anaerobic digestion (AD) of agricultural and human wastes is a proven technology, well suited for the climatic conditions (i.e. 15-30°C ambient temperatures) and high organic loading rates that are characteristic of decentralized sanitation in much of the developing world (e.g. 3.2 – 7.2 kg VS/m³/day) (Sánchez, Borja et al. 2001, Gerardi 2003). When effectively implanted, AD results in reduced emission of volatile organics, noxious odors, greenhouse gases (e.g. CH₄, CO₂), and physio-chemical and microbiological contaminants (Steinfeld, Gerber et al. 2006, Holm-Nielsen, Al Seadi et al. 2009), directly benefiting the environment and health and well-being of local residents. Moreover AD is able to convert the biochemical energy and nutrients present in human and animal excreta (4.5 g total N per L urine; 1 kWh per kg carbohydrate) into biogas (which can reduce the local deforestation pressure when used as an alternative to wood for fuel) and fertilizer, providing an incentive for rural communities to install and maintain digesters (Jonsson, Stinzinger et al. 2004, Pham, Rabaey et al. 2006). Elimination of the mechanization required for stirred reactors by employing gravity conveyance and the utilization of low-cost, readily available materials (e.g. polyethylene or masonry construction with PVC connections) has made AD an increasingly viable treatment option in resource-limited settings (Lansing, Botero et al. 2008, Arthur, Baidoo et al. 2011). Practical limitations

on capital cost, and thus reactor HRT and volume, as well as temperature and operating conditions however, often result in incomplete mineralization of organic matter. As a consequence, AD effluent typically contains organic matter at levels that exceed allowable limits for direct discharge (e.g. > 200 mg BOD/L) (Marchaim 1992, Lansing, Viquez et al. 2008). Additionally, because of the anaerobic nature of waste treatment, the nutritive content of digestate is primarily contained in nitrogen as NH_3 and phosphorus as ortho- PO_4 . Thus, to enable more complete waste treatment and to facilitate aerobic stabilization of nutrients (i.e. conversion of NH_3 to $\text{NO}_2^-/\text{NO}_3^-$), secondary, aerobic processes (e.g. treatment wetlands) that increase costs without adding value or resource-recovery are commonly employed (Mowat, Singh et al. 1986, Kantawanichkul, Somprasert et al. 2003).

As an alternative to aerobic treatment, we hypothesize that the microbial fuel cell (MFC) might serve as an alternative, secondary treatment process for digestate to enable more complete waste oxidation and provide an additional form of decentralized energy, as electrical power. The MFC is an emerging waste-to-energy technology that couples microbial oxidation of organic matter with reduction of oxygen without mechanical aeration of waste (e.g. activated sludge), which is energy intensive. (Allen and Bennetto 1993, Logan, Hamelers et al. 2006, Logan and Regan 2006). This is accomplished by splitting the process into two coupled half reactions. The first is anaerobic oxidation of organic matter catalyzed by metal reducing microorganisms that transfer respire electrons to an anode contained within the anodic half-cell. The second is reduction of oxygen (directly or mediated) by a cathode contained within the cathodic half-cell. The electrons acquired by the anode from oxidation of organic

matter are conducted as electrical current through an external electrical circuit to the cathode where they are utilized to reduce oxygen. Necessary charge neutrality is maintained by diffusion of protons generated by the anode half reaction and consumed by the cathode half reaction through a perm-selective membrane separating the anodic and cathodic half-cells that excludes oxygen from the anodic half-cell.

Thermodynamic favorability of the net reaction, oxidation of organic matter by oxygen, results in electrical power delivered to the external circuit by the electrical current generated by the separated half reactions. Alternatively, MFCs can be operated as microbial electrolysis cells (MECs) in which electrical power is applied to the external circuit to drive the net reaction faster than it will naturally occur.

The anodic reaction of MFCs fed with simple substrates (e.g. acetate) is relatively well-understood, with reaction rates (expressed as current density) reaching an apparent limit of 10 A/m^2 electrode surface area catalyzed by pure culture organisms (e.g. *G. sulfurreducens*) or mixed, environmental biofilms (Torres, Krajmalnik-Brown et al. 2009, Strycharz, Malanoski et al. 2011). This upper limit for current equates to a theoretical COD removal rate (RCOD) of $71.6 \text{ g ThCOD/m}^2/\text{d}$ (see calculations in Section 3.1).

Data on MFCs fed with actual waste streams is still relatively sparse, but it has been noted that those fed with high-strength wastes (e.g. $> 1,000 \text{ mg COD/L}$) exhibit reductions in Coulombic efficiency (ratio of amount of organic matter oxidized by the anode to total amount of organic matter oxidized in the anodic half-cell, where the difference can result from other oxidation processes such as un-intended oxygen infiltration into the anodic half-cell or methanogenesis) and non-linear relationships

between organic loading and current density (Min, Kim et al. 2005, Feng, Wang et al. 2008, Zhang, Zhao et al. 2012). For this reason, it is hypothesized that a partially degraded digester effluent could serve as an optimized input to a MFC for final polishing and additional energy capture.

The MFC field trials described here were conducted at the Costa Rica, where more than 2,000 low-cost digesters have been installed for the treatment of agricultural and human wastes, and where the benefits of AD are well documented (Huttunen and Lampinen 2005, Lansing, Botero et al. 2008, Lansing, Viquez et al. 2008). The Escuela de Agricultura de la Región Tropical Humeda (EARTH) University, in the Limon province of the country, is uniquely positioned, in that the campus has installed seven full-scale digesters for on-site waste treatment that have been in operation for eight years, and many students, faculty, and staff are highly educated on digestion principles.

Herein, we report on field testing of MFCs as a secondary treatment process for three high-strength waste streams: dormitory wastewater (combined grey/black waste stream), dairy manure, and swine manure. Each received initial treatment by full-scale anaerobic digesters maintained on the campus. MFCs were continuously fed with digestate over the course of four weeks in-country, and experiments were later repeated in a controlled laboratory setting to further evaluate electrochemical performance and elucidate cathode limitations. Specific objectives of the project included:

1. To characterize treatment efficiency, with respect to chemical oxygen demand (COD), total solids (TS), and volatile solids (VS) from full-scale digesters and MFCs

2. To characterize and compare electrochemical performance of field MFCs using two-electrode configuration with respect to current, power, and anode and cathode potentials
3. To characterize and compare MFC electrochemical performance in three-electrode mode, whereby the cathode reaction was non-limiting
4. To perform a mass balance on AD-MFC processes, including energy output as well as pollutant and nutrient loads

We aim to demonstrate some of the challenges associated with deployment and scaling of the waste water fed-MFC technology, and the fundamental electrochemical challenges that remain at the cathode reaction of MFCs. Results indicate a maximum volumetric power from MFCs of 5-13 W/m³ under the continuous flow of substrate, equating to a daily energy production of 1.5 – 3.8 MJ/day. Biogas energy yields, in comparison, provided > 100 times more energy than the MFCs—ranging from 150-820 MJ/day. MFC power/energy production was ultimately constrained by the cathode reaction (representing an overpotential of ~0.500 V), as well as substrate limitations in the already digested waste.

4.2 Materials & Methods

4.2.1 Digester Study Site

Digesters utilized for primary treatment were located on the campus of EARTH University (Limon Province, Costa Rica at 10°N, 83°W), an international college for sustainable agricultural practice and engineering. A total of seven large-

scale ($> 30 \text{ m}^3$) anaerobic digesters that were constructed on campus provide on-site treatment of dairy and swine manure from four animal production farms, as well as a combined grey-black water stream from three student dormitories. Digesters are operated at ambient temperature ranging from 22-30°C.

The effluent from three of these digesters separately treating dairy, swine, and human waste served as the input to the MFCs. All of the digesters were Taiwanese-model, flow-through reactors comprised of polyethylene or PVC bag, PVC tubing, and plastic hosing for the transport of biogas (Figure 4-1) (Lansing, Botero et al. 2008, Lansing, Viquez et al. 2008).



Figure 4-1. Un-mechanized, anaerobic digesters treating agricultural waste on the campus of EARTH University (Limon, Costa Rica). Photo on left shows biogas collection in polyethylene bags with PVC connections. Photo on right shows a two-stage digester treating swine waste, along with suspended biogas collection bags.

Both the swine and dormitory digesters utilized a two-stage digestion design, where two polyethylene bags were linked in series via PVC pipe to partially separate hydrolysis/acidogenesis and methanogenesis. Length-to-width (circumference) ratios of each of the swine and dormitory digester bags were 21:5 and 20:2.5, respectively.

For dairy waste, a singular polyethylene bag (21:8, L : W) served as the sole reactor.

For both the dairy and swine digesters, manure was manually washed from animal stalls twice per day and conveyed in open concrete channels to the digester inlet, which yielded an average daily flow of 2.18 m³/d (dairy) and 4.35 m³/d (swine).

Coarse solids separation preceded digestion in each case.

The human waste digester was fed with flush toilets and shower/sink water from three student dormitories, two laboratories, and one student cafeteria, yielding an average daily flow of 18-25 m³ /d, with variability due to weekday/weekend population differences. Human waste was routed through a septic tank for solids/grease separation, with the supernatant subsequently fed to the digester.

Physical and hydrodynamic characteristics of the three digesters are provided in Table 4-1.

Table 4-1. Physical and Hydrodynamic Design Characteristics of Digesters

Digester	Waste Source	Digester Age (yr)	Loadings per day	Washing time (min)	Digester volume (m ³)	Hydraulic retention time (d)	Organic Loading Rate (kg COD/m ³ /day)
1 ^a	50 Swine	8	1	45	61	14	0.166 – 0.232
2 ^a	60 Cows	8	1	20	85	39	0.146 – 0.162
3	Grey-Black Water	4	Continuous	NA	132	6	0.195 ^b

^a Cow and swine digesters were previously characterized (Lansing et al., 2008).

^b Calculated on the basis of influent COD concentration and hydraulic retention time.

4.2.2 Sampling and Environmental Analysis

Aqueous samples were collected and preserved for analysis during sampling of digester effluent, and pre- and post-MFC treatment at HRTs between 5 min and 3 h.

Grab sampling was performed from the effluent of each digester three times over the course of the study period (July-August 2012), and was used as both inoculum and substrate for MFCs. Dairy and swine digesters were sampled during morning or afternoon washings when effluent flow was at a maximum. For subsequent laboratory-based experiments, approximately 3 L of effluent from each digester was collected less than 24 h before departure from Costa Rica. Digestate was maintained on ice during transport and, at all other times stored at 4°C until use in MFC experiments.

All samples collected in the field were preserved at 4°C and analyzed within 24 h for COD, TS, VS, pH, and alkalinity according to Standard Methods (APHA, 1976). Nutrient samples were acidified (pH < 2; 5N H₂SO₄), filtered to 0.22 µm (for NO₃/NO₂-N, NH₃-N, PO₄-P), and stored at 4°C until analysis. Nutrient concentrations were determined by continuous flow colorimetry using an autoanalyzer with autosampler (Bran & Luebbe TRAACS 2000). Analysis for NH₃-N, NO₂+NO₃-N, TKN, and TP was performed following EPA methods 350.1, 353.1, 351.2, and 365.4, respectively (O'Dell 1993, O'Dell 1993, O'Dell 1993).

4.2.3 MFC Reactor Designs & Fabrication

Three dual-chamber MFC reactors were fabricated and tested in the laboratory prior to field experiments in Costa Rica (see Chapter 3 for detailed design). Briefly, MFCs were machined in-house on a CNC milling machine (Haas Mini Mill) using stock from Plexiglas sheet (0.635-cm thick) and graphite block (G10 grade; Mersen graphite), and were designed as plug-flow reactors with an up-flow, baffle design (Figure 4-2).

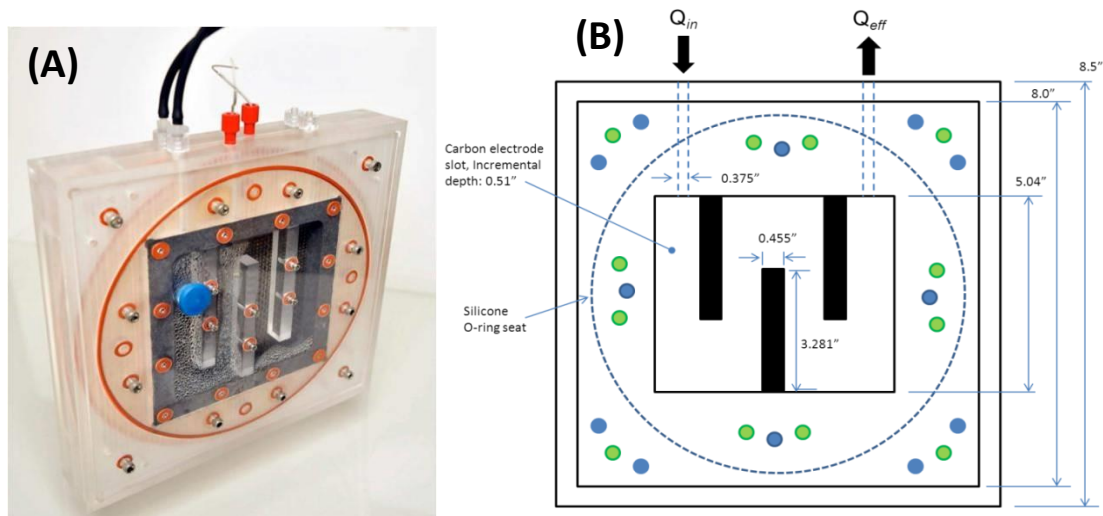


Figure 4-2. Photo (A) and schematic (B) showing the front view of dual chamber, plug-flow MFC reactor. Schematic (not to scale) provides dimensioning of reactor and baffled flow chamber. (V_{an} , 101 mL; V_{cath} , 202 mL; anode depth, 0.5 in; cathode depth, 1 in.

Anodic and cathodic half-cell volumes were 101 mL and 202 mL, respectively, and the exposed anode surface area was 12.80 cm x 12.80 cm ($A_{an} = 163.88 \text{ cm}^2$) for all trials. A Ag/AgCl (3M NaCl) reference electrode (RE-5B, Bioanalytical Systems, Inc.) was mounted inside the anodic half-cell of each MFC. Untreated carbon cloth (Fuel Cell Earth; CC6) served as the anode material. A platinum catalyst layer containing Nafion was applied to the same type of cloth, resulting in 0.45 mg Pt/cm². Squares of the Pt-loaded cloth ($A_{cath} = 163.88 \text{ cm}^2$) served as the cathode for field trials. For subsequent trials in the laboratory, graphite granules packed into the cathode half-cell (Grade 4012; Asbury Graphite; 0.935 cm diam.) served as the cathode. Graphite connected to titanium wires via nylon screws and nuts served as the current collector for the external circuit at both electrodes. The added resistance from electrical connection points was less than 5 Ω in all cases. Electrodes were physically compressed on either side of an anion exchange membrane (AEM, AMI-2000; Ultrex Corp.) in electrode-membrane-electrode configuration. Removal of residual organic

matter and metals from graphite was achieved via 24-hr soaks in 1M NaOH and 1 M HCl, respectively, followed by neutralization in deionized water.

4.2.4 MFC Loading & Operation

Two MFC trials were performed in the field, and the latter was repeated six months later in the laboratory. For field trials, digester effluent that had been sampled and maintained under anoxic conditions for ≤ 5 h, was amended with sodium acetate (10 mM $\text{NaCH}_3\text{COO}^-$), and subsequently gassed with 99% N_2 for 30 min. The amended Digestate was initially fed to the anode chambers of MFC-1, -2, and -3, corresponding to human, dairy, and swine waste, respectively, and served as both inoculum and substrate for the anodic reaction. Flow was turned while the cell potential was maintained at 0.350 V (details provided below) until the onset of catalytic activity (i.e. current production) was observed. At which point, the MFCs were switched to a low flow rate using a peristaltic pump on a timer interval (Q: 0.6 mL/min; HRT: 2.8 h) (Fisher FH100X; 3/8" Tygon) to continuously replenish organic matter and avoid stagnation and solids settling. The same digestate with the acetate amendment served as the substrate over the course of field experiments. No attempts were made to control oxygen levels in the influent reservoirs, and MFCs were maintained at ambient temperature (22-30°C). MFC treatment efficiencies were characterized by sampling influent/effluent points from each of the three anode half cells, a minimum of three times during maximal, stable current production.

For trials subsequently performed in the laboratory, undigested wastewater solids, sampled from the Blue Plains sewage treatment plant in Washington D.C.,

were used as both inoculum and substrate to grow the anodic biofilms, as described in Chapter 3. These MFCs were maintained on a continuous, recycled flow of undigested solids (Q: 20 mL/min) and were electrochemically characterized, as detailed below, for ≥ 1 week after a stable, maximum current was achieved.

Un-amended digestate was then fed to MFCs at a constant flow rate of approximately 20 mL/min (HRT, 5 min), and digestate was continuously recycled from a reservoir that served as both influent and effluent to the MFC. MFCs were maintained at 30°C, and no attempts were made to control for oxygen levels in the digestate.

4.2.5 MFC Electrochemical Analysis

Field MFCs were operated in a 2-electrode configuration using custom designed miniature low-power consuming (battery powered) potentiostats (Northwest Metasystems, Inc.) capable of maintaining a fixed cell voltage ($V_{cell}: E_{cathode} - E_{anode}$) for long-term operation. When just inoculated with AD digestate, open circuit voltages (OCVs) of these MFCs were less than 0.25 V resulting in no current generation until sufficient biofilm formation occurred at the anodes. Once sufficient biofilm formation occurred, OCVs increased above the fixed cell voltage maintained by the potentiostats, triggering the potentiostat to discharge the MFCs. A cell voltage of 0.350 V was used because it is typically the cell voltage that results in maximum power production by MFCs and is comparable to passively discharging current across a variable resistor that is maintained equivalent to the cell's internal resistance. Current and voltage measurements were collected with a data logger (DI-710, DATAQ Instruments, Inc.), logging to an SD data card that was periodically downloaded to a PC. Point measurements of anode and cathode potential (vs. Ag/AgCl, 3M KCl) were also made

3-4 times per day for the duration of field experiments using a hand held multimeter (179, Fluke Corporation). On day 15, the MFCs were allowed to equilibrate for approximately 12 h at open circuit (R_{ext} : 200,000 Ω) prior to performing polarization analysis. Polarization was performed by incrementally reducing external resistance from 200,000 Ω to 2 Ω using a resistor substitution box (Elenco, RS-500) and allowing 25-35 minutes for cell voltage to equilibrate at each resistance value. Separate measurements of anode and cathode potential (vs. Ag/AgCl, 3M NaCl) were also made at each resistance value during polarization. Current (I) and power (P) were calculated according to Ohm's law ($P = IV$ and $V = IR$).

For experiments subsequently performed in the laboratory (United States Naval Research Laboratory, Washington DC, USA, 38.822457,-77.023154), electrochemical analysis was performed using a Solartron 1470E multichannel potentiostat (1470E, Amtek) and Multistat software program (Scribner Associates) when the potentiostat was actually working and not being repaired for the n^{th} time. The anodic biofilms were grown in potentiostatic mode (i.e., 3-electrode configuration), with the anode (working electrode) maintained -0.200 V vs. the Ag/AgCl, 3M reference electrode (≈ 0.005 V vs. SHE) located in the anodic half-cell (BioAnalytical Systems, Inc.) and the cathode serving as the counter/auxiliary electrode. Such a potentiostated configuration ensures that the rate of anode microbial catalyzed oxidation of waste organic matter by the anode is not limited by cathodic overpotential or internal resistance which occurs under two-electrode configurations. This enables determination of the maximum rate of microbial catalyzed oxidation of organic matter possible by the anode as a function of potential applied to the anode. It

also enables determination of the threshold potential for which application of a more positive potential negligibly increases the reaction rate (i.e., I_{Lim} : limiting current). The applied potential of -0.200 V vs. Ag/AgCl was chosen because it approximates threshold potential that known anode reducing bacteria (ARB, e.g. *G. sulfurreducens*) can metabolically utilize for biofilm growth and still achieve limiting rates of organic matter oxidation coupled with transfer of respired electrons to the electrode (Torres, 2010) (Strycharz-Glaven and Tender 2012).

Slow-scan cyclic voltammetry (CV) of the anodes was performed at the start of the experiment, at the onset of catalytic activity, and when maximum current production (i_{max}) to characterize biofilm development. CVs were performed *in-situ* under the same three-electrode configuration using the following parameters: the initial cathodic voltammetric scan ($v < 0$) swept the anode potential from $E_{initial} = -0.800$ V vs. Ag/AgCl to $E_{final} = +0.300$ V vs Ag/AgCl, and was followed immediately by a anodic voltammetric scan from +0.300 V vs. Ag/AgCl to -0.800 V vs. Ag/AgCl; all scans were performed at rates (v) of 1, 2, and 5 mV/sec. In preliminary experiments, it was determined that voltammetric scan rates > 1 mV/s distorted limiting current and peak potentials. Thus, only 1 mV/s scans are displayed in this report.

Once a maximal electric current was achieved under potentiostated conditions (attributed to fully grown anode biofilms), the MFCs were switched to a 2-electrode configuration by connecting the potentiostat reference and counter/auxiliary electrode input leads to the cathode (i.e., the reference electrode not used) and given 24-48 hours to reach a stable open circuit voltage (OCV). Polarization was then performed (V_{cell}

was swept from OCV to 0.005 V; scan rate of 0.1 mV/s). Point measurements of cathode potential during polarization were also recorded to quantify cathode overpotentials. Following polarization, power output was characterized under 2-electrode configuration, where the cathode was poised 0.200 V positive of the anode. Power was calculated via Ohm's law (i.e. $P = IV$), and all current and power measurements were normalized by anode geometric surface area (163.88 cm²) and/or anodic volume (101 mL). All experiments were conducted, at a minimum, in triplicate, and statistical analysis on resulting current/power densities were conducted using the Student's t-test at $\alpha > 99\%$ and t_{crit} : 2.552.

4.3 Results & Discussion

4.3.1 Digester Treatment Efficiencies from Field Study

Two of the three digesters (dairy and swine) were previously characterized in studies by Lansing et al. (Lansing, Botero et al. 2008, Lansing, Viquez et al. 2008) over the course of 9 months for both treatment capacity and biogas production. For the current study, only COD and solids (TS and VS) removal by the digesters were evaluated (Figures 4-3 and 4-4; Table 4-2). Digester treatment values presented here are based on grab sampling of the influent and effluent on three separate occasions (July- Aug. 2012). MFC treatment values are based on comparison of the MFC effluent to MFC influent, sampling each a minimum of two times during continuous

flow operation in-country, and three times during lab experiments in the US (see Section 4.3.2).

Influent organic loads to the dairy and swine digesters had increased relative to previous reports (Lansing, 2008a; 2008b), which we attribute to a decrease in the volume of washing water and/or seasonal variations. Influent COD levels to the dairy and swine digesters were, respectively, 6,334 mg/L and 3,243 mg/L, corresponding to organic loading rates of 0.162 kg COD/m³/d and 0.232 kg COD/m³/d (0.121 and 0.115 kg VS/m³/d), respectively. COD removal efficiencies were comparable to historical data on the digesters, exceeding 85% COD removal by the dairy digester and 93% COD removal by the swine digester after eight years of continuous operation.

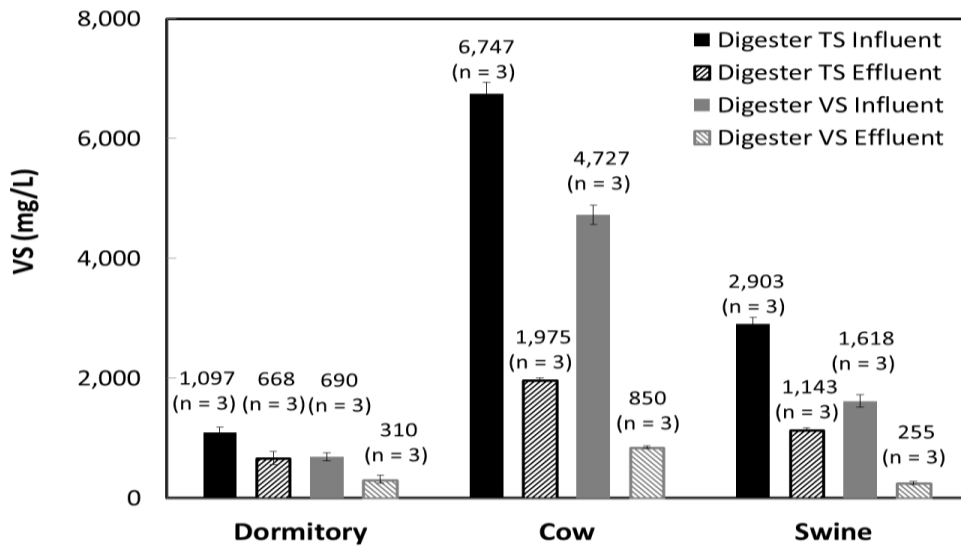


Figure 4-3. TS and VS concentrations (mg/L) at Digester Influent (solid bars) and Digester effluent (hashed bars). TS levels are represented in black; VS levels are represented in grey.

Enhanced COD removal by the swine digester may be due to its different design, being comprised of dual plug-flow reactors in series that enhance hydrolytic and fermentative capacity in comparison to the singular reactor bag that served as the dairy digester (Zahller, Bucher et al. 2007, Parawira, Read et al. 2008). The treatment

efficacy of these particular digesters in comparison to similar, plug flow systems has been previously noted (Lansing, Viquez et al. 2008), and importantly, this data further attests to their robust and long-term performance in a resource-limited setting. In comparison to COD, the total and volatile solids removal rates were somewhat reduced, but in line with the historical data on the dairy and swine digesters. An average of 71% and 61% removal of TS, and 82% and 84% removal of VS was achieved by the dairy and swine digesters, respectively.

Although loading rates had increased somewhat since 2008, the EARTH systems are operated at significantly lower organic loads than literature recommendations for similar plug-flow systems (e.g. 1-6 kg VS/m³/d) (Lettinga 1995, Buysman 2009). An inverse relationship is predicted between organic loading and percent removal rates, with > 60% VS removal predicted at loading rates less than 1 kg/m³/d (Dairy waste biogas handbook- Burke). Thus, the high efficiency for COD and solids removal in these particular digesters is likely attributed to their operation at the lower end of this range.

The dormitory waste was a combined grey/black water stream, and delivered the lowest organic load of the three digesters tested (0.071 kg COD/m³/d; 0.115 kg VS/m³/d). COD removal efficiencies, which had not been previously characterized, were also lower than the other two (74.8% COD reduction), and yielded an effluent stream with higher organic loads than the swine digestate (i.e. 343 mg COD/L in dorm digestate; 220 mg COD/L in swine digestate). Solids removal by the dormitory waste stream was also less efficient than either of the agricultural digesters, and, despite a

lower influent concentration, achieved only 39% and 55% removal of TS and VS, respectively.

The low removal capabilities of the dormitory digester may be the combined result of the digester's relatively short hydraulic retention time (HRT, 6 d), and the presence of surfactants and cleaning products in the influent stream (i.e. visible foaming of the waste stream was observed during sample collection). The fact that the dorm digester was receiving a comparably low organic loading rate (i.e. 0.115 kg VS /m³/d), but treating a significantly lower fraction of the waste suggests that methanogenic activity within the digester was inhibited. It was not assessed if biogas production by the dormitory digester was also inhibited, as the digester was installed after the previous digestion characterization studies occurred.

Table 4-2. Summary of environmental indicators and treatment performance from digesters treating dormitory, cow, and swine waste. Data is presented as the mean \pm standard deviation (n).

		Dormitory Wastewater Digester			Dairy Manure Digester			Swine Manure Digester		
		Digester Influent	Digester Effluent	Removal (%)	Digester Influent	Digester Effluent	Removal (%)	Digester Influent	Digester Effluent	Removal (%)
CO D	(mg/L)	1361 \pm 51 (n=3)	343 \pm 2 (n=3)	74.8%	6334 \pm 276 (n=3)	1108 \pm 41 (n=3)	82.5%	3243 \pm 71 (n=3)	220 \pm 5 (n=3)	93.2%
TS	(mg/L)	1097 \pm 83 (n=3)	668 \pm 107 (n=3)	39.1%	6747 \pm 190 (n=3)	1975 \pm 26 (n=3)	70.7%	2903 \pm 107 (n=3)	1143 \pm 32 (n=3)	60.6%
VS	(mg/L)	690 \pm 71 (n=3)	310 \pm 68 (n=3)	55.1%	4727 \pm 161 (n=3)	850 \pm 22 (n=3)	82.0%	1618 \pm 107 (n=3)	255 \pm 26.5 (n=3)	84.2%
pH			6.23			6.70			7.05	

4.3.2 Microbial Fuel Cell—Treatment Efficiencies

Organics Removal

Field: Field MFC experiments (at a fixed cell voltage, V_{cell} , of 0.350 V) used COD as the sole indicator of treatment efficiency. Figure 4-4 displays the levels of COD in influent and effluent samples to both digesters and fuel cells. Based on comparison of MFC effluent to MFC influent (i.e., AD digestate), MFC treatment efficiency appears to correlate with the COD level of the digestate, in that the MFC receiving the highest influent COD (dairy digestate, 1108 mg/L) also achieved the greatest rate of COD removal (46% reduction; COD_{eff} , 600 mg/L).

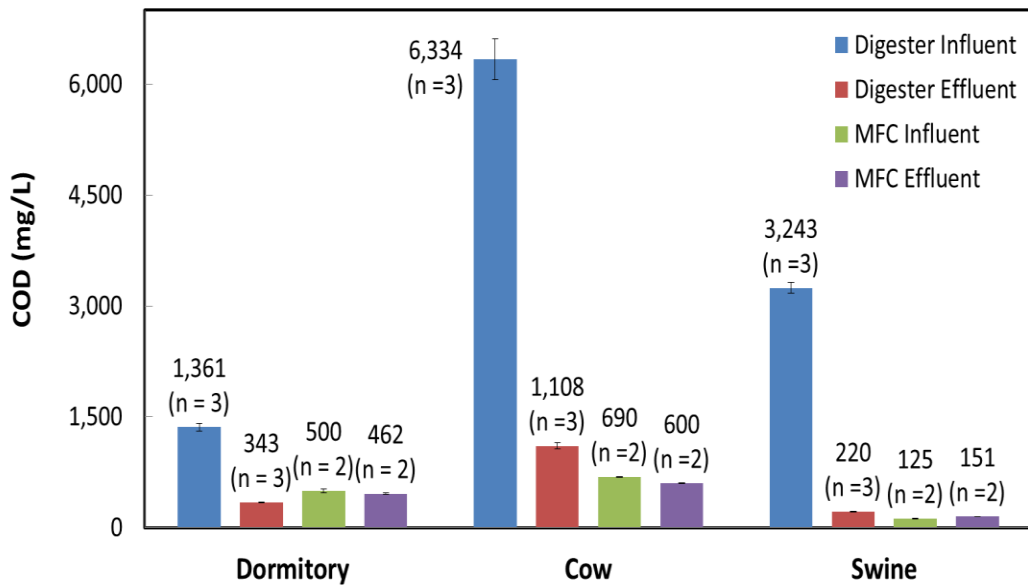


Figure 4-4. COD concentrations (mg/L) from field experiments for: (1) Digester Influent (blue); (2) Digester Effluent (Red); (3) MFC Influent (Green); and (4) MFC Effluent (Purple). Values are presented as the mean (sample size), and error bars represent the standard deviation.

COD from the swine digestate was reduced by 31.6% to a final effluent of 151 mg/L. No COD reductions could be detected from the dormitory digestate through MFC treatment (i.e. 0% removal). Cumulative COD removal from dairy, swine, and dormitory waste by the combined AD-MFC treatment process was thus 90.5%, 95.0%, and 75.0%, respectively. For comparison, AD alone yielded 85%, 93%, and 75% COD removal from dairy, swine, and dorm waste.

Laboratory: Laboratory trials (at a fixed anode potential of -0.200 V vs. Ag/AgCl) evaluated levels of COD, TS, and VS in wastewater samples at the influent and effluent of MFCs as indicators of treatment efficiency. Figures 4-5 displays MFC influent and effluent COD and VS concentrations and Figure 4-6 displays MFC removal rates (% , kg/m³/d) from laboratory experiments.

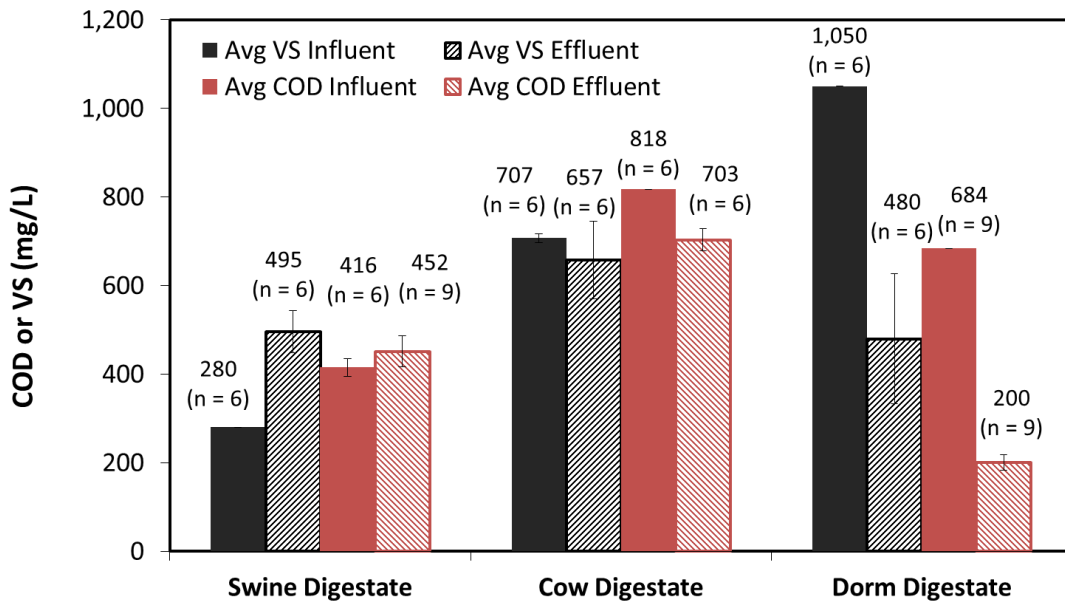


Figure 4-5. Laboratory COD (red) and VS (black) levels at the influent (solid bars) and effluent (hashed bars) of the MFCs when operated at a fixed anode potential of -0.200V vs. Ag/AgCl. Triplicate MFCs were each sampled a minimum of two times. Data values represent the mean (n), and error bars represent the standard deviation.

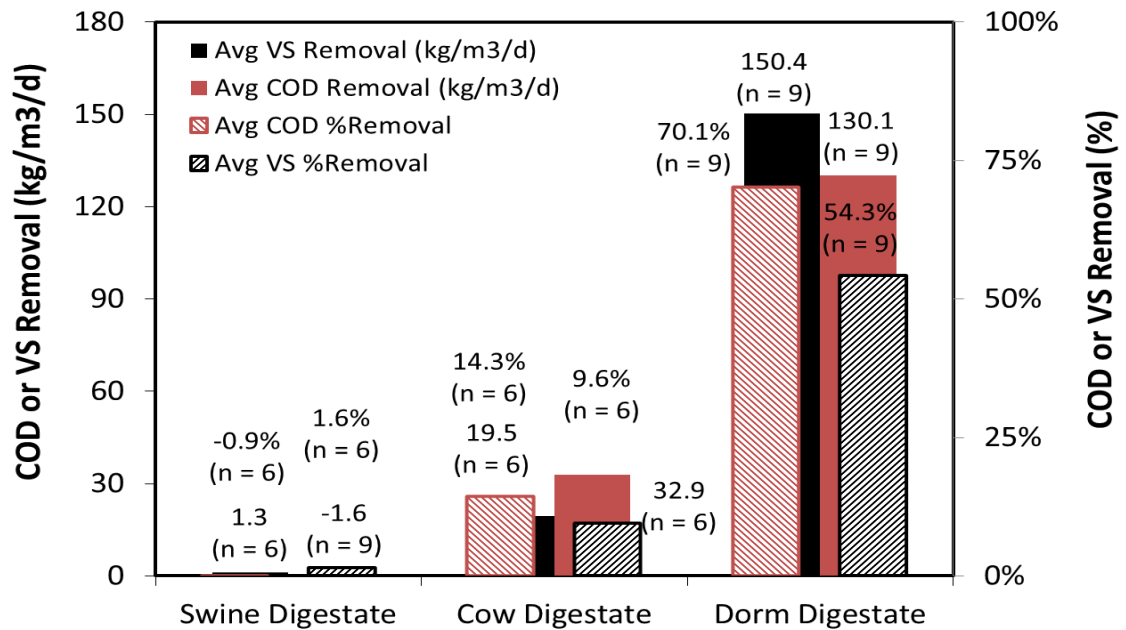


Figure 4-6. COD (Red) and VS (Black) removal rates from MFCs fed with Swine, Cow, and Dormitory Digestate. Removal efficiencies were calculated as a percentage decrease from influent to effluent (%; hashed bars) and as a daily rate (kg/m³/d, solid bars).

Laboratory MFCs fed with dairy and swine digestate achieved lower removal rates (e.g. 0% and 14.3% COD removal, L respectively), in comparison with field experiments. COD and VS removal from the dorm digestate was significantly higher however (70% COD and 54% VS removal). Samples of dormitory digestate collected at the end of field trials and preserved for laboratory experiments contained approximately double the concentration of organic matter—343 mg COD/L versus 684 mg COD/L—than those samples collected and used during field trials. MFC treatment efficiencies may correlate with digester performance. The short HRT of the dormitory digester (i.e., 6 d HRT) may have contributed to higher variability in effluent COD, VS, and TS concentrations. The remaining organic content of dormitory digestate may have had a higher soluble or biologically relevant fraction, which was, in turn, more readily degraded in the MFC. This is consistent with the

results described in Chapter 3, where digestion period serves as an inverse predictor of MFC treatment efficiency. These results corroborate this model, wherein the least treated digestate (i.e. dormitory digestate), yielded the highest levels of COD and VS removal, though this was only true in the laboratory setting, under conditions of a non-limiting cathode.

In comparison to COD levels in the effluent of a treatment wetland (i.e., 2.3 mg/L COD in wetland effluent) that receives the dairy and swine digestate (Lansing, Viquez et al. 2008), the MFC did not provide the same level of COD removal (i.e. >99% removal of COD after wetland treatment). The contribution of dilution rates to calculations of wetland treatment performance was unaccounted for though, and is likely significant, as the treatment wetlands receive both digester effluent and stream diversion inputs. Further evaluation of MFC vs. wetland technology for digestate post-treatment would require inclusion of cost-benefit metrics such as economics, resource recovery, required footprint, etc.

4.3.3 Microbial Fuel Cell—Energy Production

2-Electrode Current/Power—Field Experiments

MFC trials performed in-country utilized miniature, two-electrode potentiostats to maintain a voltage difference of 0.350 V between the anode and cathode of each MFC. The utility of this type of electrochemical instrumentation, which can be powered by the MFC itself (Tender, Gray et al. 2008) is that it allows

true assessment of amount electrical power that can generated by the waste-fed MFCs in oxidizing residual organic matter contained in the AD digestate. Such 2-electrode measurements are however subject to cathode limitations. This is exhibited as an excessive cathode overpotential in which the cathode potential shifts disproportionately negative with current through the external circuit compared to the concomitant positive shift in anode potential. Such 2-electrode measurements are also subject to internal resistance due to low ionic permeability of the membrane required to separate the anode and cathode half cells. Both factors conspire to greatly reduce the rate of organic matter oxidation achieved by effectively driving the anode potential negative the threshold potential. In comparison, this does not occur when operating the MFC in a 3-electrode configuration in which the anode potential is poised vs. a reference electrode positioned in the anodic half-cell, but which requires power to be inputted to the MFC. Point measurements of the anode and cathode potential during biofilm growth (Figure 4-3) revealed the development of significant cathode overpotentials for all of our MFCS as experienced by other (Popat, Ki et al. 2012) (Oh, Min et al. 2004). At the onset of the in-country MFC field trials, cathode OCPs ranged from 0.390 to 0.490 V vs. Ag/AgCl (~ 0.590V - 0.690 V vs. SHE). After 48 h of current discharge however, all cathode potentials dropped by > 0.250 V, and after 200 h, all cathode potentials were < 0 V vs. Ag/AgCl (~ 0.200 V vs. SHE), representing an overpotential of > 0.500 V relative to the theoretical reduction potential of oxygen to water at pH 7 ($E^{0'}$, 0.791 V vs. SHE, $O_2 + 4H^+ + 4e^- \rightarrow 2H_2O$). The cathode chambers were continuously aerated during all experiments. It is therefore unlikely that low bulk

oxygen concentrations are responsible for the cathodic overpotentials we observed but rather associated with proton and/or hydroxyl limitations (Popat, Ki et al. 2012).

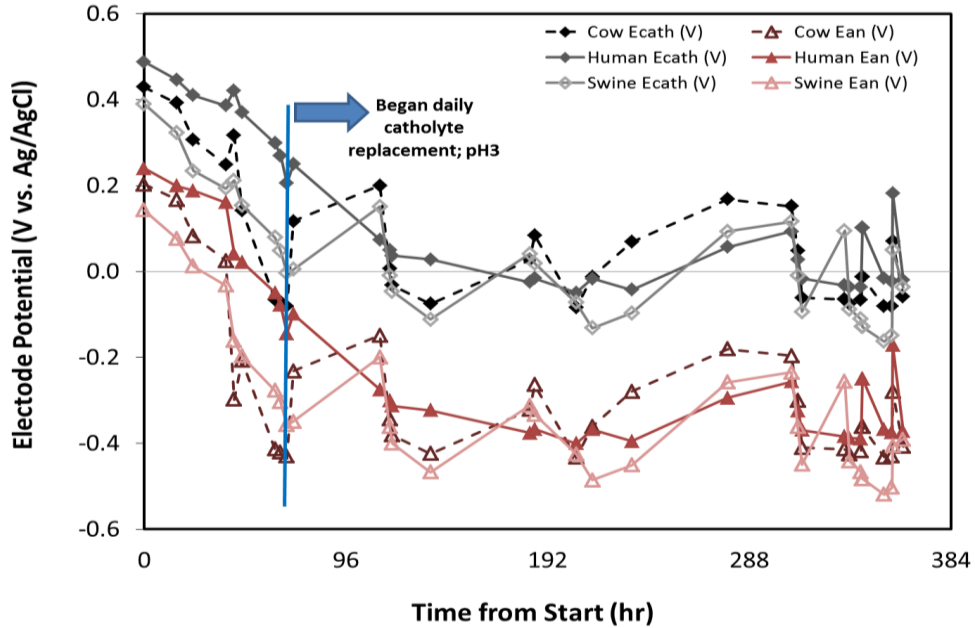


Figure 4-7. Convergence of anode (diamond symbols) and cathode (triangle symbols) potentials during biofilm development of MFCs operated in the field. Anodes were fed with digestate from a dairy manure digester (dashed line, closed symbol), Swine manure digester (solid line, open symbol), and Dormitory wastewater digester (solid line, closed symbol). After hour 60, the catholyte was replaced daily with pH 3 seawater.

For two days following inoculation, these MFCs were incapable of maintaining an open circuit cell voltage > 0.250 V, presumably because anodes had not become sufficiently colonized by ARB. Thereafter, anodes became sufficiently reduced and MFCs were maintained at a cell voltage of 0.350 V while being discharged. Even with the addition of sodium acetate (10 mM) as a supplemental carbon source, the cathodic limitations had the effect of limiting maximum current production to ≤ 4 mA (≈ 300 mA/m²; or ≈ 40 A/m³). The transient spikes in current after this point (Figure 4-4) were due to the addition of dilute acid to the cathode chamber. See section 4.3.4 for description of acid effects on the fuel cell.

The digestate source had some effect on the development of anodic biofilms, in that anodes fed with swine and dairy digestate achieved a potential < -0.250 V vs. Ag/AgCl within 60 h, while the time required for the dormitory-fed anode to become equally reduced was double that of the other two (112 hours) (Figure 4-9). This could be due to either a lower concentration of relevant, anode respiring microorganisms in the dormitory waste compared to the other two wastes, and/or inhibition by surfactants, etc. in the dormitory waste stream. Similar to AD systems, the effect of surfactants or other inhibitory compounds on MFC performance has not yet been evaluated. Despite the increased lag time of the dormitory digestate, all waste streams yielded comparable anode potentials after ≈ 300 h.

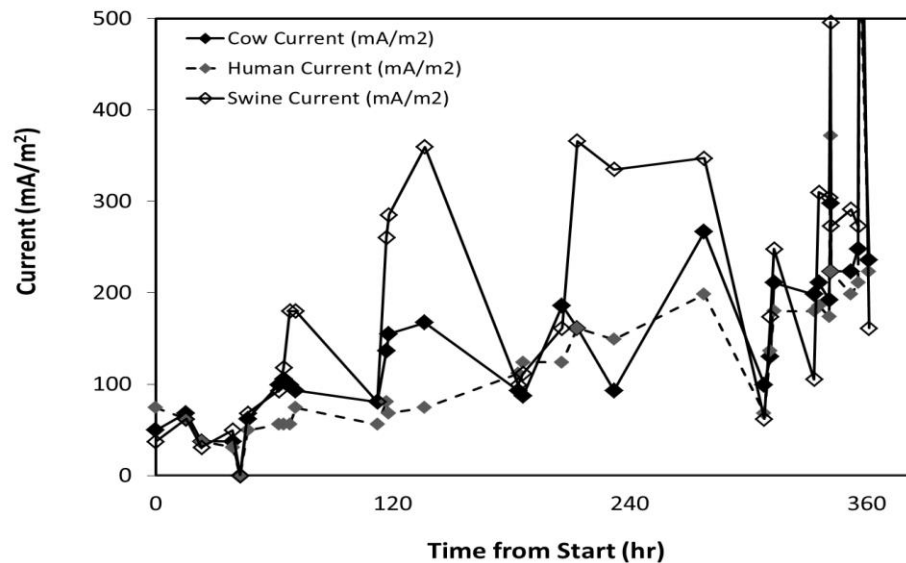


Figure 4-8. Current production (mA/m²) during biofilm development of MFCs fed with digestate from a dairy manure digester (filled symbols, solid line), Swine manure digester (open symbols, dashed line), and Dormitory wastewater digester (closed symbols, dashed line); continuous flow experiment with 2.8 h HRT; V_{cell} : 0.350 V.

Current production from dormitory, dairy, and swine digestate was, respectively, 3.4 mA, 3.6 mA, and 4.4 mA after 360 h of operation at 0.350 V_{cell}

(Figure 4-10). On the basis of anodic volume or surface area, this equates to 34 A/m³ or 210 mA/m² (dormitory); 36 A/m³ or 248 mA/m² (dairy); and 44 A/m³ or 272 mA/m² (swine). Equivalent volumetric power based on anodic half-cell volume was 11.9 W/m³ (dormitory); 12.6 W/m³ (dairy); and 15.4 W/m³ (swine). In field and laboratory experiments, the dormitory digestate yielded the lowest current production (see Section 4.3.5), consistent with the notion that this waste stream is slightly inhibitory and reduces activity of both methanogenic and anode respiring microorganisms.

Polarization analysis was performed after 300 hours of operation in the field, and was preceded by 24 h of equilibration at open circuit conditions. Results of field polarization are displayed in Figure 4-9. All MFCs achieved an open circuit potential (OCP) of > 0.790 V, with $E_{anode, OCP}$ of -0.583 V (dormitory) vs. Ag/AgCl (~-0.383 V vs. SHE), -0.580 V (dairy) vs. Ag/AgCl (~-0.380 V vs. SHE), and -0.534 V (swine) vs. Ag/AgCl (~-0.334 V vs. SHE); and $E_{cathode, OCP}$ of +0.261 V (dormitory) vs. Ag/AgCl (~+0.461 V vs. SHE), +0.210 V (dairy) vs. Ag/AgCl (~+0.410), and +0.229 V (swine) vs. Ag/AgCl (~+0.429 V vs. SHE). Maximum power achieved by the dormitory, dairy, and swine digestate was, respectively, 1.31 mW, 1.27 mW, and 0.57 mW. On the basis of anodic volume or surface area, this equates to 13.1 W/m³ or 81.3 mW/m² (dormitory); 12.7 W/m³ or 78.8 W/m² (dairy); and 5.7 W/m³ or 35.1 mW/m² (swine). The reduced power output by the swine digestate was likely due to the anodic reaction (Figure 4-9B), which achieved a lower OCP than the other two and also had a larger shift in potential during polarization. This was not observed in lab trials, where

the swine digestate yielded the highest maximum power production (See Section 4.3.5).

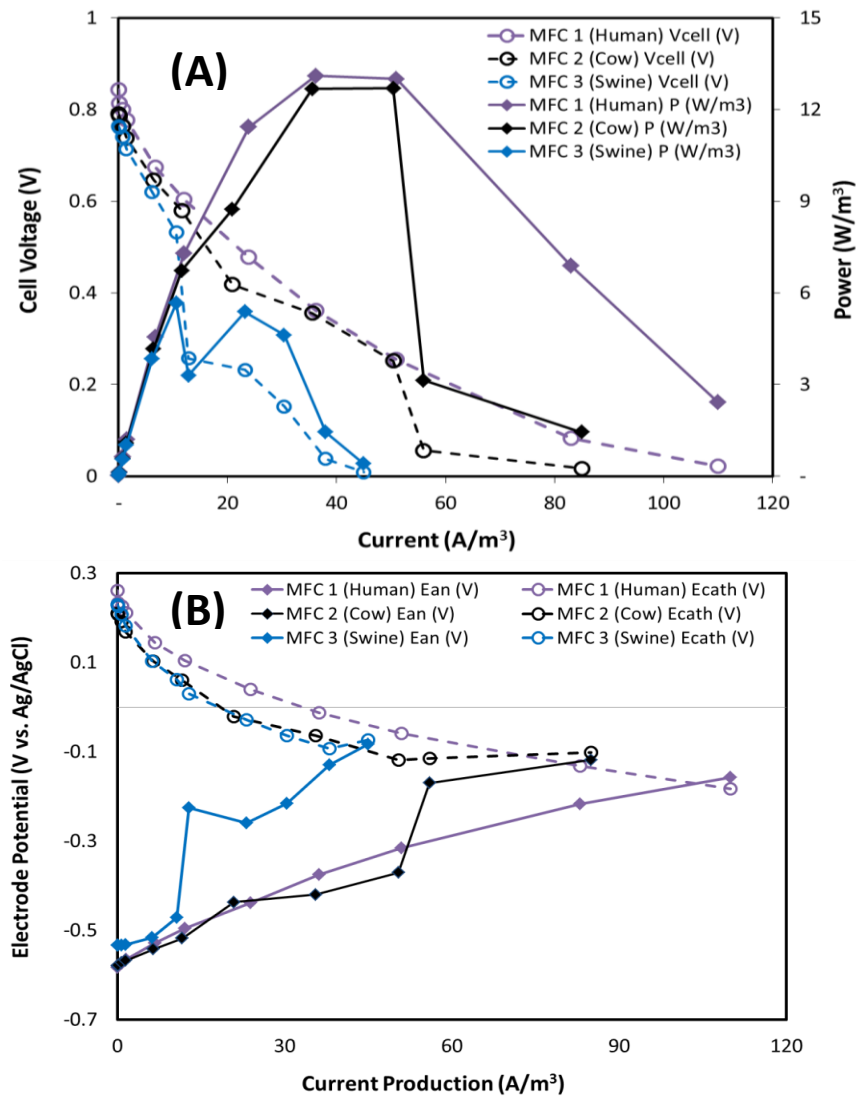


Figure 4-9. Polarization analysis performed in-country on MFCs fed with digestate from a dairy manure digester (black lines), Swine manure digester (blue lines), and Dormitory wastewater digester (purple lines). Polarization was performed through reductions in external resistance from 200,000 Ω to 2 Ω , and recording stable current production after 25 min. Figure (A) shows power (mW/m^2 ; solid lines), and cell voltage (V; dashed lines), as a function of and current (mA/m^2). Figure (B) shows anode potentials (closed symbols) and cathode potentials (open symbols) as a function of current (mA/m^2).

4.3.4 Cathodic Overpotential & pH Effects

The development of cathodic overpotentials was intimately related to the development of the anodic biofilm. In all cases, the anode potential shifted > 0.400 V from the start of the experiment to the point of maximum current production, and stabilized near -0.350 V vs. Ag/AgCl, consistent with presence of a catalytically active biofilm. (Strycharz-Glaven and Tender 2012, Strycharz-Glaven and Tender 2012). At the point when anode potentials reached -0.350 V, current production had increased from approximately 0.6 mA to 1.5 mA (hr 150), which coincided with a drop in cathode potential of approximately 0.500 V from the starting OCP. Presumably, the rate of electron transfer from the anode to cathode was initially faster than the oxygen reduction kinetics at the cathode, resulting in significant charge accumulation and thus, significant cathode overpotential. As has been previously noted (Popat, Ki et al. 2012, Yuan, Zhou et al. 2013), the cathode reaction in MFCs (waste-fed and otherwise) is hindered by the low concentration of protons at the circum-neutral pH conditions required for biological growth. Specifically, the rate of mass transport of protons and hydroxyls within the diffusion layer (i.e. electrode-electrolyte interface) is insufficient, leading to localized pH gradients and dramatic reductions in the rate of abiological reduction of oxygen (Popat, Ki et al. 2012). Acceleration of the cathodic reaction at neutral pH represents a significant impediment to the scaling and advancement of bioelectric technology.

In an attempt to minimize cathode pH limitations during the first trial, 0.5 M H_2SO_4 was replaced as the catholyte after the establishment of a reduced anode (E_{an} , -0.400 V vs. Ag/AgCl) and catalytic activity (> 2 mA) (data not shown). This had the

effect of immediately and permanently raising the cathode potential from -0.100 V to ≥ 0.500 V vs. Ag/AgCl, but also resulted in acidification of the anode chamber and the cessation of current production within two days. Based on these results, it was hypothesized that cathodic pH limitations could be mitigated with the continuous, slow addition of acid to the cathode at a rate equal to the rate of electron/proton release at the anode.

For field trial 2, minimization of cathode pH limitations was evaluated by replacing the catholyte daily, starting at hour 60, and adjusting it to \approx pH 3.0. The catholyte was brackish seawater collected from the Caribbean coast of Costa Rica and stored at 4°C until use, chosen to provide conductivity and minimize solution resistance. Spikes in electrode potentials and current production were observed each time the catholyte was replaced. This had the effect of creating transient spikes in current and power that could not be sustained for more than a few hours (Figure 4-8). These spikes became more pronounced as current production increased, suggesting that the capability for current and power production (i.e. metabolic activity) by the anodic biofilm had grown over time, but was significantly impaired by the cathode reaction. Spikes in current production up to 9.5 mA (589 mA/m² or 95 A/m³; dormitory), 13.1 mA (812 mA/m² or 131 A/m³; swine), and 10.2 mA (632 mA/m² or 102 A/m³; dairy) occurred immediately following the addition of pH 3 seawater as the catholyte, but the effect was transient, with current falling again after < 1 h of catholyte replacement. Catholyte pH was also checked after each addition of fresh seawater (pH 3), and was found to have increased by more than 5 units in < 24 h, with effluent catholyte between pH 8-9.5 in all cases. This may be indicative of a relatively

rapid rate of proton consumption by the cathode that is not matched by the rate of OH⁻ transport across the membrane.

4.3.5 Laboratory Experiments

The MFC experiments conducted in the field were subsequently repeated in triplicate in the laboratory, using a 3-electrode configuration to evaluate the MFC limiting current production from digestate oxidation when not constrained by the cathode reaction or internal resistance. Anodic biofilms of triplicate MFCs, grown under continuous flow of undigested solids achieved steady-state limiting current densities of $813 \text{ mA/m}^2 \pm 133 \text{ mA/m}^2$ ($131 \text{ A/m}^3 \pm 21.5 \text{ A/m}^3$) for $V_{anode} = 0.200 \text{ V}$ vs. Ag/AgCl ($\sim 0.000 \text{ V}$ vs. SHE) after approximately 120 h of growth (Figure 3-13 in Chapter 3). Undigested solids were also used to recover a stable, maximum current between testing of the three digested wastes. Each time a comparable, stable current production was achieved ($800\text{-}1,000 \text{ mA/m}^2$; $129\text{--}161 \text{ A/m}^3$). See Chapter 3 for full description of results with undigested waste.

Swine, dairy, and dormitory digestate was subsequently fed to triplicate MFCs, and flow was recycled (3 L total volume) until substrate was depleted, as evidenced by a decline in current density to $< 50 \text{ mA/m}^2$ ($\approx 0.8 \text{ mA}$). Significantly less current (approximately 10-20%) could be extracted from the digestate than from the undigested wastewater solids, likely owing to a lower fraction of easily degradable organic matter. In all cases, current production rapidly declined once flow of digested waste began but stabilized after approximately 24 h (Figure 4-10). With a fixed anode potential of -0.200V vs. Ag/AgCl, the average current density from the swine, dairy,

and dormitory digestate was $93.0 \pm 16.6 \text{ mA/m}^2$, $165 \pm 62.9 \text{ mA/m}^2$, and $86.0 \pm 16.5 \text{ mA/m}^2$. On the basis of anodic volume, this equates to $15 \pm 2.8 \text{ A/m}^3$ (swine); $27 \pm 10.2 \text{ A/m}^3$ (dairy); and $14 \pm 2.7 \text{ A/m}^3$ (dormitory). These values represent the average, stable current production from the triplicate MFCs after approximately 24 h of continuous, recycled flow without acetate amendments.

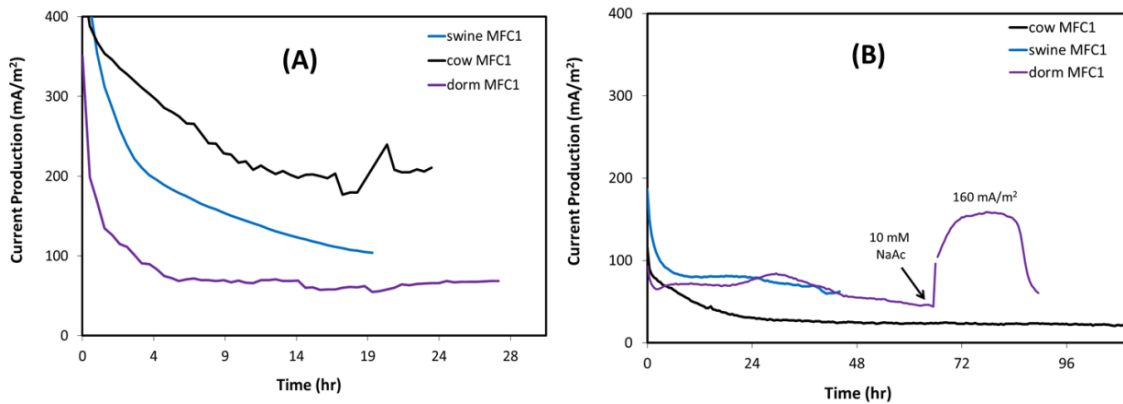


Figure 4-10. Current production from lab trials of MFCs fed with Swine (blue), Cow (Black), and Dormitory (purple) digestate; continuous flow experiment with 5 min HRT. Figure A displays current production with a fixed anode potential of -0.200V vs. Ag/AgCl; Figure B displays current production with a fixed cell voltage of 0.200V.

When the dormitory digestate was later augmented with sodium acetate (10 mM NaAc in Figure 4-11), current increased and stabilized at $681 \pm 265 \text{ mA/m}^2$ ($110 \pm 43 \text{ A/m}^3$), again at a fixed anode potential of -0.200 V vs. Ag/AgCl. This represents a > 600% increase in current from the un-amended digestate, and suggests that significantly higher levels of current production could be attained by reducing the dilution rate of substrate to anodic bacteria (i.e. by increasing the flow rate or reducing HRT of the digested waste). This is analogous to optimizing the food-to-microbe

(F/M) ratios in fixed-film wastewater treatment processes (Tchobanoglous, Burton et al. 2003, Metcalf, Eddy et al. 2010).

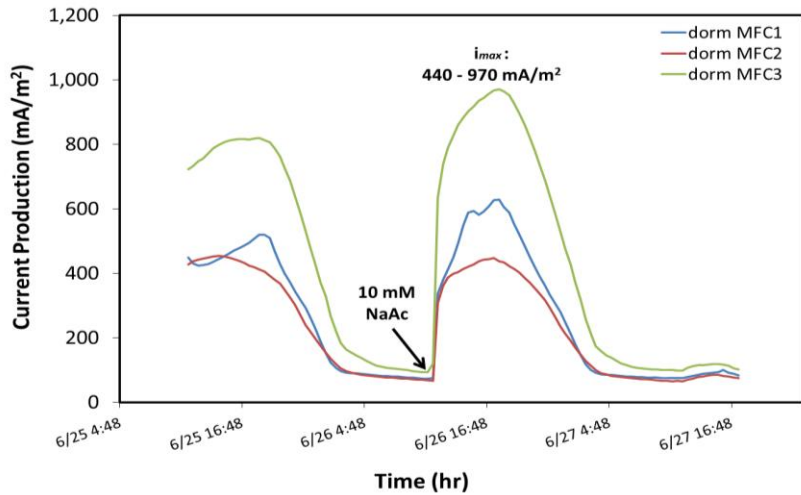


Figure 4-11 Chronoamperometric plot of current as a function of time during lab trials of triplicate MFCs fed with dormitory digestate, illustrating effect of substrate concentration on current when digestate is spiked with sodium acetate (10 mM NaAc). Current production is displayed at a fixed anode potential of -0.200V vs. Ag/AgCl.

The same acetate augmentation was later repeated when the cell voltage was fixed at 0.200 V (2-electrode configuration), and yielded an average, stable current and power of $158 \pm 16 \text{ mA/m}^2$ (25 A/m^3); 31 mW/m^2 (5 W/m^3) from dormitory digestate (Figure 4-10B). This represents a 76% decline in current production in 2- versus 3-electrode configuration under non-limiting substrate conditions.

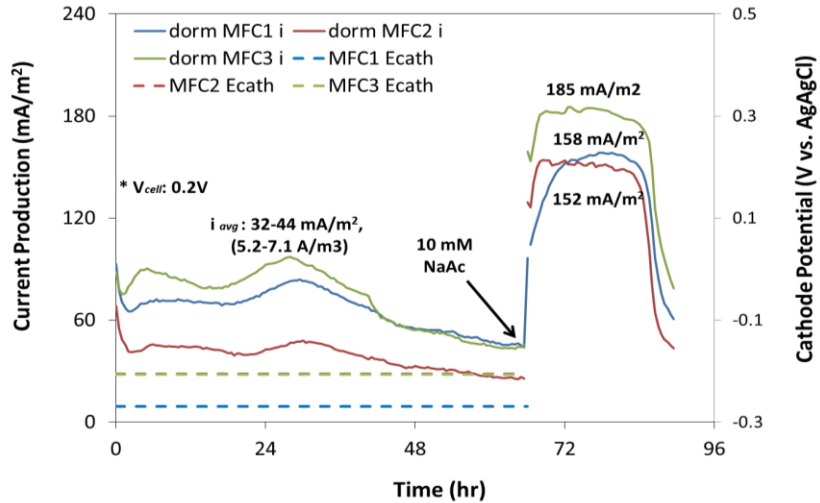


Figure 4-12. Current production from triplicate MFCs fed with dormitory digestate; continuous flow experiment with 5 min HRT; V_{cell} : .200V. Values represent the average, stable current for the experimental condition.

Dairy digestate was similarly augmented with sodium acetate (10 mM) while the cell voltage was fixed at 0.200 V, which resulted in average current/power of 82 mA/m^2 (13 A/m^3 ; 3 W/m^3) representing a 50% decrease in current production from the three-electrode experiment under non-limiting substrate conditions (Figure 4-12). The magnitude of current/power production observed when operated in two-electrode experiments is comparable to what was observed in the field. Importantly though, this confirms the cathodic limitation that was observed in field experiments, and the substrate limitations of using a digested waste stream. Although the digestate still contained a relatively high level of organic matter (i.e. $> 250 \text{ mg VS/L}$; $> 400 \text{ mg COD/L}$), it is likely the case that this was primarily recalcitrant material (e.g. humus; lignin) that would require a significantly longer period for microbial decomposition. These results also highlight an ill-understood phenomena in MFCs - optimization of the anodic reaction (i.e. optimized ARB substrate levels) often comes at the expense of the cathodic reaction (i.e. charge accumulation and cathodic overpotential also increase as anodic reaction rates increase), resulting in energy and power assessments

that are primarily a function of membrane and cathode limitations, and not a representation of the theoretical energy extraction from a given waste source. Efforts must be taken to identify and isolate the limiting reaction, so that energy potential is not under-represented.

Polarization analysis performed in the lab yielded average maximum power densities of $5.0 \pm 0.2 \text{ W/m}^3$ (dormitory; $n = 3$); $8.0 \pm 1.2 \text{ W/m}^3$ (dairy; $n = 3$); and $10.0 \pm 1.6 \text{ W/m}^3$ (swine; $n = 3$) at cell voltages between 0.27 V and 0.31 V. Lab trials yielded somewhat lower levels of limiting power and current, compared to what was observed in the field (Figure 4-13). Average maximum power from field and lab evaluations was, respectively, 81.3 mW/m^2 ($n = 1$) vs. $28 \pm 1.3 \text{ mW/m}^2$ ($n = 3$) from dormitory digestate; 78.8 mW/m^2 ($n = 1$) vs. $52 \pm 7.4 \text{ mW/m}^2$ ($n = 3$) from dairy digestate; and 35.1 mW/m^2 ($n = 1$) vs. $60 \pm 10.1 \text{ mW/m}^2$ ($n = 3$) from swine digestate. Limiting current densities during polarization were also somewhat lower than what was achieved in field trials (i.e. i_{max} , 375 mA/m^2 vs. 700 mA/m^2), which is likely indicative of the substrate limitation of the waste when not amended with acetate. The reduced power extraction from dormitory digestate was observed in polarization, as it was in all electrochemical measurements, suggesting again that the surfactants or other anti-microbial agents may impair ARB activity and reduce energy gains in any domestic waste-fed MFC system.

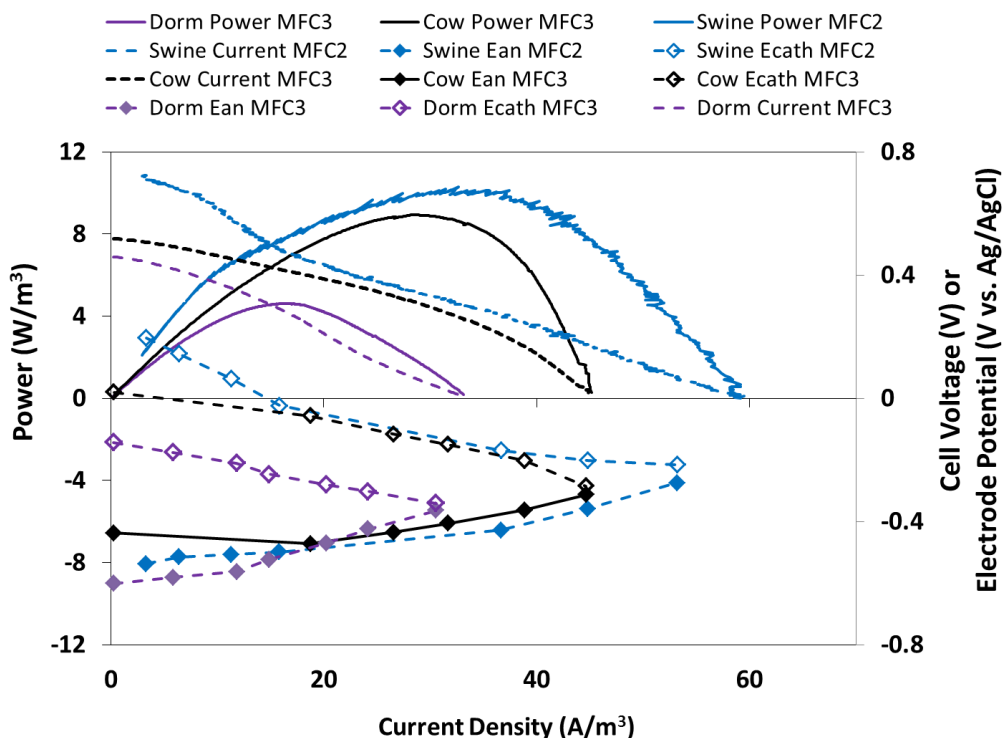


Figure 4-13. Polarization analysis from lab trials of MFCs fed with Swine (blue), Cow (Black), and Dormitory (purple) digestate. Power curves (solid lines); cell voltage (dashed lines); cathode potential (open symbols); anode potential (closed symbols).

In all cases power density was constrained by the cathode reaction during polarization. Average shifts in electrode potentials from open circuit to closed circuit conditions were: $\Delta E_{anode, dormitory}, 0.253 \pm 0.035 \text{ V}$ ($n = 3$) and $\Delta E_{cathode, dormitory}, 0.178 \pm 0.024 \text{ V}$; $\Delta E_{anode, dairy}, 0.229 \pm 0.086 \text{ V}$ ($n = 3$) and $\Delta E_{cathode, dairy}, 0.320 \pm 0.052 \text{ V}$; $\Delta E_{anode, swine}, 0.206 \pm 0.090 \text{ V}$ ($n = 3$) and $\Delta E_{cathode, swine}, 0.395 \pm 0.022 \text{ V}$ (Figure 4-13). Graphite granules were replaced twice during lab experiments to check for cathode bio-fouling; however, no significant difference in cathode OCP or overpotential were observed with the clean granules. The significant polarization of the cathode is consistent with field experiments, demonstrating that cathodic losses constrain MFC current/power production.

4.3.6 Voltammetry

Slow scan voltammetry was used to confirm the electrochemical current response of the anode reaction when fed with undigested vs. digested waste. Representative voltammograms are displayed in Figure 4-14. In comparison to voltammetric responses from undigested waste, all digestate-fed anodes exhibited significantly smaller redox peaks and approximately $\frac{1}{4}$ to $\frac{1}{2}$ the limiting current response at anode potentials > 0 V vs. Ag/AgCl (voltammogram in red in Figure 4-15). Such voltammetric features confirm the substrate deficiencies that were observed during chronoamperometry of the digested waste. Positive (i.e. anodic) current response began at anode potentials greater than -0.500 V vs. Ag/AgCl and maximum, limiting current response was observed at anode potentials > 0 V vs. Ag/AgCl. This provides a valuable thermodynamic baseline for ARB activity, in that anode potentials must remain within this window to provide a sufficient energetic benefit for microbially catalyzed anode respiration. If cathodic activity becomes significantly limited, such that excess charge builds up at both cathode and anode, it has the effect of eliminating the thermodynamic benefit for the biofilm and creating a condition equivalent to open circuit operation.

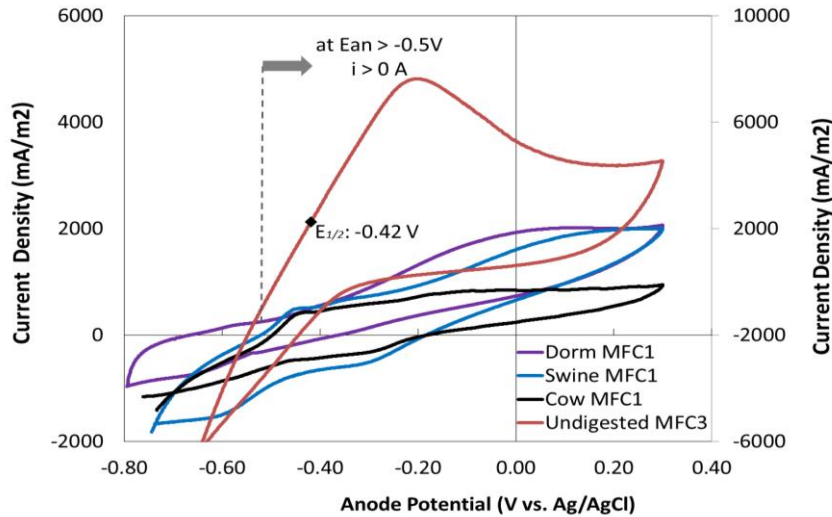


Figure 4-14. Representative voltammograms from MFCs fed with cow (black), swine (blue), and dormitory (purple) digestate. Voltammogram from undigested latrine solids (red line) is provided for comparison of magnitude of current production and current-potential dependency. Scans were recorded at 0.001 V/s from -0.8 V to +0.3 V and back to -0.8 V vs. Ag/AgCl, 3M KCl

4.3.7 Mass Balance of Wastewater Treatment & Energy Production

An empirical mass balance over the digester and MFC was performed for laboratory experiments on the basis of: COD, VS, and energy resulting from each process. Calculations were carried out in units of kg/d for masses, m³/d for flows, and MJ/d for energy. The energy content (HHV) of biogas was approximated as 25.7 kJ/L (Murphy, McKeogh et al. 2004, Buysman 2009), and the maximum power production by the MFCs, as predicted by polarization analysis during laboratory experiments, was used to estimate energy output from the MFC. Table 4-3 summarizes the field and lab results, respectively, of the mass balance for dormitory, swine, and dairy waste. Maximum MFC power density (5-13 W/m³) translated into an equivalent daily energy production of 1.5 – 3.8 MJ/day assuming a continuous flow of swine, cow, and dormitory digestate at a rate of 4.36, 2.18, and 22.0 m³/d, respectively (based on

influent flow rate to full-scale digesters). Biogas energy yields, in comparison, provided ≥ 100 times more energy than the MFCs—ranging from 150- 820 MJ/day. This is consistent with previous empirical and theoretical work on estimated energy production from AD & MFC systems (Clauwaert, Toledo et al. 2008, Weld and Singh 2011). On a daily basis, the digesters discharged 1.8 – 15 kg COD and 1.2 – 23 kg VS, where the highest mass rates corresponded to the dormitory digester; MFCs discharged 1.5 – 4.4 kg COD and 1.4 – 10.1 kg VS per day. A similar mass balance was performed on field data as well; results are in Appendix B.

Table 4-3 Empirical mass balance for COD, VS, and energy produced by AD-MFC treatment; laboratory MFC data was used for all calculations

	Parameter	Dormitory Waste	Swine Waste	Dairy Waste
	Q (m³/day)	22	4.36	2.18
	COD_{in}-AD (kg/day)	22.9	14.1	13.8
Lab Samples	COD_{eff}-AD (kg/day)	15.1	1.81	1.78
Lab samples	COD_{eff}-MFC (kg/day)	4.40	1.97	1.53
	VS_{in}-AD (kg/day)	15.2	7.05	10.3
Lab Samples	VS_{eff}-AD (kg/day)	9.06 - 23.1	1.22 - 1.88	1.54 - 1.54
Lab Samples	VS_{eff}-MFC (kg/day)	5.08 - 10.6	2.16	1.43
	E_{out}-AD (MJ/day)	824	154	707
	E_{out}-MFC (MJ/day)	1.90	3.77	1.51

4.4 Conclusions

In this continued study on the use the MFC for post-treatment of anaerobically digested waste, we demonstrate the comparative results of field and lab MFC deployment at the effluent of dairy, swine, and dormitory digesters. Results indicate a maximum volumetric power of 5-13 W/m³ under the continuous flow of substrate,

equating to a daily energy production of 1.5 – 3.8 MJ/day. Biogas energy yields, in comparison, provided > 100 times more energy than the MFCs—ranging from 150-820 MJ/day. MFC power/energy production was ultimately constrained by the cathode reaction (representing an overpotential of ~0.500 V), as well as substrate limitations is the already digested waste. COD removal efficiencies in the MFC ranged from 0-70%, equating to daily removal rates of 0 – 0.778 kg COD/m³/d (HRT, 168 min) and 0-130 kg COD/m³/d (HRT, 5 min).

Acknowledgements

This work was supported by in part by a grant from the University of Maryland's Institute for International Affairs through their International Travel Fund, the Department of Environmental Science and Technology at the University of Maryland, as well as the Bill & Melinda Gates Foundation (Grant 01566000547) and the US Naval Research Laboratory. K.G. was also supported by a fellowship from the A. James Clark School of Engineering at UMD. We thank the laboratory staff and students at EARTH University, including Jane Yeomans, Herbert Arrieta, Luis Emilio Pineda, and Oscar Hugo Mendez Esquivel. We also thank Greg Phillips at DC WATER (Washington D.C.) for assistance with nutrient analysis.

Chapter 5 : Iron(II)-Dependent Denitrification by a High-Current Density Bio-Cathode

5.1 Introduction

Extraction of energy from wastewater by microbial fuel cells (MFC) is an often-proposed application of bioelectrochemical systems (BES) (Lefebvre, Uzabiaga et al. 2011, McCarty, Bae et al. 2011, Logan and Rabaey 2012, Schröder 2012). Conversion of the biochemical energy stores in domestic sewage ($\approx 14\text{-}16$ kJ/g COD; $0.4 - 23.3$ kWh/m³ or $1.5\text{-}96$ kJ/m³) would represent significant reductions in energy consumption by the water and wastewater sectors, where demand currently represents 2 - 4% of the US national energy budget (e.g. $0.2 - 1.0$ kWh/m³ required for treatment of sewage) (Christensen and McCarty 1975, McCarty 1975, Mitchel and Gu 2010, Rothausen and Conway 2011).

The anodic reaction of MFCs is relatively well understood, whereby anode respiring bacteria (ARB, e.g. *Geobacter sulfurreducens*, *Shewanella putrefaciens*) serve as electrochemical catalysts capable of coupling oxidation of organic matter with reduction of a non-corrosive electrode (e.g. graphite) (Bond, Strycharz-Glaven et al. 2012). The rate at which ARB can transfer electrons to the anode (measured as anodic current density) in waste-fed MFCs is primarily limited by the low concentration of substrate (i.e. 1-3 mM acetate) in domestic sewage (Rabaey, Clauwaert et al. 2005,

Rodrigo, Cañizares et al. 2007). By controlling the substrate dilution rate however (i.e. reducing retention times), waste-fed anodes can achieve relatively high current densities (e.g. 2-4 A/m²) and minimal anodic overpotential (e.g., 0.070 V) representing a relatively optimized anode reaction and a high potential for energy/power generation from waste (Katari and Scott 2010).

Realization of energy from waste-fed MFCs, however, is dependent on a non-limiting cathode (i.e. > -2 A/m² current density and minimized overpotential). The vast majority of waste-fed MFCs to date have relied on the oxygen reduction reaction (ORR) at the cathode, owing to its high thermodynamic potential (i.e. +0.791 V vs. SHE, pH7) and availability of oxygen as a sustainable oxidant (i.e. air). It is increasingly recognized however, that abiotic oxygen reduction is not optimal for MFC cathodes owing to the requirements for circum-neutral pH and temperature (i.e. pH 7, 30°C)—conditions that are required for biological growth at the anode, but that simultaneously reduce ORR kinetics by limiting the concentration of protons and increasing activation energy (Baturina and Smirnova 2013). The low solubility of oxygen in freshwater (8.2 mg/L at 25°C) further contributes to ORR rate reductions, albeit to a lesser degree as predicted by the Nernst equation (Gil, Chang et al. 2003, Freguia, Rabaey et al. 2008, Rismani-Yazdi, Carver et al. 2008, Papat, Ki et al. 2012). These conditions result in dramatic reductions in cathode potential, cell voltage, and power (i.e. $V_{cell} = E_{cath} - E_{an}$; $P = IV_{cell}$). Moreover, known abiological oxygen reduction catalysts (e.g. platinum) are rapidly fouled by organic waste by-products (e.g. hydrogen sulfide), and are ill-suited for scalable, cost-appropriate systems (Jang, Chang et al. 2004, Niessen, Schröder et al. 2004).

Biological catalysis of oxygen reduction represents one promising, low cost solution to cathode limitations that has received considerable attention (Freguia, Tsujimura et al. 2010, Ter Heijne, Strik et al. 2010, Strycharz-Glaven, Glaven et al. 2013). Oxygen reducing bio-cathodes have been successfully enriched from a number of environmental sources, including aerobic/anoxic sludges, soils, as well as fresh and seawater (Huang et. al, 2011; Rosenbaum et al., 2011). Analysis of the microbial composition of electrode-attached biofilms has revealed a high diversity of organisms, often dominated by members of the *Proteobacteria* and *Bacteroidetes* phyla (Erable et al., 2012; Rabaey et al., 2008; Zhang et al., 2011).

Certain members of these phyla are known to thrive in micro aerobic zones (such as the benthic marine layer or the oxic-anoxic interface in freshwater sources), where they derive a relatively small energetic benefit by coupling iron-oxidation to oxygen reduction, i.e. ΔG° , 29 kJ/mol Fe(II) (Neubauer, Emerson et al. 2002, Bird, Bonnefoy et al. 2011, Hedrich, Schlömann et al. 2011). Microbial electrode oxidation may be thought of as an analogous process to biological iron oxidation in micro aerobic environments and may explain the presence of iron-oxidizing species reported in bio-cathode biofilms (Strycharz-Glaven, Glaven et al. 2013).

A number of oxygen reducing bio-cathodes have achieved cathodic current densities exceeding 1 A/m², and the onset of biological catalysis has been demonstrated at potentials exceeding 0.100 V vs. Ag/AgCl (\approx 0.300 V vs. SHE) (Freguia, Tsujimura et al. 2010, Ter Heijne, Strik et al. 2010, Strycharz-Glaven, Glaven et al. 2013). While oxygen reducing bio-cathodes hold great promise for

certain BES applications, their applicability to waste-driven MFCs may prove to be limited because of the added complexity and cost of a second biological reactor that may require aeration to maintain oxygen levels and that does not serve an essential waste treatment function. Thus, a significant need exists for a waste-relevant reduction reaction occurring at thermodynamically favorable potentials (i.e. $E_c > 0$ V vs. SHE) for MFC cathode reactions in order to improve power output.

An alternative to oxygen reduction is biologically mediated denitrification, which is catalyzed by anaerobic organisms that couple iron(II) oxidation to nitrate reduction. A review of the relevant half reactions (Table 5-1) indicates that the thermodynamic potential range for iron-dependent nitrate reduction is similar to that of iron-dependent oxygen reduction.

Similar to oxygen reducing species, microorganisms capable of coupling Fe(II) oxidation to NO_3^- reduction do so for a relatively small energetic benefit, i.e. $\Delta G^{\theta'}$, -264.9 kJ/mol NO_3^- ; -53.0 kJ/ e^- eq for complete denitrification (NO_3^-/N_2 , $n = 5$) with ferrous carbonate (FeCO_3) oxidation (Benz, Brune et al. 1998, Bird, Bonnefoy et al. 2011, Hedrich, Schlömann et al. 2011, Carlson, Clark et al. 2012). In comparison, Fe(III) reducing bacteria (such as *Geobacter* spp.), identified as anode microbial catalysts, may derive -816.6 kJ/mol or -102.1 kJ/ e^- eq from the oxidation of acetate (McCarty 1975). The speciation of the $\text{Fe}^{2+}/\text{Fe}^{3+}$ couple, as well as the NO_3^-/N_2 (+0.710 V), $\text{NO}_3^-/\text{NO}_2^-$ (+0.430 V), or $\text{NO}_3^-/\text{NH}_4^+$ (+0.360 V) reduction pair greatly influences the energy available of the reaction. For example, microbial oxidation of ferrous carbonates, the most frequently reported microbial reductant at circum-neutral pH occurs in a potential window of +0.220 V ($\text{NO}_3^-/\text{NO}_2^-$) to +0.549 V (NO_3^-/N_2)

(Straub, Benz et al. 1996, Benz, Brune et al. 1998). This metabolic flexibility allows anaerobic iron-oxidizing bacteria to thrive in a variety of habitats.

Nitrate dependent iron oxidizing bacteria have been successfully isolated from anaerobic sediments, as well as from marine, brackish, fresh and wastewaters, where they have primarily been identified as *Proteobacteria* (Nielsen and Nielsen 1998, Straub, Benz et al. 2001, Straub and Schink 2004, Hedrich, Schlömann et al. 2011). The majority of reports utilize ferrous carbonates as the electron donor for culturing the bacteria in solution, with limited reporting on the effects of using less soluble iron species for iron oxidation (Kumaraswamy, Sjollem et al. 2006). The energetics, as well as kinetics, of strict autotrophic growth on iron(II) are extremely poor (Neubauer, Emerson et al. 2002, Hedrich, Schlömann et al. 2011). Autotrophic species that have been identified have all exhibited significantly slower growth and NO_3^- reduction kinetics (Widdel, Schnell et al. 1993, Straub and Schink 2004). As such, iron-dependent nitrate reducing bacteria have primarily been found to be heterotrophs, requiring an auxiliary carbon source for growth on iron. Similarities in microbial composition and thermodynamic range of iron-dependent nitrate reducers to the microbial composition of characterized oxygen reducing bio-cathode biofilms (Benz, Brune et al. 1998, Straub, Benz et al. 2001, Hedrich, Schlömann et al. 2011) suggests that selective enrichment for nitrate reducers could result in a bio-cathode community optimized for nitrate rich waste streams.

Table 5-1. Redox half reactions and associated formal potentials relevant to bio-cathodes

Reaction	Half Reaction Equation	Biological Formal Potential ($E^{0'}$, V vs. SHE)
1		
2	$O_2 + 4H^+ + 4e^- \rightarrow 2H_2O$	+0.791
3	$2NO_3^- + 12H^+ + 10e^- \rightarrow N_2 + 6H_2O$	+0.749
4	$NO_3^- + 2H^+ + 2e^- \rightarrow NO_2^- + H_2O$	+0.420
5	$NO_3^- \rightarrow NH_4^+$	+0.360
6	$Fe^{2+} \rightarrow Fe^{3+} + e^-$ (pH 2)	-0.770
7	$Fe^{2+}(\text{citrate}) \rightarrow Fe^{3+}(\text{citrate}) + e^-$	-0.370
8	$FeCO_3 \rightarrow Fe(OH)_3 + e^-$	-0.200
9	$Fe^{2+}(\text{EDTA}) \rightarrow Fe^{3+}(\text{EDTA})$	-0.096
10	$Fe^{2+}/\alpha\text{-FeOOH}_{\text{solid}}$	+0.274
11	$Fe^{2+}/\alpha\text{-Fe}_2\text{O}_3 \text{ solid}$	+0.287
12	$Fe^{2+}/Fe_3O_4 \text{ solid}$	+0.314

*Values are provided at biological standard conditions (298K, 1 atm, 1 M activity except $[H^+] = 10^{-7}$; adapted from Bird et al, (2011); McCarty (1974)

Increasing the solubility of the Fe^{2+} through chelation with EDTA has been shown to improve microbial energetics, described as reaction 9 in Table 5-1 (Kumaraswamy, Sjollem et al. 2006); however, it is unclear if enrichment on more favorable electron donors would impact the catalytic redox potential in an electrode-grown biofilm.

A number of the technological hurdles currently associated with the MFC make the possibility of a denitrifying bio-cathode appealing. First, a nitrate reducing bio-cathode capable of high-rate nitrate removal at $> 0V$ vs. $Ag/AgCl$ (i.e. $> 1 A/m^2$) could represent significant improvements in in power/energy from MFCs (i.e. $V_{cell} = E_{cath} - E_{an}$; $P = iV$). In addition, the anaerobic respiratory pathways of denitrifiers open up the possibility for an anaerobic, single-chamber MFC reactor, thereby eliminating costly and ineffective oxygen-exclusion membranes (e.g. Nafion). Such elimination

would further reduce internal resistance, theoretically increasing power, and significantly reduce reactor cost and complexity. From an environmental perspective, a bio-cathode would provide the added benefits of nitrate/nitrite removal from waste streams, which are regulated as contaminants by the USEPA; and elimination of energy requirements for cathode aeration, either biological or abiotic.

Previously reported work on bio-cathodic denitrification has been limited, and to date, there has been no electrochemical characterization of a mixed community performing denitrification at the cathode. The early work of Gregory et al., (2004) (Gregory, Bond et al. 2004) and more recently Su et al, (2012) (Su, Zhang et al. 2012) reported bio-cathodic denitrification at a poised electrode; however, in both cases, strains of ARB not known to catalyze iron-dependent denitrification were used (i.e. *G. sulfurreducens* and *Pseudomonas alcaliphila*). As a result, highly reducing electrode potentials were required (-0.500 V vs. Ag/AgCl; \approx -0.300 V vs. SHE) to maximize the energetic benefit from electrode oxidation. While these studies demonstrate plausibility of cathode-dependent denitrification, catalytic activity at such a reduced potential would require that power be supplied to a MFC (i.e., a microbial electrolysis cell, MEC) to drive the reaction since typical MFC/MEC anode potentials are $>$ -0.200 V vs Ag/AgCl (\approx 0.00 V vs SHE).

In contrast to the above pure culture studies, Rabaey and colleagues have successfully enriched for mixed-consortia denitrifying bio-cathodes in dual-chamber, MFC configurations where power/energy can theoretically be realized from the fuel cell (Clauwaert, Rabaey et al. 2007, Viridis, Rabaey et al. 2008, Viridis, Rabaey et al. 2010, Viridis, Read et al. 2011). Under conditions of maximum current production (i.e.

closed circuit between anode and cathode; $E_{an} \approx E_{cath}$), where no power is realized, reports of cathode potentials have ranged from -0.480 V to -0.306 V vs. Ag/AgCl (\approx -0.280 V to -0.106 V vs. SHE) (Clauwaert, Rabaey et al. 2007, Viridis, Rabaey et al. 2008, Viridis, Read et al. 2011). The correlation between MFC power production and nitrate loading rates in these MFCs; however, current/power limitations caused by cathodic overpotential were not elucidated. Clauwaert et al. (2007) and Viridis (2008) both report high rates of NO_3^- removal under short-circuit conditions (e.g. 0.100 – 0.400 kg $\text{NO}_3\text{-N}/\text{m}^3/\text{d}$); however, denitrification could not be accomplished by the cathode when the MFC was operated to produce maximum power (i.e. V_{cell} , 0.300 V; E_{cath} , 0.00V vs. SHE) or at open circuit conditions. Although cathodic overpotential was not elucidated in either case, these factors, as well as their relatively low open circuit voltages, are both consistent with a significant cathode limitation where ultimate power output will be significantly reduced.

From a microbial enrichment perspective, little has been reported concerning organic carbon requirements of iron(II)-dependent denitrifiers, with the presumption that strict autotrophic organisms would grow to utilize the electrode as the sole source of electrons (Park, Kim et al. 2005, Clauwaert, Rabaey et al. 2007, Puig, Coma et al. 2012). As noted above, the majority of isolates performing iron-dependent denitrification have been heterotrophic. It is thus likely that denitrifying bio-cathodes will also require an auxiliary carbon source for growth. One report from (Jeremiase, Hamelers et al. 2012) may also support this hypothesis, where start-up time of an H_2 producing bio-cathode was significantly reduced when supplied with an organic carbon source.

Drawing from the biological precedent that has been established for Fe(II)-dependent denitrification, we aim to illustrate methods for the systematic enrichment for a high current density bio-cathode reaction for BES application. Specific objectives of the project are:

1. To perform planktonic growth experiments to enrich for Fe(II)-dependent denitrifying organisms from environmental inocula
2. To transfer environmental enrichments to electrochemical growth reactors and further isolate the consortia for a denitrifying consortia that uses an electrode as the sole electron donor
3. To electrochemically characterize the bio-cathode using chronoamperometry and slow-scan voltammetry under catalytic and non-catalytic (non-turnover) conditions
4. To microbiologically characterize scrapings from the bio-cathode using 16s rRNA gene sequencing

Results indicate that the enriched bio-cathode catalyzes cathode oxidation coupled to NO_3^- reduction at potentials less than $-0.150 \text{ V vs. Ag/AgCl}$ ($\approx 0.050 \text{ V vs. SHE}$). The bio-cathode has an apparent limiting current density of 3.2 A/m^2 , which is reached at cathode potentials less than $-0.350 \text{ V vs. Ag/AgCl}$ ($\approx -0.150 \text{ V vs. SHE}$). This is the highest current density reported to date from a denitrifying bio-cathode, and is comparable in magnitude to the current production by mixed- and pure culture anodic biofilms.

5.2 Materials & Methods

5.2.1 Sampling

Environmental inocula were collected from three sites: (1) freshwater sediment from the Potomac River (Rock Creek tributary) in Washington, D.C. at approximately 38° 55' 49.18", -77° 3' 39.66"; (2) freshwater sediment from Paint Branch Creek in College Park, MD at approximately +38° 59' 37.94", -76° 56' 14.20", and (3) denitrifying biomass from a sewage treatment plant in Washington, D.C (DC Water Blue Plains facility). At freshwater sites, anaerobic sediments were collected in plastic containers filled approximately half-full with sediment and at least 200 mL of overlying water. Sediment samples were collected using anaerobic techniques, but no attempts were made to preserve the natural redox gradients. Denitrifying biomass was collected in plastic, screw-top containers with no headspace from a sampling point in the recycle line for nitrifying/denitrifying biomass at the Blue Plains facility. In all cases, the samples were stored on ice and used as inoculum within six hours of sampling.

5.2.2 Aqueous Enrichment for Iron(II)-Dependent Denitrifying Organisms

Enrichment for iron(II)-dependent denitrifying organisms was performed, using methods modified from Benz et al, (1998) (Benz, Brune et al. 1998) (Straub and Schink 2004). A freshwater, bicarbonate buffered media was used; the media contained (per L): 2.52 g NaHCO₃, 0.3 g NH₄Cl, 0.05 g MgSO₄ x 7H₂O, 0.4 g MgCl₂ x 6H₂O, 0.6 g KH₂PO₄, 0.1 g CaCl₂ x 2H₂O, 0.606 g KNO₃, 1 mL SL9 Mineral

Solution and 2 mL Vitamin Solution (Dworkin, Falkow et al. 2006). One half of all enrichments contained acetate (0.15 g/L NaCH₃COOH) to evaluate dependence on an auxilliary carbon source. Media pH was adjusted to 7.2 and filter sterilized (0.22 µm). Anoxic stock solutions of ferrous chloride (60 g/L FeCl₂) and ferrous sulfate (200 g/L FeSO₄) were prepared in deionized water while continually flushing with N₂ (99%) to avoid abiotic iron(II) oxidation. Iron solutions were prepared immediatley prior to use and filter sterilized (0.22 µm) into anoxic media. The final concentrations of electron donor (Fe²⁺) and electron acceptor (NO₃⁻) in solution were 6 mM and 10 mM, respectively; yielding electron-donor (NO₃⁻) limited conditions. For cathodic electrochemical growth experimens, ferrous iron and vitamins were omitted from the media.

Serum bottles (150 mL) were filled aseptically with 75 mL media and flushed with N₂/CO₂ (80:20 v/v) for 25 min to remove dissolved oxygen. Iron(II) was added via sterile filtration from an anoxic stock solution to achieve a final concentration of 6 mM. Reaction of the iron(II) with carbonates and phosphates in solution resulted in a milky white precipitate. For the aqueous inoculum (denitrifying biomass), 20% (v/v) was added anaerobically via syringe, and for sediment samples, 33% (v/v) was added to anoxic media via pipette. Following inoculation, bottles were flushed for an additional 10 min in liquid and headspace, then sealed with butyl rubber stoppers and incubated at 30°C in the dark. Bottles were incubated horizontally to maximize interaction between bacteria and iron particles, and were manually agitated every 1-2 days. Transfers to fresh media were performed every 2-5 weeks using aseptic, anaerobic techniques.

5.2.3 Electrochemical Enrichment Experiments

Experimental Set-Up

Electrode-dependent growth experiments were performed according to the methods of (Strycharz-Glaven and Tender 2012) and (Strycharz-Glaven, Glaven et al. 2013) using single-chamber electrochemical cells (250 mL total volume; approximately 175 mL aqueous volume; Ace Glass 6959-48). Two identical graphite rods (0.635 cm diameter, approximately 4 cm submerged length) served as the working electrode (WE) and counter electrode (CE), respectively, and a reference was a silver/silver chloride electrode (Ag/AgCl, 3M KCl, ≈ 0.200 V vs. SHE). Graphite rods were sterilized via autoclave in partially assembled cells prior to start-up.

Single-chamber cells were filled with approximately 175 mL media (6 mM NO_3^- as electron acceptor) and were continuously purged with the anaerobic gas mix (N_2/CO_2 80:20 v/v). Cells were maintained on stir plates at a rate of '3' (VWR Brand), and temperature was controlled at 30°C with a recirculating water bath. All cells were wrapped in black cloth to inhibit growth of photosynthetic organisms. Enrichment cultures from Paint Branch Creek and DC Water (provided 2.5 mM $\text{NaCH}_3\text{COO}^-$ as organic carbon during enrichment) were used as inoculum for two identical cells, referred to as **DN1 and DN2**, respectively. Each cell was inoculated via syringe at a rate of 10% (v/v) using equal volumes from the two enrichments (total inoculation volume of 16 mL) and initially maintained in batch mode. Inoculation was performed using anaerobic, aseptic techniques. For both DN1 and DN2, once a negative catalytic current was observed that exceeded background levels ($\leq -4 \mu\text{A}$; -5 mA/m^2) (see *Electrochemical Methods* section), cells were placed on flow mode, whereby

anaerobic media was continuously supplied to the cells using a peristaltic pump. For initial experiments (DN1 & DN2), flow rate was adjusted periodically to evaluate the effect of dilution rate on current production and nitrate removal. Cells were thus maintained at dilution rates between $0.19 - 0.75 \text{ hr}^{-1}$ (HRT: 318 - 1250 min). Successive transfer from one of the original cathodes (DN2) was performed into a new electrochemical cell to refine the microbial consortia and evaluate any differences in the electrochemical signature of the biofilm. The DN2 cathode was sampled in-situ using a sterile canula needle and syringe to remove 10 mL of electrode scrapings plus media, which was immediately used to inoculate a new cell, which was maintained as described in the previous paragraph.

Electrochemical Analysis

All electrochemical cells were maintained on a Solartron 1470E multi-channel potentiostat (Solartron Analytical) and Multistat software program (Scribner Assoc.). Immediately following inoculation, cathodes (working electrode, WE) were maintained in open circuit conditions (vs. Ag/AgCl) for 48 hr to facilitate attachment and charge accumulation. Cathodic biofilms were subsequently grown via chronoamperometry, with the WE maintained at a fixed potential (E). For initial experiments with environmental enrichments, the WE of DN1 and DN2 was held at 0.00 V and -0.250 V vs. Ag/AgCl, respectively. For all subsequent experiments using the transferred bio-cathode, the WE was held at -0.250 V vs. Ag/AgCl unless otherwise indicated.

Slow-scan cyclic voltammetry (CV) was performed at several points during growth: (1) prior to inoculation under abiotic conditions; (2) immediately following

inoculation; (3) at the onset of catalytic activity; and (4) at maximum cathodic current production. CVs were performed in-situ, and scan parameters were as follows: for the initial anodic scan the cathode potential was changed from $E_i = +0.350$ V vs. Ag/AgCl to $E_f = -0.500$ V vs. Ag/AgCl, and was followed immediately by a cathodic scan from -500 mV vs. Ag/AgCl to $+350$ mV vs. Ag/AgCl; all scans during growth were performed at rates (ν) of 1, 2, and 5 mV/sec. Once cathodes reached a steady-state, maximum limiting current at poised potential, voltammetry was performed at increasing scan rates: 0.2, 2, 10, 20, 100, 200 mV/s (sequentially). All current measurements were normalized by cathode geometric surface area (Graphite rod SA: 8.30 cm²; Carbon cloth two-sided SA: 12.9 cm²).

5.2.4 Environmental Analyses

Aqueous samples were collected from the influent and effluent of the flow reactors. Samples were immediately acidified (pH < 2), filtered (0.22 μ m), and stored at 4°C until nutrient analysis. Nutrient concentrations were determined by continuous flow colorimetry using an autoanalyzer with autosampler (Bran & Luebbe TRAACS 2000). Analysis for $\text{NH}_3\text{-N}$, $\text{NO}_2^- \text{-N}$, and $\text{NO}_3^- \text{-N}$ was performed following EPA methods 350.1 and 353.1 respectively (O'Dell 1993, O'Dell 1993, O'Dell 1993).

5.2.5 Confocal Microscopy

Carbon cloth modified with the denitrifying bio-cathode was removed from the reactor after maximum, stable current production (approximately 0.5 mA) was maintained for > 4 d. The electrode was prepared for microscopy as follows: carbon cloth was cut with a sterile blade and rinsed three times in sterile-filtered PBS buffer

(1X; pH 8). Biofilms were subsequently stained for 10 min according to the manufacturer's instructions at the concentration of 3 μ L stain per 1 mL PBS, then rinsed twice and de-stained in PBS (1X) for 10 min. The sample was then mounted on a glass cover slide with one drop of mounting oil for imaging. A Nikon TE-2000e inverted confocal microscope was used to examine the biofilms within the 400-700 nm excitation range. Four different x,y coordinates across the biofilm were randomly chosen for imaging.

5.2.6 Phylogenetic DNA Analysis and Clone Library Generation

Scrapings of the DN2-T1 cathode biofilm were taken after > 10 d of continuous, stable current production (> 600 mA/m²). Electrode sampling was performed in an anaerobic glove box (Coy brand) using a sterile blade and syringe. Electrode scrapings plus media were preserved in three 10-mL syringes for < 10 min before inoculation of triplicate electrochemical cells. The cells were identical to those described in section 2.3.1, except that a carbon cloth flag (CC6, Fuel Cell Earth) with titanium wire lead was used as the working electrodes in each cell (2.54 cm by 2.54 cm; total geometric surface area, 12.9 cm²). Biofilm-modified electrodes were removed from electrochemical cells after maximum, steady-state current production was maintained for > 4 d. Electrodes were preserved in sterile polypropylene containers at -20°C until DNA extraction. DNA extraction and genetic analysis is currently underway.

5.3 Results & Discussion

5.3.1 Aqueous Phase Enrichment

Two of the environmental samples (Potomac sediment and denitrifying biomass) were initially inoculated in media containing ferrous sulfate (10 mM) as the sole electron donor, which resulted in the unintentional enrichment of sulfate reducing bacteria, as qualitatively evidenced by visibly reduced conditions (i.e. darkening of soils) and the production of odorous compounds (presumably hydrogen sulfide) 1-2 weeks after inoculation. Importantly however, transfers of the two cultures and inoculation of the Paint Branch sediment were subsequently performed into fresh media containing ferrous chloride (10 mM) as sole electron donor. In all cases, this resulted in visible oxidation of the ferrous iron, as evidenced by the development of a vivid, rust-colored precipitate in all bottles (Figure 5-1). Qualitatively, both sediment samples were able to oxidize the ferrous carbonates at a faster rate than the denitrifying biomass, though ferric precipitates were visible in all samples after five days of incubation. Equal volumes of the initial enrichments on FeCl_2 were used as inoculum for the electrochemical reactors.

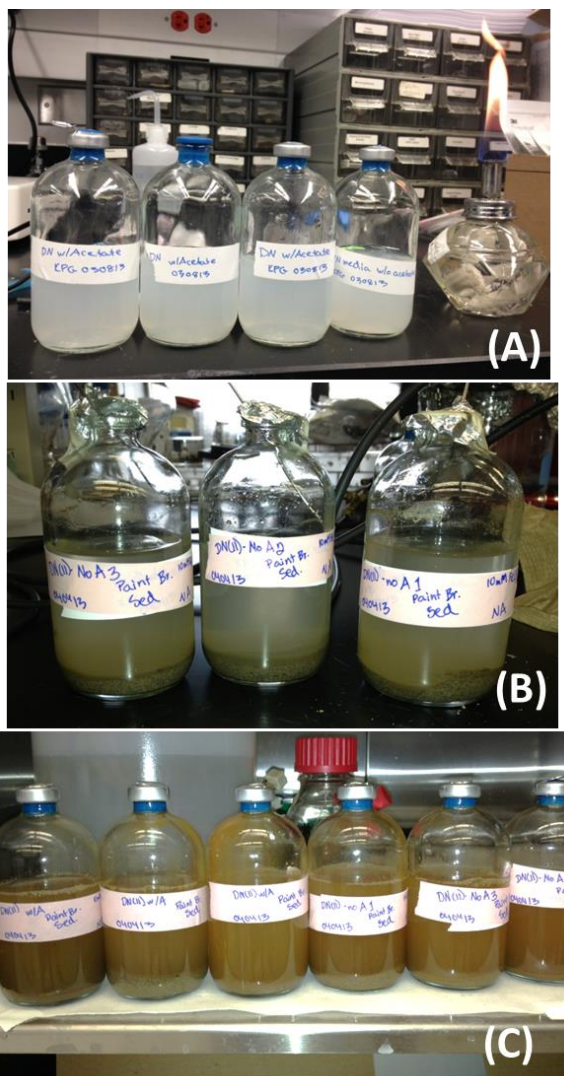


Figure 5-1 Photographs of un-inoculated serum bottles, where milky color results from FeCO_3 precipitates (A); serum bottles immediately after inoculation with sediment enrichments (B); and serum bottles containing environmental enrichments seven days after inoculation, showing development of orange-brown precipitate, consistent with Fe(III) precipitation through microbial oxidation of ferrous carbonates (C).

5.3.2 Cathodic Enrichment

Current Profiles

Following inoculation, 48 h of open circuit conditions were maintained, where cathodes came to a maximum stable potential versus the Ag/AgCl reference electrode.

For both DN1 and DN2, this initial OCP was approximately -0.06 V vs. Ag/AgCl (OCP vs. Ag/AgCl). Subsequently, the cathodes in reactors DN1 and DN2 were poised at 0.00 V vs. Ag/AgCl and -0.250 V vs. Ag/AgCl, respectively.

After ~600 hours at a fixed potential (0.00 V vs. Ag/AgCl) and under the continuous flow of media, no significant cathodic current could be detected from DN1, as shown in Figure 5-2. On day 12 of the experiment, a small catalytic wave was observed in a voltammogram performed at 0.2 mV/s (inflection at approximately -0.100 V vs. Ag/AgCl; Figure 5-6), though this phenomenon was not observed in subsequent CVs, which appeared featureless (data not shown). The DN1 experiment was also repeated at a later date and yielded the same result.

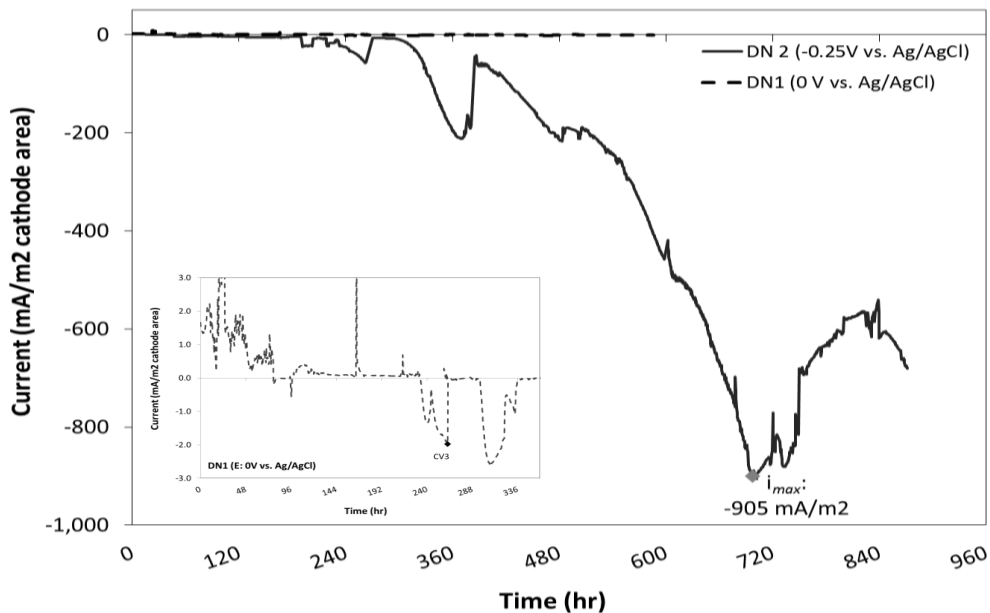


Figure 5-2 Current profile during biofilm growth of denitrifying cells. DN1 and DN2 were maintained at fixed potentials of 0V and -0.25V vs. Ag/AgCl, 3M KCl. Figure inset shows enlarged current profile from DN1 cell. Raw current was normalized to cathode surface area (8.30 cm²).

The inability to develop a bio-cathode at 0.00 V vs. Ag/AgCl may be related to the thermodynamics of initial enrichments on ferrous carbonates, which is energetically more favorable for iron-oxidizing bacteria than solid iron oxide species (see Table 5-1). The significant lag period, approximately 220 hours, of the DN2 cathode also supports this hypothesis, where, presumably, a significant metabolic adaptation was required by cells to shift from growth on the semi-soluble ferrous carbonates to an insoluble electrode poised at -0.250 V vs Ag/AgCl (\approx -0.050 V vs. SHE).

In contrast, DN2 developed a small cathodic current (\sim -5 mA/m²) within 48 hours after initial poisoning of the electrode at -0.250 V vs. Ag/AgCl, and the onset of exponential growth was observed after approximately 220 hours (Figure 5-2). This lag period is significantly longer than what has been observed during growth of anode respiring biofilms from environmental cultures (e.g. 72- 120 h anodic growth period for a wastewater-grown biofilm; see Chapter 3). Under a controlled dilution rate of 0.09 hr⁻¹ (Q: 0.275 mL/min) the bio-cathode required approximately 400 hours to reach a maximal current production of \sim -900 mA/m² (based on geometric surface area of the electrode, 8.30 cm²) at a fixed cathode potential of -0.250 V vs. Ag/AgCl (Figure 5-2). Under the production of stable current from the original bio-cathode (DN2), the flow rate of media to reactors was increased (Q: 0.550 mL/min), which did not stimulate additional increases in current production, suggesting that catalytic activity was not limited by loading rate of nitrate. Similarly, doubling the concentration of nitrate in solution by spiking with concentrated, de-gassed KNO₃, did not yield significant increases in current.

Although reductant concentrations did not affect catalytic activity, increasing the rate of mixing in all reactors (approx. 20% stir rate increase) resulted in a 5-10% increase in current ($\sim 30\text{-}100\text{ mA/m}^2$ increase). Presumably, this was due to improved diffusion, and thus mass transport between the electrode, biofilm, bulk solution or some combination thereof. Further increasing the stir rate did not yield any additional increase to current, and eliminating stirring entirely resulted in current reductions of 12 to 50%. Similar stir-rate dependence was observed in all bio-cathode transfers. This may suggest that the bulk concentration of reductant (NO_3^-), product (e.g. OH^-), or of minerals in solution was sufficient to maintain metabolic activity at the lowest flow rate, but diffusion of nitrate, electrons, or other metabolic by-products into or out of the biofilm is rate limiting.

The experimental conditions we describe here, i.e. reactors provided with a continuous flow (vs. batch loading) of media, provide valuable information on the mechanism of electron transfer from electrode to biofilm, where such conditions preclude the use of soluble electron mediators or bacteria grown in suspension for current production (Marsili, Baron et al. 2008). In the case of the bio-cathode described here, growth and stable current production under continuous media flow is consistent with bacterial species that are, in contrast, colonizing the electrode and using the cathode directly as an electron donor to drive denitrification.

Electrode scrapings taken from the original cathode (DN2) were used to inoculate an identical cell (**identified as DN2-T1 in figures**). Exponential growth from the transferred biofilm began within 48 h of inoculation, and reached a similar level of stable density, $\sim 950\text{ mA/m}^2$. DN2-T2 and all subsequent cathode transfers achieved

maximum current production by hour 135. Start-up time of the transfer was thus reduced by 60% relative to the original environmental enrichment. Subsequent transfers from the 2nd generation cathode (DN2-T2) were performed onto carbon cloth (12.9 cm² geometric area; **labeled as DN-DNA in figures**), which reached stable current production of ~ -2,150 mA/m²—more than double the current achieved by the graphite rod. Presumably, this is due to the higher ratio of electrochemically active-to-geometric surface area resulting from the cloth's weave, as has been previously noted in Richter et al, (2009).

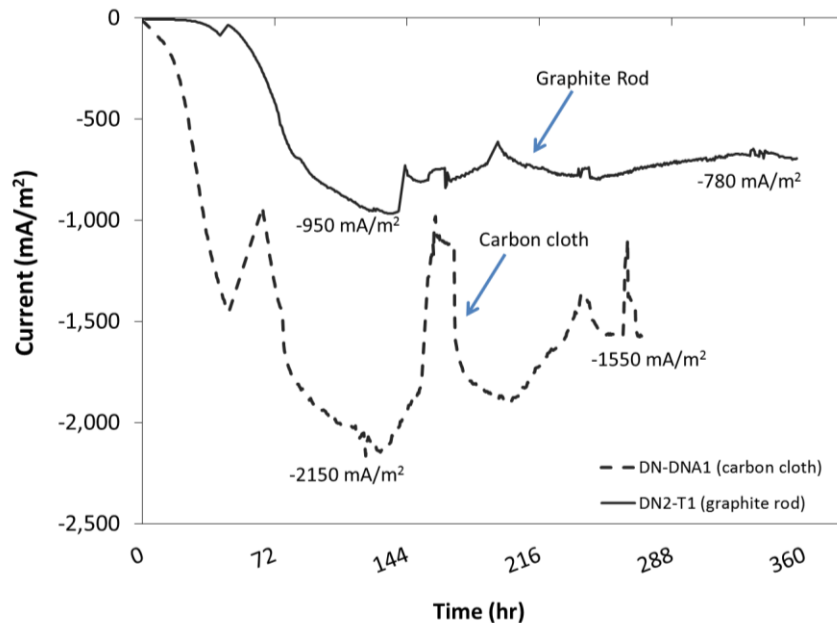


Figure 5-3 Chronoamperometry showing current production from denitrifying bio-cathode on graphite rod (solid line) and carbon cloth (dashed line). Electrodes were maintained at -0.25V vs. Ag/AgCl and current was normalized by geometric surface area (graphite rod, 8.30 cm²; carbon cloth, 12.9 cm²)

The dependence on an organic carbon source for iron(II)-dependent denitrification was subsequently evaluated in both the original (DN2) and transferred (DN2-T2) cultures. Under the flow of media containing all ingredients except acetate (2.5 mM NaCH₃COO⁻) cathodic current from DN2 remained stable. This may be

attributable to the presence of autotrophic organisms from the original enrichment culture that were able to grow, either planktonically or on the electrode as biofilm, in the original electrochemical cell. In the transferred biofilm, a 24% decrease in current (from -855 mA/m^2 to -647 mA/m^2), was observed after 82 h of media flow lacking any organic carbon. Importantly though, this was still within the window of current production observed from DN2-T1 over the 600 h of operation, and thus may not be indicative of lithotrophic metabolism.

Nitrate was confirmed as the microbial oxidant for both the original and transferred biofilms under the flow of media containing all ingredients except KNO_3 . These experiments are referred to as **non-turnover** conditions in figures. In all cases, current production sharply declined under non-turnover conditions to reach background levels ($\pm 4 \mu\text{A}$) within 24 hours (Figure 5-4), consistent with nitrate serving an essential metabolic function and that current production was directly dependent on its availability to the biofilm. Upon re-introduction of nitrate to cells, stable current production resumed within 2-3 hours.

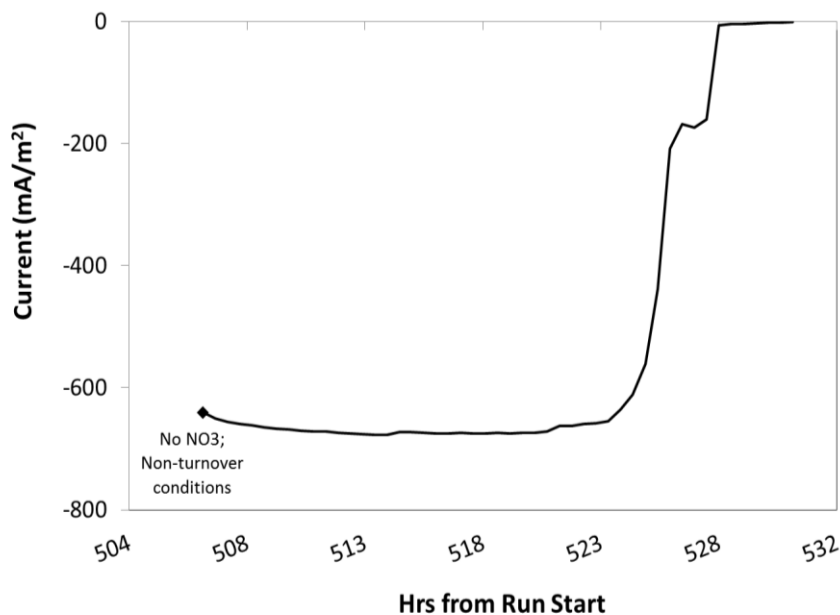


Figure 5-4 Chronoamperometric plot (EWE, -0.25V vs. Ag/AgCl) illustrating the decline in current to background levels within 24 h of flowing media without nitrate as an electron acceptor to the DN2-T1 bio-cathode.

Voltammetry

Slow-scan cyclic voltammetry (CV) was performed immediately before and after inoculation of each reactor, and corresponded to background (abiotic) and pre-growth conditions, respectively. In all cases, abiotic CVs were featureless, and no evidence of abiotic NO_3^- reduction was observed within the potential window of +0.5V to -0.5V vs. Ag/AgCl (Figure 5-5). The absence of characteristic hydrogen and oxygen reduction peaks during abiological scans also confirmed the exclusion of oxygen and hydrogen gas from the reactor media (Baturina and Smirnova 2013).

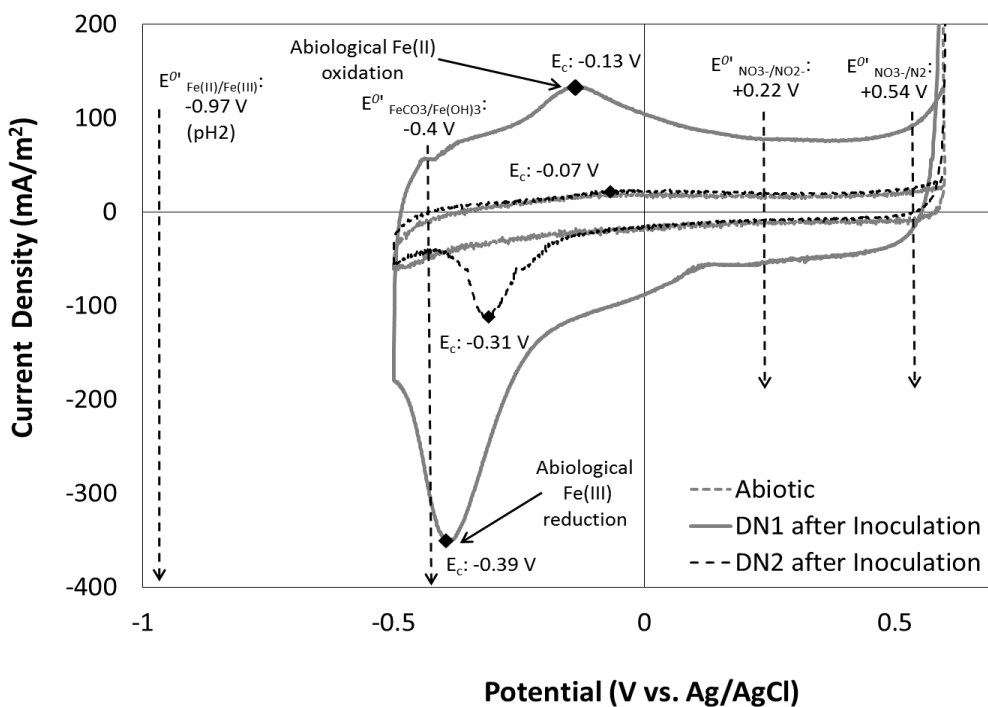


Figure 5-5 Voltammograms captured immediately before and after inoculation with the environmental enrichments. Scan before inoculation is featureless, consistent with abiological, anoxic conditions. Scans after inoculation show abiological oxidation and reduction of ferrous and ferric iron, respectively ($v = 1$ mV/s from +0.55V to -0.6V vs. Ag/AgCl).

In the case of the initial DN1 and DN2 reactors, CVs performed immediately following inoculation with the environmental enrichments, exhibited defined peaks, which we attribute to the abiological oxidation and reduction, respectively, of ferrous and ferric iron on graphite (Figure 5-5). The addition of ferrous chloride to anaerobic, bicarbonate buffered media generated a FeCO₃ precipitate, thus predicting a FeCO₃/Fe(OH)₃ redox couple with a theoretical potential of -0.400 V vs. Ag/AgCl (\approx -0.20 V vs. SHE). The cathodic scan (initial sweep from +0.500 to -0.500 V) revealed a reduction peak (occurring between -0.310 V and -0.390 V vs. Ag/AgCl), consistent with abiological reduction of ferric iron precipitates. Similarly, the subsequent anodic

scan (from -0.500 V to +0.500 V) yields a smaller oxidation peak, presumably corresponding to the re-oxidation of soluble ferrous iron generated during the cathodic scan. Peak separation was approximately 0.260 V, possibly indicating that the abiological mid-point potential ($E_m^{\theta'}$) of the $\text{FeCO}_3/\text{Fe}(\text{OH})_3$ couple on graphite was approximately -0.260V vs. Ag/AgCl . Importantly, this provided a abiological datum for comparing and analyzing catalytic and non-turnover voltammograms.

The shift in peak potentials, as well as the overall change in the peak shape (i.e. a broader, less sharp oxidative peak) may have been caused by the initial reduction of Fe(III) to Fe(II), which presumably increased the fraction soluble iron in the reactor. Previous work by (Nicholson and Shain 1964) demonstrated a similar phenomenon, where voltammograms associated with solid, or semi-solid compounds in direct contact with the electrode exhibited sharp, highly defined peaks, and successively increasing the solubility of compounds resulted in less refined, broader peak shapes.

Slow-scan CV (at 0.2 and 1 mV/s) was repeated several times during the course of biofilm growth (Figure 5-7). The redox peaks that were observed following inoculation, presumably associated with iron(II)/iron(III), were not observed after seven days, which corresponds to the approximate dilution time for the reactor after media flow began. During the initial seven days, the presence of small amounts of ferrous iron in the reactors may have served as an alternative, more energetically favorable, electron donor, which may have also contributed to the prolonged lag phase (~ 9 d) that was observed before the onset of catalytic activity.

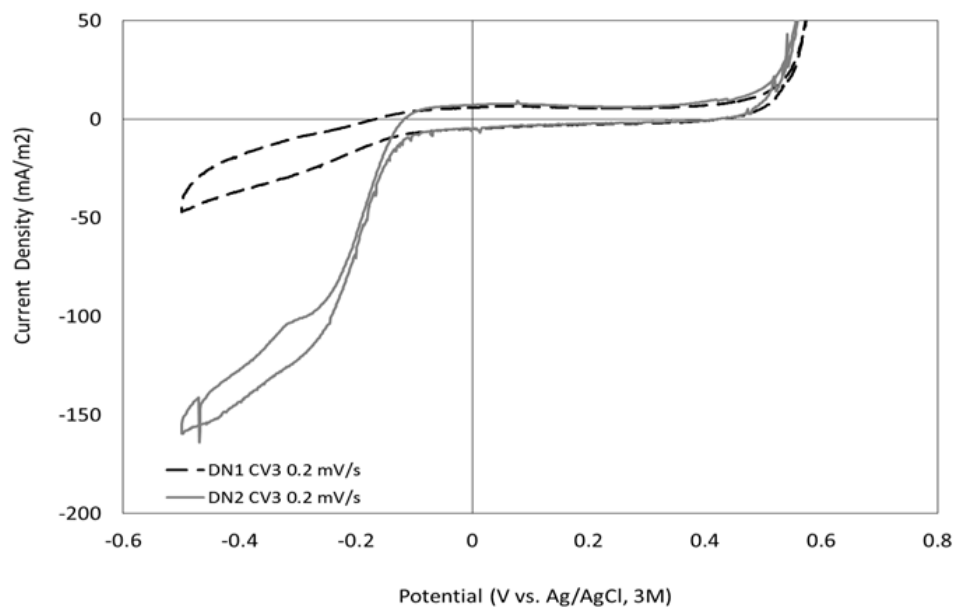


Figure 5-6 Representative slow scan voltammograms of cathodes at the onset of catalytic activity, $v = 0.0002$ V/s. DN1 (dashed line) and DN2 (solid line) were grown at fixed potentials of 0V and -0.25V vs. Ag/AgCl, respectively.

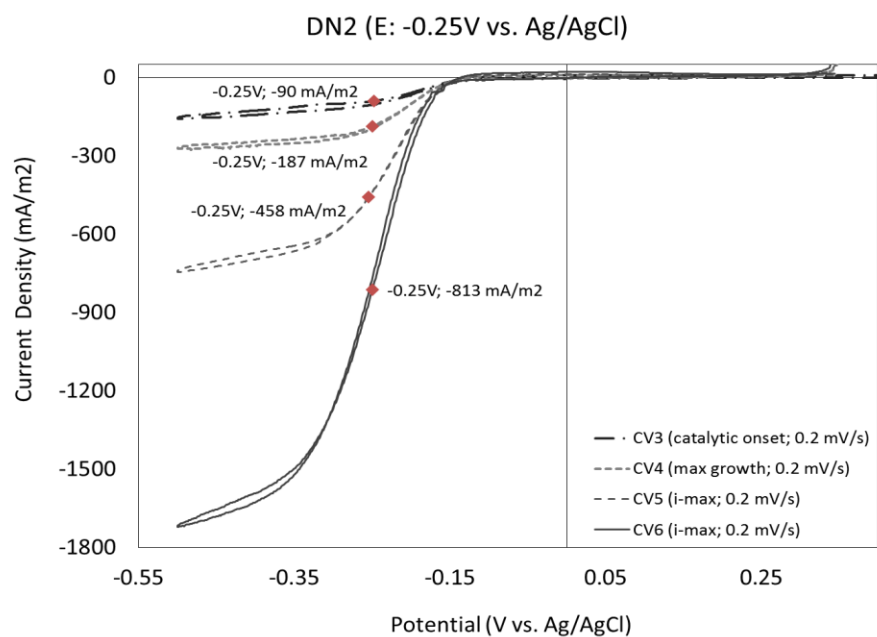


Figure 5-7 Slow-scan voltammetry of original NO_3 -reducing bio-cathode (DN2) at various points along the growth curve. Scan parameters: 0.2 mV/s; Ewe: +350 mV to -500 mV and back to +350 mV vs. Ag/AgCl.

The production of logarithmic current commenced around day 9, and evidence of a Nernst-Monod current-potential dependency (i.e., a sigmoid-shaped voltammetric feature) could be interpreted from all subsequent CVs (Figure 5-6). Nernst-Monod kinetics have previously been applied to interpret CV of catalytically active biofilms (e.g. *G. sulfurreducens*) but not of NO_3^- reducing bio-cathode. A sigmoid-shaped current-potential dependency was observed for all CVs recorded at 0.2 mV/s under turnover conditions (i.e., when substrate, nitrate, was present). During early growth, the onset of catalysis occurred at approximately -0.130 V vs. Ag/AgCl (\approx 0.07 V vs. SHE) and the mid-point of the catalytic wave centered at approximately -0.180 V vs. Ag/AgCl (\approx -0.02 V vs. SHE) confirmed by the first derivative of the CV; Figure 5-9). Cathodic current saturated at potentials below -0.270 V vs. Ag/AgCl (\approx -0.07 V vs. SHE). CV repeated at faster rates (1, 2, 5, 10, 20, 100, and 200 mV/s) exhibited increasing distortion as expected due to kinetics of one or steps involved in the catalytic process, and a clear catalytic mid-point could not be observed at $v > 20$ mV/s (Figure 5-8).

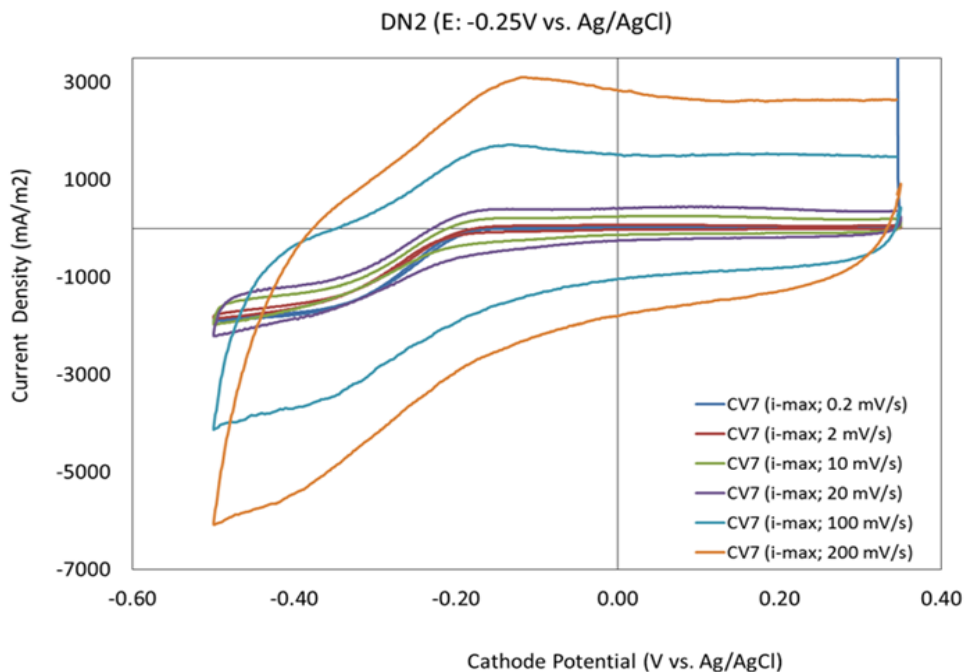


Figure 5-8 Representative voltammograms of the original bio-cathode (DN2) cathode at maximal current production. Scans were performed at 0.2, 2, 10, 20, 100, and 200 mV/s, E: +0.3V to -0.5V and back to +0.3V vs. Ag/AgCl.

CV was also performed periodically after current production stabilized in each bio-cathode. In all instances, the mid-point potentials of CVs were observed to shift by approximately - 0.050 to - 0.070 V (more negative) after prolonged operation at a fixed potential of -0.250 V vs. Ag/AgCl (\approx -0.05 V vs. SHE). This was confirmed with a first derivative analysis of the voltammograms (Figure 5-8).

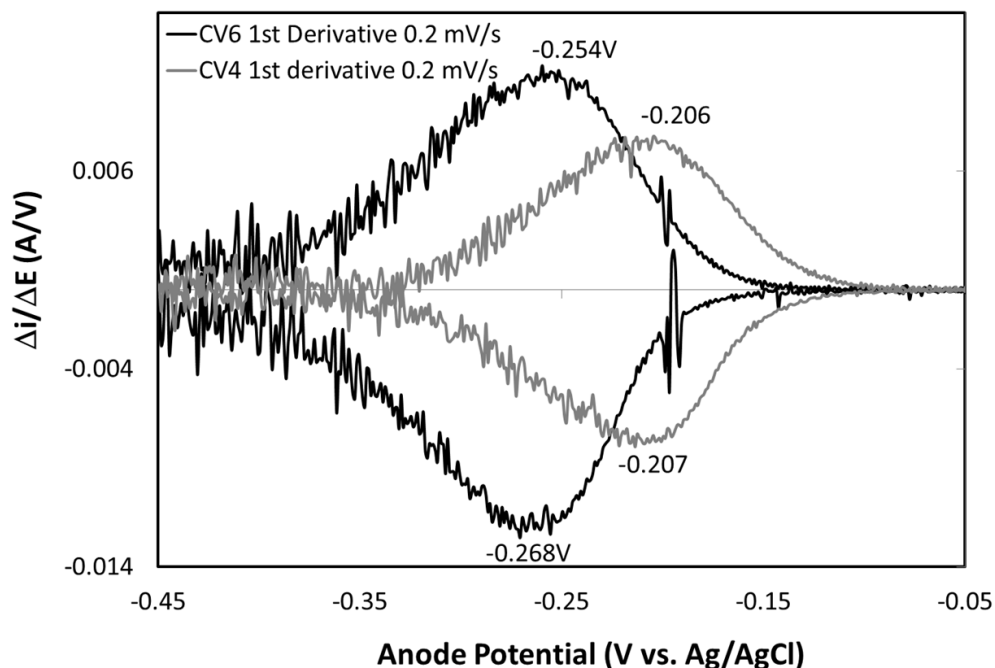


Figure 5-9 First derivative analysis of voltammograms of the DN2-T1 bio-cathode. Voltammograms were recorded immediately after cathodes reached maximum stable current operation (in grey) and 18 days later (in black); scan parameters: 0.2 mV/s from +0.3 V to -0.5V and back to +0.3V vs. Ag/AgCl.

Importantly, the shift in CVs coincided with significant increases in the saturation current, albeit at lower cathodic potentials. Key features of CV (mid-point potential; saturation current; catalytic onset) were highly reproducible from the original (DN2) bio-cathode to all subsequent transfers, suggesting a highly stable and non-transformed biofilm was catalyzing electrode oxidation.

Previous Nernst-Monod models for bio-catalytic behavior (Richter, Nevin et al. 2009) (Strycharz-Glaven and Tender 2012) have theorized a five step mechanism for bio-anode catalyzed acetate oxidation by *Geobacter sulfurreducens*. Here, we propose an analogous five step mechanism for bio-cathode catalyzed nitrate reduction reported here.

1. Electron transfer from the cathode surface to redox cofactors adjacent to the anode surface, resulting in current production
2. Electron transport through the biofilm via incoherent multistep electron hopping, also referred to as redox conduction, whereby electron transport through the biofilm occurs by a sequence of electron transfer reactions through a network of immobile redox cofactors
3. Transfer of electrons from redox cofactors to cells within the biofilm
4. Binding and reduction of substrate (NO_3^-) in cells consuming electrons and yielding products
5. Diffusion of cellular substrate in (e.g. nitrate from media into biofilm) and products out (e.g. NO , N_2O , OH^- out of the biofilm)

Drawing on a limiting case analysis performed on the analogous 5-step model for *Geobacter sulfurreducens* bio-anode oxidation of acetate, the sigmoid shape of slow-scan CV reported in this study for bio-cathode reduction of nitrate indicates that the rate of Step 1 is fast, and that neither Step 1 nor Step 5 is the rate-limiting step in the process (Richter, Nevin et al. 2009) (Strycharz, Malanoski et al. 2011).

Non-turnover CV

Non-turnover voltammograms were recorded after the cessation of appreciable current production ($\pm 4 \mu\text{A}$; 4.8 mA/m^2) when media lacking nitrate was flushed into reactors containing DN2 and DN2-T2. Figure 5-10 displays representative non-

turnover voltammograms at 2, 5, and 10 mV/s. CVs captured the presence of distinct and highly reproducible redox peaks which we attribute to the biofilm redox cofactors accessible by the electrode via steps 1 and 2 above. In the absence of an electron acceptor, redox cofactors within the biofilm become oxidized and reduced, respectively, when the cathode potential is driven very negative or very positive vs. the redox cofactor formal potential during voltammetry. In the case of DN2 and DN2-T2, two sets of redox peaks near equal in size were observed in all scans from 0.2 to 100 mV/s.

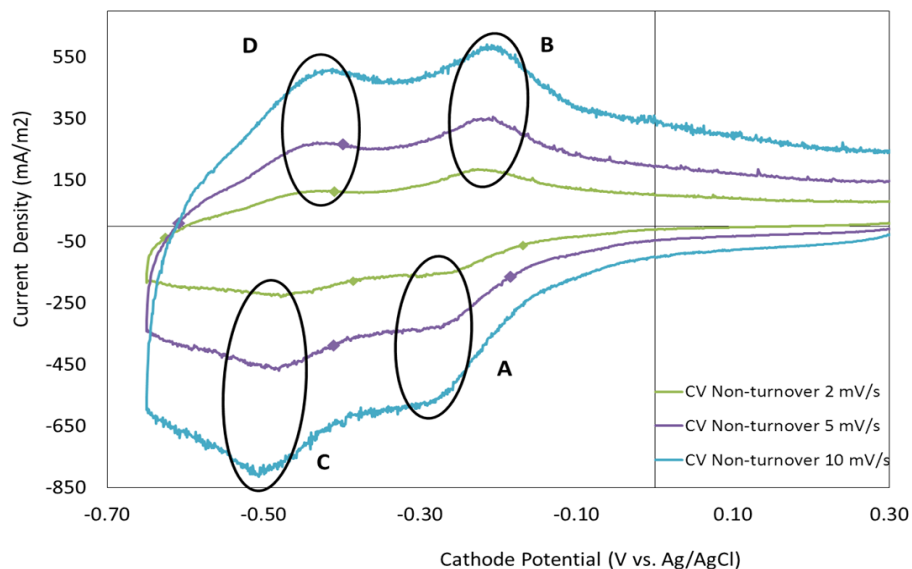


Figure 5-10 Representative non-turnover voltammograms from bio-cathode DN2, captured at $i < 4 \mu\text{A}$ in the absence of NO_3^- as electron acceptor. Scans were recorded at 2 mV/s (green line), 5 mV/s (purple line), and 10 mV/s (teal line).

The first set of peaks (A and B in Figure 5-10) was centered at approximately -0.240 V vs. Ag/AgCl (≈ -0.040 V vs. SHE), nearly identical to the mid-point potential of turnover voltammograms (Figure 5-8). A second set of peaks (C and D) was centered at -0.450 V vs. Ag/AgCl (≈ -0.250 V vs. SHE) and were similar in size to A

and B. This suggests that the redox cofactor involved in Steps 1, 2, and 3 above can be sequentially reduced by two electrons, where electron repulsion inside the molecule makes it thermodynamically more challenging to perform the second reduction reaction. It therefore requires a more negative potential (-0.210 V) to drive the second electron into the molecule (Bard and Faulkner 1980). Further drawing on the same limiting case analysis as above, alignment of the A/B voltammetric peaks with the mid-point potential of catalytic CVs depicted in Figure 5-6 suggests that electrons associated with generation of peaks A/B ($E^{0'} = -0.240$ V vs. Ag/AgCl, ≈ -0.040 V vs. SHE) are the ones used by the cells in Step 4. If so, then Step 2 or 3 of the above proposed mechanism is the rate limiting step of the bio-cathode catalyzed nitrate reduction reaction reported here. Alternatively, it may be the case that electrons associated with generation of voltammetric peaks C/D ($E^{0'} = -0.450$ V vs. Ag/AgCl, ≈ -0.250 V vs. SHE) are the ones used by the cells in Step 4. If this is the case, then Step 4 is the rate limiting step.

Sweep-rate analysis was also performed on non-turnover CVs to evaluate the effect of scan rate on peak height and area. With baseline subtraction, the net height of redox peaks was evaluated at 0.2, 1, 2, 10, 20, 50, 100, and 150 mV/s. A linear dependency ($R^2, \geq 89\%$) was found between peak height and the square root of scan rate (from 0.2 to 50 mV/s) for each redox peak (Figure 5-11). This is consistent with diffusive electron transport through the biofilm expected for redox conduction involving immobile redox cofactors (Richter, Nevin et al. 2009, Strycharz, Malanoski et al. 2011, Strycharz-Glaven and Tender 2012).

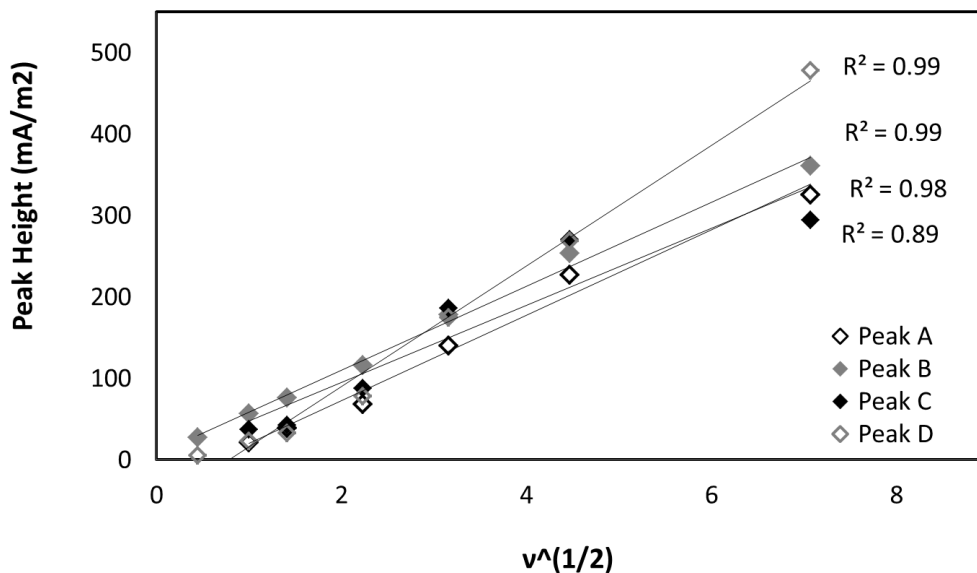


Figure 5-11 Relationship between height of visible redox peaks (A, B, C, D in Figure 5-9) and the square root of scan rate during non-turnover voltammetry. Linear regression lines are overlaid with correlation coefficient. Baseline correction was accounted for in calculating peak height.

5.3.3 Confocal Imaging

Imaging of DNA at the electrode surface was performed after stable current generation on carbon cloth squares was maintained for ≈ 4 d. Confocal images revealed a relatively dense biofilm, with cells extending up to 60 μm from the electrode surface, with coverage extending to the majority of the electrode surface. A representative three-dimensional image is shown in Figure 5-12, where there was some evidence of radial growth of biofilm around individual carbon fibers.

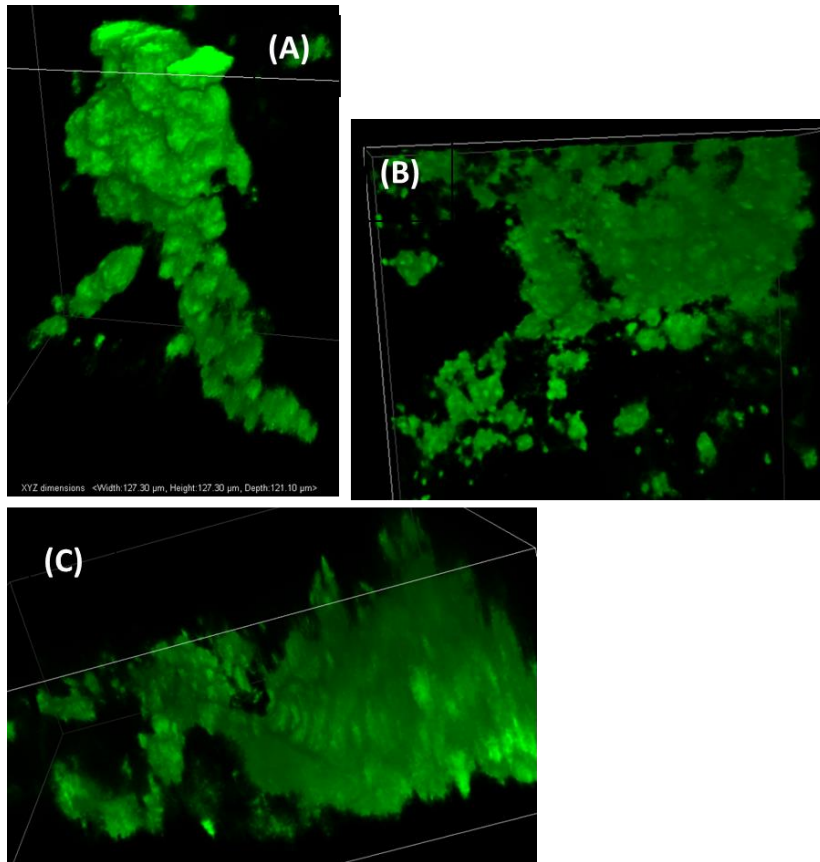


Figure 5-12 Confocal laser scanning microscopy images performed on carbon cloth, modified with denitrifying bio-cathode. Images show the presence of DNA at the electrode surface.

5.3.4 NO₂-NO₃ Transformations—Treatment Efficiencies

The influent and effluent of electrochemical cells containing the denitrifying bio-cathode were sampled under the conditions of maximum, stable current production and analyzed for nitrate (NO₃-N), nitrite (NO₂-N), and ammonia (NH₃-N) to assess possible nitrate reduction pathways of the bio-cathodic biofilm. A number of iterations were also performed to assess the effect of electrode surface area or HRT on NO₃-N removal rates. A summary of influent/effluent nutrient composition and the associated removal rates for each electrode/HRT combination is provided in Tables 5-2 and 5-3.

Table 5-2 Nitrate-Nitrogen Removal Rates from Denitrifying Cathode
(values presented as mean \pm stdev, n)

Electrode Material	Electrode Surface Area (cm ²)	HRT (min)	[NO ₃ -N] Influent (mg/L)	[NO ₃ -N] Effluent (mg/L)	% Removal NO ₃ -N	Loading Rate (g NO ₃ -N/m ³ /day)	Loading Rate (g NO ₃ -N/m ² /day)	Removal Rate (g NO ₃ -N/m ² /day)
Graphite Rod	8.30	636	64.8 \pm 4.59 (n = 5)	41.15 \pm 12.4 (n = 5)	36.9%	147	30.95	11.4
Graphite Rod	8.30	1250	64.8 \pm 4.59 (n = 5)	54.36 \pm 2.16 (n = 3)	14.2%	75	15.75	2.2
Graphite Rod	8.30	2134	64.8 \pm 4.59 (n = 5)	49.56 \pm 7.09 (n = 2)	23.8%	44	9.22	2.2
Carbon Cloth	12.90	1250	64.8 \pm 4.59 (n = 5)	45.11 \pm 2.33 (n = 7)	30.6%	75	10.12	3.1

Table 5-3 Nitrite- and Ammonia-Nitrogen Removal Rates from Denitrifying Cathode
(values presented as mean \pm stdev, n)

	Influent (mg/L)	Effluent (mg/L)	% Removal
NO ₂ -N	0.20 \pm 0.29 (n = 5)	0.91 \pm 1.27 (n = 5)	-357%
NH ₃ -N	83.5 \pm 5.99 (n = 4)	79.0 \pm 1.24 (n = 5)	5%

The concentration of nitrate added to the media (0.606 g KNO₃/L; 6 mM NO₃⁻) is equivalent to 84.0 mg NO₃-N/L, or a loading rate of 0.190 kg NO₃-N/m³/d (HRT, 0.442 d). Observed nitrate concentrations in the assayed influent samples were somewhat lower however (64.8 mg NO₃-N/L), which is equivalent to a loading rate of 0.147 kg NO₃-N/m³/d. This may be due in part to precipitation of nitrate within the media and/or dilution rates for the colorimetric assay (~1:40); however, to provide conservative estimates of treatment efficiency, empirical measurements were used for all calculations. As previously noted, reactors were operated under conditions of continuous flow, such that the concentration of electron acceptor was non-limiting for

cell growth and for current production. In this way, we conservatively estimate the removal efficiencies from this bio-cathode under the condition of maximum catalytic activity. To better estimate maximum removal efficiencies, a reactor design that maximizes the surface area-to-volume ratio should be employed, as in fixed-film wastewater processes (e.g. trickling filter; anaerobic filter).

In all cases, there was significant removal of $\text{NO}_3\text{-N}$ ($p < 0.05$) by the bio-cathode (avg. removal, 14.2 – 36.9%), with associated daily removal rates of 2.20 – 11.4 $\text{g NO}_3\text{-N/m}^2\text{/day}$ (based on electrode surface area), or 10 – 54 $\text{g NO}_3\text{-N/m}^3\text{/day}$ (based on cell volume). A small increase in the concentration of $\text{NO}_2\text{-N}$ was observed (0.71 mg N/L); however, this represents $< 7\%$ of the net removal of $\text{NO}_2+\text{NO}_3\text{-N}$, suggesting that the bio-cathode was, at a minimum, reducing nitrate to nitric or nitrous oxide. The change in $\text{NH}_3\text{-N}$ concentration from influent to effluent (4.51 mg/L) was insignificant relative to the starting concentration (83.5 mg/L), indicating that reduction of NO_3^- to NH_3 was not a metabolic pathway of the biofilm.

Interestingly, maximum removal efficiency of $\text{NO}_3\text{-N}$ was achieved with the bio-cathodes on graphite rods, despite their smaller surface area and lower current production. Both DN2 and DN2-T2 achieved higher rates of nitrate removal, as both a percentage of the influent (i.e. 36.9% removal) and as a daily removal rate (i.e. 11.4 $\text{g NO}_3\text{-N/m}^2\text{/day}$). These results may suggest that additional denitrifying organisms, transferred from the enrichment cultures, were growing in suspension in the original bio-cathode and were contributing to nitrate reduction but not to current production. As successive transfers of the electrode-attached biofilm were performed to new bioreactors, the suspended cells were likely eliminated from growth conditions.

Alternatively, results may be related to the HRT/NO₃-N loading rate—in the case of the original DN2 bio-cathode (grown on a graphite rod with geometric surface area of 8.30 cm²), the flow rate of media to the reactors was altered to assess the effect of hydraulic retention time (HRT), and thus loading rate, on removal efficiencies. Maximum removal was achieved at the lowest retention time (highest loading rate), though we did not observe a linear correlation between loading rate and removal rate, as has been reported elsewhere (Clauwaert, Rabaey et al. 2007). Bio-cathodes transferred and grown on squares of carbon cloth as the working electrode (geometric surface area, 12.90 cm²), saw an increase in NO₃-N removal from 14.2% to 30.6%, relative to the graphite rod (at an equivalent loading rate, 75 g NO₃-N/m³/d). On a volumetric basis, this represents a lower removal rate than has previously been reported elsewhere (Clauwaert, Rabaey et al. 2007). In reports by Rabaey and colleagues, graphite granules were used to fill the cathode chamber, significantly improving the ratio of electrode surface area-to-reactor volume, i.e. minimizing void volume. Similar, conflicting analyses of volumetric- versus surface area-based efficiencies are common throughout MFC literature, with no clear metric as yet to compare performance from disparate reactor configurations. Based on the high level of current density achieved however, further studies are warranted to evaluate treatment efficiencies.

5.4 Conclusions

Herein, we report on enrichment strategies for iron(II)-dependent denitrifying bacteria, and their subsequent application as the basis for a high-current bio-cathode. The cathodic biofilm grown on carbon cloth yielded -2 A/m² of current production at a

fixed potential of -250 mV vs. Ag/AgCl. Catalytic voltammetry exhibited a mid-point potential of -0.250 V vs. Ag/AgCl (≈ -0.050 V vs. SHE). This level of current production is significantly higher than has been previously reported by denitrifying bio-cathodes, and is comparable in magnitude to what has been reported from mixed-culture anodic biofilms.

5.5 Acknowledgements

This work was supported in part by the US Naval Research Laboratory as well as the Bill & Melinda Gates Foundation (Grant #01566000547). K.G. was also supported by a fellowship from the A. James Clark School of Engineering at UMD. We thank Mark Ramirez and Greg Phillips at DC WATER for assistance with sampling and nutrient analysis.

Chapter 6 : Sand-Modified Anode for Increased Power Generation from Benthic Microbial Fuel Cell

6.1 Introduction

To date, benthic microbial fuel cells (BMFCs) remain the only viable bioelectric system—having been successfully deployed to power sensors and remote monitoring devices in the marine environment (Rabaey, Clauwaert et al. 2005, Rodrigo, Cañizares et al. 2007). BMFCs rely on a number of biogeochemical processes at the benthic interface of water bodies to sustain and optimize power generation: (1) sedimentary organic matter (SOM), primarily derived from marine phytoplankton at a rate of approximately 27×10^{15} g per year (Kim, Min et al. 2005), serves as the biochemical energy source for the anodic (i.e. oxidation) reaction; (2) a naturally occurring redox gradient (i.e. 0.7-0.8V) develops across the first 5-10 mm of the sediment-water interface, serving as the barrier between anodic (anoxic) and cathodic (oxic) reactions as well as the de facto proton exchange membrane (PEM) (Liu, Ramnarayanan et al. 2004); (3) the high conductivity levels of seawater (i.e. $>30,000$ $\mu\text{S}/\text{cm}$) minimize solution resistance to ion transport; and (4) there is evidence that naturally occurring biofilms develop on the BMFC cathode and catalyze oxygen reduction (Strycharz-Glaven, Glaven et al. 2013), a factor currently plaguing wastewater-fed MFCs.

A common BMFC configuration is illustrated in Figure 6-1, where the BMFC anode is typically embedded a few inches below the surface of the sediment and is electrically connected via an abiotic circuit, to a cathode suspended in the overlying seawater. A resistor or load in series provides the potential drop between anode and cathode to generate current/power (i.e. Ohm's law; $V_{cell} = iR_{ext}$ & $P = iV_{cell}$). After re-establishment of anoxic conditions around the anode, a biofilm comprised mainly of dissimilatory metal reducing bacteria forms on its surface. These microorganisms, termed *anode respiring bacteria* (ARB), serve as biological catalysts that couple the oxidation of organic matter (e.g. acetate) with the reduction of a non-consumed electrode (e.g. graphite). Protons and electrons released at the anode travel across the PEM and abiotic circuit, respectively, and converge at the cathode to reduce oxygen molecules present in the overlying seawater.

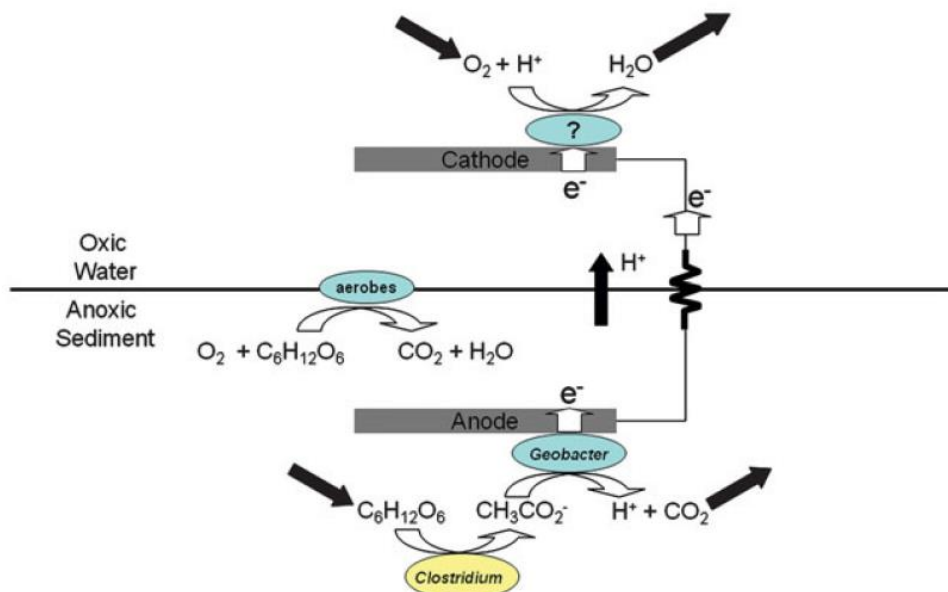


Figure 6-1. Courtesy: Tender (2011). Schematic representation of benthic microbial fuel cell (BMFC). Sedimentary organic matter is depicted as glucose, which is fermented to acetate by Clostridia, which is in turn oxidized by ARB at the anode surface (represented as Geobacter). At the cathode, oxygen, present in the overlying water, is reduced, either abiotically or by a spontaneously-formed cathodic biofilm. The resulting electric current flows through the external circuit connecting the electrodes where power can be utilized to operate an oceanographic sensor.

Despite the relative success of BMFC systems, predictions for their expanded utility are currently tempered by consistently low power densities, as summarized in Table 6-1. In comparison to the highest performing BMFC design (105 mW/m^2) (Lowy, Tender et al. 2006), many MFCs fed with wastewater or refined substrates (e.g. acetate) achieve an order of magnitude greater power production (Delaney, Bennetto et al. 1984, Katuri and Scott 2010, Pant, Van Bogaert et al. 2010). Much of the work to improve BMFC power generation has focused on electrode materials (e.g. platinum, or Mn-/Ni-modified graphite) to improve the kinetics of electron transfer at the anode (Vega and Fernandez 1987). While these efforts have resulted in moderate power increases, they assume that electron transfer kinetics, rather than mass transport of substrate, is the rate limiting step at the anode reaction.

Table 6-1 Review of Benthic Microbial Fuel Cells to Date

Reference	Lab/Field	Sediment Source/ Deployment Site	Electrochemical Condition	Anode Material	Anode Surface Area (m ²)	Anode Footprint Area (m ²)	i_{max} (mA)	i_{max} (mA/m ²)	P _{max} (mW)	P_{max} (mW/m ²)	V _{cell} at P _{max} (V)
<i>Reimers, 2001</i>	Lab	Tuckerton, NJ Salt Marsh	R _{ext} (NG)	52-mesh Pt	0.01	NG	0.75	75.00	0.120	12.0	0.16
<i>Reimers, 2001, Harvesting E</i>	Lab	Tuckerton, NJ Salt Marsh	R _{ext} (300 Ω)	Carbon fiber	0.01	NG	0.06	5.77	1.00	100.0	NG
<i>Tender, 2002, Harnessing microbe</i>	Field	Tuckerton, NJ Salt Marsh	R _{ext} (NG)	Graphite Plate	0.34	0.183	25.62	140.00	3.11	17	0.2
<i>Tender, 2002, Harnessing microbe</i>	Field	Newport, OR Estuary	R _{ext} (NG)	Graphite Plate	0.34	0.183	20.13	110.00	4.94	27.0	0.27
<i>Bond, 2002, Electrode-reducing</i>	Lab	NG	NG	Graphite Plate	0.01	NG	NG	NG	0.10	16.0	NG
<i>Holmes, 2004</i>	Lab	Boston, MA Marine Harbor	R _{ext} (1 kΩ)	Graphite Plate	0.0032	NG	0.10	30.00	0.01	2.9	0.095
<i>Holmes, 2004</i>	Lab	West Falmouth, MA Salt Marsh	R _{ext} (1 kΩ)	Graphite Plate	0.0032	NG	0.09	29.00	0.01	2.7	0.092
<i>Holmes, 2004</i>	Lab	Gunston Cove, VA Freshwater	R _{ext} (1 kΩ)	Graphite Plate	0.0032	NG	0.07	21.00	0.004	1.4	0.067
<i>Lowy, 2006, Harvesting E II</i>	Field	Tuckerton, NJ Salt Marsh	V _{cell} (NG)	Graphite Plate	0.18	0.183	12.08	66.00	3.66	20.0	0.3
<i>Lowy, 2006, Harvesting E II</i>	Field	Tuckerton, NJ Salt Marsh	V _{cell} (NG)	Graphite Plate, AQDS Modified	0.18	0.183	102.48	560.00	17.93	98.0	0.24
<i>Lowy, 2006, Harvesting E II</i>	Field	Tuckerton, NJ Salt Marsh	V _{cell} (NG)	Graphite Plate, Mn ²⁺ /Ni ²⁺ Modified	0.05	0.457	159.95	350.00	47.99	105.0	0.35
<i>Reimers, 2006, MFC E</i>	Field	Monterey Bay, CA Ocean Cold Seep	0.3 V _{cell}	Graphite Rod	0.24	0.007	20.50	85.00	8.201	34.0	0.4
<i>Tender, 2008, First demo</i>	Field	Washington, DC Freshwater River	0.35 V _{cell}	Graphite Plates	5.20	NG	68.57	13.19	24.0	4.0	0.35
<i>Tender, 2008, First demo</i>	Field	Tuckerton, NJ Salt Marsh	0.35 V _{cell}	Graphite Plates	2.20	NG	102.86	46.75	36.0	16.0	0.35
<i>Song, 2011, Effect of sediment</i>	Lab	Taihu, China Eutrophic Lake	R _{ext} (1 kΩ; 0.15V)	Graphite Felt	0.01	0.00318	0.40	125.00	0.018	5.7	0.0004

Despite the large quantity of organic matter in marine sediments, the rapid oxidation of ARB substrates (namely acetate and butyrate) likely leads to concentration gradients, and thus mass transport limitations, at the anode. Compounding this limitation, embedment of the anode in relatively impermeable sediments, especially in the case of high organic matter, low porosity soils likely results in significant mass transport limitations. Furthermore, substrate replenishment in BMFCs can only be accomplished through diffusive, tidal action or anaerobic fermentation of complex organics (e.g. glucose, cellulose). Previous results from an idealized electrochemical flow cell containing an anode modified with *Geobacter sulfurreducens*, strain DL1 found that a minimum substrate loading rate of 0.366 mmol acetate/L/min (equivalent to a dilution rate of $D = 3 \text{ hr}^{-1}$) was necessary to maintain a maximal current production of 5 A/m^2 (Strycharz-Glaven and Tender 2012), a significantly more rapid consumption rate than the naturally occurring turnover rate of acetate found in marine sediments (e.g. 19-330 $\mu\text{mol acetate/L}_s/\text{h}$) (Bond and Lovley 2003, Gil, Chang et al. 2003). Studies examining the role of mass transport and organic matter availability at the BMFC anode have similarly found that natural diffusion of organics is insufficient to maximize power generation and there is a time-dependent decline in the concentration of small molecule organics under closed circuit conditions (Nielsen, Wu et al. 2009, Hong, Kim et al. 2010).

It is thus hypothesized that BMFCs, especially those deployed in low-porosity, organic-rich sediments, are hindered by the mass transport of substrate and protons at the anode surface. Power generation is impeded by the development of concentration gradients near the anode surface during current discharge. We hypothesize that increasing the diffusion rate of organic matter to the anode will reduce the likelihood of a substrate limitation for ARB, thereby improving power production. Similarly, to increase the diffusion rate of protons away from the

anode will reduce the likelihood of a proton gradient, i.e. anode acidification. The purpose of this study is to evaluate the efficacy of a structural, sand-modification of the BMFC anode against these inherent limitations of BMFC configurations, and quantify improvements in power generation in both lab and field trials.

6.2 Materials & Methods

6.2.1 Lab-Scale BMFC Evaluation

Sediment & Seawater Sources

Marine sediment was collected from two sites: (1) a Salt Marsh located at the Rutgers University Marine Field Station (RUMFS) near Tuckerton, New Jersey at approximately 39°30.5'N, 74°19.6'W, and (2) the SPAWAR Marine Base in San Diego Bay, California. The sites were chosen because previously deployed BMFCs generated relatively high and comparable levels of power production, and, qualitatively, the sediments appeared to have comparable physio-chemical characteristics. At both sites, sediment was collected via shovel in 5-gallon plastic buckets, filled approximately half-full with sediment, and at least one gallon of overlying seawater. No attempts were made to preserve the natural redox gradients of the sediments. From each site, an additional 40mL of sediment and 10mL seawater was collected without headspace in sterile containers and stored on ice for analysis of total organic carbon (TOC), particle size distribution, and porosity. The TOC analysis was conducted using a high-temperature combustion TOC analyzer (Shimadzu TOC-V).

BMFC Configuration

Figure 6-1 illustrates the set-up of the lab-scale BMFCs, which were configured as artificial microcosms of the marine sediment-water ('benthic') interface. Similar batch configurations have been previously employed to evaluate BMFCs in laboratory settings (Park and Zeikus 2003, Lowy and Tender 2008). Two-liter beakers were filled with 800 mL marine sediment and 1200 mL artificial seawater, and allowed to rest at room temperature (25°C) overnight. Artificial seawater was prepared from a commercially available synthetic salt blend (Instant Ocean Inc., Spectrum Brands) at a concentration of 125 mL salt to 3.79 L deionized water—to achieve a standard conductivity of ~30,000 $\mu\text{S}/\text{cm}$. The anode was subsequently buried 1-2 cm below the sediment surface, and the cathode was suspended within 10 cm of the anode in the overlying seawater. An Ag/AgCl, 3M KCl reference electrode (BASi Inc.) was positioned in solution with the cathode, with the tip less than 3 cm from the water surface. All BMFCs were positioned in a water bath maintained at 30°C. To maintain conductivity/salinity levels, seawater evaporation during the course of the experiment was replaced with a deionized water (DIW) source. Dissolved oxygen (DO) concentrations in the overlying seawater were periodically monitored with fiber optic sensors (Ocean Optics R Sensor Probe and Neofox Viewer software).

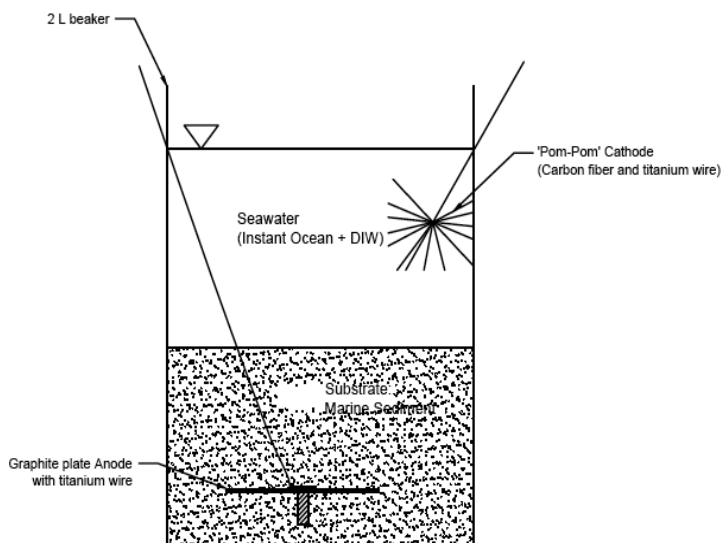


Figure 6-2 Lab-Scale BMFC Reactor (not to scale). 2-L beaker is filled with 800 mL marine sediment and 1200 mL artificial seawater. Graphite plate anode is embedded in the sediment, carbon cloth cathode is suspended in overlying seawater, and Ag/AgCl reference

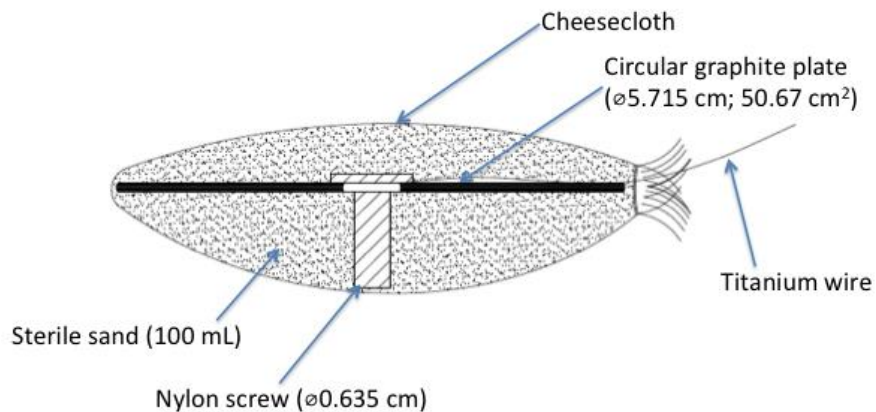


Figure 6-3 Schematic of sand-modified anode used for lab evaluations (not to scale)

Circular anodes were cut from rough graphite plates (Mersen Graphite; G10 grade 0.3175 cm thickness) using a hole saw ($\varnothing 5.715$ cm; $\varnothing 0.635$ cm center cut-out). Organic matter and metals, respectively, were leached from the graphite via 24-hr soaks in 1M NaOH and 1 M HCl,

followed by 24 hours in DIW. Electrical contact was made via titanium wire ($\varnothing 0.0635$ cm; McMaster-Carr) wound around a nylon screw ($\varnothing 0.635$ cm), and secured with a nylon washer and nut. Electrical resistance of the graphite-titanium connection was checked with a handheld voltmeter (Fluke), and found to be less than 5Ω for all anodes. The two-sided surface area for both the control and sand-modified anodes was 50.67 cm^2 . The sand-modified anodes, as illustrated in Figure 6-2, were embedded in 100 mL of washed sea sand (Acros Organics) that was previously sterilized via autoclave, and then wrapped in three layers of cheesecloth and sealed via cinched, insulated wire. An additional anode was prepared with 100 mL of marine sediment, and similarly wrapped in cheesecloth to differentiate any effects of the sand layer vs. cheesecloth. All cathodes were made from 10cm x 10 cm squares of plain weave carbon cloth (US Composities; FG-CARB575), pulled apart into strands, and wound around titanium wire to make a press-fit connection.

Electrochemical Analysis

All electrochemical analysis was performed using a Solartron 1470E multichannel potentiostat (Solartron analytical) and Multistat software program (Scribner Associates). The anodic biofilms were grown in potentiostatic mode, whereby the anode (working electrode) was maintained at a fixed potential of +0.3V vs. Ag/AgCl, the cathode served as the counter/auxiliary electrode, and an Ag/AgCl, 3M (+205 mV vs. SHE) (BioAnalytical Systems, Inc.) served as the reference electrode. By maintaining the anode at a positive (i.e. oxidizing) potential, we ensure that it can serve as a potent oxidant for bacterial respiration—effectively maximizing the thermodynamic driving force of the electron transfer step from bacteria to electrode.

Potentiostated configurations also ensure that the anode is not limited by any cathodic overpotential that can develop under two-electrode configurations.

Slow-scan cyclic voltammetry (CV) of the anodes was performed at (1) the start of the experiment; (2) the onset of catalytic activity; and (3) maximum current production (i_{max}). Multiple CVs during the course of biofilm development allowed for analysis of capacitance, resistance, and sigmoidal current profiles at the anodic reaction. CVs were performed in-situ under the same three-electrode configuration, and scan parameters were as follows: the initial cathodic scan ($v < 0$) swept the anode potential from $E_i = +0.3V$ vs. Ag/AgCl to $E_f = -0.8V$ vs Ag/AgCl, and was followed immediately by a anodic scan from $-0.8V$ vs. Ag/AgCl to $+0.3V$ vs. Ag/AgCl; all scans were performed at a rate (v) of 1 mV/sec.

Once a maximal electric current was achieved under potentiostated conditions, the BMFCs were switched to two-electrode configuration (WE: Anode; CE/RE: Cathode), and given 24-48 hr to reach a steady-state open circuit voltage (OCV). Polarization was then performed (V_{cell} was swept from OCV to 0.02V; scan rate of 0.1 mV/s). Point measurements of cathode potential during polarization were also recorded to quantify any cathode polarization (i.e. deviation of E_{cath} to less than 0.2-0.3 V vs. Ag/AgCl). After polarization, power output was characterized under two-electrode configuration, whereby the cathode was held 350 mV positive of the anode (i.e. $V_{cell} = 0.35V$). Power was calculated via Ohm's law (i.e. $P = iV$), and all current and power measurements were normalized by anode surface area (50.67 cm^2). All experiments were conducted, at a minimum, in triplicate, and statistical analysis on resulting current/power densities were conducted using the Student's t-test at $\alpha > 99\%$ and $t_{crit}: 2.552$.

6.2.2 Field Deployment of Sand-Modified BMFC

Deployable BMFCs

Scaled-up versions of the control and sand-modified anodes from the lab were designed as illustrated in Figure 6-3 and 6-4. The deployable anodes were built from identical graphite disks (\varnothing 40.64 cm; 3.81 cm thickness) that had been previously modified with an inner inset circle (\varnothing 20.32 cm; 2.54 cm depth) and a \varnothing 2.54 cm center through-hole. To facilitate shallow-water deployment, the anodes were further modified to include a 7.6cm x 7.6cm acrylic block and heli-coil insert to allow for manual anode embedment via a threaded extension pole. Electrical connection to both anodes was made via marine insulated electrical leads that terminated in wet pluggable connectors. Approximately 5 cm of conductor cable was exposed and connected to the graphite via ring terminal and a titanium bolt, and the connection was subsequently sealed in water insulating epoxy.

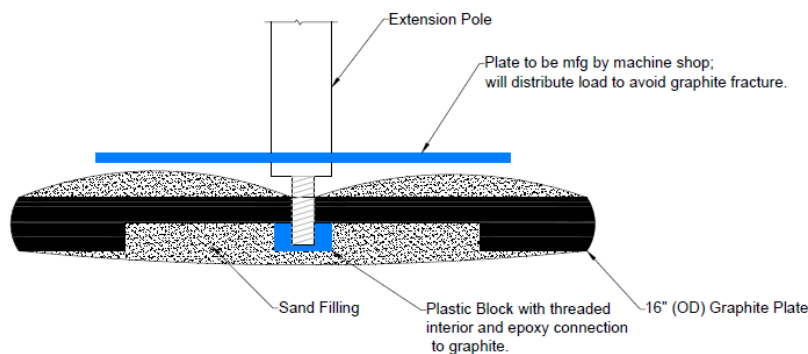


Figure 6-4 Schematic of Sand-Modified Anode

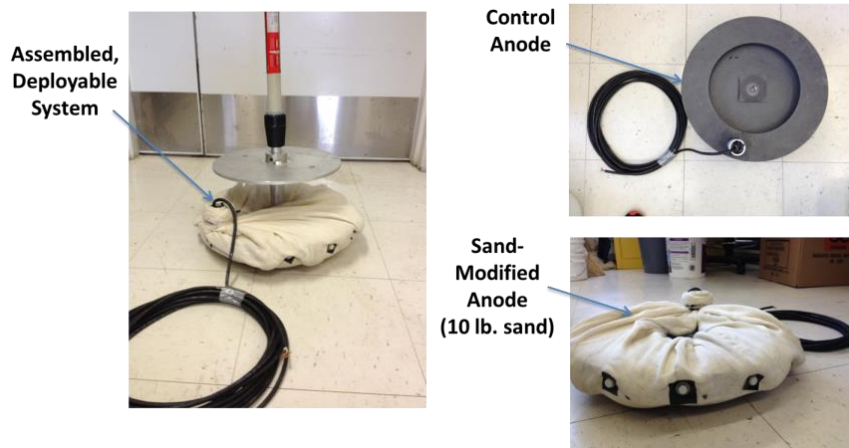


Figure 6-5 Photos of (A) Assembled, Deployable Anode; (B) Control Anode; and (C) Sand-Modified Anode

One anode was embedded in 4.54 kg of fine-grained construction sand (previously sterilized via autoclave) and then wrapped in three layers of cheesecloth. The sand was held in place by securing the cheesecloth to the graphite with titanium bolts around the perimeter of the graphite plate (spaced at 10.16 cm o.c.). Both the control and sand-modified deployed anodes yielded a two-sided surface area of 0.259 m² (footprint area of 0.130 m²). Identical cathodes were made from graphite fiber bottle brushes (ø15.24cm; 1.82 m length), similarly connected via marine insulated electrical leads. Both anodes were buried, with their surface approximately 10cm below the sediment surface, and cathodes were suspended via floats (describe) in the overlying water, approximately 2 ft. from the anode.

Field Electrochemical Evaluation

All BMFCs were deployed in a salt marsh at the Rutgers University Marine Field Station (RUMFS), located near Tuckerton, NJ (39°30.5'N, 74°19.6'W) on June 16, 2012. Immediately after anode embedment, both control & sand-modified BMFCs were connected to custom

designed miniature low-power consuming (battery powered) potentiostats (Northwest Metasystems, Inc.) capable of maintaining a fixed cell voltage ($V_{cell}: E_{cathode} - E_{anode}$) for long-term operation. Control and sand-modified BMFCs were maintained at a cell voltage (V_{cell}) of 0.35 V for the duration of the deployment. The fixed cell voltage of 0.35 V represents the cell voltage that most commonly results in maximum power production during polarization of BMFCs, and is comparable to passively discharging current across a variable resistor that is maintained equivalent to the cell's internal resistance. Current and voltage measurements were collected with a DataQ data collection device, logging to an SD data card that was periodically downloaded to a PC. Point measurements of anode and cathode potential were also made versus a Ag/AgCl seawater reference electrode.

6.3 Results & Discussion

6.3.1 Sediment Characterization

A summary of physio-chemical sediment characteristics from the Tuckerton, NJ salt marsh and the San Diego Bay, CA sites are presented in Table 6-2. Importantly, deployed BMFCs have exhibited high variability in both electrical output as well as sediment characteristics with some evidence that current production can be correlated with TOC levels (Tender et al., in preparation). In comparison with sediments from other deployment sites, the Tuckerton and San Diego sediments contained relatively high levels of TOC but were less porous. TOC was not differentiated into its dissolved and suspended fractions, so it cannot be directly linked to bioavailable ARB substrates. However, in field deployments, these sites have generated higher current densities despite a decreased porosity. Thus, it is likely that TOC numbers correlated

with concentrations of known ARB substrates (e.g. acetate, lactate), and an anode structure with increased diffusion would benefit in these sediments.

Table 6-2 Physical & Chemical characteristics of sediment collected from the Tuckerton, NJ Salt Marsh and the San Diego, CA marine station

Sediment	Date Sampled	Average Particle Size (μm)	Total Organic Content (%)	Porosity (%)	Soil Classification
RUMFS	2012	30	2.19	57.1	Medium silt
SPAWAR	11/2010	32.8		56.3	Coarse silt
SPAWAR	4/2010	218	0.44	51.4	Medium-fine sand
RUMFS	2010	17.8		68.6	Medium silt
SPAWAR	2010	24.3	1.88	78.0	Medium silt

6.3.2 Laboratory Evaluation

Table 6-3 summarizes the electrochemical performance of the control and sand-modified anodes in RUMFS & SPAWAR sediment. Upon embedment of the anode, all control and sand-modified BMFCs achieved $\text{OCV} \geq 0.4 \text{ V}$ and $E_{\text{an}} \leq -0.3 \text{ V}$ within 48 hr (see plot in Batch 3), at which time all anodes were poised at +300 mV vs. Ag/AgCl. The onset of catalytic activity, as evidenced by an initial current increase, was observed in all cells within 72 hours of poisoning. The time required to reach maximum current production varied from 120-350 hours, with sand-modified BMFCs reaching max current in a shorter time frame. The unmodified (control) anodes in RUMFS sediment achieved maximum current between 29-38 mA/m^2 (mean: 35 mA/m^2 ; stdev: 3 mA/m^2 ; n = 9). Sand-modified RUMFS BMFCs reached 62-113 mA/m^2 (mean: 86 mA/m^2 ; stdev: 14 mA/m^2 ; n = 11), representing a 148% increase in maximum (3-electrode) current production over the control anodes. Figure 6-5 depicts representative current versus time

plots during biofilm growth. Comparable improvements in the SPAWAR sediment were achieved (Figure 6-7), albeit with a higher variation in mean current and power production (SD, 18 mA/m² and 9 mW/m², respectively). High variability in the performance of SPAWAR sediment has also been observed at fuel cell deployments in San Diego (*unpublished data; Snider & Tender*).

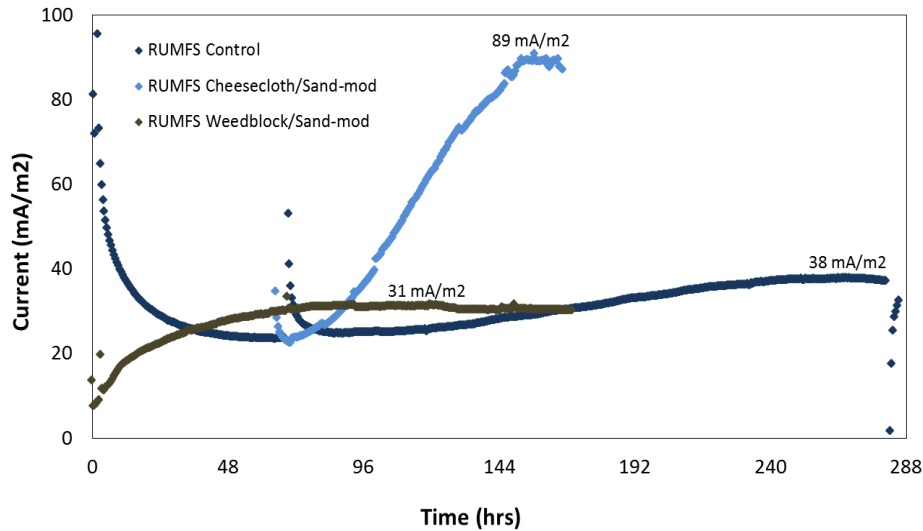


Figure 6-6 Representative growth curves of lab-scale BMFCs using Tuckerton, NJ Salt Marsh sediment. Experiments conducted in three-electrode mode, where E_{an} : 0.3V vs. Ag/AgCl. All current measurements were normalized by anode surface area (50.67 cm²).

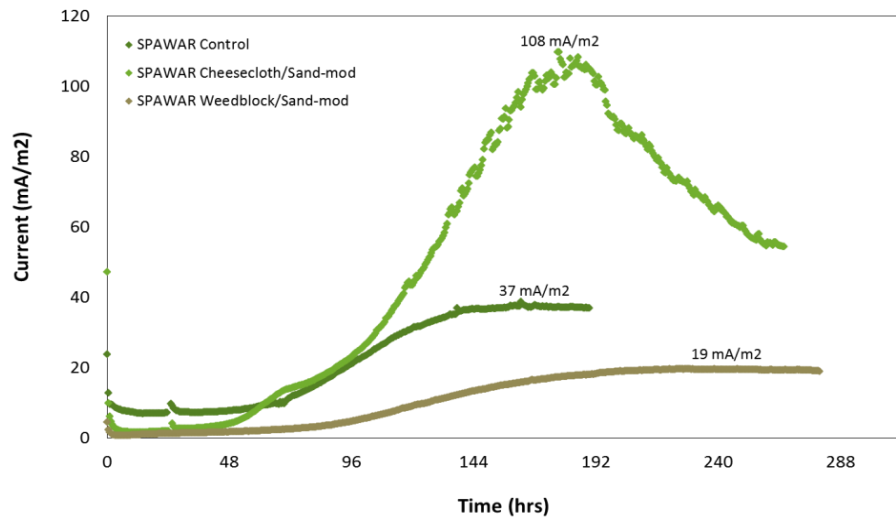


Figure 6-7 Representative growth curves of lab-scale BMFCs using San Diego Bay (SPAWAR) marine sediment. Experiments conducted in three-electrode mode, where E_{an} : 0.3V vs. Ag/AgCl. All current measurements were normalized by anode surface area (50.67 cm²).

All BMFCs, operated at open circuit for 24 hours after reaching i_{max} , achieved $\geq 0.57V$ OCV. Subsequent polarization (V_{cell} : OCV to 0.02V at 0.1mV/sec) also revealed significant improvements in maximum power with the sand modification (300% and 65% increase in P_{max} of RUMFS and SPAWAR, respectively). Representative polarization curves for RUMFS data are illustrated in Figure 6-8. For both sediment types, the increase in i_{max} and P_{max} using the sand-modification was statistically significant at the level of $\alpha > 99\%$ (Student's T-test).

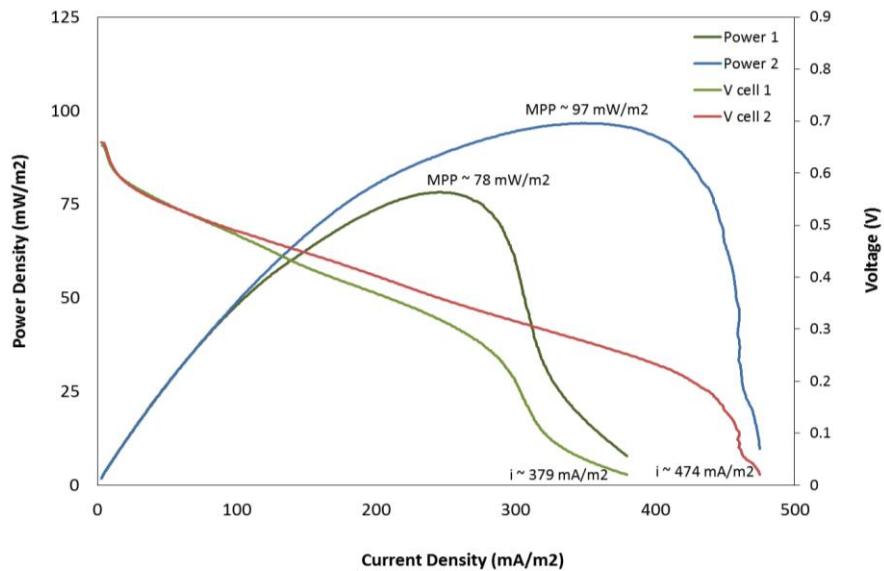


Figure 6-8 Representative polarization and IV plots from lab-scale BMFCs with sand-modified anodes, using Tuckerton, NJ Salt Marsh sediment. BMFC was held at open circuit for 24-48 hrs. prior, then scanned from open circuit to 0.1V; scan rate of 0.1 mV/s. All current/power measurements were normalized by anode surface area (50.67 cm²).

Steady-state evaluation at a fixed cell voltage of 0.35V after polarization confirmed the increase power from the sand modification—with a 156% increase in steady-state power production from RUMFS cells (26 mW/m² vs. 74 mW/m²; n = 8). Long-term evaluation at a fixed cell voltage yielded a more accurate measure of power production than fuel cell polarization—with polarization over predicting power output by a factor of two. Importantly,

evaluation at a fixed cell voltage occurred after current production peaked and began to decline, likely skewing the lab values downward. It has been previously observed that BMFCs cannot sustain maximum current production indefinitely in batch, lab-scale configurations (Lowy, Tender et al. 2006), presumably due to the development of substrate concentration gradients around the anode, which are remedied by natural diffusion, convection, and tidal action in field deployments. This phenomenon was also observed in the current study; however, it was noted that the sand-modified anodes somewhat prolonged the duration of current production—i.e. 480 hr versus > 500 hr where $i > 30 \text{ mA/m}^2$, which corroborates the hypothesis that such a modification reduced substrate depletion zones and improved mass transport around the anode.

Importantly, significant cathode polarization was observed during polarization of all lab-scale BMFCs, i.e. the shift in E_{cath} accounted for >50% of ΔV_{cell} during polarization. Figure 6-7 describes the shift in cathode potential during polarization of one sand-modified BMFC, where cathode polarization accounted for 62% of the overall fuel cell polarization and the cathode is driven near 0 mV vs. Ag/AgCl at short-circuit conditions. Cathode overpotential is well documented in MFCs and other biological fuel cells that rely on the oxygen reduction reaction (ORR) at the cathode:



The potential at which ORR takes place in MFCs is often driven far below the theoretical 1.23V vs. SHE (1.03V vs. Ag/AgCl; applicable for 4-electron ORR), owing to the low concentration of H^+ and OH^- ions at the circumneutral-pH conditions that are required for biological growth (i.e. mass transport), and the low activity of graphite or carbon cloth for catalyzing oxygen reduction (i.e. kinetics). This has the effect of limiting the maximum achievable cell voltage (i.e. $V_{cell} = E_{cath} - E_{an}$), and thus the maximum power production (i.e. $P =$

iV_{cell}). Previous field deployments of BMFCs have recorded sustained cathode potentials of 200-350 mV vs. Ag/AgCl at maximum power production. DO concentrations in the overlying water were maintained >6 mg/L (data not show), suggesting that our lab-scale cathodes were limited by either electrochemically active surface area or by the absence of naturally occurring marine bio-cathodes that develop in the field (Strycharz-Glaven, Glaven et al. 2013).

Slow-scan voltammetry (performed in-situ at 1 mV/s; E_{an} : -0.8 to +0.3V vs. Ag/AgCl) confirmed the presence of current-potential (i-E) dependency, consistent with Nernst-Monod kinetics, and the presence of oxidative peaks (illustrated in Figures 6-8 and 6-9) (Strycharz-Glaven et al., 2012). The limiting current observed during voltammetry at 1 mV/s typically over predicted the maximum three-electrode current production by a factor of two. Scans performed at slower rates (0.1 mV/sec) displayed oxidative peaks that were closer in magnitude to the maximum current achieved (not shown). For both control and sand-modified anodes, the oxidative peak on the cathodic scan of the CV occurred in a potential window of E_{an} : -200 mV to 0 mV vs. Ag/AgCl (Figures 6-8 and 6-9). No previous attempts to perform in-situ voltammetry on BMFCs have been reported on in the literature. In comparison however, to anodic CVs from idealized, electrochemical cells with ARB-modified anodes, the in-situ BMFC-CVs revealed significant mass-transport limitations and irreversibility at the anodic reaction. Both control and sand-modified CVs changed from peak-shaped to sigmoidal when switching from oxidative to reductive responses, suggesting that either a quasi-reversible or two separate irreversible reactions were dominating the anodic process. Peak splitting—a phenomena observed in acetate-depleted ARB biofilms—was observed in both the control and sand-modified CVs. Despite an increase in current with the sand-modification, this suggests that the anodic biofilm may continue to be limited by substrate availability and may benefit from further increases to mass transport.

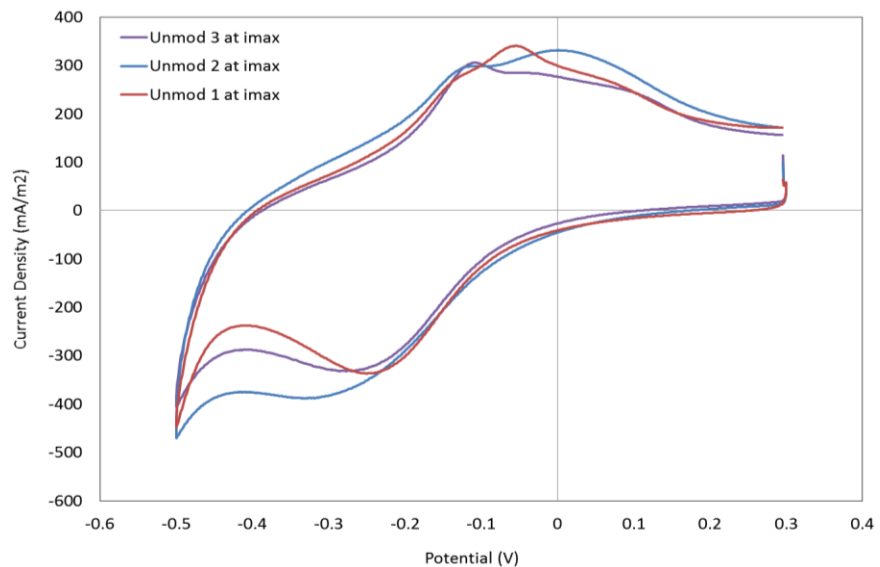


Figure 6-9 Representative voltammetry of control anodes using Tuckerton, NJ Salt Marsh sediment (RUMFS 100410 Batch). Scans performed at 0.1 mV/s from 0.3V --> -0.5V vs. Ag/AgCl. All current measurements were normalized by anode surface area (50.67 cm²).

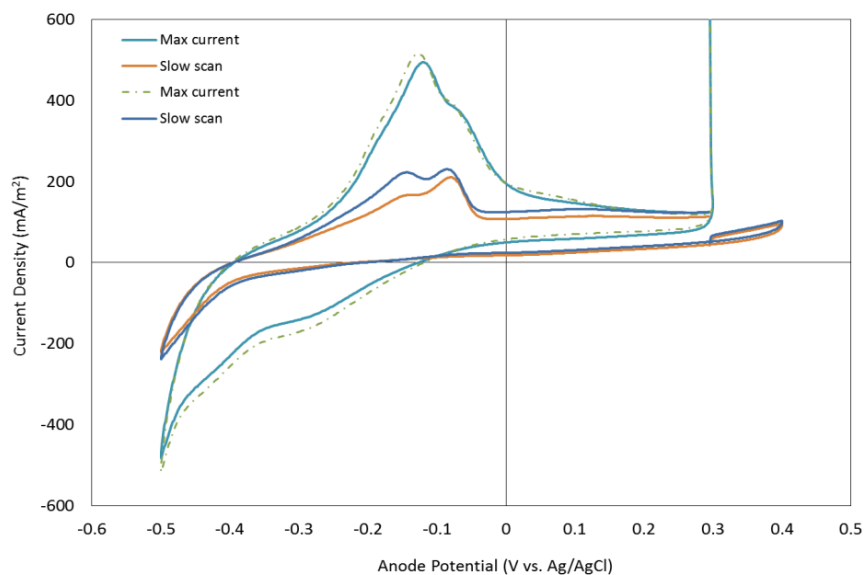


Figure 6-10 Representative voltammetry of sand-modified anodes using Tuckerton, NJ Salt Marsh sediment (RUMFS 100410 Batch). Scans performed at 0.1 mV/s from 0.3V --> -0.5V vs. Ag/AgCl. All current measurements were normalized by anode surface area (50.67 cm²).

Table 6-3 Performance Summary from Lab-Scale Control & Sand-Modified Anodes

	RUMFS Control	RUMFS Sand-Modified	SPAWAR Control	SPAWAR Sand-Modified
Mean particle size (d_p) (μm)	18 ± 0.09	--	24.3	--
Porosity (%)	57	--	78	--
Percent Organic Content (%)	2.19	--	1.88	--
Initial E_{an}^0 vs. Ag/AgCl (mV)	-367 ± 26^a (n = 3)	-402 ± 19 (n = 5)		
OCV (V)	0.597 ± 0.005	0.640 ± 0.030	0.645 ± 0.031	0.700 ± 0.03
i_{max} (mA/m^2) (E_{an} : 0.3V vs. Ag/AgCl)	34 ± 4 (n = 6)	85.2 ± 15 (n = 8)	37 ± 13 (n = 4)	93 ± 18 (n = 3)
P_{max} (Polarization) (mW/m^2)	13 ± 2.3 (n = 6)	53.4 ± 41.5 (n = 8)	12 ± 6 (n = 4)	19 ± 9 (n = 3)
P_{ss} (at 0.35V _{cell}) (mW/m^2)	10 ± 2 (n = 5)	26 ± 10 (n = 8)	12 (n = 1)	23 (n = 2)
Mean sediment particle size (d_p) (μm)	18 ± 0.09			
P_{max} (Anode step polarization) (mW/m^2)	14.7 ± 2.5 (n = 3)	20.4 ± 12.5 (n = 5)	NA	NA
I_{sc} (Anode step polarization) (mA/m^2)	36.6 ± 3.5 (n = 3)	75.6 ± 16.4 (n = 5)	NA	NA
Power Lifetime (hr where $i > 30 \text{ mA}/\text{m}^2$)	~480 hr	< 500 hr	> 700 hr	> 600 hr

6.3.3 Field Deployment

The control and sand-modified BMFCs were deployed in a shallow water salt marsh near Tuckerton, NJ on June 14th, 2012. The anode was manually embedded approximately 10 cm below the sediment surface with the cathode suspended in the overlying seawater. All BMFCs were maintained at a fixed cell voltage of 0.35V for the duration of the experiment. When data logging began on June 27th (13 days after deployment), the control and sand-modified BMFCs were producing 20 and 130 mW/m^2 , respectively (normalized by the anodic surface area)—representing more than a six-fold power improvement. Point measurements of anode and cathode

potential were also made on day 13 using a Ag/AgCl seawater reference. At a cell voltage of 0.35V, the control E_{an} was +0.02V vs. Ag/AgCl—comparable to anodic potentials of additional BMFCs deployed nearby (E_{an} : -0.003 to 0.029V vs. Ag/AgCl) (unpublished data; Tender et al.). Interestingly, the potential of the sand-modified anode was significantly lower ($E_{an, sand}$: -0.29V vs. Ag/AgCl), suggesting an increase in the anodic oxidation reaction (i.e. accelerated rate of electron transfer at the anode). Cathode potentials for both BMFCs were comparable (0.32-0.37V vs. Ag/AgCl), confirming that the increased performance was due to a factor at the anodic reaction. Furthermore, a decrease in anode potential is frequently observed in BMFC literature reporting increases in power performance (Vega and Fernandez 1987, He, Shao et al. 2007).

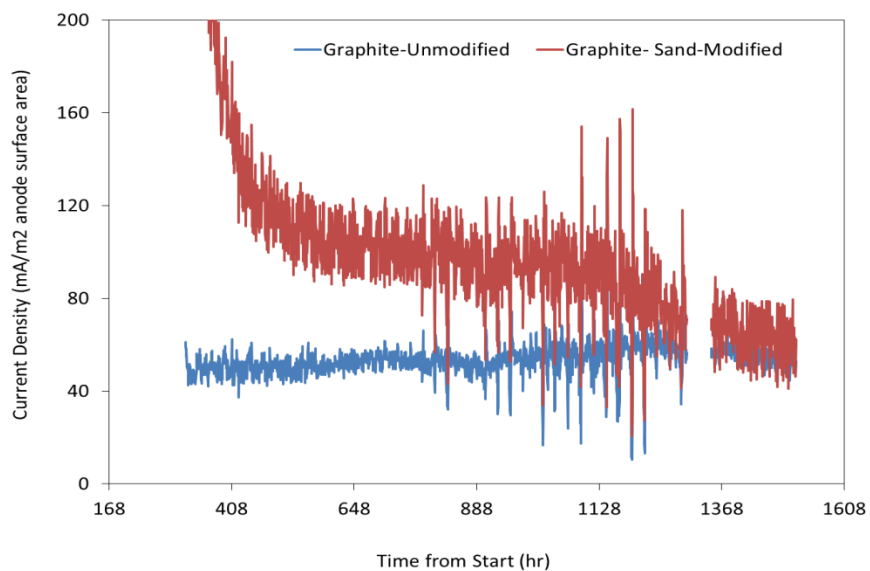


Figure 6-11 Current Density from Control and Sand-Modified BMFCs deployed at Tuckerton, NJ Salt Marsh. Current production was normalized by anode surface area of 0.259 m².

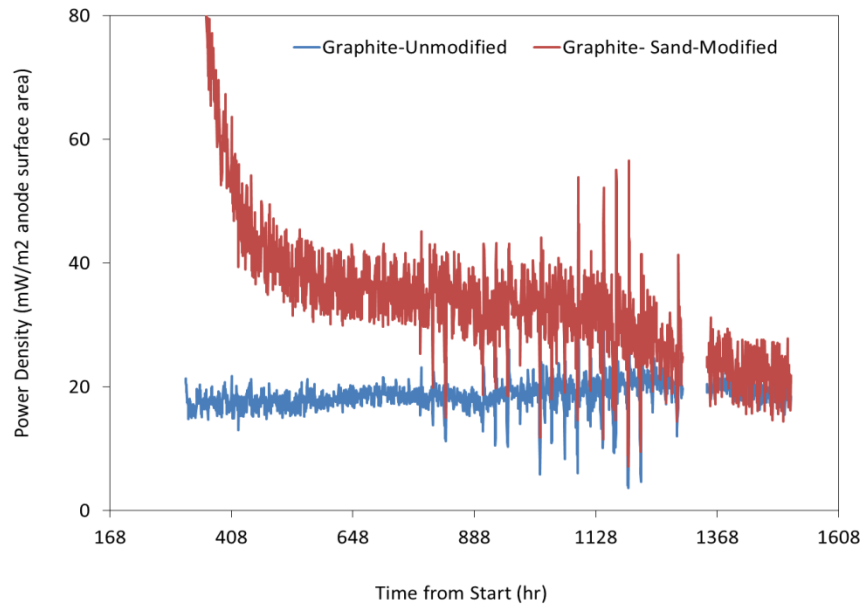


Figure 6-12 Power density from Control and Sand-Modified BMFCs deployed at Tuckerton, NJ Salt Marsh. Power production was normalized by anode surface area of 0.259 m².

Power production from the sand BMFC thereafter declined (Figure 6-11), but continued to produce > 50% more power than the control for over 1000 hours (41 days). After 58 days however, the sand BMFC maintained only a small advantage in power production (~15%), and the two cells appeared to be converging at a power density of ~20 mW/m², which is within the range of power densities observed from the control anodes in the lab-scale experiments. It is hypothesized that the convergence in power densities may have been due to the escape of sand from the relatively permeable cheesecloth that was maintaining the anode structure. Voltage and data logging continued for 130 days, until the experiment was terminated by a weather event (Tropical Storm Sandy).

6.4 Conclusions

This study reports on efforts to improve power densities in lab- and field-scale BMFCs with the use of a structural sand-modification to mitigate mass transport limitations of substrate to the BMFC anode. An increase in current of > 148% was achieved in lab-scale testing with an environmental sediment source, and an average control versus sand current production of: 35 mA/m² (± 3 mA/m²; n = 9) versus 86 mA/m² (14 mA/m²; n = 11), respectively. Deployment of control and sand-modified BMFC prototypes were performed in a salt marsh near Tuckerton, NJ (USA), with the sand BMFC sustaining a >50% increase in power generation for >40 days, relative to the control. Max power densities from the sand-modified anode near the upper limit of what has been achieved from the BMFC design, representing a simplistic design modification to improve electrical output and simplify BMFC deployment.

6.5 Acknowledgements

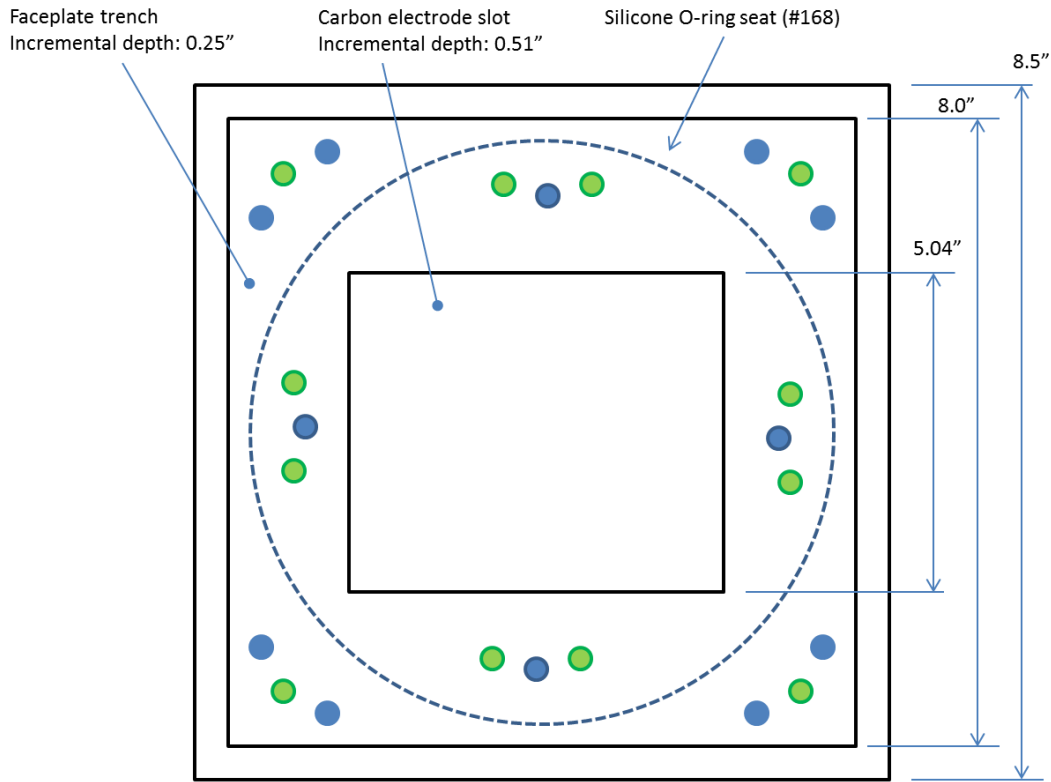
This work was supported by the Naval Research Laboratory and the Office of Naval Research. We thank Rose Petrecca, Joe Debarro, and staff of the Tuckerton, New Jersey Field Station of Rutgers University, Institute of Marine and Coastal Sciences for assistance in fuel cell deployment and retrieval. Marius Pruessner also assisted with BMFC deployment and monitoring.

Appendices

Table 6-4 Summary of analytical methods used for environmental analysis of samples

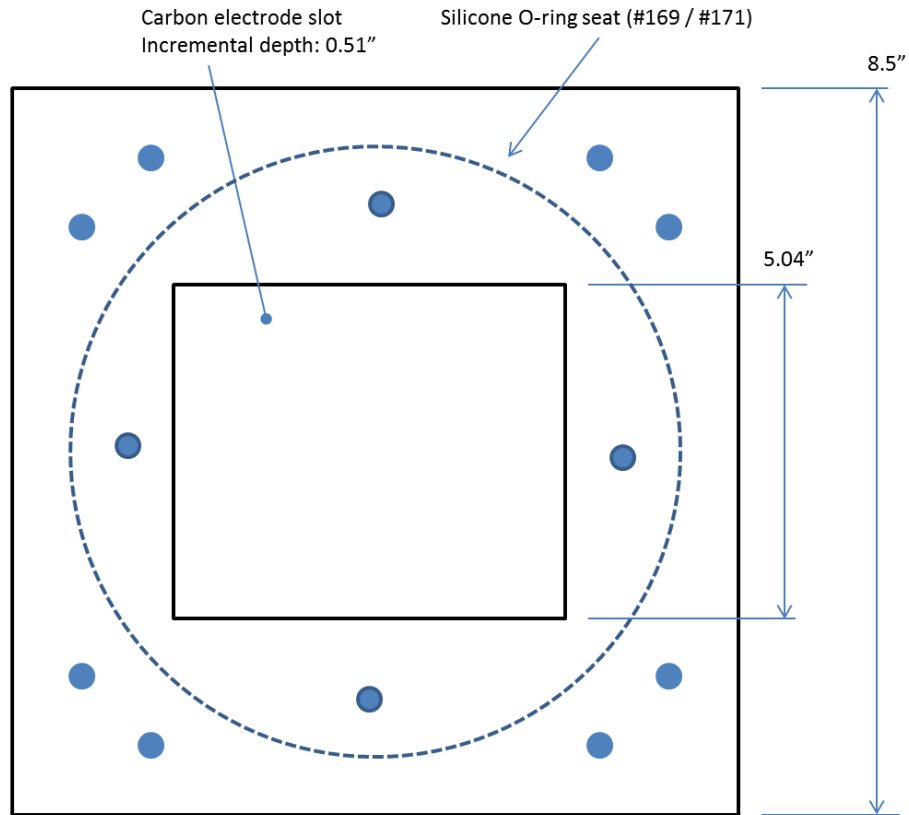
Analyte	Analytical Method	Reference
COD	Reactor Digestion	Hach 8000; Jirka et al. (1975)
TS, TSS, VS	Standard Methods	APHA (1992); EPA 2540 B
TN, NO ₃ /NO ₂ -N, NH ₃ -N, PO ₄ -P, TP	Continuous Flow Colorimetry (TRAACS 2000)	O'Dell & EPA (1993)
pH	pH probe + mV meter (Accumet 950)	
Alkalinity (mg CaCO ₃ /L)	Titration	APHA (1992)
Conductivity	Conductivity probe + meter (Hach Model 51975)	
CH ₄	Gas Chromatography (Agilent HP5890)	Freedman & Gosset (1989)
Dissolved oxygen	DO probe + mV meter	NA
<i>E.coli</i> & Fecal coliforms	Filtration + physical enumeration	APHA (1992)
Organic Acids (AD/MFC effluent only)	High performance liquid chromatography	NA

Microbial Fuel Cell Design



- Faceplate Locking Screws: 8-32 thread, 1/2" long
Use #10 silicone O-rings **(REPLACE W/ #11 O-RINGS) – next line down (REPLACE W/ #11 O-RINGS)**
- Flow Chamber Locking Screws 8-32 thread, 5/8" long
Use #10 / #12 silicone O-rings (larger rings for recessed screw heads)
- Flow Chamber Locking Screws 8-32 thread, 5/8" long
No O-ring

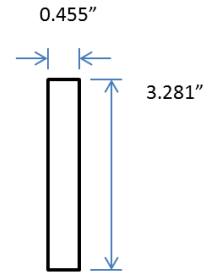
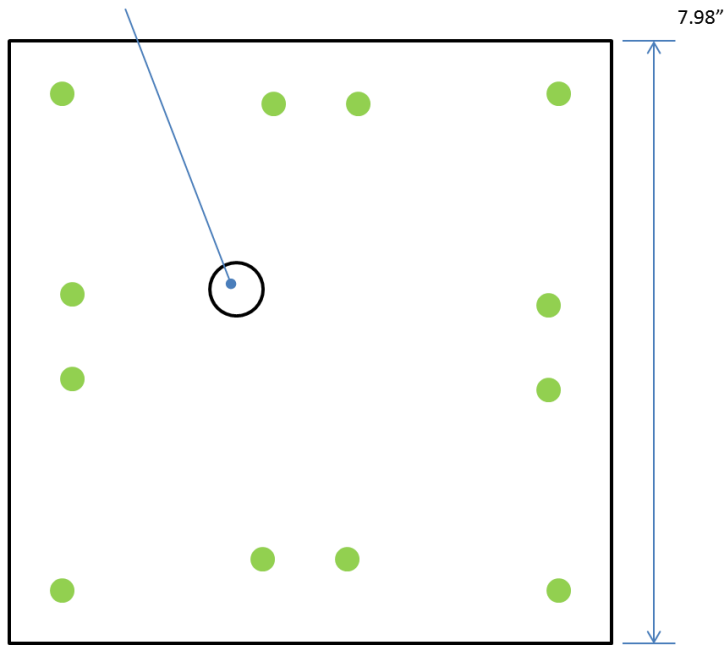
Flow Chamber: Top View



- Flow Chamber Locking Screws 8-32 thread, 5/8" long
Use #10 silicone O-rings **(REPLACE W/ #11 O-RINGS)**
- Flow Chamber Locking Screws 8-32 thread, 5/8" long
No O-ring

Flow Chamber: Back View

Hole for 1/2" rubber stopper:
dissolved O2 and electrode

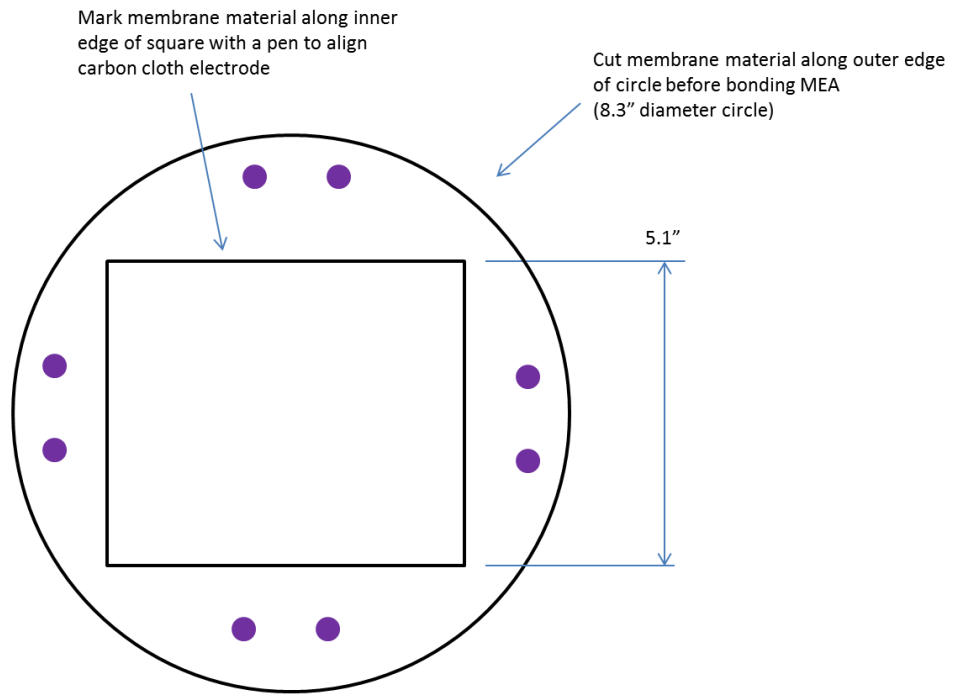


Baffles
3/8" thick

Faceplate

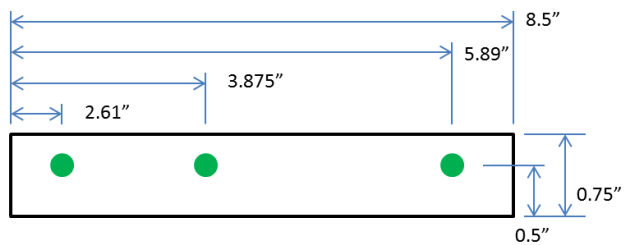
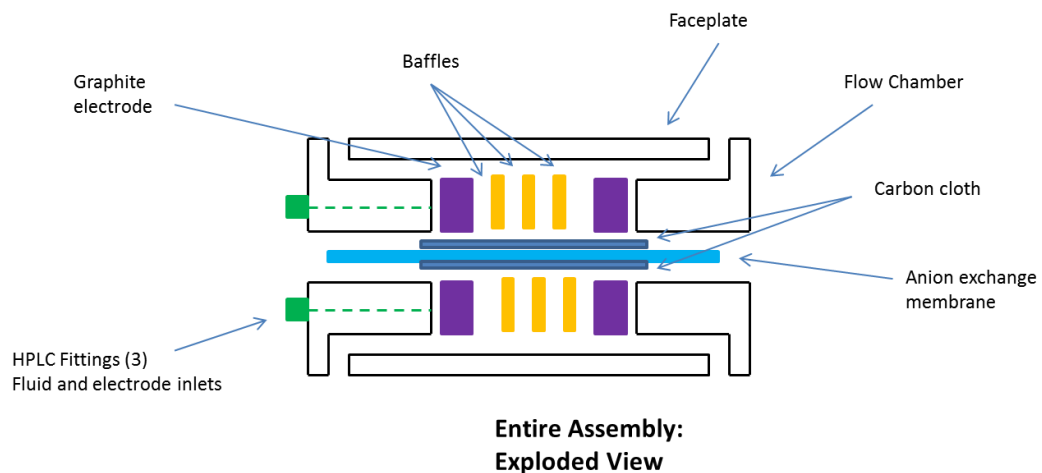
Note: designed for 12% compression
with 1/16" soft rubber gasket material

● Faceplate Locking Screws: 8-32 thread, 1/2" long



Membrane Cutting Template

- Use a #5 punch to transfer marked holes into membrane



notes:

- (1) all three HPLC fittings are tapped 1/4"-28
- (2) Fluidic inlets are drilled with 3/16" bit
- (3) Electrode hole (middle) drilled with 1/8" bit

SMA Data & Results

Table 6-5 Summary of calculations and results from SMA assay on methanogenic inoculum

Bottle	V _{vw} (L)	VSS _i (g)	X _{ss,1} (g/L)	X _{ss,2} (g/L)	ΣQ ₁ CH ₄ (mL)	ΣCH ₄ -COD (g COD)	Dt ₁ (d)	ΣQ ₂ CH ₄ (mL)	ΣCH ₄ -COD ₂ (g COD)	Dt ₂ (d)	SMA ₂ (g COD-CH ₄ /g VSS-day)
C1	0.059	2.02			9.73	0.0259	3			1	
C2	0.059	2.02			10.57	0.0281	3			1	
C3	0.059	2.02			10.67	0.0284	3			1	
A1	0.050	1.71	0.129	0.857	11.76	0.0313	3	12.38	0.0329	1	0.0192
A2	0.050	1.71	0.129	0.857	11.68	0.0311	3	12.74	0.0339	1	0.0198
A3	0.050	1.71	0.129	0.857	11.14	0.0296	3	11.11	0.0295	1	0.0173
G1	0.050	1.71	0.129	0.857	13.23	0.0352	3	15.80	0.0420	1	0.0245
G2	0.050	1.71	0.129	0.857	11.90	0.0317	3	14.11	0.0375	1	0.0219
G3	0.050	1.71	0.129	0.857	13.91	0.0370	3	15.02	0.0399	1	0.0233

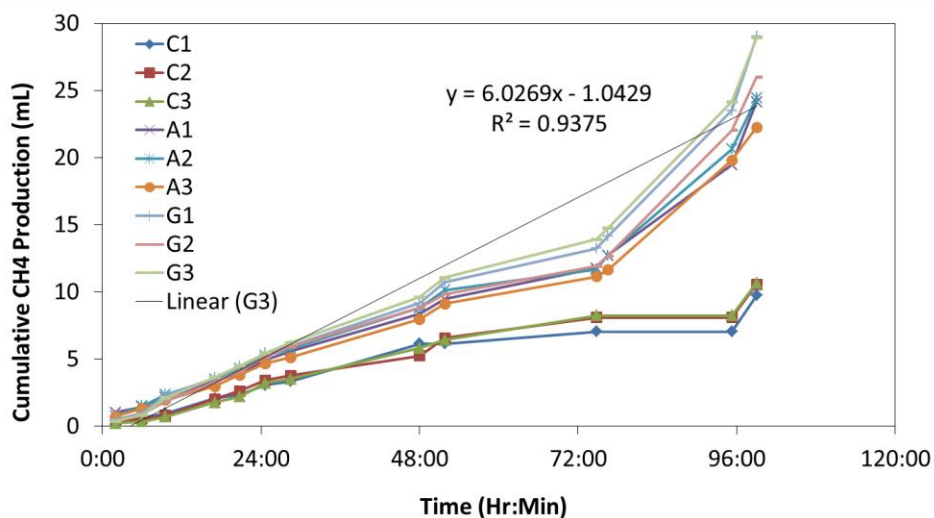


Figure 6-13 Cumulative CH₄ production during SMA assay on methanogenic inoculum

BMP Data

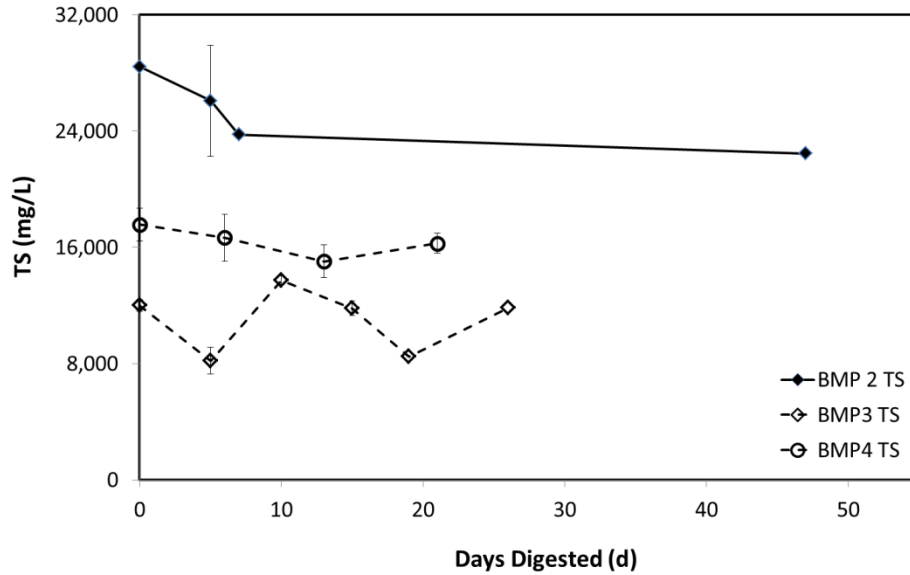


Figure 6-14 Average TS in mg/L during digestion of latrine solids during BMP2 (solid symbols); BMP3 (open diamonds); and BMP4 (open circles). Data points represent the Mean \pm SD (mg/L COD, n = 4-6)

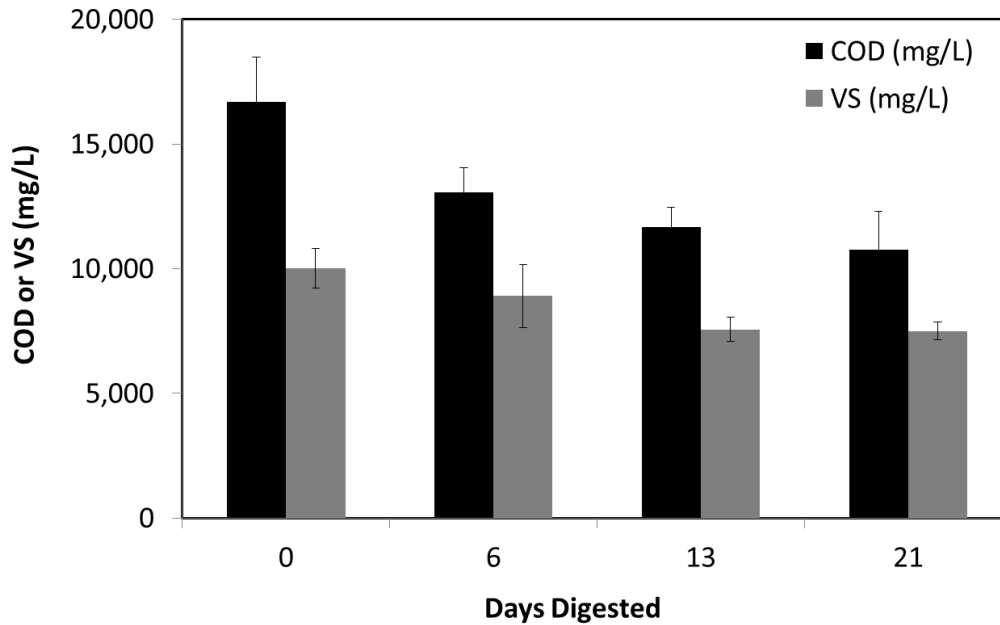


Figure 6-15. Average COD (in black) and VS (in grey) during digestion of wastewater in BMP4. Data points represent the Mean \pm SD (mg/L COD, n = 4-6)

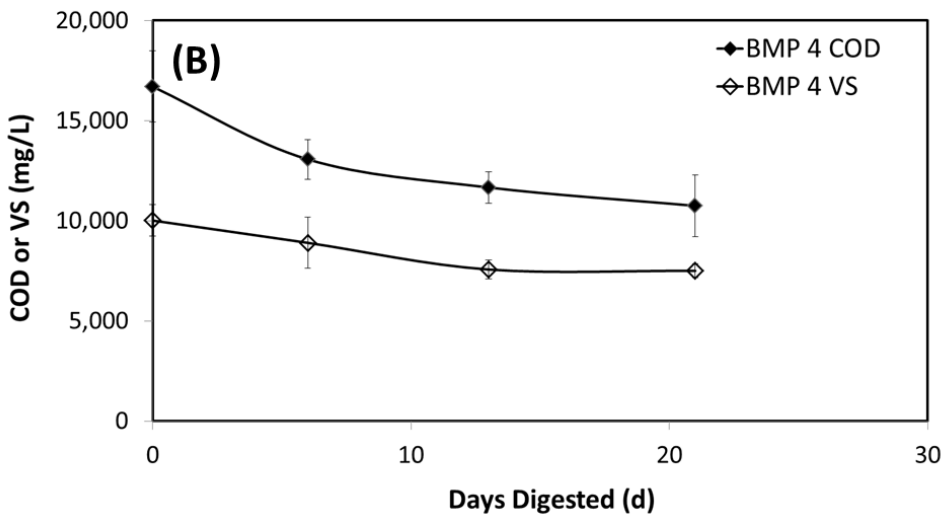
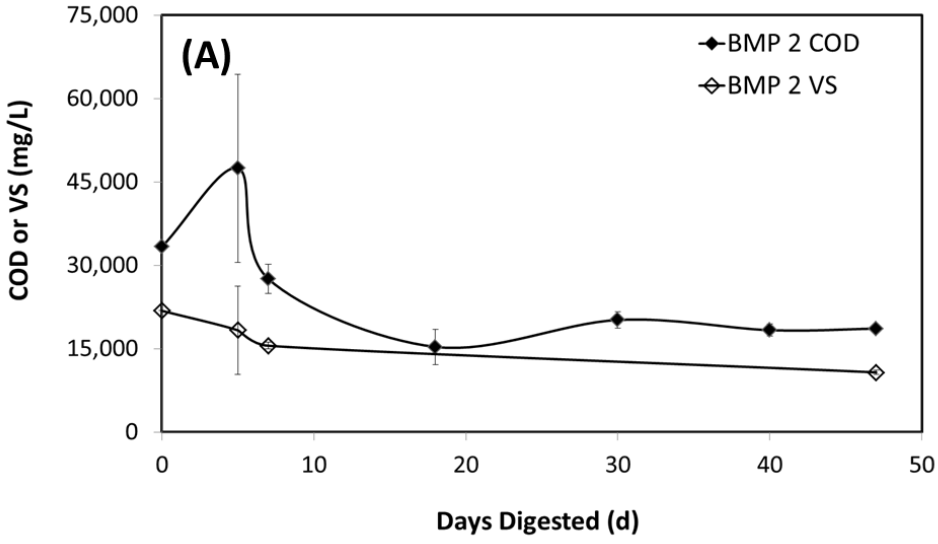
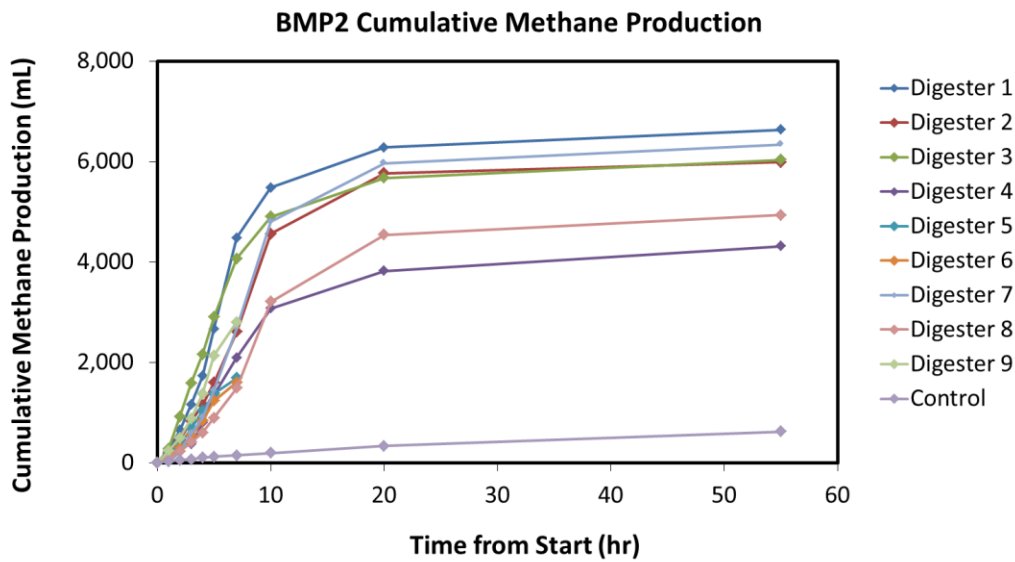
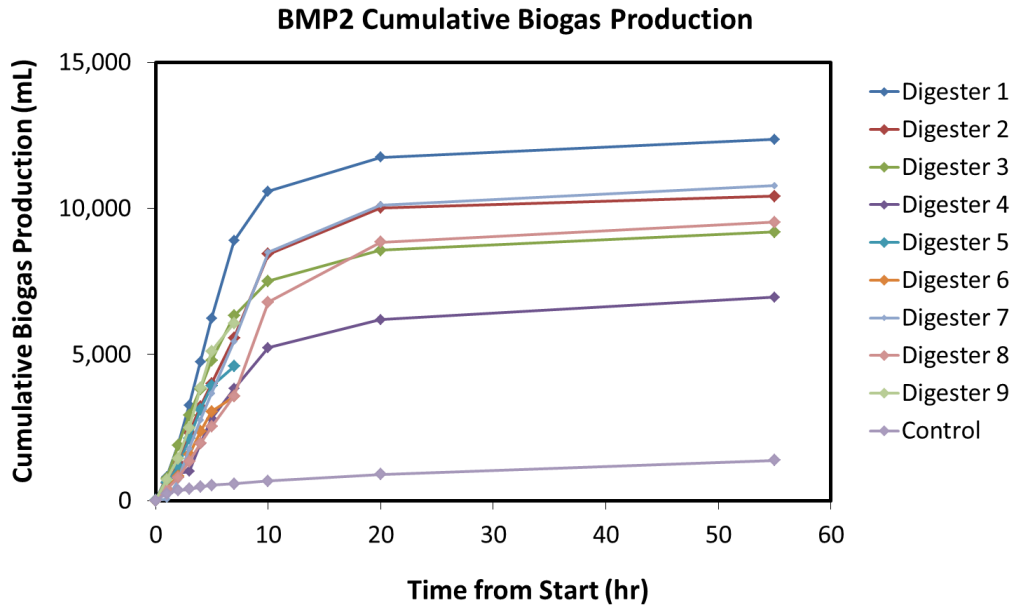


Figure 6-16. Average COD (solid symbols) and VS (open symbols) during digestion of latrine solids during BMP2 (Figure A) and BMP4 (Figure B). Data points represent the average \pm standard deviation (mg/L COD or mg/L VS) of triplicate reactors.



Field Deployments (Ch.4)

US Lab Experiments

Table 6-6. Summary of electrochemical performance of MFCs fed with agricultural digestate in laboratory experiments. Values are presented as mean \pm standard deviation (n).

	Swine Average	Cow Average	Dorm Average
i_{ss} (Ean: -0.2V vs. Ag/AgCl) (mA/m ²)	93 \pm 17 (n = 3)	165 \pm 63 (n = 3)	86 \pm 17 (n = 3)
i_{ss} (Ean: -0.2V vs. Ag/AgCl) (A/m ³)	15 \pm 2.8 (n = 3)	27 \pm 10 (n = 3)	14 \pm 2.7 (n = 3)
$w/acetate, i_{ss}$ (Ean: -0.2V vs. Ag/AgCl) (mA/m ²)	NA	NA	681 \pm 265 (n = 3)
$w/acetate, i_{ss}$ (Ean: -0.2V vs. Ag/AgCl) (A/m ³)	NA	NA	110 \pm 43 (n = 3)
i_{ss} (Vcell: 0.2V) (mA/m ²)	71 \pm 7.9 (n = 3)	26 \pm 3.4 (n = 3)	59 \pm 18 (n = 3)
P_{ss} (Vcell: 0.2V) (mW/m ²)	14 \pm 1.6 (n = 3)	5.0 \pm 0.7 (n = 3)	12 \pm 3.6 (n = 3)
i_{ss} (Vcell: 0.2V) (A/m ³)	12 \pm 1.2 (n = 3)	4.0 \pm 0.5 (n = 3)	10 \pm 2.9 (n = 3)
P_{ss} (Vcell: 0.2V) (W/m ³)	2.0 \pm 0.2 (n = 3)	1.0 \pm 0.1 (n = 3)	2.0 \pm 0.6 (n = 3)
$w/acetate, i_{ss}$ (Vcell: 0.2V) (mA/m ²)	NA	82 \pm 16.7 (n = 3)	158 \pm 15.9 (n = 3)
$w/acetate, P_{ss}$ (Vcell: 0.2V) (mW/m ²)	NA	16 \pm 3.4 (n = 3)	31 \pm 3.5 (n = 3)
$w/acetate, i_{ss}$ (Vcell: 0.2V) (A/m ³)	NA	13 \pm 2.7 (n = 3)	25 \pm 2.7 (n = 3)
$w/acetate, P_{ss}$ (Vcell: 0.2V) (W/m ³)	NA	3 \pm 0.6 (n = 3)	5.0 \pm 0.6 (n = 3)
P_{max} (mW/m ²)	60 \pm 10 (n = 3)	52 \pm 7.4 (n = 3)	28 \pm 1.3 (n = 3)
P_{max} (W/m ³)	10 \pm 1.6 (n = 3)	8 \pm 1.2 (n = 3)	5.0 \pm 0.2 (n = 3)
ΔE_{an} during polarization (mV)	206 \pm 90 (n = 3)	229 \pm 86 (n = 3)	253 \pm 35 (n = 3)
ΔE_{cath} during polarization (mV)	395 \pm 22 (n = 3)	320 \pm 52 (n = 3)	178 \pm 24 (n = 3)
OCV_{max} (mV)	701 \pm 34 (n = 3)	548 \pm 37 (n = 3)	495 \pm 31 (n = 3)
Power Lifetime (hr to $i < 1$ mA)	< 20	19	30

NA refers to an experimental condition that was not evaluated.

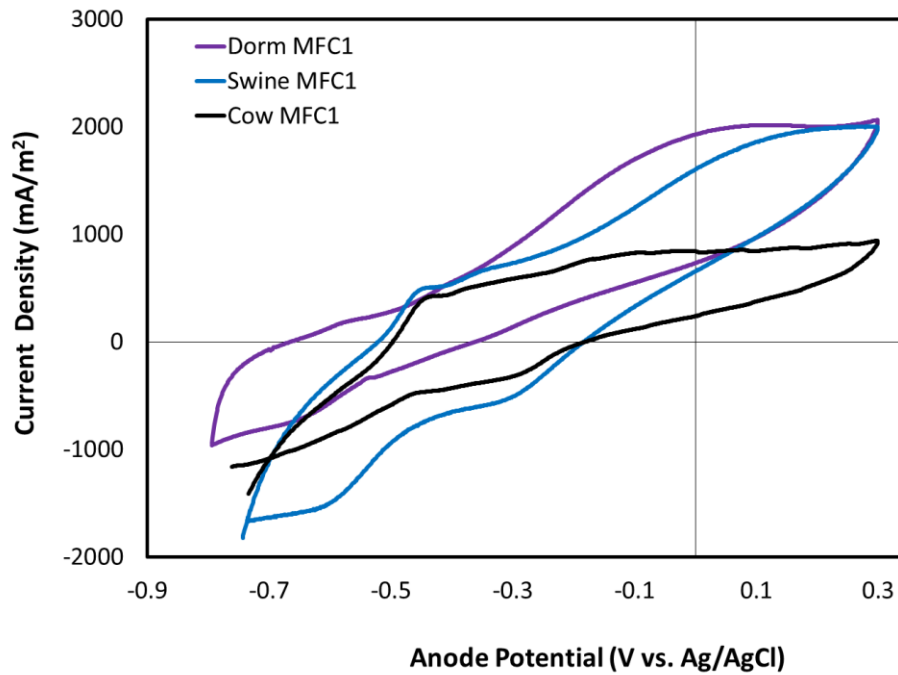
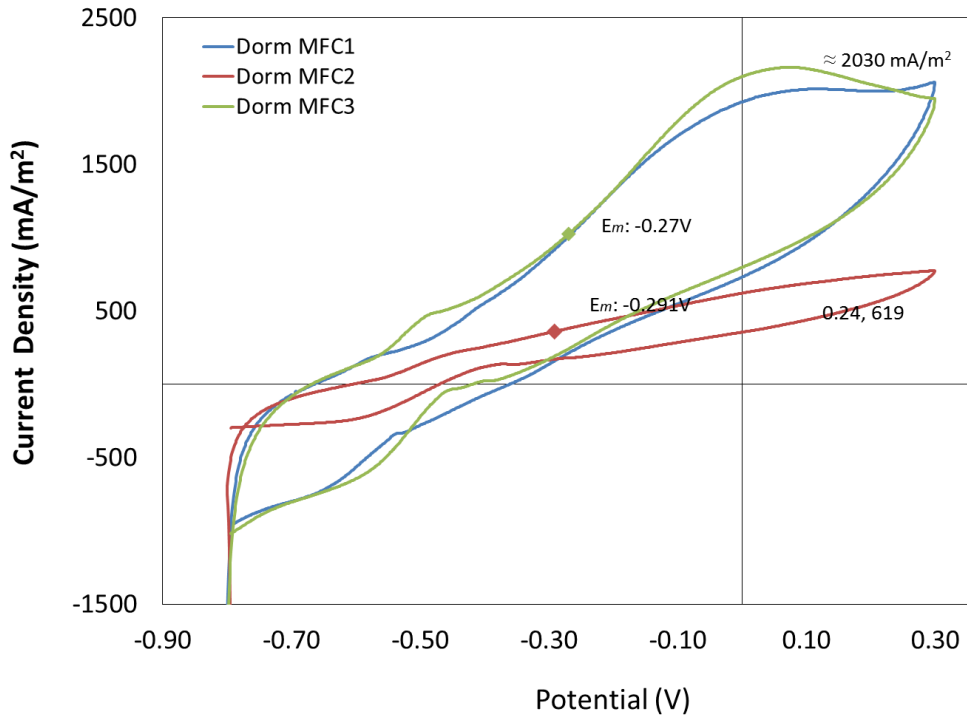


Figure 6-17. Representative voltammograms from MFCs fed with cow (black), swine (blue), and dormitory (purple) digestate. Scans were recorded at 0.001 V/s from -0.8 V to +0.3 V and back to -0.8 V vs. Ag/AgCl, 3M KCl

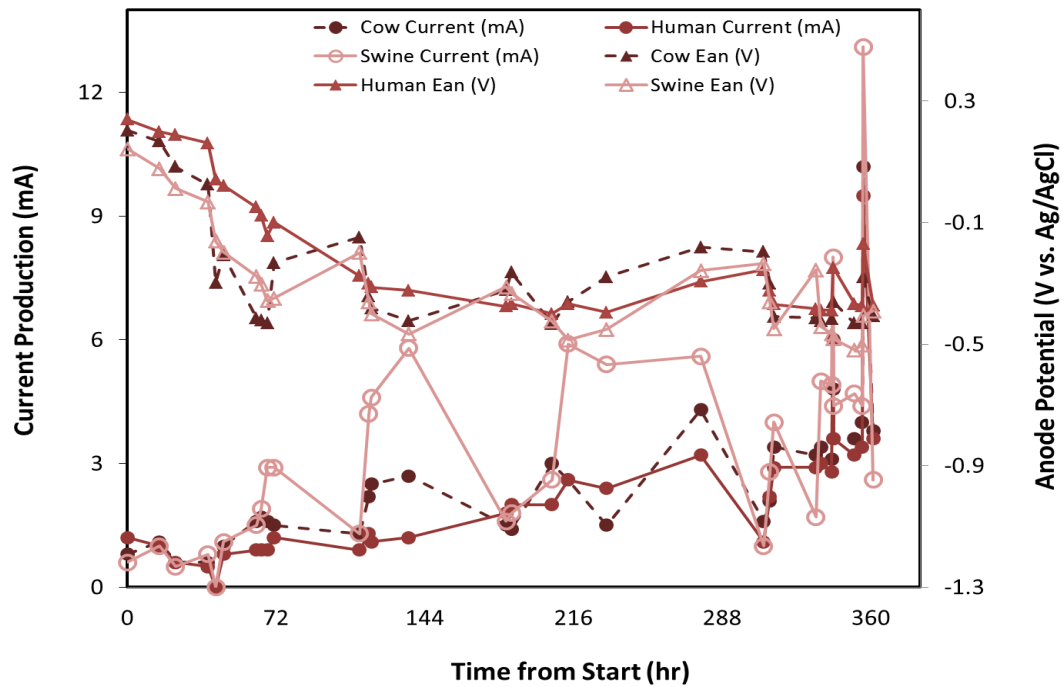


Figure 6-18. Development of anode potential (triangular symbols) and current production (circular symbols) from MFCs fed with Human (closed symbols, solid line); Cow (closed symbols, dashed line); and Swine (open symbols, solid line) Digestate; continuous flow experiment, V_{cell} , 0.35V.

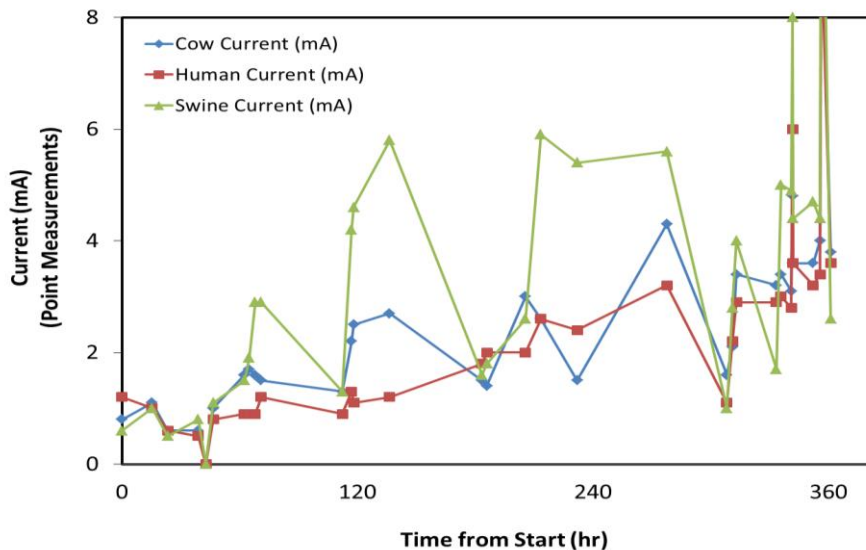


Figure 6-19. Current production (mA) during biofilm development of MFCs fed with Cow (blue), Swine (green), and Dormitory (red) digestate; continuous flow experiment with 2.8 h HRT; V_{cell} : 0.350 V.

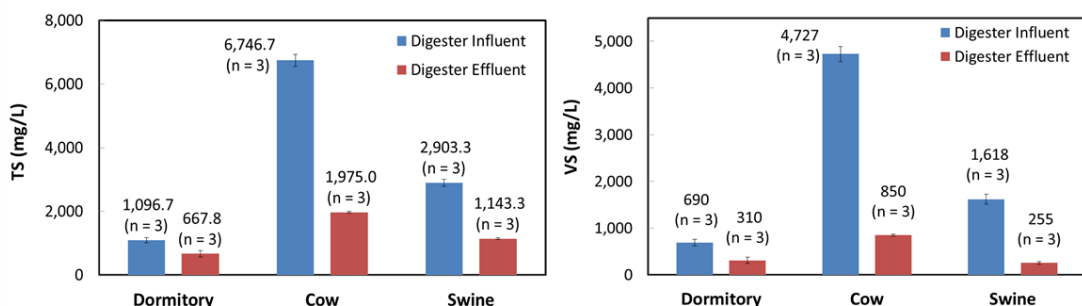


Figure 6-20. Total solids (TS) and Volatile Solids (VS) at the influent and effluent of Dormitory, Cow, and Swine Digesters. Values are presented as the mean (sample size), and error bars represent the standard deviation.

Table 6-7. Summary of electrochemical performance of MFCs fed with agricultural digestate

	Swine Average	Swine Stdev	Cow Average	Cow Stdev	Dorm Average	Dorm Stdev
i_{ss} (Ean: -0.2V vs. Ag/AgCl) (mA/m ²)	93 ± 17 (n = 3)	16.6	165	62.9	86	16.5
i_{ss} (Ean: -0.2V vs. Ag/AgCl) (A/m ³)	15	2.8	27	10.2	14	2.7
$w/acetate$, i_{ss} (Ean: -0.2V vs. Ag/AgCl) (mA/m ²)	DNR	DNR	DNR	DNR	681	264.6
$w/acetate$, i_{ss} (Ean: -0.2V vs. Ag/AgCl) (A/m ³)	DNR	DNR	DNR	DNR	110	43.0
i_{ss} (Vcell: 0.2V) (mA/m ²)	71	7.9	26	3.4	59	17.9
P_{ss} (Vcell: 0.2V) (mW/m ²)	14	1.6	5	0.7	12	3.6
i_{ss} (Vcell: 0.2V) (A/m ³)	12	1.2	4	0.5	10	2.9
P_{ss} (Vcell: 0.2V) (W/m ³)	2	0.2	1	0.1	2	0.6
$w/acetate$, i_{ss} (Vcell: 0.2V) (mA/m ²)	DNR	DNR	82	16.7	158	15.9
$w/acetate$, P_{ss} (Vcell: 0.2V) (mW/m ²)	DNR	DNR	16	3.4	31	3.5
$w/acetate$, i_{ss} (Vcell: 0.2V) (A/m ³)	DNR	DNR	13	2.7	25	2.7
$w/acetate$, P_{ss} (Vcell: 0.2V) (W/m ³)	DNR	DNR	3	0.6	5	0.6
P_{max} (mW/m ²)	60	10.1	52	7.4	28	1.3
P_{max} (W/m ³)	10	1.6	8	1.2	5	0.2
ΔE_{an} during polarization (mV)	206	90	229	86	253	35

ΔE_{cath} during polarization (mV)	395	22	320	52	178	24
OCV_{max} (mV)	701	34	548	37	495	31
Power Lifetime (hrs to $i < 1$ mA)	< 20 h	NA	19	0.0	30	NA

Table 6-8 Empirical mass balance for COD, VS, and energy produced by AD-MFC treatment process; combined lab & field data

	Dormitory Waste	Swine Waste	Dairy Waste
Q (m3/day)	22	4.36	2.18
COD_{in}-AD (kg/day)	22.9	14.1	13.8
Field Samples COD_{eff}-AD (kg/day)	7.55	0.959	2.42
Lab Samples COD_{eff}-AD (kg/day)	15.1	1.81	1.78
Field Samples COD_{eff}-MFC (kg/day)	10.2	0.658	1.31
Lab samples COD_{eff}-MFC (kg/day)	4.40	1.97	1.53
VS_{in}-AD (kg/day)	15.2	7.05	10.3
Field Samples VS_{eff}-AD (kg/day)	6.82	1.11	2.42
Lab Samples VS_{eff}-AD (kg/day)	9.06 - 23.1	1.22 - 1.88	1.54 - 1.54
Field Samples VS_{eff}-MFC (kg/day)	NA	NA	NA
Lab Samples VS_{eff}-MFC (kg/day)	5.08 - 10.6	2.16	1.43
E_{out}-AD (MJ/day)	824	154	707
E_{out}-MFC (MJ/day)	1.90	3.77	1.51

Table 6-9 Empirical mass balance for COD, VS, and energy produced by AD-MFC treatment process; field MFC data was used for all calculations

	Dormitory Waste	Swine Waste	Dairy Waste
--	-----------------	-------------	-------------

	Q (m³/day)	22	4.36	2.18
	COD_{in}-AD (kg/day)	22.9	14.1	13.8
Field Samples	COD_{eff}-AD (kg/day)	7.55	0.959	2.42
Field Samples	COD_{eff}-MFC (kg/day)	10.2	0.658	1.31
	VS_{in}-AD (kg/day)	15.2	7.05	10.3
Field Samples	VS_{eff}-AD (kg/day)	6.82	1.11	2.42
Field Samples	VS_{eff}-MFC (kg/day)	NA	NA	NA
	E_{out}-AD (MJ/day)	824	154	707
	E_{out}-MFC (MJ/day)	1.90	3.77	1.51

Bibliography

- Aelterman, P. R., K. Clauwaert, P. Verstraet, W. (2006). "Microbial fuel cells for wastewater treatment." Water Science & Technology **54**(8): 9-15.
- Allen, R. M. and H. P. Bennetto (1993). "Microbial fuel-cells: Electricity production from carbohydrates." Journal Name: Applied Biochemistry and Biotechnology; (United States); Journal Volume: 39-40 **39-40**: Medium: X; Size: Pages: 27-40.
- Amani, T., M. Nosrati and T. Sreekrishnan (2010). "Anaerobic digestion from the viewpoint of microbiological, chemical, and operational aspects-a review." Environmental Reviews **18**(NA): 255-278.
- An, B. X., T. R. Preston and F. Dolberg (1997). "The introduction of low-cost polyethylene tube biodigesters on small scale farms in Vietnam." Livestock Research for Rural Development **9**(2): 27-35.
- APHA, AWWA and WEF (2005). Standard methods for the examination of water and wastewater. Washington, D.C.
- APHA. (1976). Standard Methods for the Examination of Water and Wastewater 14ed, APHA American Public Health Association.
- Appels, L., J. Baeyens, J. Degrève and R. Dewil (2008). "Principles and potential of the anaerobic digestion of waste-activated sludge." Progress in Energy and Combustion Science **34**(6): 755-781.
- Arthur, R., M. F. Baidoo, A. Brew-Hammond and E. C. Bensah (2011). "Biogas generation from sewage in four public universities in Ghana: A solution to potential health risk." Biomass and Bioenergy **35**(7): 3086-3093.
- Atayol, A. A. and A. Sofuoğlu (2003). Anaerobic co-treatability of olive mill wastewaters and domestic wastewater, İzmir Institute Of Technology, İzmir.
- Austin, G. and G. Morris (2012). Biogas production in Africa. Bioenergy for Sustainable Development in Africa, Springer: 103-115.
- Bachmann, A., V. L. Beard and P. L. McCarty (1985). "Performance characteristics of the anaerobic baffled reactor." Water Research **19**(1): 99-106.
- Barber, W. P. and D. C. Stuckey (1999). "The use of the anaerobic baffled reactor (ABR) for wastewater treatment: a review." Water Research **33**(7): 1559-1578.
- Barbir, F. (2005). PEM Fuel Cells: Theory and Practice. Burlington, MA, Elsevier Academic Press.
- Bard, A. J. and L. R. Faulkner (1980). Electrochemical methods: fundamentals and applications, Wiley New York.
- Baturina, O. A. and A. E. Smirnova (2013). Chapter 4 - Catalytic Processes Using Fuel Cells, Catalytic Batteries, and Hydrogen Storage Materials. New and Future Developments in Catalysis. L. S. Steven. Amsterdam, Elsevier: 69-97.
- Bennetto, H. P., J. Stirling, K. Tanaka and C. Vega (1983). "Anodic reactions in microbial fuel cells." Biotechnology & Bioengineering **25**: 559-568.
- Benz, M., A. Brune and B. Schink (1998). "Anaerobic and aerobic oxidation of ferrous iron at neutral pH by chemoheterotrophic nitrate-reducing bacteria." Archives of Microbiology **169**(2): 159-165.

Bernard, O., Z. Hadj-Sadok, D. Dochain, A. Genovesi and J.-P. Steyer (2001). "Dynamical model development and parameter identification for an anaerobic wastewater treatment process." Biotechnology and Bioengineering **75**(4): 424-438.

Bhat, P. R., H. N. Chanakya and N. H. Ravindranath (2001). "Biogas plant dissemination: success story of Sirsi, India." Energy for Sustainable Development **5**(1): 39-46.

Bird, L. J., V. Bonnefoy and D. K. Newman (2011). "Bioenergetic challenges of microbial iron metabolisms." Trends in Microbiology **19**(7): 330-340.

Bitton, G. (2005). Wastewater microbiology, Wiley. com.

Bogte, J., A. Breure, J. Van Anandel and G. Lettinga (1993). "Anaerobic treatment of domestic wastewater in small scale UASB reactors." Water Science & Technology **27**(9): 75-82.

Bond, D. R. and D. R. Lovley (2003). Appl. Environ. Microbiol. **69**: 1548.

Bond, D. R., S. M. Strycharz-Glaven, L. M. Tender and C. I. Torres (2012). "On Electron Transport through Geobacter Biofilms." ChemSusChem **5**(6): 1099-1105.

Buysman, E. (2009). Anaerobic Digestion for Developing Countries with Cold Climates Masters Thesis, University of Wageningen.

Carlson, H. K., I. C. Clark, R. A. Melnyk and J. D. Coates (2012). "Toward a mechanistic understanding of anaerobic nitrate-dependent iron oxidation: balancing electron uptake and detoxification." Frontiers in microbiology **3**.

Chaggu, E. J., W. Sanders and G. Lettinga (2007). "Demonstration of anaerobic stabilization of black water in accumulation systems under tropical conditions." Bioresource Technology **98**(16): 3090-3097.

Chang, I., H. Moon, O. Bretschger, J. Jang, H. Park, K. H. Nealson and B. H. Kim (2006). "Electrochemically active bacteria (EAB) and mediator-less microbial fuel cells." J Microbiol Biotechnol **16**(2): 163-177.

Cheng, S., H. Liu and B. E. Logan (2006). "Increased performance of single-chamber microbial fuel cells using an improved cathode structure." Electrochemistry Communications **8**(3): 489-494.

Choi, M.-J., K.-J. Chae, F. F. Ajayi, K.-Y. Kim, H.-W. Yu, C.-w. Kim and I. S. Kim (2011). "Effects of biofouling on ion transport through cation exchange membranes and microbial fuel cell performance." Bioresource Technology **102**(1): 298-303.

Christensen, D. R. and P. L. McCarty (1975). "Multi-Process Biological Treatment Model." Journal (Water Pollution Control Federation) **47**(11): 2652-2664.

Clauwaert, P., K. Rabaey, P. Aelterman, L. De Schampelaire, T. H. Pham, P. Boeckx, N. Boon and W. Verstraete (2007). "Biological denitrification in microbial fuel cells." Environmental Science & Technology **41**(9): 3354-3360.

Clauwaert, P., R. Toledo, D. v. d. Ha, R. Crab, W. Verstraete, H. Hu, K. Udert and K. Rabaey (2008). "Combining biocatalyzed electrolysis with anaerobic digestion." Water Science and Technology **57**(4): 575-580.

Corcoran, E., C. Nellesmann, E. Baker, R. Bos, D. Osborn and H. Savelli (2010). Sick Water? The central role of wastewater management in sustainable development.

Cusick, R., B. Bryan, D. Parker, M. Merrill, M. Mehanna, P. Kiely, G. Liu and B. Logan (2011). "Performance of a pilot-scale continuous flow microbial electrolysis cell fed winery wastewater." Applied Microbiology and Biotechnology **89**(6): 2053-2063.

Daly, H. E. (1997). Beyond growth: the economics of sustainable development, Beacon Press.

Davidson, C. I., H. S. Matthews, C. T. Hendrickson, M. W. Bridges, B. R. Allenby, J. C. Crittenden, Y. Chen, E. Williams, D. T. Allen and C. F. Murphy (2007). "Viewpoint: Adding sustainability to the engineer's toolbox: A challenge for engineering educators." Environmental Science & Technology **41**(14): 4847-4849.

Delaney, G. M., H. P. Bennetto, J. R. Mason, S. D. Roller, J. L. Stirling and C. F. Thurston (1984). J. Chem. Technol. Biotechnol., Biotechnol. **34**: 13.

Du, F., B. Xie, W. Dong, B. Jia, K. Dong and H. Liu (2011). "Continuous flowing membraneless microbial fuel cells with separated electrode chambers." Bioresource Technology **102**(19): 8914-8920.

Dworkin, M., S. Falkow, E. Rosenberg, K. Schleifer and E. Stackebrandt, Eds. (2006). The Prokaryotes: Vol.6: Proteobacteria, Springer.

El-Fadel, M. and M. Massoud (2001). "Methane emissions from wastewater management." Environmental Pollution **114**(2): 177-185.

Elbeshbishy, E., G. Nakhla and H. Hafez (2012). "Biochemical methane potential (BMP) of food waste and primary sludge: Influence of inoculum pre-incubation and inoculum source." Bioresource Technology **110**: 18-25.

Fan, Y., H. Hu and H. Liu (2007). "Sustainable Power Generation in Microbial Fuel Cells Using Bicarbonate Buffer and Proton Transfer Mechanisms." Environmental Science & Technology **41**(23): 8154-8158.

Feng, Y., X. Wang, B. Logan and H. Lee (2008). "Brewery wastewater treatment using air-cathode microbial fuel cells." Applied Microbiology and Biotechnology **78**(5): 873-880.

Ferrer, I., M. Garfí, E. Uggetti, L. Ferrer-Martí, A. Calderon and E. Velo (2011). "Biogas production in low-cost household digesters at the Peruvian Andes." Biomass and Bioenergy **35**(5): 1668-1674.

Foley, J. M., R. Rozendal, C. Hertle, P. Lant and K. Rabaey (2010). "Life cycle assessment of high-rate anaerobic treatment, microbial fuel cells, and microbial electrolysis cells." Environmental Science & Technology **44**(9): 3629-3937.

Fornero, J. J., M. Rosenbaum and L. T. Angenent (2010). "Electric power generation from municipal, food, and animal wastewaters using microbial fuel cells." Electroanalysis **22**(7-8): 832-843.

Freguia, S., K. Rabaey, Z. Yuan and J. Keller (2008). "Sequential anode–cathode configuration improves cathodic oxygen reduction and effluent quality of microbial fuel cells." Water Research **42**(6–7): 1387-1396.

Freguia, S., S. Tsujimura and K. Kano (2010). "Electron transfer pathways in microbial oxygen biocathodes." Electrochimica Acta **55**(3): 813-818.

Fricke, K., F. Harnisch and U. Schroder (2008). "On the use of cyclic voltammetry for the study of anodic electron transfer in microbial fuel cells." Energy & Environmental Science **1**(1): 144-147.

Friedrich, E., S. Pillay and C. Buckley (2009). "Carbon footprint analysis for increasing water supply and sanitation in South Africa: a case study." Journal of Cleaner Production **17**(1): 1-12.

Garfí, M., L. Ferrer-Martí, V. Villegas and I. Ferrer (2011). "Psychrophilic anaerobic digestion of guinea pig manure in low-cost tubular digesters at high altitude." Bioresource Technology **102**(10): 6356-6359.

Garfí, M., P. Gelman, J. Comas, W. Carrasco and I. Ferrer (2011). "Agricultural reuse of the digestate from low-cost tubular digesters in rural Andean communities." Waste management **31**(12): 2584-2589.

Gerardi, M. H. (2003). The Microbiology of Anaerobic Digesters. Hoboken, N.J., John Wiley & Sons.

Gil, G.-C., I.-S. Chang, B. H. Kim, M. Kim, J.-K. Jang, H. S. Park and H. J. Kim (2003). "Operational parameters affecting the performance of a mediator-less microbial fuel cell." Biosensors and Bioelectronics **18**(4): 327-334.

Gil, G. C., I. S. Chang, B. H. Kim, M. Kim, J. K. Jang, H. S. Park and H. J. Kim (2003). Biosens. Bioelectron. **18**: 327.

Goldstein, N. C., R. L. Newmark, C. D. Whitehead, E. Burton, J. McMahon, G. Ghatikar and D. May (2008). "The Energy-Water Nexus and information exchange: challenges and opportunities." International Journal of Water **4**(1): 5-24.

Grau, J., C. Cathala, R. Riquelme, C. Nuques, Y. Galaz, S. Brackmann and S. Duret-Piquion (2009). Haiti: Water and Sanitation in Intermediate Cities: 25.

Gregory, K. B., D. R. Bond and D. R. Lovley (2004). "Graphite electrodes as electron donors for anaerobic respiration." Environmental Microbiology **6**(6): 596-604.

Haller, L., G. Hutton and J. Bartram (2007). "Estimating the costs and health benefits of water and sanitation improvements at global level." J Water Health **5**(4): 467-480.

Hansen, K. H., I. Angelidaki and B. K. Ahring (1998). "Anaerobic digestion of swine manure: inhibition by ammonia." Water Research **32**(1): 5-12.

Hayes, T. (1979). "Anaerobic Digestion of Cattle Manure.[book auth.]." AD Stafford.

He, Z., Y. L. Huang, A. K. Manohar and F. Mansfeld (2008). "Effect of electrolyte pH on the rate of the anodic and cathodic reactions in an air-cathode microbial fuel cell." Bioelectrochemistry **74**(1): 78-82.

He, Z., H. B. Shao and L. T. Angenent (2007). "Increased power production from a sediment microbial fuel cell with a rotating cathode." Biosensors & Bioelectronics **22**(12): 3252-3255.

Hedrich, S., M. Schlömann and D. B. Johnson (2011). "The iron-oxidizing proteobacteria." Microbiology **157**(6): 1551-1564.

Holm-Nielsen, J. B., T. Al Seadi and P. Oleskowicz-Popiel (2009). "The future of anaerobic digestion and biogas utilization." Bioresource Technology **100**(22): 5478-5484.

Hong, S. W., H. S. Kim and T. H. Chung (2010). "Alteration of sediment organic matter in sediment microbial fuel cells." Environmental Pollution **158**(1): 185-191.

Hu, Z. (2008). "Electricity generation by a baffle-chamber membraneless microbial fuel cell." Journal of Power Sources **179**(1): 27-33.

Hutton, G. and L. Haller (2004). Estimating the costs and health benefits of water and sanitation improvements at global level. S. a. H. Water. Geneva, WHO.

Huttunen, S. and A. Lampinen (2005). "Bioenergy technology evaluation and potential in Costa Rica."

Jang, J. K., I. S. Chang, K. H. Kang, H. Moon, K. S. Cho and B. H. Kim (2004). "Construction and operation of a novel mediator-and membrane-less microbial fuel cell." Process Biochemistry **39**(8): 1007-1012.

Jensen, P., H. Ge and D. J. Batstone (2011). "Assessing the role of biochemical methane potential tests in determining anaerobic degradability rate and extent." Water Science & Technology **64**(4): 880-886.

Jeremiase, A. W., H. V. M. Hamelers, E. Croese and C. J. N. Buisman (2012). "Acetate enhances startup of a H₂-producing microbial biocathode." Biotechnology and Bioengineering **109**(3): 657-664.

Jiang, D., M. Curtis, E. Troop, K. Scheible, J. McGrath, B. Hu, S. Suib, D. Raymond and B. Li (2011). "A pilot-scale study on utilizing multi-anode/cathode microbial fuel cells (MAC MFCs) to enhance the power production in wastewater treatment." International Journal of Hydrogen Energy **36**(1): 876-884.

Jiang, X., S. G. Sommer and K. V. Christensen (2011). "A review of the biogas industry in China." Energy Policy **39**(10): 6073-6081.

Jimenez, B., D. Mara, R. Carr and F. Brissaud (2010). Wastewater Treatment for Pathogen Removal and Nutrient Conservation: Suitable Systems for Use in Developing Countries. Wastewater Irrigation and Health: Assessing and Mitigating Risk in Low-Income Countries. P. Drechsel. London, UK, Earthscan: 149-169.

Jonsson, H., A. R. Stinzing, B. Vinneras and E. Salomon (2004). Guidelines on the Use of Urine and Faeces in Crop Production. EcoSanRes Programme. Stockholm, Stockholm Environment Institute: 43.

Kantawanichkul, S., S. Somprasert, U. Aekasin and R. Shutes (2003). "Treatment of agricultural wastewater in two experimental combined constructed wetland systems in a tropical climate." Water Science & Technology **48**(5): 199-205.

Katukiza, A., M. Ronteltap, C. Niwagaba, J. Foppen, F. Kansime and P. Lens (2012). "Sustainable sanitation technology options for urban slums." Biotechnology Advances **30**(5): 964-978.

Katuri, K. P. and K. Scott (2010). "Electricity generation from the treatment of wastewater with a hybrid up-flow microbial fuel cell." Biotechnology and Bioengineering **107**(1): 52-58.

Kim, J. R., B. Min and B. E. Logan (2005). Appl. Microbiol. Biotechnol. **68**: 23.

Kim, M., M. S. Hyun, G. M. Gadd, G. T. Kim, S. J. Lee and H. J. Kim (2009). "Membrane-electrode assembly enhances performance of a microbial fuel cell type biological oxygen demand sensor." Environmental Technology **30**(4): 329-336.

Klavon, K. H., S. A. Lansing, W. Mulbry, A. R. Moss and G. Felton (2013). "Economic analysis of small-scale agricultural digesters in the United States." Biomass and Bioenergy **54**: 36-45.

Koottatep, T., N. Surinkul, C. Polprasert, A. Kamal, D. Kone, A. Montangero, U. Heinss and M. Strauss (2004). Treatment of septage in constructed wetlands in tropical climate-- Lessons learnt after seven years of operation. 9th International IWA Specialist Group Conference on Wetlands Systems for Water Pollution Control, Avignon, France, Water Science & Technology.

Kujawa-Roeleveld, K. and G. Zeeman (2006). "Anaerobic Treatment in Decentralised and Source-Separation-Based Sanitation Concepts." Reviews in Environmental Science and Biotechnology **5**(1): 115-139.

Kumaraswamy, R., K. Sjollema, G. Kuenen, M. Van Loosdrecht and G. Muyzer (2006). "Nitrate-dependent [Fe (II) EDTA]²⁻ oxidation by *Paracoccus ferrooxidans* sp. nov., isolated from a denitrifying bioreactor." Systematic and applied microbiology **29**(4): 276-286.

Langergraber, G. and E. Muellegger (2005). "Ecological Sanitation—a way to solve global sanitation problems?" Environment international **31**(3): 433-444.

Lansing, S., R. Botero and J. Martin (2008). "Waste treatment and biogas quality in small-scale agricultural digesters." Bioresource Technology **99**(13): 5881-5890.

Lansing, S., R. B. Botero and J. F. Martin (2008). "Waste treatment and biogas quality in small-scale agricultural digesters." Bioresource Technology **99**(13): 5881-5890.

Lansing, S., J. Viquez, H. Martinez, R. Botero and J. Martin (2008). "Quantifying electricity generation and waste transformations in a low-cost, plug-flow anaerobic digestion system." Ecological Engineering **34**(4): 332-348.

Lansing, S., J. Viquez, H. Martínez, R. Botero and J. Martin (2008). "Quantifying electricity generation and waste transformations in a low-cost, plug-flow anaerobic digestion system." ecological engineering **34**(4): 332-348.

LeBlanc, R. J., P. Matthews and R. P. Richard (2009). Global atlas of excreta, wastewater sludge, and biosolids management: moving forward the sustainable and welcome uses of a global resource, UN-HABITAT.

Lee, C. C. and S. D. Lin (2000). Handbook of environmental engineering calculations, McGraw-Hill New York.

Lefebvre, O., A. Uzabiaga, I. Chang, B.-H. Kim and H. Ng (2011). "Microbial fuel cells for energy self-sufficient domestic wastewater treatment—a review and discussion from energetic consideration." Applied Microbiology and Biotechnology **89**(2): 259-270.

Legros, G., I. Havet, N. Bruce and S. Bonjour (2009). The Energy Access Situation in Developing Countries. New York, NY: 142.

Lettinga, G. (1995). "Anaerobic digestion and wastewater treatment systems." Antonie van leeuwenhoek **67**(1): 3-28.

Lettinga, G. and M. J. Lexmond (2001). Anaerobic digestion for sustainable development : selected proceedings of the farewell seminar for Prof. Dr Ir Gatzke Lettinga, held in Wageningen, The Netherlands, 29-30 March 2001. London, IWA Publishing.

Lin, J.-G., Y.-S. Ma, A. C. Chao and C.-L. Huang (1999). "BMP test on chemically pretreated sludge." Bioresource Technology **68**(2): 187-192.

Liu, H., S. A. Cheng and B. E. Logan (2005). "Production of electricity from acetate or butyrate using a single-chamber microbial fuel cell." Environmental Science & Technology **39**(2): 658-662.

Liu, H. and B. E. Logan (2004). "Electricity generation using an air-cathode single chamber microbial fuel cell in the presence and absence of a proton exchange membrane." Environmental Science & Technology **38**(14): 4040-4046.

Liu, H., R. Ramnarayanan and B. E. Logan (2004). Environ. Sci. Technol. **38**: 2281.

Logan, B., B. Hamelers, R. Rozendal, U. Schroder, J. Keller, S. Freguia, P. Aelterman, W. Verstraete and K. Rabaey (2006). "Microbial fuel cells: methodology and technology." Environmental Science & Technology **40**: 5181 - 5192.

- Logan, B. and J. Regan (2006). "Electricity-producing bacterial communities in microbial fuel cells." Trend Microbiol **14**: 512 - 518.
- Logan, B. E. (2008). Microbial Fuel Cells. Hoboken, NJ, John Wiley & Sons.
- Logan, B. E. (2012). "Essential data and techniques for conducting microbial fuel cell and other types of bioelectrochemical system experiments." ChemSusChem **5**(6): 988-994.
- Logan, B. E. and K. Rabaey (2012). "Conversion of Wastes into Bioelectricity and Chemicals by Using Microbial Electrochemical Technologies." Science **337**(6095): 686-690.
- Lovely, D. R. (1993). "Dissimilatory Metal Reduction." Annual Reviews of Microbiology **47**: 263-290.
- Lovley, D. R. (2006). "Bug juice: harvesting electricity with microorganisms." Nature Reviews Microbiology **4**(7): 497-508.
- Lovley, D. R. and E. J. P. Phillips (1988). "Novel Mode of Microbial Energy Metabolism: Organic Carbon Oxidation Coupled to Dissimilatory Reduction of Iron or Manganese." Appl. Environ. Microbiol. **54**(6): 1472-1480.
- Lowy, D. A. and L. M. Tender (2008). "Harvesting energy from the marine sediment–water interface: III. Kinetic activity of quinone- and antimony-based anode materials." Journal of Power Sources **185**(1): 70-75.
- Lowy, D. A., L. M. Tender, J. G. Zeikus, D. H. Park and D. R. Lovley (2006). "Harvesting energy from the marine sediment–water interface II: Kinetic activity of anode materials." Biosensors and Bioelectronics **21**(11): 2058-2063.
- Madigan, M. T., J. M. Martinko, J. Parker and T. D. Brock (1997). Biology of microorganisms, prentice hall Upper Saddle River, NJ.
- Mara, D. (2003). Domestic wastewater treatment in developing countries. London, UK, Earthscan.
- Mara, D. and N. J. Horan (2003). Handbook of water and wastewater microbiology, Academic press.
- Marchaim, U. (1992). Biogas processes for sustainable development. Shmona, Israel, Food and Agriculture Organization.
- Marland, G., T. A. Boden, R. Griffin, S. Huang, P. Kanciruk and T. Nelson (1989). Estimates of CO₂/emissions from fossil fuel burning and cement manufacturing, based on the United Nations energy statistics and the US Bureau of Mines cement manufacturing data, Oak Ridge National Lab., TN (USA).
- Marsili, E., D. B. Baron, I. D. Shikhare, D. Coursolle, J. A. Galnick and D. R. Bond (2008). "Shewanella secretes flavins that mediate extracellular electron transfer." Proceedings of the National Academy of Sciences **105**(10): 3968-3973.
- Marsili, E., J. Sun and D. R. Bond (2010). "Voltammetry and Growth Physiology of *Geobacter sulfurreducens* Biofilms as a Function of Growth Stage and Imposed Electrode Potential." Electroanalysis **22**(7-8): 865-874.
- McCarty, P. L. (1975). "Stoichiometry of Biological Reactions." Progress in Water Technology **7**: 157-172.
- McCarty, P. L., J. Bae and J. Kim (2011). "Domestic Wastewater Treatment as a Net Energy Producer–Can This be Achieved?" Environmental Science & Technology **45**(17): 7100-7106.

McCullough, J. S., D. H. Moreau and B. L. Linton (1993). *Financing Wastewater Services in Developing Countries*, WASH Technical Report No. 80. Washington, D.C.: 46.

Metcalf, L., H. Eddy and G. Tchobanoglous (2010). Wastewater engineering: treatment, disposal, and reuse, McGraw-Hill.

Mihelcic, J. R., J. C. Crittenden, M. J. Small, D. R. Shonnard, D. R. Hokanson, Q. Zhang, H. Chen, S. A. Sorby, V. U. James and J. W. Sutherland (2003). "Sustainability science and engineering: the emergence of a new metadiscipline." Environmental Science & Technology **37**(23): 5314-5324.

Min, B., J. Kim, S. Oh, J. Regan and B. Logan (2005). "Electricity generation from swine wastewater using microbial fuel cells." Water Research **39**(20): 4961-4968.

Min, B., J. Kim, S. Oh, J. M. Regan and B. E. Logan (2005). "Electricity generation from swine wastewater using microbial fuel cells." Water Research **39**(20): 4961-4968.

Mitchel, R. and J. Gu, Eds. (2010). Environmental Microbiology. Hoboken, NJ, John Wiley & Sons, Inc.

Montangero, A. and M. Strauss (2002). *Faecal Sludge Treatment*. S. F. I. f. E. S. Technology. IHE Delft, EAWAG: 42.

Moody, L., R. Burns, G. Bishop, S. Sell and R. Spajic (2011). "Using biochemical methane potential assays to aid in co-substrate selection for co-digestion." Applied Engineering in Agriculture **27**(3): 433-439.

Moon, H., I. S. Chang, J. K. Jang and B. H. Kim (2005). "Residence time distribution in microbial fuel cell and its influence on COD removal with electricity generation." Biochemical Engineering Journal **27**(1): 59-65.

Mosey, F. (1983). "Mathematical modelling of the anaerobic digestion process: regulatory mechanisms for the formation of short-chain volatile acids from glucose." Water Science & Technology **15**(8-9): 209-232.

Mowat, D. N., J. B. Singh and S. K. Vyas (1986). "Nutritive value of methane fermentation residue produced from cattle and swine wastes." Microbial Biomass Proteins **1**: 167-173.

Murphy, J. D., E. McKeogh and G. Kiely (2004). "Technical/economic/environmental analysis of biogas utilisation." Applied Energy **77**(4): 407-427.

Neubauer, S. C., D. Emerson and J. P. Megonigal (2002). "Life at the Energetic Edge: Kinetics of Circumneutral Iron Oxidation by Lithotrophic Iron-Oxidizing Bacteria Isolated from the Wetland-Plant Rhizosphere." Applied and Environmental Microbiology **68**(8): 3988.

Nicholson, R. S. and I. Shain (1964). "Theory of stationary electrode polarography. Single scan and cyclic methods applied to reversible, irreversible, and kinetic systems." Analytical Chemistry **36**(4): 706-723.

Nielsen, J. L. and P. H. Nielsen (1998). "Microbial nitrate-dependent oxidation of ferrous iron in activated sludge." Environmental Science & Technology **32**(22): 3556-3561.

Nielsen, M. E., D. M. Wu, P. R. Girguis and C. E. Reimers (2009). "Influence of substrate on electron transfer mechanisms in chambered benthic microbial fuel cells." Environmental Science & Technology **43**(22): 8671-8677.

Niessen, J., U. Schröder, M. Rosenbaum and F. Scholz (2004). "Fluorinated polyanilines as superior materials for electrocatalytic anodes in bacterial fuel cells." Electrochemistry Communications **6**(6): 571-575.

O'Dell, J. W. (1993). Method 350.1 Determination of Ammonia Nitrogen by Semi-Automated Colorimetry. O. o. R. a. Development. Cincinnati, US EPA: 1-15.

O'Dell, J. W. (1993). Method 351.2 Determination of Total Kjeldahl Nitrogen by Semi-Automated Colorimetry. O. o. R. a. Development. Cincinnati, US EPA: 1-15.

O'Dell, J. W. (1993). Method 353.2 Determination of Nitrate-Nitrite by Automated Colorimetry. O. o. R. a. Development. Cincinnati, US EPA.

Oh, S., B. Min and B. Logan (2004). "Cathode performance as a factor in electricity generation in microbial fuel cells." Environmental Science & Technology **38**: 4900 - 4904.

Owen, W. F., D. C. Stuckey, J. B. Healy Jr, L. Y. Young and P. L. McCarty (1979). "Bioassay for monitoring biochemical methane potential and anaerobic toxicity." Water Research **13**(6): 485-492.

Pant, D., G. Van Bogaert, L. Diels and K. Vanbroekhoven (2010). "A review of the substrates used in microbial fuel cells (MFCs) for sustainable energy production." Bioresource Technology **101**(6): 1533-1543.

Parameswaran, P., C. I. Torres, H. S. Lee, R. Krajmalnik-Brown and B. E. Rittmann (2009). "Syntrophic Interactions Among Anode Respiring Bacteria (ARB) and Non-ARB in a Biofilm Anode: Electron Balances." Biotechnology and Bioengineering **103**(3): 513-523.

Parameswaran, P., H. S. Zhang, C. I. Torres, B. E. Rittmann and R. Krajmalnik-Brown (2010). "Microbial Community Structure in a Biofilm Anode Fed With a Fermentable Substrate: The Significance of Hydrogen Scavengers." Biotechnology and Bioengineering **105**(1): 69-78.

Parawira, W., J. S. Read, B. Mattiasson and L. Björnsson (2008). "Energy production from agricultural residues: High methane yields in pilot-scale two-stage anaerobic digestion." Biomass and Bioenergy **32**(1): 44-50.

Park, D. H. and J. G. Zeikus (2003). Biotechnol. Bioeng. **81**: 348.

Park, H. I., D. k. Kim, Y.-J. Choi and D. Pak (2005). "Nitrate reduction using an electrode as direct electron donor in a biofilm-electrode reactor." Process Biochemistry **40**(10): 3383-3388.

Parkin, G. F. and W. F. Owen (1986). "Fundamentals of anaerobic digestion of wastewater sludges." ASCE Journal of Environmental Engineering **112**(5).

Pham, T. H., K. Rabaey, P. Aelterman, P. Clauwaert, L. De Schampelaire, N. Boon and W. Verstraete (2006). "Microbial Fuel Cells in Relation to Conventional Anaerobic Digestion Technology." Engineering in Life Sciences **6**(3): 285-292.

Popat, S. C., D. Ki, B. E. Rittmann and C. I. Torres (2012). "Importance of OH⁻ Transport from Cathodes in Microbial Fuel Cells." ChemSusChem **5**(6): 1071-1079.

Pozio, A., L. Giorgi, M. De Francesco, R. Silva, R. Lo Presti and A. Danzi (2002). "Membrane electrode gasket assembly (MEGA) technology for polymer electrolyte fuel cells." Journal of Power Sources **112**(2): 491-496.

Puig, S., M. Coma, J. Desloover, N. Boon, J. s. Colprim and M. D. Balaguer (2012). "Autotrophic denitrification in microbial fuel cells treating low ionic strength waters." Environmental Science & Technology **46**(4): 2309-2315.

Rabaey, K., P. Clauwaert, P. Aelterman and W. Verstraete (2005). "Tubular Microbial Fuel Cells for Efficient Electricity Generation." Environmental Science & Technology **39**(20): 8077-8082.

Rabaey, K. and W. Verstraete (2005). "Microbial fuel cells: novel biotechnology for energy generation." Trends Biotechnol **23**: 291 - 298.

Rajan, R., J.-G. Lin and B. T. Ray (1989). "Low-level chemical pretreatment for enhanced sludge solubilization." Research Journal of the Water Pollution Control Federation: 1678-1683.

Rajendran, K., S. Aslanzadeh and M. J. Taherzadeh (2012). "Household Biogas Digesters—A Review." Energies **5**(8): 2911-2942.

Raposo, F., M. A. De la Rubia, V. Fernández-Cegrí and R. Borja (2012). "Anaerobic digestion of solid organic substrates in batch mode: An overview relating to methane yields and experimental procedures." Renewable and Sustainable Energy Reviews **16**(1): 861-877.

Redlinger, T., J. Graham, V. Corella-Barud and R. Avitia (2002). "ECOLOGICAL TOILETS IN HOT ARID CLIMATES."

Richter, H., K. P. Nevin, H. Jia, D. A. Lowy, D. R. Lovley and L. M. Tender (2009). "Cyclic voltammetry of biofilms of wild type and mutant *Geobacter sulfurreducens* on fuel cell anodes indicates possible roles of OmcB, OmcZ, type IV pili, and protons in extracellular electron transfer." Energy & Environmental Science **2**(5): 506-516.

Rismani-Yazdi, H., S. M. Carver, A. D. Christy and O. H. Tuovinen (2008). "Cathodic limitations in microbial fuel cells: An overview." Journal of Power Sources **180**(2): 683-694.

Rodrigo, M. A., P. Cañizares, J. Lobato, R. Paz, C. Sáez and J. J. Linares (2007). "Production of electricity from the treatment of urban waste water using a microbial fuel cell." Journal of Power Sources **169**(1): 198-204.

Rothausen, S. G. and D. Conway (2011). "Greenhouse-gas emissions from energy use in the water sector." Nature Climate Change **1**(4): 210-219.

Rozendal, R., T. Sleutels, H. Hamelers and C. Buisman (2008). "Effect of the type of ion exchange membrane on performance, ion transport, and pH in biocatalyzed electrolysis of wastewater." Water Science and Technology **57**(11): 1757-1762.

Rozendal, R. A., H. V. Hamelers, K. Rabaey, J. Keller and C. J. Buisman (2008). "Towards practical implementation of bioelectrochemical wastewater treatment." Trends in biotechnology **26**(8): 450-459.

Schievano, A., G. D'Imporzano, S. Salati and F. Adani (2011). "On-field study of anaerobic digestion full-scale plants (Part I): an on-field methodology to determine mass, carbon and nutrients balance." Bioresource Technology **102**(17): 7737-7744.

Schröder, U. (2012). "Editorial: Microbial Fuel Cells and Microbial Electrochemistry: Into the Next Century!" ChemSusChem **5**(6): 959-959.

Schönning, C. and T. A. Stenström (2004). Guidelines on the safe use of urine and faeces in ecological sanitation systems, EcoSanRes Programme.

Sleutels, T., H. Hamelers, R. Rozendal and C. Buisman (2009). "Ion transport resistance in Microbial Electrolysis Cells with anion and cation exchange membranes." International Journal of Hydrogen Energy **34**(9): 3612-3620.

Sneddon, C., R. B. Howarth and R. B. Norgaard (2006). "Sustainable development in a post-Brundtland world." Ecological Economics **57**(2): 253-268.

Steinfeld, H., P. Gerber, T. Wassenaar, V. Castel and C. De Haan (2006). Livestock's long shadow: environmental issues and options, Food & Agriculture Org.

Stenström, T.-A. (2001). "Reduction efficiency of index pathogens in dry sanitation compared with traditional and alternative waste water treatment systems." Internet Dialogue on Ecological Sanitation (15 Nov.–20 Dec. 2001).

Straub, K. L., M. Benz and B. Schink (2001). "Iron metabolism in anoxic environments at near neutral pH." FEMS Microbiology Ecology **34**(3): 181-186.

Straub, K. L., M. Benz, B. Schink and F. Widdel (1996). "Anaerobic, nitrate-dependent microbial oxidation of ferrous iron." Applied and Environmental Microbiology **62**(4): 1458-1460.

Straub, K. L. and B. Schink (2004). Appl. Environ. Microbiol. **70**: 5744.

Strauss, M., S. A. Larmie and U. Heinss (1997). "Treatment of sludges from on-site sanitation - low-cost options." Water Science and Technology **35**(6): 129-136.

Strauss, M., S. A. Larmie and U. Heinss (1997). "Treatment of Sludges from On-Site Sanitation: Low-Cost Options." Water Science and Technology **35**(6): 129-136.

Strycharz, S. M., A. P. Malanoski, R. M. Snider, H. Yi, D. R. Lovley and L. M. Tender (2011). "Application of cyclic voltammetry to investigate enhanced catalytic current generation by biofilm-modified anodes of *Geobacter sulfurreducens* strain DL1 vs. variant strain KN400." Energy & Environmental Science **4**(3): 896-913.

Strycharz-Glaven, S. M., R. H. Glaven, Z. Wang, J. Zhou, G. J. Vora and L. M. Tender (2013). "Electrochemical investigation of a microbial solar cell reveals a nonphotosynthetic biocathode catalyst." Applied and Environmental Microbiology **79**(13): 3933-3942.

Strycharz-Glaven, S. M. and L. M. Tender (2012). "Study of the Mechanism of Catalytic Activity of *G. sulfurreducens* Biofilm Anodes during Biofilm Growth." ChemSusChem **5**(6): 1106-1118.

Strycharz-Glaven, S. M. and L. M. Tender (2012). "Study of the mechanism of catalytic activity of *G. sulfurreducens* biofilm anodes during biofilm growth." ChemSusChem **5**(6): 1106-1118.

Su, W., L. Zhang, D. Li, G. Zhan, J. Qian and Y. Tao (2012). "Dissimilatory nitrate reduction by *Pseudomonas alcaliphila* with an electrode as the sole electron donor." Biotechnology and Bioengineering **109**(11): 2904-2910.

Sánchez, E., R. Borja, P. Weiland, L. Travieso and A. Martín (2001). "Effect of substrate concentration and temperature on the anaerobic digestion of piggery waste in a tropical climate." Process Biochemistry **37**(5): 483-489.

Sørensen, A. H. and B. K. Ahring (1993). "Measurements of the specific methanogenic activity of anaerobic digester biomass." Applied Microbiology and Biotechnology **40**(2): 427-431.

Tchobanoglous, G., F. L. Burton, H. D. Stensel and Metcalf & Eddy. (2003). Wastewater engineering : treatment and reuse. Boston, McGraw-Hill.

Tchobanoglous, G., F. L. Burton, H. D. Stensel and Metcalf & Eddy. (2003). Wastewater engineering : treatment and reuse. Boston, McGraw-Hill.

Tender, L., M. T. Carter and R. W. Murray (1994). "Cyclic Voltammetric Analysis of Ferrocene Alkanethiol Monolayer Electrode Kinetics Based on Marcus Theory." Analytical Chemistry **66**(19): 3173-3181.

Tender, L., S. Gray, E. Groveman, D. Lowy, P. Kauffman, J. Melhado, R. Tyce, D. Flynn, R. Petrecca and J. Dobarro (2008). "The first demonstration of a microbial fuel cell as a viable power supply: Powering a meteorological buoy." Journal of Power Sources **179**(2): 571-575.

Ter Heijne, A., D. P. B. T. B. Strik, H. V. M. Hamelers and C. J. N. Buisman (2010). "Cathode Potential and Mass Transfer Determine Performance of Oxygen Reducing Biocathodes in Microbial Fuel Cells." Environmental Science & Technology **44**(18): 7151-7156.

Thien Thu, C. T., P. H. Cuong, L. T. Hang, N. V. Chao, L. X. Anh, N. X. Trach and S. G. Sommer (2012). "Manure management practices on biogas and non-biogas pig farms in developing countries—using livestock farms in Vietnam as an example." Journal of Cleaner Production **27**: 64-71.

Torres, C. I., R. Krajmalnik-Brown, P. Parameswaran, A. K. Marcus, G. Wanger, Y. A. Gorby and B. E. Rittmann (2009). "Selecting Anode-Respiring Bacteria Based on Anode Potential: Phylogenetic, Electrochemical, and Microscopic Characterization." Environmental Science & Technology **43**(24): 9519-9524.

UN (2010). The Millenium Development Goals Report. New York, United Nations Department of Economic and Social Affairs: 76.

UNEP (1998). Appropriate Technology for Sewage Pollution Control in the Wider Caribbean Region. Kingston, Jamaica, UNEP 224.

UNEP and E. Corcoran (2010). Sick Water?: The Central Role of Wastewater Management in Sustainable Development: a Rapid Response Assessment, UNEP/Earthprint.

USDOE and EG&G (2004). Fuel Cell Handbook. U. O. o. F. Energy. Morgantown, WV, USDOE: 7-18.

USEPA and CHP (2001). Opportunities for Combined Heat and Power at Wastewater Treatment Facilities: Market Analysis and Lessons from the Field. U. E. P. Agency. Washington, D.C., USEPA.

Vega, C. A. and I. Fernandez (1987). Bioelectrochem. Bioenerg. **17**: 217.

Vega, J. A., C. Chartier and W. E. Mustain (2010). "Effect of hydroxide and carbonate alkaline media on anion exchange membranes." Journal of Power Sources **195**(21): 7176-7180.

Virdis, B., K. Rabaey, R. A. Rozendal, Z. Yuan and J. Keller (2010). "Simultaneous nitrification, denitrification and carbon removal in microbial fuel cells." Water Research **44**(9): 2970-2980.

Virdis, B., K. Rabaey, Z. Yuan and J. Keller (2008). "Microbial fuel cells for simultaneous carbon and nitrogen removal." Water Research **42**(12): 3013-3024.

Virdis, B., S. T. Read, K. Rabaey, R. A. Rozendal, Z. Yuan and J. Keller (2011). "Biofilm stratification during simultaneous nitrification and denitrification (SND) at a biocathode." Bioresource Technology **102**(1): 334-341.

Voinov, A. and H. Cardwell (2009). "The Energy-Water Nexus: Why Should We Care?" Journal of Contemporary Water Research & Education **143**(1): 17-29.

Wang, Y., Y. Zhang, J. Wang and L. Meng (2009). "Effects of volatile fatty acid concentrations on methane yield and methanogenic bacteria." Biomass and Bioenergy **33**(5): 848-853.

Wang, Z., J. Ma, Y. Xu, H. Yu and Z. Wu (2013). "Power production from different types of sewage sludge using microbial fuel cells: A comparative study with energetic and microbiological perspectives." Journal of Power Sources **235**(0): 280-288.

Weld, R. and R. Singh (2011). "Functional stability of a hybrid anaerobic digester/microbial fuel cell system treating municipal wastewater." Bioresource Technology **102**(2).

Widdel, F., S. Schnell, S. Heising, A. Ehrenreich, B. Assmus and B. Schink (1993). "Ferrous iron oxidation by anoxygenic phototrophic bacteria." Nature **362**(6423): 834-836.

Yadvika, Santosh, T. Sreekrishnan, S. Kohli and V. Rana (2004). "Enhancement of biogas production from solid substrates using different techniques - a review." Bioresource Technology **95**(1): 1-10.

Yuan, Y., S. Zhou and J. Tang (2013). "In Situ Investigation of Cathode and Local Biofilm Microenvironments Reveals Important Roles of OH⁻ and Oxygen Transport in Microbial Fuel Cells." Environmental Science & Technology **47**(9): 4911-4917.

Zahller, J., R. Bucher, J. Ferguson and H. Stensel (2007). "Performance and stability of two-stage anaerobic digestion." Water Environment Research **79**(5): 488-497.

Zhang, G., Q. Zhao, Y. Jiao, K. Wang, D.-J. Lee and N. Ren (2012). "Efficient electricity generation from sewage sludge using biocathode microbial fuel cell." Water Research **46**(1): 43-52.

Zhang, J., Ed. (2008). PEM Fuel Cell Electrocatalysts and Catalyst Layers: Fundamentals and Applications. Vancouver, Springer.